Chapter 6

MAJOR AND TRACE ELEMENT GEOCHEMISTRY

6.1 INTRODUCTION

In this chapter are examined the major and trace element analyses of samples representative of the petrographic ranges of igneous and metamorphic variations. Samples were omitted that contained large veins of secondary minerals, or had suffered recent weathering effects.

The analytical data sample set consists of 80 XRF analyses of the lavas and dykes, 12 electron microprobe analyses of fresh volcanic glasses, and a further 17 major and trace element analyses performed by earlier researchers. REE analyses obtained by Dr P. Hellman, using facilities at the University of Cambridge in the course of a joint study with the author, are also presented. All of the analytical data are given in Appendices 1 and 2, and the analytical procedures are outlined in Appendix 6.

Geochemical effects of the alteration are examined by a comparison of the petrography and normative compositions of the samples and inter-element correlations within the data set, by comparisons of pillow core and rim analyses, and by variations within massive lava flows. Primary igneous geochemical variations are then assessed, and used to constrain the petrogenesis of the lavas and dolerites. The validity of various basalt discriminant diagrams currently in use is tested with these Macquarie Island data.

Some discussion of the major and trace element geochemistry of the lavas and dolerites has been presented in the literature, particularly in Griffin & Varne (1980), included as Appendix 8. Wherever possible repetition of this work has been avoided in this chapter and the reader is directed, by appropriate reference, to the relevant publication.

6.2 GEOCHEMICAL EFFECTS OF THE ALTERATION AND METAMORPHISM

Geochemical effects of low grade metamorphism on rocks of basaltic composition have been shown to be both complex and variable (Cann, 1969; Myashiro *et al.*, 1971; Hart, 1973; Smewing, 1975; Coish, 1977). Reviews of the range of metamorphic conditions considered to be present in the oceanic crust note the diversity of alteration trends recorded in different studies (Hart *et al.*, 1973; Aumento *et al.*, 1976; Coleman, 1977).

Many studies have concentrated on basalts altered under low greenschist facies metamorphism (Cann, 1969; Coish, 1977; Humphris & Thompson, 1978a,b) or on basalts altered during ocean-floow weathering (Andrews, 1977; Barager *et al.*, 1977; Pritchard *et al.*, 1979). Surprisingly little information is available on basalts affected by zeolite facies metamorphism (Andrews *et al.*, 1975; Wood *et al.*, 1976).

The various studies suggest that only the H_2O content and the Fe^{3+}/Fe^{2+} ratio, of the rock, show consistent increases during alteration occurring regardless of local environment, metamorphic conditions or degree of crystallinity of the rock (Aumento *et al.*, 1976). It is also apparent that alteration is most intense around fractures and other permeable zones in the rocks and that major variations may exist between the glassy rim and crystalline core of a pillow lava as a result of alteration. Ludden & Thompson (1979) have demonstrated these latter points particularly well for the rare earth elements. There is also strong evidence to suggest that certain trace elements, particularly Ti, Zr, Y and Nb, are little affected by alteration and metamorphism to moderate grades (Cann, 1970; Pearce & Cann, 1971, 1973; Wood *et al.*, 1976; Pearce & Norry, 1979).

6.2.1 H_2O abundances and Fe^{3+}/Fe^{2+} ratios

The lavas and dolerites analyzed in this study have a range of loss on ignition (LOI) values from 0.84 wt.% to 5.93 wt.% (Figure 6.1). Results of CO_2-H_2O^+ analyses of selected samples (Table 6.1) show that the LOI values are principally H_2O^+ unless calcite is an abundant secondary phase; a feature of the samples that have undergone ocean-floor weathering. A maximum value of 3.25 wt.% CO_2 was obtained for sample 35, other samples containing from 0.12 to 0.99 wt.% CO_2 (Table 6.1).

Moore (1970) has documented the low water contents of fresh basalts, with values ranging up to 0.98 wt.% H_2O^+ for alkaline basalts but less than 0.5 wt.% for K-poor tholeiites. Similar results have been recorded from fresh oceanic basalt glasses by Melson *et al.* (1976) and in this thesis as the microprobe analyses of fresh volcanic glasses total 100 ± 1 wt.% (Appendix 1). Consequently the high LOI values recorded from the crystalline samples are interpreted as principally an effect of the alteration processes.

A breakdown of the samples into subsets with the same grade of alteration shows a general decrease of the LOI value with increasing grade of alteration. Samples from the ocean-floor weathering zone have a wide LOI range, reflecting the erratic style of this type of alteration. The LOI values of samples from higher grades of alteration are more uniform. The highest LOI mean value (3.58 wt.%) for rocks from a particular metamorphic grade occurs in the zeolitized samples, decreasing to 2.28 wt.% for samples which have undergone upper greenschist facies metamorphism. This variation presumably results from the decrease in water content of the dominant secondary phases (in the respective grades of alteration), from clay minerals (20 wt.% H_2O) through zeolites (12-16 wt.% H_2O) to chlorites (10-12 wt.% H_2O) and epidote (2-4 wt.% H_2O) and finally amphibole (2-3 wt.% H_2O).

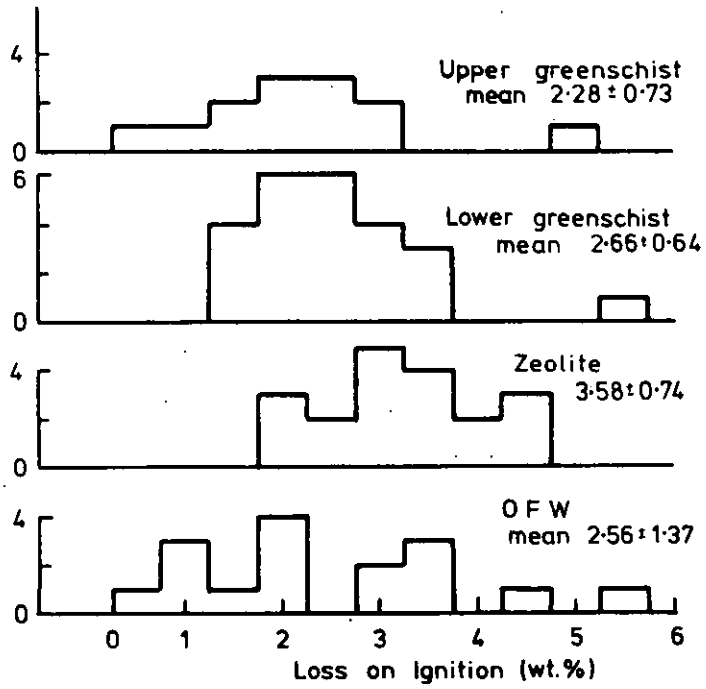

Figure 6.1 Histograms of loss on ignition for lavas and dykes from different metamorphic grades.

Table 6.1

CO_2 AND H_2O ANALYSES OF LAVAS AND DYKES.

Alteration	Sample Number	CO_2†	H_2O†	ε	LOI
Ocean-floor weathering	35	3.25	2.44	5.69	5.72
	38265	0.59	4.03	4.62	3.50*
	38391	0.99	1.54	2.53	2.28
Zeolite	157	0.98	3.36	4.34	3.67
	38188	0.40	3.55	3.95	3.39
Lower Greenschist	56D	0.24	1.76	2.00	1.63
	56G	0.32	2.08	2.40	2.75
	108C	0.35	1.45	1.80	1.76
	119	0.20	2.50	2.70	2.75
	199	0.12	1.43	1.55	1.76
	38310	0.22	4.06	4.28	4.13
Upper Greenschist (Dykes)	153	0.13	1.87	2.00	5.03
	38157	0.18	2.29	2.47	2.72
	38236	0.77	2.43	3.20	3.26
	38451	0.19	2.07	2.26	2.42

† Analyses by J. Cocker.
* Analysis by P. Robinson. (Analyst, Geology Dept., University of Tasmania)

The second major geochemical effect of the alteration is a modification of the Fe_2O_3 content of the samples compared with fresh basalts. Although it is impossible to know exactly what the pristine igneous Fe_2O_3 values of the samples might have been, Myashiro *et al.* (1970) have shown that fresh basalts have a Fe_2O_3/FeO weight ratio range of 0.1 to 0.3. This is equivalent to a range of 0.92 to 0.79 in the weight ratio Fe^{2+}/Fe_T (= total Fe), used from this point on, in this thesis.

Although there is a considerable range in Fe^{2+}/Fe_T values from samples of similar degrees of alteration, the histograms in Figure 6.2 demonstrate a progressive increase in this ratio with increasing grades of metamorphism. Samples metamorphosed at zeolite facies grade and below dominate the low end of the Fe^{2+}/Fe_T range, with values from 0.38 to 0.62, with lower greenschist facies samples having a range of 0.55 to 0.74, and then the upper greenschist facies and higher grade samples from the dyke swarm zones with a range from 0.74 to 0.97.

The observed variation in Fe^{2+}/Fe_T values of these samples supports the conclusion, based on the secondary mineralogical studies (described in Chapter 5), that the metamorphic process was strongly oxidizing at the lower grades and became progressively more reducing with increasing metamorphic grade. Also, the relatively large ranges both in LOI and in Fe^{2+}/Fe_T within each group of samples from the various metamorphic grades illustrate the incomplete nature of the metamorphism and the variation in degree of alteration within the samples.

In summary, the lavas and dolerites probably show a gain in H_2O under all conditions of metamorphism and alteration recorded in these rocks. This gain is probably at a maximum at low grades of metamorphism. Fe^{2+}/Fe_T values are more variable within grades of metamorphism than LOI contents but show overall group decreases up to and including conditions

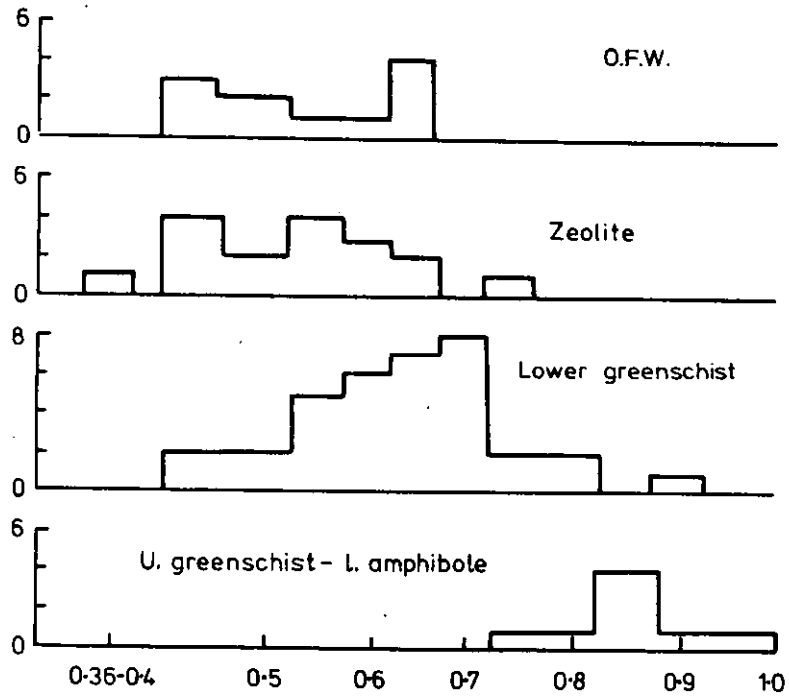

Figure 6.2 Histograms of Fe^{2+}/Fe_{T*} for lavas and dykes of different metamorphic grades.
* total as FeO

of lower greenschist facies metamorphism. The Fe^{2+}/Fe_T values are apparently increased during upper greenschist facies metamorphism. To aid the petrologic interpretation of these data the analyses have been recalculated to a volatile-free basis with $Fe^{2+}/Fe_T = 0.85$ (the mid-range value from Miyashiro *et al.*, 1970).

6.2.2 Comparison of petrography and CIPW normative and major element chemistry

The samples vary normatively from basanitic through alkaline olivine basalts to olivine tholeiites and rarely quartz tholeiites (Figure 6.3). This range is in excellent agreement with the observations made from the petrography (Chapter 4). In the analyzed set, of 21 lavas recognized petrographically to have alkaline affinities, 15 contain normative Ne; and of 23 lavas with oceanic tholeiite petrographic affinities, 14 are ol- hy-normative and 6 contain less than 2 wt.% normative ne.

To check this result more rigorously, a Wilke stepwise discriminant analysis was performed on the analyses of lavas obtained by the author which were petrographically defined as either alkaline or tholeiitic. The discriminant analysis was successful in that 16 of the 18 tholeiitic samples and 11 of the 13 alkaline samples were correctly identified. Components of the Wilke discrimination function were SiO_2, CaO, Na_2O and LOI with standardized function values of 1.477, 1.307, -0.744 and 0.477 respectively. The significance of the discrimination was 99.5%.

The systematic relationship between the relict petrographic features and the bulk chemistry and normative composition of the samples suggests strongly that the alteration and metamorphism has had little effect on the present geochemistry of the samples. This is not in conflict with the observed secondary mineralogical reconstitution of the samples but indicates that away from fracture surfaces, or areas of major fluid movement, the fluid/rock ratios were low.

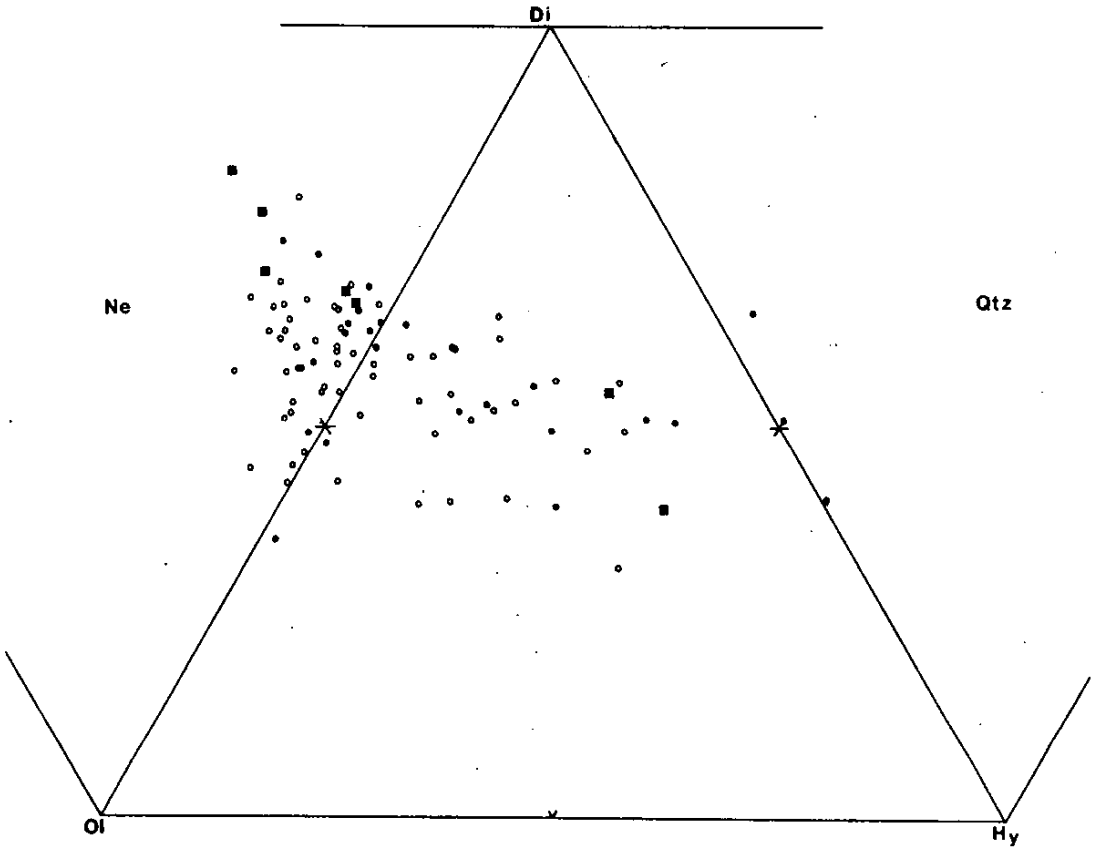

Figure 6.3 Plot of relative proportions of normative ol, hy, di, ne and Q in Macquarie Island basalts (open circles), dolerites (filled circles), and volcanic glasses (filled squares). CIPW norm calculations were performed on major element analyses recalculated volatile-free with Fe^{2+}:total Fe = 0.85. Two volcanic glasses, four basalts, and one dolerite have >5 wt.% ne, and could be termed basanitoids.

6.2.3 Core-rim variations in pillow lavas and variations across a massive flow

To examine the geochemical effects of the alteration on a local scale in the samples, analyses have been performed on core and rim material from two pillow lavas and on four samples obtained from the edge to the central zone of a massive lava flow. The rim material from the pillow lavas is hyalocrystalline and the cores holocrystalline. These samples should show the maximum geochemical effects of the alteration, apart from areas abutting veins. All samples have undergone lower greenschist facies metamorphism and were selected to allow comparison between the samples and other similar studies in the literature.

Relative to their core compositions, the rims of the pillow lavas are depleted in Al_2O_3, Fe_2O_3, MgO, CaO and Sr, and enriched in SiO_2, FeO and Na_2O. LOI, Fe_T, Ni and Cr show opposing variations in the two pillow core-rim pairs (Table 6.2). The remaining elements show little variation. The magnitude of the variations is much smaller and generally opposed to results from a comparable study of pillow lavas in the Betts Cove ophiolite (Coish, 1977). They could equally well arise from minor differences in plagioclase and olivine proportions in the core relative to the rim, as from metamorphic effects. For example, a difference of +5 wt.% plagioclase (An_{85}) between the core and rim will account for the observed variations in CaO, Al_2O_3 and Sr, and much of that in SiO_2 and Na_2O. Samples from the massive flow show no systematic or major variations in major and trace element abundances with position relative to the edge of the flow (Table 6.2).

Rare earth elements (REE) have been obtained for these samples as part of a project to study the mobility of these elements (Hellman & Henderson, 1977; Hellman *et al*, 1978). However, no evidence for mobilization of the REE is provided by these results. The Masuda-Coryell

Table 6.2

RIM-CORE PILLOW LAVA AND EDGE-CORE MASSIVE FLOW ANALYSES

	Pillow		Pillow		Massive Flow			
Sample No.	43B	43B	108	108	56A	56D	56G	56I
Analysis	core	edge	core	edge	edge	1.0m	2.0m	core
SiO_2	49.24	50.20	49.17	50.20	48.17	48.58	49.76	47.80
TiO_2	1.60	1.59	1.35	1.35	1.03	1.03	1.06	1.05
Al_2O_3	16.15	15.81	15.22	14.79	18.68	18.95	18.34	18.51
Fe_2O_3	5.09	4.09	5.05	4.69	2.17	1.45	2.27	2.47
FeO	4.06	4.68	5.30	5.95	4.45	4.35	4.07	4.46
MnO	0.19	0.19	0.15	0.15	0.12	0.12	0.11	0.12
MgO	7.31	6.67	7.29	7.25	7.94	7.79	8.07	8.08
CaO	10.36	9.87	11.52	10.85	11.72	12.33	11.91	12.25
Na_2O	3.27	3.66	2.85	2.91	2.95	2.59	3.19	2.57
K_2O	0.63	0.84	0.51	0.51	0.25	0.20	0.25	0.20
P_2O_5	0.29	0.28	0.20	0.18	0.17	0.17	0.21	0.17
LOI	1.71	1.81	1.75	0.35	2.08	1.63	2.75	1.89
Total	99.59	99.95	100.37	100.13	99.71	99.21	100.19	99.17
Ni	55	61	54	49	87	87	86	92
Cr	142	137	103	110	311	294	294	273
Zr	115	117	78	82	71	60	68	61
Y	39	38	40	41	18	20	23	23
Nb	21	23	8	8	14	12	14	14
Rb	12	10	13	14	1	0	4	0
Sr	221	197	145	133	213	210	207	199
Co	37	37	40	41	30	30	32	30
Sc	36	35	42	42	34	35	35	35
Fe^{2+}/Fe	0.47	0.56	0.54	0.59	0.70	0.77	0.67	0.67
Fe/Fe+Mg	0.60	0.59	0.57	0.56	0.69	0.71	0.70	0.68

plots of REE abundances show no differences between the samples, within the experimental error of the analyses (Figure 6.4).

These data suggest minimal element mobility on local scales and provide corroborative evidence for the overall conclusion that the alteration and metamorphism has had little effect on the geochemistry of the samples.

6.2.4 Inter-element correlations of major and trace elements

A matrix of Pearson correlation coefficients for major and trace elements in the data set is presented in Table 6.3. The elements have been arranged into three groups based on their respective correlations, or lack thereof. *Group I* is composed of the major elements SiO_2, Al_2O_3, FeO_T, MnO, MgO, CaO and Na_2O; *group II* is composed of Y, Zr and TiO_2; and *group III* is composed of K_2O, P_2O_5, Nb, Sr and Rb.

Within group I the positive correlation between CaO and Al_2O_3 and the negative correlations of these elements with the remainder of the major elements of group I suggest that plagioclase may have played a major role in the evolution of these rocks; corroborating observations based on the petrography of the rocks (Chapter 4).

MgO and FeO_T do not correlate at a significant level. However MgO negatively correlates with SiO_2, Al_2O_3, CaO and Na_2O, and Y and TiO_2 in group II; and FeO negatively with Al_2O_3, CaO and positively with MnO and Y, Zr, and TiO_2 in group II. This suggests that abundances of these two elements have not been greatly affected. This is also implied by negative correlations of the Mg/Mg+Fe of the samples with Ni and Cr abundances (Figure 6.5), a systematic relation generally found as a result of igneous processes.

The group II elements are those which have been recognized to be relatively immobile under these conditions of metamorphism, as noted earlier (Section 6.2.1). The correlations of these elements with all

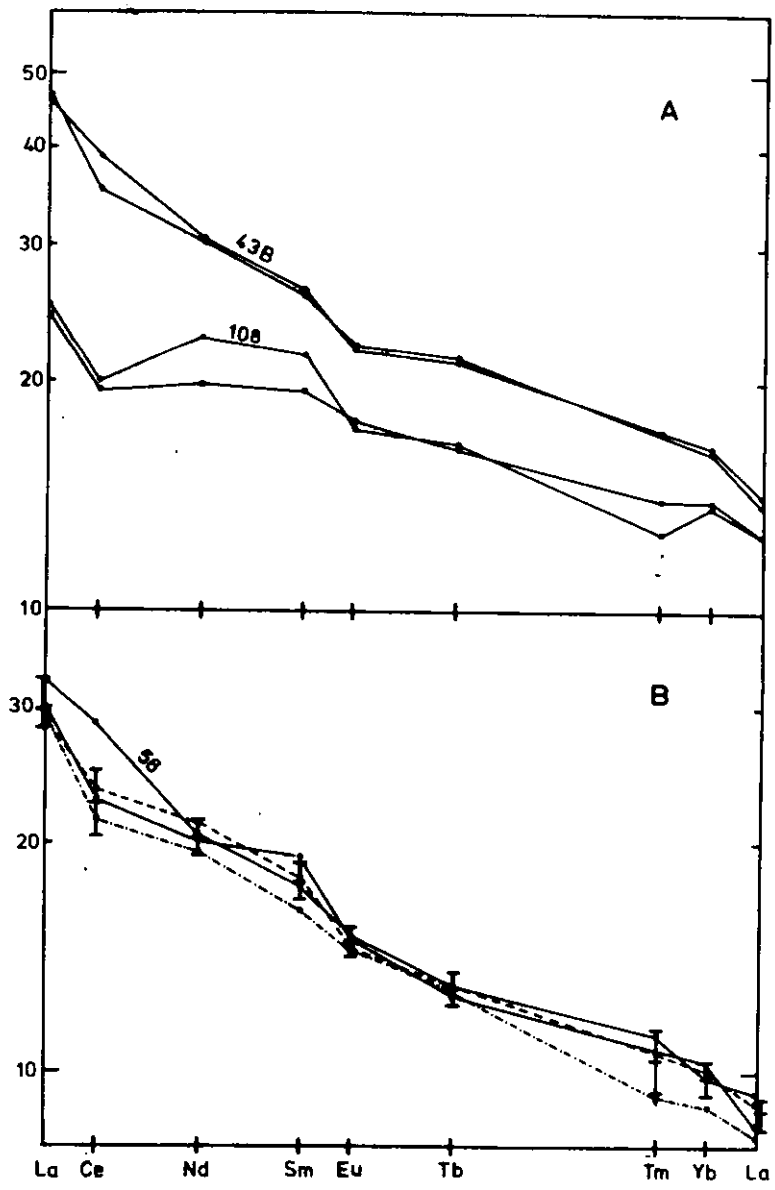

Figure 6.4 Normalised REE abundances for (A) pillow lava core (●) and rim (○) pairs and (B) massive lava samples. Error bars are drawn about the mean abundances. Chondrite normalizing values used were those of Hoskins *et al.* (1968)

Table 6.3

PEARSON CORRELATION COEFFICIENT MATRIX FOR MAJOR AND TRACE ELEMENTS IN MACQUARIE ISLAND LAVAS AND DYKES

	SiO_2	Al_2O_3	FeO_T	MnO	MgO	CaO	Na_2O	Y	Zr	TiO_2	K_2O	P_2O_5	Nb	Sr	Rb
SiO_2	-														
Al_2O_3	-0.304	-													
FeO_T		-0.785	-												
MnO	0.313	-0.640	0.802	-											
MgO	-0.452	-0.480			-										
CaO	-0.360	0.657	-0.474	-0.493	-0.435	-									
Na_2O	0.557	-0.032			-0.573		-								
Y	0.537	-0.464	0.632	0.511	-0.339	-0.277	0.464	-							
Zr	0.337	-0.387	0.445	0.480			0.319	0.627	-						
TiO_2	0.513	-0.514	0.587	0.585	-0.303	-0.330	0.441	0.831	0.871	-					
K_2O						-0.310					-				
P_2O_5								0.334	0.802	0.543	0.375	-			
Nb									0.732	0.448	0.369	0.919	-		
Sr									0.334		0.617	0.605	0.653	-	
Rb						-0.299			0.286		0.968	0.334	0.391	0.614	-

For 90 samples, 99.9% level of confidence = 0.267.

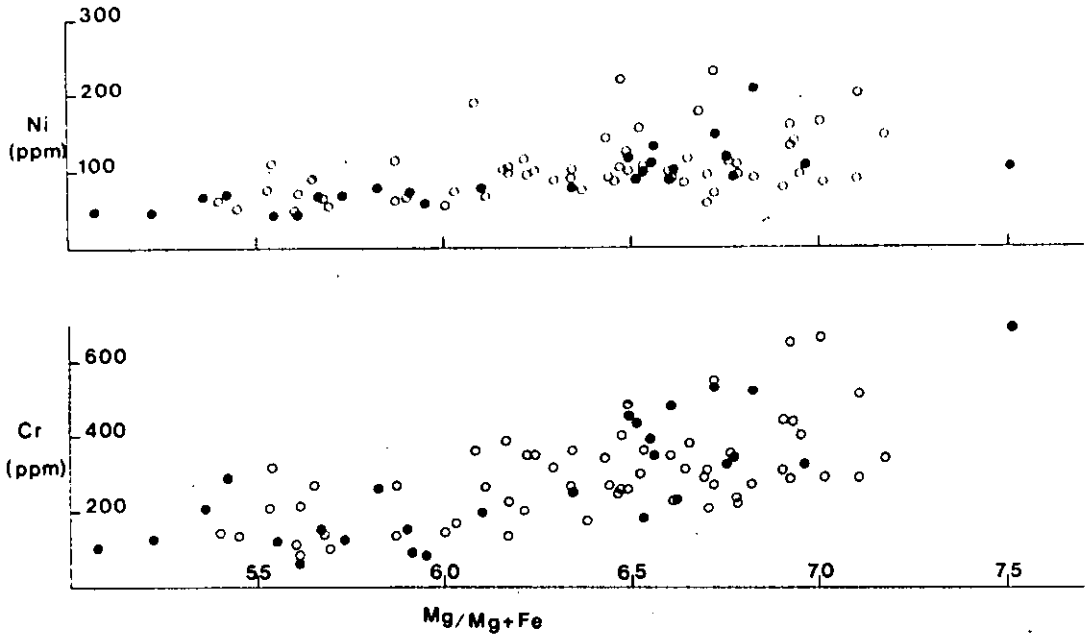

Figure 6.5 Ni and Cr contents of Macquarie Island basalts (open circles) and dolerites (closed circles), plotted against 100 Mg/Mg+Fe.

others, excepting K_2O, is in agreement with the earlier studies in confirming their immobile character. A feature of the correlations of these elements is that Zr shows the lowest correlations with the group I elements but the highest correlations with the group III elements. Evidence is presented in Section 6.3.6 to suggest that this is a feature of the petrogenesis of the samples.

All group III elements show significant correlations with each other. Correlation coefficient values of 0.919 between Nb and P_2O_5, and 0.968 between Rb and K_2O are very high and reflect the coherent geochemical behaviour of these elements. Apart from correlations of K_2O and Rb with CaO, these group III elements show no significant correlations with the major elements of group I. Although the metamorphic mobility of three of the group III elements (K_2O, Sr and Rb) has been recognized in some studies (Hart *et al.*, 1973; Wood *et al.*, 1976) their correlations with the less mobile elements of the group (Nb and P_2O_5), and with Zr in the case of Sr and Rb, suggest that their abundance and variations reflect primary processes rather than effects of the alteration and metamorphism. Later in this chapter (Section 6.3.6, Table 6.12) it is shown that the light rare earth elements (LREE) correlate closely with Nb and thus, apart from exhibiting variations comparable to the group III elements, have also not been significantly affected.

Overall, the results presented in Section 6.2 are strong evidence for the conclusion that, apart from Fe^{2+}/Fe_T and H_2O contents, geochemical effects of the alteration and metamorphism are minimal in the analyzed data set. This is not in conflict with the extensive alteration of many of the samples, described in the preceding chapter, but reaffirms the conclusions drawn regarding the local variability of the metamorphic processes; specifically the low water/rock ratios away from the major fracture surfaces and more permeable zones in the rocks.

6.3 IGNEOUS GEOCHEMISTRY

6.3.1 Petrogenesis of the lavas and dykes: implications from their geochemistry

The statistical analysis of the results discussed in the preceding sections has distinguished three groups of elements in terms of their variations in the analyzed lavas and dykes. Ni and Cr data were not available for inclusion in the statistical analysis, however correlation coefficients derived for these elements against the other elements (Table 6.4) demonstrate their membership of group I. Also, the LREE closely correlate with Nb (Table 6.12, Figure 6.16) and are assigned to group III.

In terms of geochemical behaviour, an immediate distinction can be made between the elements comprising group I and those of groups II and III. Group I elements are either major elements or elements with high solid/liquid partition coefficients for the phases either comprising likely mantle mineralogies or likely to fractionate from basaltic liquids, i.e. olivine, orthopyroxene, clinopyroxene, plagioclase, garnet and spinel. Group II and group III elements are, on the other hand, generally characterized by low solid/liquid partition coefficients for these phases and thus are "incompatible". Sr, Eu and the HREE may be exceptions to this depending on prevailing conditions, particularly P. T, P_{H_2O} and P_{O_2}.

Wood (1979) has ranked incompatible elements, including those of the groups II and III recognized here, on the basis of bulk partition coefficients, for a range of mantle compositions composed of the phases olivine, clinopyroxene, orthopyroxene, garnet and plagioclase. The last two were only present in minor modal amounts (5%) in the assumed mantle mineralogies. Experimentally determined solid/liquid partition coefficient data from Hanson (1977) were used. This ranking is compared with the components of groups II and III and geochemical patterns for

Table 6.4

CORRELATION COEFFICIENTS OF Zr WITH OTHER ELEMENTS/OXIDES FOR RECALCULATED ANALYSES.

Element/Oxide	Lavas (56*)	Dykes (24*)
SiO_2	0.026	0.170
TiO_2	0.820	0.877
Al_2O_3	0.559	0.560
Total iron (FeO)	0.543	0.421
MnO	0.563	0.280
MgO	0.161	0.220
CaO	-0.240	-0.379
Na_2O	0.083	0.215
K_2O	0.420	0.445
P_2O_5	0.799	0.872
Correlation Coefficients for:		
99% confidence	0.340	0.514
95% confidence	0.260	0.400

* Number of samples

various mid-ocean ridge basalts (MORB) as shown in Figure 6.6.

Group II elements (Zr, Ti and Y) are those with moderately low bulk partition coefficients, and show relatively little variation in abundance between the different MORB. Group III elements have lower bulk partition coefficients and show a wide range in abundances; being most enriched in the alkaline basalts from 45°N on the Mid-Atlantic Ridge. On the basis of these characteristics the group II elements are referred to as the *incompatible elements* and the group III elements as the *hygromagmatophile elements*. This terminology is similar to that of Cann *et al.* (1979). The distinction of less- and more-hygromagmatophile elements suggested by Wood *et al.* (1979) is not made.

In the following sections, variations and consequent petrogenetic implications from the major/compatible trace element, incompatible and hygromagmatophile element groups are described and discussed. This approach has been used to identify the various processes that together produced the spectrum of lavas and dykes on Macquarie Island.

6.3.2 Major element and compatible trace element variations

Both the lavas and dykes exhibit a wide chemical range which correlates with the petrographic variations from alkaline to tholeiite and aphyric to coarsely porphyritic described earlier (Chapter 4). Mean results suggest that the lavas are slightly enriched in Al_2O_3 and K_2O, and depleted in FeO_T relative to the dykes, although the high standard deviations indicate a large overlap and prevent firm conclusions being drawn. The mean composition of the combined lava and dyke data sets is similar to the average MORB composition of Cann (1971), although the Macquarie Island mean is higher in Al_2O_3, K_2O and P_2O_5, and lower in FeO_T (Table 6.5).

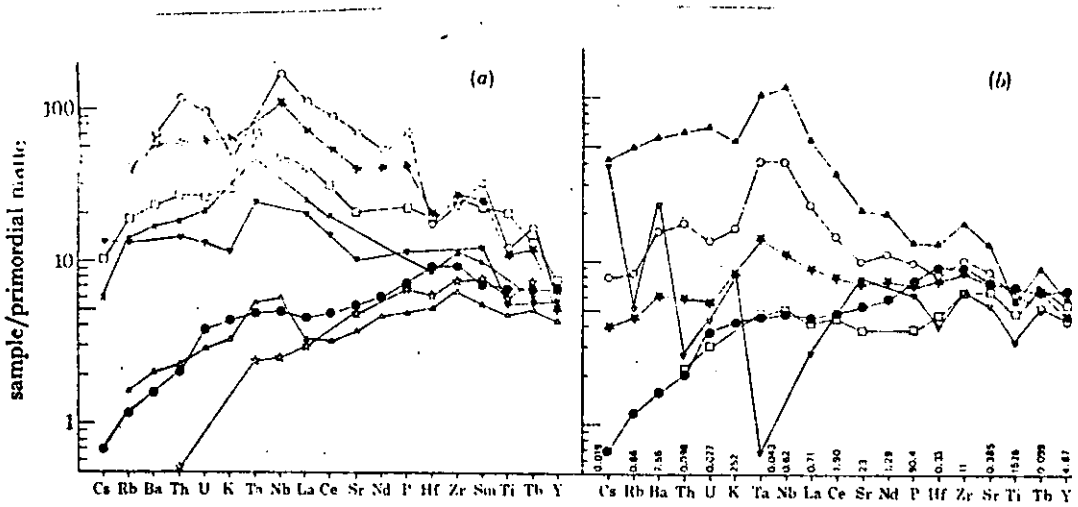

Hyg. element abundances in selected basic lavas normalized to a primordial mantle composition (micrograms per gram) which is given along the abscissa in (*b*). (*a*) Open circles are melilitite 2927 and closed stars are basanite 2679, both from southeastern Australia (Frey *et al.* 1978); open squares, crosses and inverted closed triangles are alkali basalts ISL79, T-2 and Ch50 from Eldgjá (Iceland), Terceira (Azores) and Erta Ale (Afar; Treuil & Joron 1975), respectively; open triangles and stars are representative m.o.r.b. from 63° N and 25° N in the North Atlantic ocean, respectively (Wood *et al.* 1979*a*; Joron *et al.* 1978); closed circles are average N-type m.o.r.b. (*b*) Closed triangles and open circles are E-type m.o.r.b. from 45° N and 36° N M.A.R. respectively; closed stars are tholeiite ISL28 from Askja (Iceland); open squares are N-type m.o.r.b. from the Iceland–Faeroes ridge (Wood *et al.* 1979*b*). Open inverted triangles are island arc tholeiite from Oshima, Japan (Joron & Treuil 1977).

Figure 6.6 From Tarney *et al.* (1980).

Table 6.5

Macquarie Island Lavas and Dykes:
Major Element Data Summary

MEANS AND STANDARD DEVIATIONS

	Lavas (68)	Dykes (29)	Combined	O.F.B.[1]
SiO_2	49.53 ± 1.10	49.96 ± 1.29	49.66 ± 1.17	49.61 ± 0.72
TiO_2	1.36 ± 0.37	1.41 ± 0.41	1.38 ± 0.38	1.43 ± 0.29
Al_2O_3	17.95 ± 1.90	16.58 ± 1.85	17.54 ± 1.98	16.01 ± 0.85
FeO	7.78 ± 1.31	8.60 ± 1.74	8.02 ± 1.49	11.49 ± 1.27
MgO	7.68 ± 0.99	8.08 ± 1.52	7.80 ± 1.18	7.84 ± 0.90
MnO	0.15 ± 0.03	0.16 ± 0.04	0.15 ± 0.03	0.18 ± 0.04
CaO	11.27 ± 1.18	11.42 ± 1.03	11.31 ± 1.13	11.32 ± 0.64
Na_2O	3.18 ± 0.52	3.07 ± 0.67	3.13 ± 0.57	2.76 ± 0.25
K_2O	0.68 ± 0.41	0.38 ± 0.34	0.59 ± 0.41	0.22 ± 0.12
P_2O_5	0.26 ± 0.12	0.23 ± 0.14	0.25 ± 0.12	0.14 ± 0.07

RANGES

	Lavas	Dykes
SiO_2	46.35-52.95	46.92-52.25
TiO_2	0.61- 3.04	0.61- 2.61
Al_2O_3	14.22-23.33	14.22-21.80
FeO	5.33-10.79	4.44-11.76
MgO	6.19-11.17	6.43-14.14
MnO	0.09- 0.22	0.06- 0.20
CaO	7.77-13.17	9.54-13.62
Na_2O	0.10- 1.60	0.08- 1.23
P_2O_5	0.06- 0.95	0.07- 0.82

[1] Cann (1971).

The range in CIPW normative compositions from ol- to hy-bearing to mildly ne-bearing and rarely Q-bearing has been briefly discussed in the previous section. It is important to reiterate here that this range correlates with the petrography of the samples *and* that the analyzed fresh volcanic glasses span almost the entire compositional range of the crystalline samples (Figure 6.3). The distinction between the lavas and dykes noted in their mean compositions is clearer on the normative ol-hy-di-Q diagram. The dykes tend to be less rich in ne and di than the lavas and include the few Q-normative rocks. This overall normative range and the scarcity of Q-normative varieties is generally recognized to be characteristic of ocean-floor basalts (Kay *et al.*, 1970; Cann, 1971; Thompson *et al.*, 1972; Bryan & Moore, 1977; Wood *et al.*, 1979a,b).

A further comparison with MORB chemistry is presented using an AFM diagram in Figure 6.7. Firstly, it can be noted that the dykes occupy a field nearer to the F-apex of the diagram than the lavas, although a considerable overlap is present between the two groups. Secondly, the Macquarie Island data are directly comparable to IPOD leg 49 basalts from 45°N on the Mid-Atlantic Ridge (Wood *et al.*, 1979a), although with slightly higher Mg/Mg+Fe ratios.

The Mg/Mg+Fe ratios of the lavas and dykes cover a wide range, from 0.51 to 0.72. Dykes dominate the lower end of the range (<0.54) and basalts the higher end (>0.69), with the exception of one dyke (Figure 6.5). This unusual dyke (38471) has a Mg/Mg+Fe ratio of 0.75; its MgO content of 14.74 wt.%, and Cr content (690 ppm) could be due to accumulation of olivine and Cr-spinel.

Major element abundances are plotted against the Mg/Mg+Fe ratio in Figure 6.7, allowing visualization of the statistical results given earlier. K_2O and P_2O_5 show no correlation. Na_2O, MnO, FeO, TiO_2 and SiO_2 show a negative covariance with the Mg/Mg+Fe ratio and MgO and Al_2O_3 positive covariance. The plots of SiO_2 and Al_2O_3 with the Mg/Mg+Fe ratio show a considerable scatter.

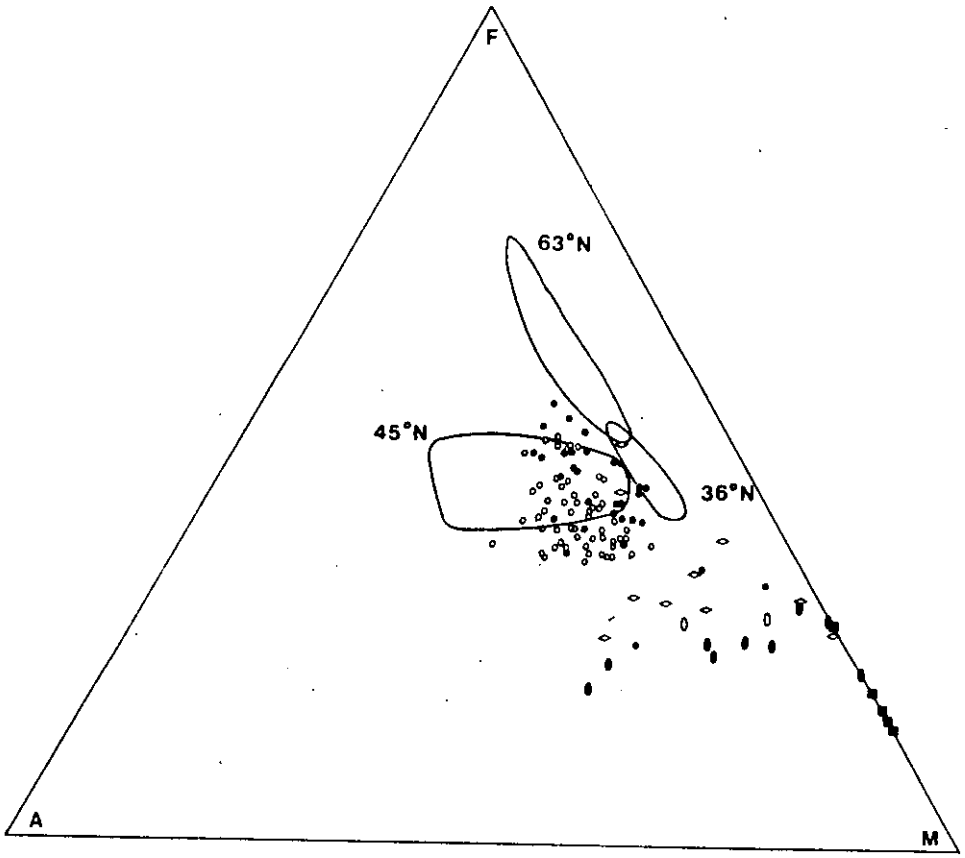

Figure 6.7 AFM diagram for Macquarie Island basalts (open circles), dolerites (filled circles), layered gabbros and wehrlites (filled ellipses, harzburgites (filled squares). Massive gabbros are shown by open rhombs except for those east of Handspike Point and above the layered rocks in the section, which are shown as open ellipses. Also outlined are fields of IPOP Leg 49 basalts from the Mid-Atlantic Ridge (Wood *et al.*, 1979a).

The range in Mg/Mg+Fe is ascribed principally to olivine control, presumably through shallow level fractionation. This is supported by the petrography of the samples (Chapter 4), and the covariance of Mg/Mg+Fe ratios and Ni abundances. Major fractionation of clinopyroxene is unlikely because of its rarity as a phenocryst phase, although resorption may have reduced its abundance to some extent. Also, CaO does not show a significant depletion with decreasing Mg/Mg+Fe, as would be expected with significant clinopyroxene fractionation. It could be argued that plagioclase accumulation would buffer this latter effect; however, Al_2O_3 decreases with the Mg/Mg+Fe ratio, particularly at lower Mg/Mg+Fe values.

At higher Mg/Mg+Fe values Al_2O_3 contents of the dykes maintain the positive correlation but many lavas show a scatter above the main trend (Figure 6.8). The Al_2O_3 enrichment in these samples is coincident with low SiO_2, and high CaO values; indicative of plagioclase accumulation.

The covariance of Cr with the Mg/Mg+Fe values may reflect either clinopyroxene or Cr-spinel fractionation. Evidence against the former mechanism has been discussed. Petrographically it has been observed that minor Cr-spinel is commonly included in olivine phenocrysts: spinel fractionation could account for the observed Cr variation, but is difficult to quantify.

The major element and compatible trace element variations are in accord with fractionation of olivine, Cr-spinel and plagioclase, and possibly minor clinopyroxene. This corroborates observations on the petrography of the samples. Significant field evidence favouring such fractionation is the presence of cumulate gabbros with suitable mineralogies on Macquarie Island. This is discussed more fully in Griffin & Varne (1980) (Appendix 8), where it is shown that phase compositions in the cumulate bodies are comparable to those of the phenocrysts in the lavas and dykes and furthermore that the cumulate gabbros exhibit major

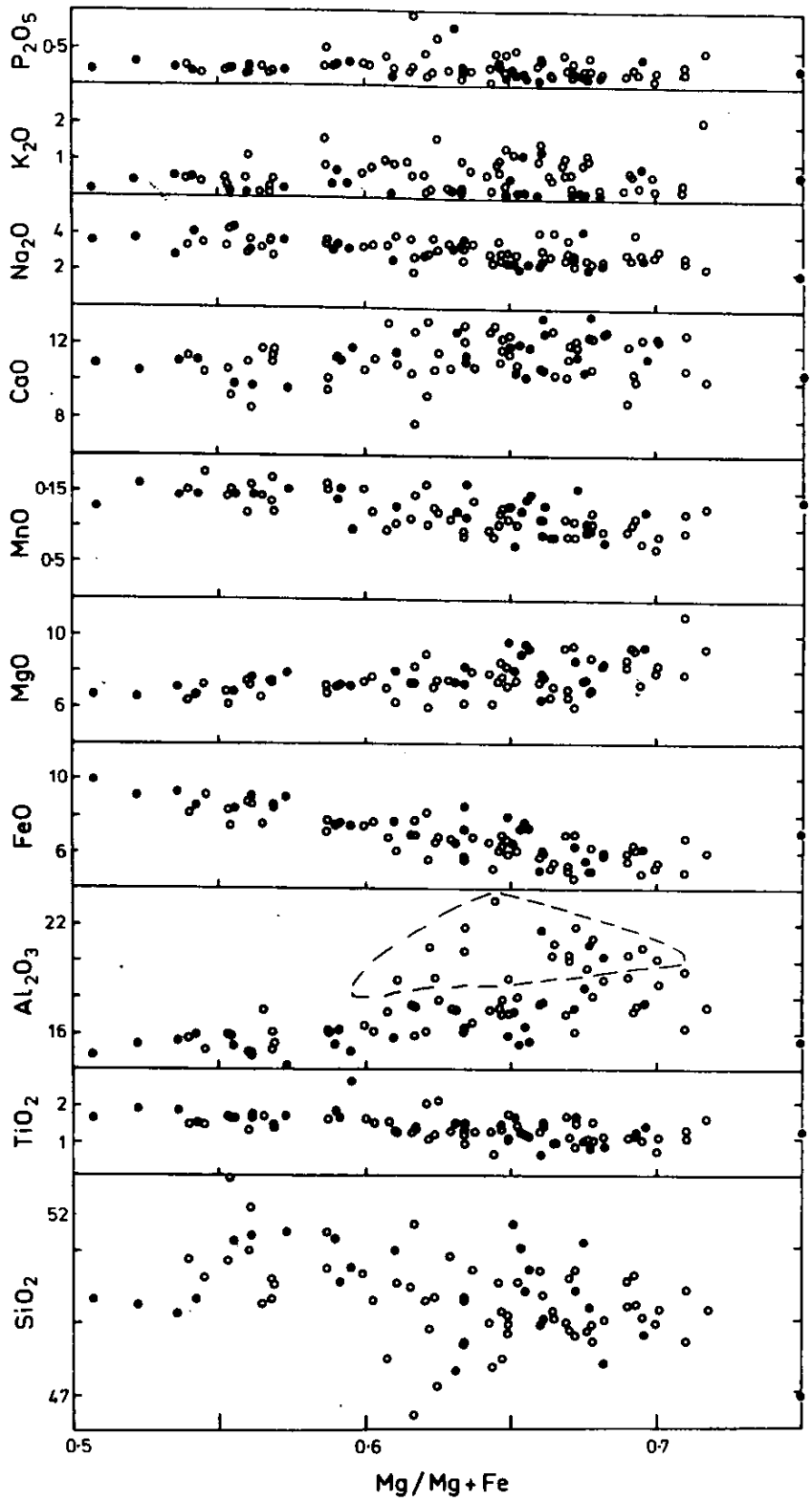

Figure 6.8 Plot of major elements (analyses recalculated volatile free) against Mg/Mg+Fe for lavas (o) and dykes (•). The field marked on the Al_2O_3 against Mg/Mg+Fe plot encloses possible plagioclase cumulates.

element geochemical variations commensurate with olivine and plagioclase fractionation from the lavas (Griffin & Varne, 1980; Figures 6.12 and 6.13).

6.3.3 Major element composition modelling and constraints on petrogenesis

Preliminary attempts have been made to model the geochemical variations more closely. Several criteria have been used to identify primitive compositions. Firstly they should have high Mg/Mg+Fe ratios. Green *et al.* (1978) noted that, using $K_{D_{ol/lq}}^{Fe/Mg} = 0.3$ (Roedder & Emslie, 1970), primitive basaltic magmas derived from source peridotite, with mineralogies similar to refractory dunites and harzburgites in ophiolite complexes, must have $Mg/Mg+Fe^{2+} = 0.68\text{-}0.75$ for up to about 30% partial melting. This range is applicable to Macquarie Island rocks where harzburgites have Mg/Mg+Fe ~ 0.89. Secondly, such liquids should have high Cr and Ni abundances, as these elements are rapidly depleted by high pressure phase fractionation. Limiting values for Cr and Ni in these lavas and dykes are 500-600 ppm and ~200 ppm respectively, comparable to primitive MORB (Green *et al.*, 1979).

Four samples meeting these criteria are presented in Table 6.6. As a basis for modelling, sample 38188 has been chosen from the four identified primitive compositions, due to its relatively low Al_2O_3 content, high CaO/Al_2O_3 and low CaO/Na_2O. These ratios would be lowered and raised, respectively by plagioclase fractionation, which would leave Mg/Mg+Fe, Ni and Cr little affected.

Mixing calculations using sample 38188 and the mineral phases olivine, clinopyroxene, plagioclase and orthopyroxene have been performed on a number of samples. The method used was that of Wright & Doherty (1971). These clinopyroxene and plagioclase compositions represent the most magnesian and calcic analyses respectively present in both lava and dyke samples and cumulate gabbros (see Griffin & Varne, 1980, for mineral compositions

Table 6.6

POSSIBLE PRIMARY LIQUIDS

Sample no.	220	234	236	38188
Type	dyke	lava	lava	lava
SiO_2	47.83	50.23	48.89	48.42
TiO_2	0.80	1.10	0.70	1.29
Al_2O_3	20.31	17.32	20.14	16.40
Fe_2O_3	1.17	1.25	1.02	1.36
FeO	5.95	6.40	5.21	6.93
MnO	0.10	0.13	0.09	0.15
MgO	8.41	9.45	7.99	11.17
CaO	12.82	10.46	12.36	10.71
Na_2O	2.40	2.79	2.90	2.89
K_2O	0.09	0.66	0.60	0.39
P_2O_5	0.12	0.21	0.09	0.28
Mg/Mg+Fe	0.716	0.725	0.732	0.742
Ni	207	158	164	199
Cr	523	652	663	514
ne	-	-	2.30	0.39
hy	0.34	8.99	-	-
ol	16.07	12.29	14.19	21.29
Zr/Nb	5.8	4.3	9.0	2.8
CaO/Al_2O_3	0.631	0.604	0.614	0.653
Al_2O_3/CaO	1.58	1.66	1.63	1.53
Zr	46	69	27	84
Y	18	28	11	27
Nb	8	16	3	30
Rb	0	16	3	7
Sr	171	219	322	232
Co	-			
Sc	-			
Zr/Y	2.56	2.46	2.45	3.11
$Ti/Yx10^2$	2.67	2.36	3.82	2.85
CaO/Na_2O	5.34	3.75	4.26	3.71

Table 6.7A

RARE EARTH ELEMENT ABUNDANCES IN MACQUARIE ISLAND LAVAS AND DYKES

Sample no.	3A	43B/B	43B/A	108C	108E	56A	56D	56G	56I	151	157	38331	64D	38133	38137	38206
Rock Type	P	P-C	P-E	P-C	P-E	ML-E	ML	ML	ML-M	P	P	P	D	D	D	D
La	39.2	15.3	15.1	8.04	8.27	9.55	9.63	10.3	9.88	11.9	14.3	30.6	58.1	14.8	7.32	5.06
Ce	75.5	31.1	34.1	17.1	17.6	20.7	18.9	25.2	20.1	17.7	25.5	57.2	113.1	34.8	16.6	13.7
Nd	29.9	18.1	18.3	11.9	13.7	12.7	11.7	12.3	12.1	15.5	13.4	21.1	38.0	18.8	8.82	9.60
Sm	6.21	4.68	4.75	3.52	3.92	3.26	2.95	3.18	3.47	3.81	3.05	4.69	6.60	4.79	2.75	3.20
Eu	1.94	1.53	1.51	1.22	1.20	1.01	1.00	1.05	1.04	1.28	0.98	1.47	2.00	1.53	0.88	1.09
Tb	1.03	1.01	1.00	0.77	0.78	0.61	0.60	0.61	0.59	0.80	0.57	0.84	1.12	1.07	0.55	0.69
Tm	-	-	0.52	0.42	0.38	0.32	0.28	0.34	-	0.42	0.24	-	-	0.50	0.27	0.37
Yb	2.42	3.23	3.28	2.79	2.74	2.01	1.79	1.95	2.05	2.65	1.67	2.58	2.62	3.11	1.81	2.70
Lu	0.38	0.47	0.48	0.43	0.43	0.31	0.28	0.32	0.29	0.42	0.27	0.35	0.40	0.46	0.29	0.43
Eu/Eu*	1.0	0.9	0.9	1.0	0.9	0.9	1.0	1.0	0.9	1.0	1.0	1.0	1.0	0.9	0.9	1.0
(La/Sm)e.f.	3.46	1.79	1.74	1.26	1.16	1.60	1.79	1.78	0.56	1.71	2.56	3.58	4.82	1.70	1.46	0.86
La/Sm	6.31	3.27	3.18	2.28	2.11	2.93	3.26	3.24	2.85	3.12	4.69	6.52	8.80	3.09	2.66	1.58

Rock type key: P = pillow; E = edge; C = core; ML = massive lava; D = dyke; M = middle.

Table 6.7B

LITERATURE REE ANALYSES OF MACQUARIE ISLAND LAVAS AND BCR STANDARD ANALYSIS.

Reference	1	1	2	2	3		4
Sample No.	279-12-1	279-3-2	26	48	BCR	Precision	BCR
Rock Type	P	P	P	P			
La	8.0	8.2	4.2	5.3	28.0	±5%	26.0
Ce	20.8	20.4	9.1	6.7	52.0	±10%	53.9
Nd	12.6	11.0	7.3	9.1	32.8	±5%	29.0
Sm	3.6	3.6	2.7	2.8	7.72	±5%	6.6
Eu	1.33	1.26	1.0	0.95	2.05	±5%	1.94
Tb	0.84	0.82	0.48	0.45	1.34	±5%	1.0
Tm	0.48	0.35	0.4	0.26	0.60	±10%	0.6
Yb	2.7	2.8	2.7	2.3	3.37	±5%	3.36
Lu	0.36	0.38	-	0	0.52	±5%	0.55
Eu/Eu*	1.0	1.0	1.2	1.1			
(La/Sm)e.f.	0.54	1.61	0.85	1.04			
La/Sm	2.22	2.28	1.56	1.89			

References:
1 - Schilling & Ridley (1975)
2 - Jakes & Gill (1970)
3 - Hellman *et al.* (1978)
4 - Flanagan (1973).

in the gabbroic rocks). The olivine composition at $Fo_{0.91}$, is slightly more magnesian than the most magnesian composition recorded in the lavas and dolerites ($Fo_{89.5}$) but only a few analyses were obtained as olivine is generally altered in these rocks. The orthopyroxene analysis is from one of the gabbroic samples. It was not initially included in the mixing calculations, because of its absence as a phenocryst phase, but was found to be necessary for accurate results to be achieved.

The results of the mixing calculations are presented in Table 6.8. The matched compositions cover the ranges of normative compositions and Mg/Mg+Fe ratios of the analyzed lavas and dykes. The importance of plagioclase and, to a lesser extent, olivine fractionation is emphasized by these results.

In the extreme of the tested compositions, sample 38337 represents 60% of one weight unit of primary liquid (38188 composition) with ~21% plagioclase fractionation together with ~7% olivine, 9.5% orthopyroxene and 2% clinopyroxene fractionation. Major plagioclase accumulation is also suggested for four of the matched compositions. The results imply that orthopyroxene and clinopyroxene could also have been involved, either through fractionation or accumulation, during the evolution of the liquids. A final feature is that the tested liquid compositions would only be expected to vary by a factor of 2 in their incompatible element abundances if they were derived from a primitive magma with constant incompatible element abundances and did not undergo open-system fractionation of the style suggested by O'Hara (1977).

It is important to emphasize that these mixing calculations only provide rough guidlines to the evolution process. Using a set of fixed phase compositions is a major simplification of the natural process, as evidenced by the observed range in phenocryst composition and experimental studies of primitive ocean-floor basalt compositions which have shown that the liquidus phase compositions are strongly influenced

Table 6.8

Mixing calculations: Macquarie Island lavas and dykes

	35	64Dy	124	38389	212	56A	38337
Ne	7.79	6.92	6.92	4.29	0.15	0.09	
Hyp							0.98
Mg/Mg+Fe	60.8	63.1	54.2	64.7	64.4	69.0	50.7
Ol	4.64	4.46	8.79	1.65	1.43	10.10	7.20
Cpx	-7.04	-6.09	1.51	-4.33	4.25	-1.87	1.95
Plag	3.08	0.14	15.05	1.75	-38.24	-17.03	20.97
Opx	11.58	9.37	5.73	9.83	5.47	-9.64	9.50
Liq	88.45	93.43	68.64	91.28	126.07	118.33	59.86
Σres	0.311	0.660	0.078	0.051	0.438	0.248	0.412
Ol					-1.25	-8.68	
Cpx					-3.25	1.65	
Plag					30.6	14.60	
Opx					-3.93	8.39	
38188					78.48	84.00	
Σres					0.272	0.176	

	210	38451	147	38425	38434	151	38449
Ne							
Hyp	1.05	4.64	10.80	12.96	14.61	16.94	22.0
Mg/Mg+Fe	54.5	66.0	56.1	59.0	62.1	67.2	65.3
Ol	9.70	8.82	18.47	17.07	8.36	23.10	12.45
Cpx	2.71	-4.64	7.64	-2.44	7.40	2.66	-7.94
Plag	17.87	-36.53	18.26	12.00	11.64	-43.27	7.25
Opx	3.15	-3.42	-13.08	-8.38	-3.15	-29.58	-6.42
Liq	65.86	134.70	68.70	81.56	75.73	146.82	93.42
Σres	0.244	0.372	0.168	0.065	0.342	0.010	0.792
Ol		-6.64				-15.74	
Cpx		3.54				-1.81	
Plag		27.40				29.48	
Opx		2.86				20.16	
38188		73.57				68.10	
Σres		0.203				0.005	

by P, T, P_{O_2} and P_{CO_2} (Green & Lieberman, 1976; Green *et al.*, 1979; Jaques & Green, 1980).

6.3.4 Major element petrogenesis

The petrographic features, geochemical variations and the results of modelling calculations are strong evidence for the derivation of the observed spectrum of lavas and dolerites on Macquarie Island through crystal fractionation processes dominated by plagioclase and olivine; but also involving clinopyroxene. The presence of complementary gabbroic rocks on the island further suggests that much of the liquid evolution was through shallow-level fractionation processes (Griffin & Varne, 1980).

There is growing experimental evidence for a picritic primary magma for ocean-floor basalts (Green *et al.*, 1979; Jaques & Green, 1980), in support of earlier ideas along this line (O'Hara, 1968) and evidence from ophiolites (Elthon, 1979). Green *et al.* (1979) have shown that picritic magma formed by segregation from orthopyroxene-bearing peridotites at about 70 km depth will evolve to primitive magnesian MORB compositions through fractionation of 15-17% olivine. Subsequent work indicates that this process requires 20-30% partial melting and that lower degrees (<18%) will produce alkaline liquids (Jaques & Green, 1980). Alternatively orthopyroxene and olivine fractionation from a slowly ascending tholeiitic picritic primary magma, in the pressure range 20-15 kb, could produce a primitive alkali olivine basaltic liquid (Malpas, 1978).

Although Malpas' mechanism satisfactorily accounts for the major and compatible trace element abundances of mid-ocean ridge basalts and the Macquarie Island lavas and dykes, major objections have been raised. Specifically, Green *et al.* (1979) found that plagioclase of An_{89} was the most calcic composition present under one-atmosphere conditions on the liquidus for the primitive DSDP3-18 glass. From this and the lack of

orthopyroxene on the liquidus they concluded that the primitive magmas were not parental to the calcic plagioclase and also the magnesian clinopyroxene (of Mg/Mg+Fe = 0.92) megacrysts of mid-ocean ridge basalts and cumulate phases of ophiolite complex layered rocks. It has been found experimentally that phases of these compositions can fractionate from second-stage melting of diapirs at depths of 1-15 km (Duncan & Green, 1980).

Bender *et al.* (1978) have studied one atmosphere liquidus phase compositions of a similar primitive mid-ocean ridge basalt glass (no. 527-1-1) and reported liquidus plagioclase compositions up to An_{89}. The apparent discrepancy would seem to be a result of temperature dependence of the plagioclase composition. $An_{78.6}$ plagioclase observed by Green *et al.* (1979) was obtained at 1210°C whereas Bender *et al.* (1978) found compositions of An_{89}, An_{81}, $An_{79.6}$ and $An_{80.0}$ at temperatures of 1235°C, 1218°C, 1215°C, 1208°C and 1205°C respectively. Thus there is only a discrepancy of ~1 An unit between the result, at similar temperatures, which must be considered to be a good agreement in view of the slightly different starting compositions, experimental and analytical techniques used.

In summary, the Macquarie Island lavas and dykes have major and compatible trace element compositions that can be explained through a mechanism of extensive shallow level crystal fractionation, dominated by plagioclase and to lesser extents olivine, clinopyroxene and spinel, from primitive liquids that in turn are a result of extensive fractionation from primary picritic magmas. The range of primary magmas present probably resulted from variations in degree of partial melting of the source or, through an initially slowly ascending magma fractionating orthopyroxene in addition to olivine.

Relevant experimental studies indicate 10-30% partial melting of the source mantle is required to produce the variation in primary

liquids and a consequent fractionation of about 20% olivine to attain the primitive liquid composition. Subsequently shallow-level fractionation or accumulation events are constrained by the mixing calculations to maximum of about 40 wt.% although this is an over-estimate as these calculations probably include some contribution from earlier processes. Using extreme cases this would suggest a range of extremely incompatible elements in the lavas and dykes of ~3x to ~10x source mantle abundances. For primitive lavas (those not having undergone shallow-level fractionation) the range would be ~4x to ~12x mantle source abundances, for a constant mantle source.

6.3.5 Incompatible and hygromagmatophile trace element variations and characterization of the volcanic rocks

Incompatible and hygromagmatophile elements can provide vital information on the nature of basalt mantle sources. Element ratios are of particular importance as these are not significantly affected by fractionation of the major basaltic phases whereas the abundances are modified. A major use of such elements has been the characterization of altered rocks, as many of these elements are immobile up to moderate grades of metamorphism. This is discussed in the following section which is drawn principally from Griffin & Varne (1980).

Ranges and mean values for low abundance elements analyzed in the lavas and dolerites are presented in Table 6.9. Apart from Sr, the mean results are comparable to depleted ocean-floor basalts. Observed ranges (Table 6.9) are also similar.

The best comparison of the incompatible trace element chemistry of the Macquarie Island lavas and dykes with ocean-floor basalts is through the use of the various discriminant functions. They have been used to characterize altered and metamorphosed basalts, and assign them to particular tectonic environments (e.g. Pearce & Cann, 1971, 1973; Bloxam & Lewis, 1972). This also allows a testing of the usefulness of

Table 6.9

Macquarie Island Lavas and Dykes:
Trace Element Data Summary

MEANS AND STANDARD DEVIATIONS

	Lavas	Dykes	Combined	O.F.B.*
Ti	8160 ± 2220	8460 ± 2460	8280 ± 2280	9000
Ni	110 ± 50	102 ± 51	107 ± 50	114
Cr	302 ± 119	288 ± 155	297 ± 132	300
Zr	88 ± 29	94 ± 31	90 ± 30	90
Y	27 ± 8	27 ± 10	27 ± 9	30
Nb	22 ± 16	18 ± 16	21 ± 15	25
Rb	11 ± 8	7 ± 9	10 ± 8	-
Sr	258 ± 118	228 ± 99	247 ± 112	145
Co	38 ± 5	43 ± 8	40 ± 8	32
Sc	36 ± 4			40

* from Pearce (1981)

RANGES

	Lavas	Dykes	O.F.B.
Ti	3660 - 18240	3660 - 15660	
Ni	52 - 302	42 - 273	58- 320
Cr	103 - 663	63 - 690	30-1260
Zr	32 - 163	33 - 149	28- 178
Y	11 - 45	9 - 53	16- 57
Nb	1 - 73	2 - 52	
Rb	0 - 35	0 - 32	
Sr	114 - 806	112 - 548	
Co	30 - 49	26 - 52	
Sc	29 - 42		

these discriminant functions; Macquarie Island being the sole ophiolite composed of young oceanic crust.

On the Ti-Zr diagram of Pearce & Cann (1973) the Macquarie Island data fall mainly within the ocean-floor basalt field (OFB) with some data points in the OFB-low K tholiite field (LKT), where overlap occurs with the low-K tholeiites if island arcs (Figure 6.9). On their Ti-Zr-Y diagram (Figure 6.10) the majority of the Macquarie Island data falls within the OFB field but some data points occur in the "within-plate" basalt field (WPB) defined by ocean island or continental basalts. On their Ti-Zr-Sr diagram (Figure 6.11), the Macquarie Island data points define a band from the OFB field into the LKT field.

These discriminant diagrams, using Ti, Zr, Y and Sr, classify most of the Macquarie Island rocks as ocean-floor basalts, but the remainder are unlike typical ocean-floor basalts (Varne & Rubenach, 1972). Similarly ambiguous results are achieved using the Zr-Zr/Y diagram (Figure 6.12) of Pearce & Norry (1979). On the Ti-Cr diagram developed by Pearce (1975) to discriminate between ocean-floor basalts and island-arc tholeiites, the Macquarie Island rocks with Ti abundances generally greater than 5000 ppm and ranging up to 15 000 ppm (Figure 6.10), and Cr abundances generally greater than 100 ppm and ranging up to 600 ppm (Figure 6.5), would fall within the OFB field.

The Macquarie Island rocks that fall within the OFB fields on the various discriminant diagrams tend to have relatively high Ti/Zr ratios, Na(Na+K) > 0.9, K/Rb > 360, and relatively low K_2O and Nb abundances. They resemble the "depleted" oceanic tholeiites of Engel *et al.* (1965) and the Group-I ocean-floor basalts of Bryan *et al.* (1976). The samples that plot outside the OFB fields tend to have relatively high Nb contents and low Zr/Nb, Y/Nb, Ti/Zr and K/Rb ratios, to be relatively enriched in K and Sr, and to be ne-normative. These rocks resemble volcanics from the so-called "anomalous" ridge segments, e.g. the FAMOUS area (near 36°N on the Mid-Atlantic Ridge).

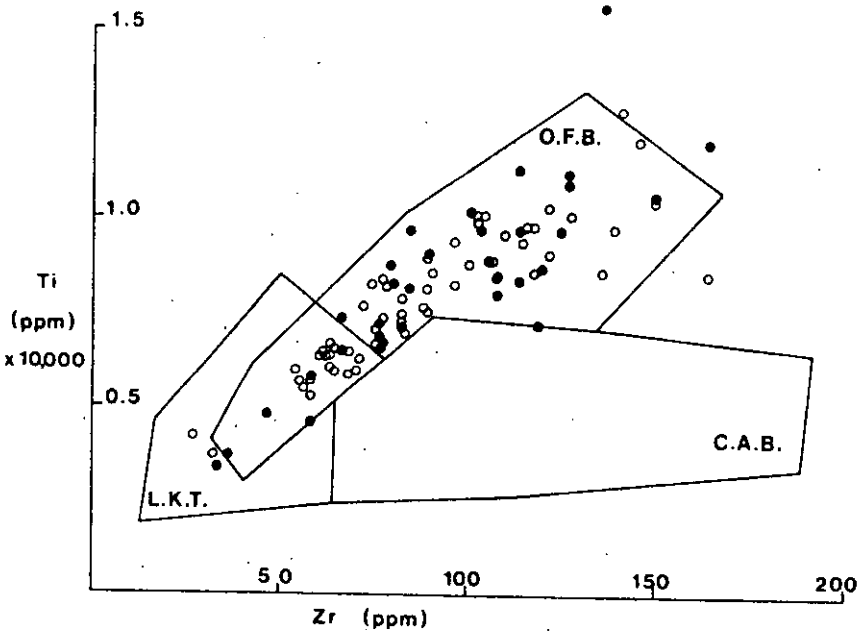

Figure 6.9 Ti and Zr contents of Macquarie Island basalts (open circles) and dolerites (closed circles) plotted on a basalt classification and discrimination diagram of Pearce & Cann (1973). Ocean-floor basalts plot in the O.F.B. field, and in the field that overlaps into the low-potassium tholeiite (L.K.T.) field. Calc-alkali basalts also plot in this overlapping field and in the C.A.B. field.

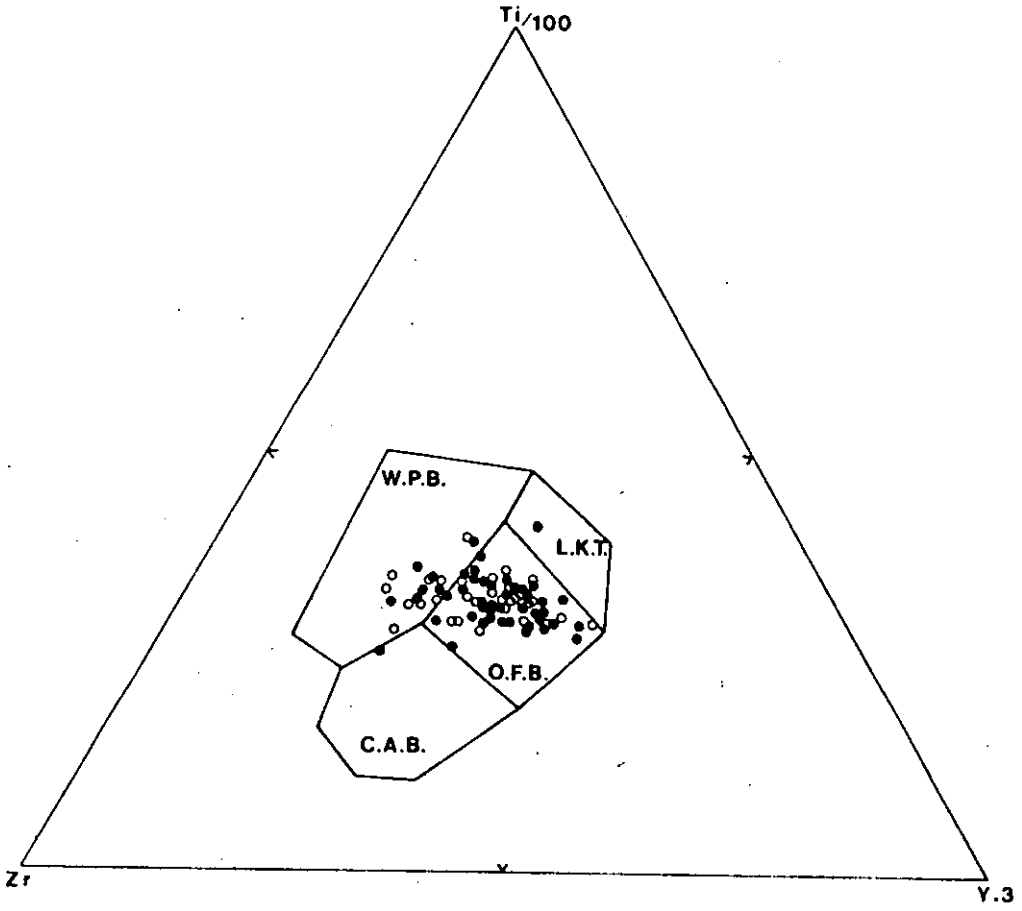

Figure 6.10 Ti, Zr, and Y contents of Macquarie Island basalts (open circles) and dolerites (filled circles) in a discrimination triangle of Pearce & Cann (1973). Fields as in Fig. 6.9 , with the addition of a "within-plate" basalt field (W.P.B.).

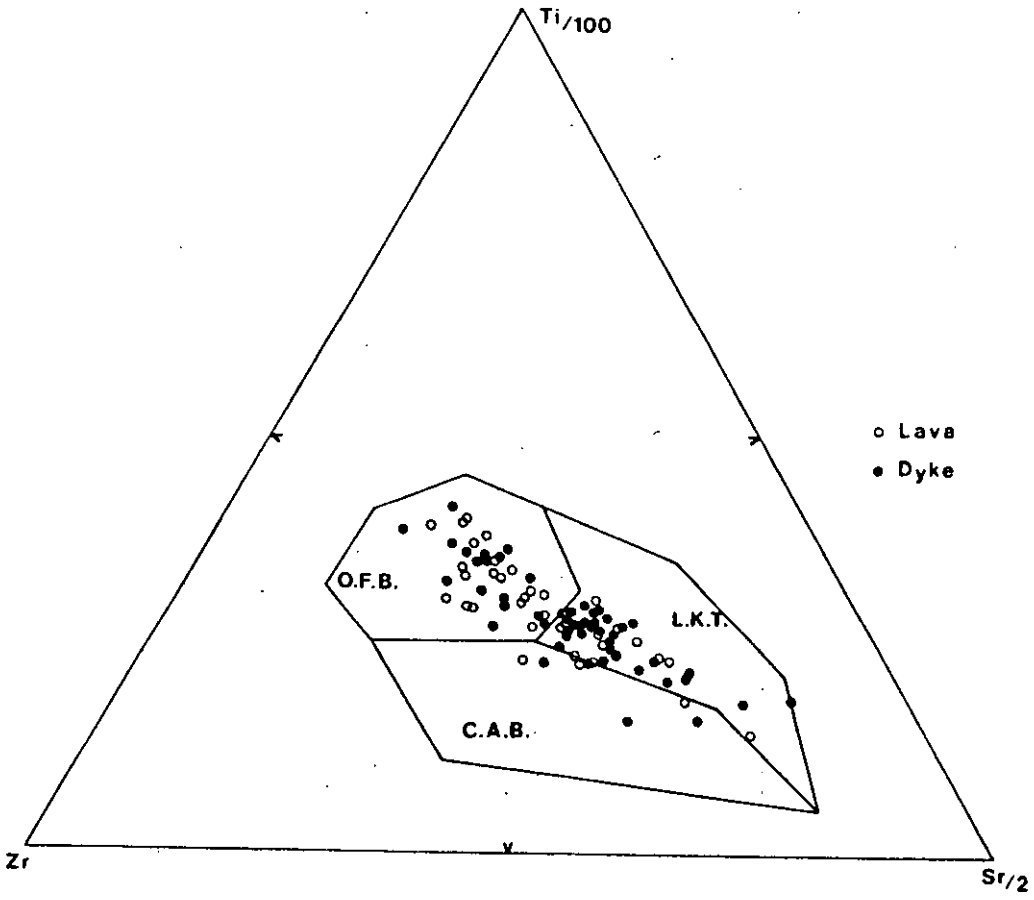

Figure 6.11 Ti, Zr, and Sr contents of Macquarie Island basalts (filled circles) and dolerites (open circles) in a discrimination triangle of Pearce & Cann, 1973). Fields as in Fig. 6.9.

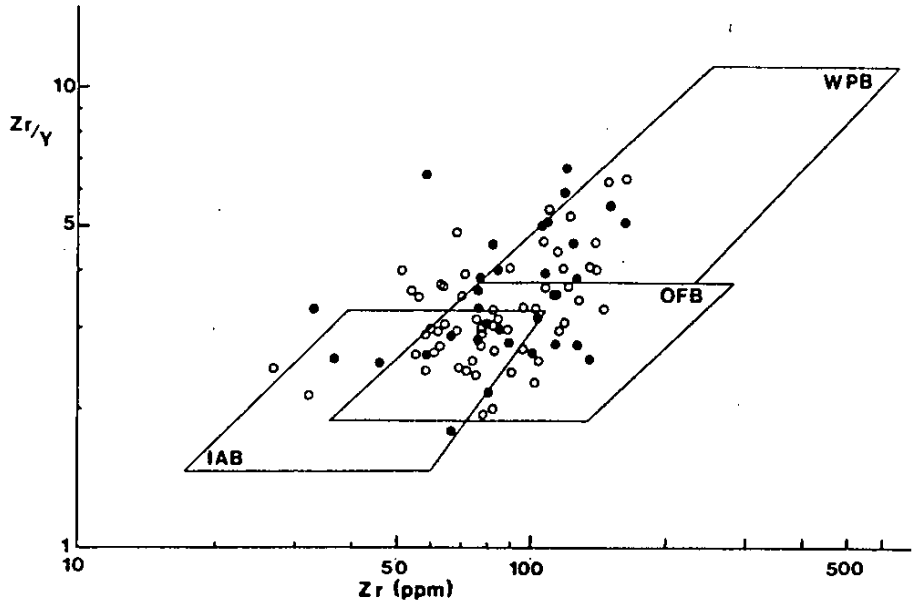

Figure 6.13 Zr and Y contents of Macquarie Island basalts and dolerites plotted on the Zr-Zr/Y diagram of Pearce & Norry (1979). Fields as in Fig. 6.9 and Fig. 6.10.

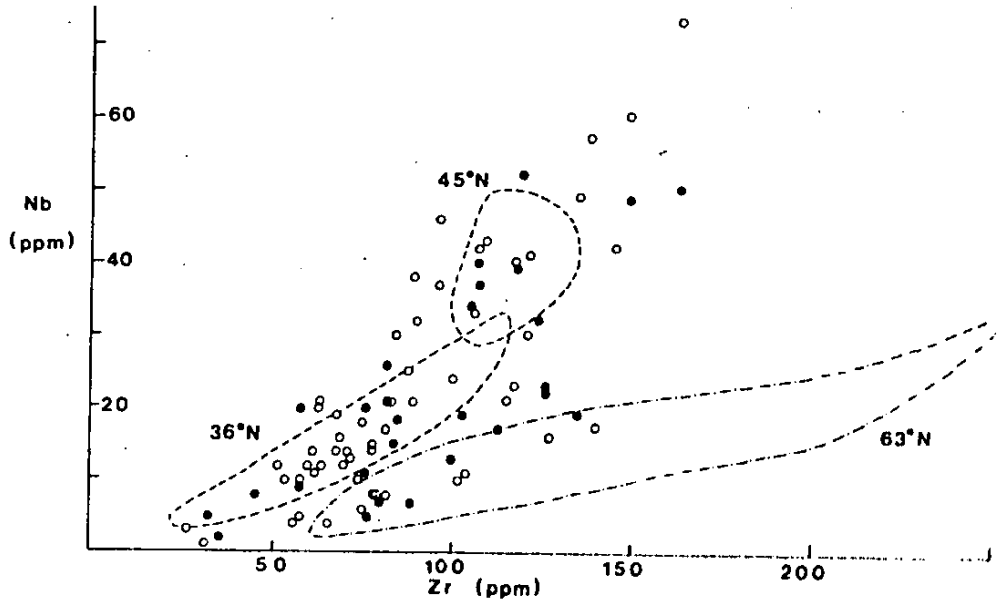

Figure 6.12 Zr and Nb contents of Macquarie Island basalts and dolerites. Also outlined are fields for IPOD Leg 49 basalts from the Mid-Atlantic Ridge (Wood *et al.*, 1979a)

The "non-OFB" data do not form a group distinct from the OFB data. This continuum in compositions is well shown in a Zr/Nb diagram (Figure 6.13). Rocks from near 36°N and 45°N on the Mid-Atlantic Ridge have Zr/Nb ratios in the range 3 to 7, and Nb contents generally higher than those of rocks from near 63°N where Zr/Nb ratios range from approximately 7 up to high values of 18 or more that were formerly considered to be diagnostic of ocean-floor basalts (Pearce & Cann, 1973; Erlank & Kable, 1976). Most of the Macquarie Island rocks plot in the same fields as 36°N and 45°N rocks, but range more widely when considered as a group (Figure 6.13).

REE analyses of samples covering this range in trace element abundances are presented in Table 6.10. These have been grouped by profile on a Masdua-Coryell plot in Figure 6.14 and demonstrate the correlation of the LREE with other hygromagmatophile element ratios, re-emphasize the continuous nature of the trace element variations, and further the correlation of Macquarie Island volcanics with those from "anomalous" ridge segments (cf. Langmuir *et al.*, 1977).

An important result arising from this grouping of the samples is an apparent relationship to the degree of metamorphism of the samples. Samples which have undergone metamorphism up to and including zeolite facies alteration are characterized by high La/Sm and La/Yb ratios whereas those of greenschist facies metamorphic grade have markedly lower values for these ratios (Table 6.11). Although this is in apparent agreement with studies which emphasize the susceptibility of the LREE to mobilization during metamorphism (Hellman *et al.*, 1978; Ludden & Thompson, 1979) the good positive correlations of the LREE with the other incompatible and hygromagmatophile elements are strong evidence against this interpretation. Alternatively these results suggest a *temporal evolution* of the lava and dyke compositions, assuming the least altered rocks are the youngest. This evolution is manifested by an

Table 6.10

Selected Major and Trace Element Ratios in the REE Data Subset.

Sample Number	La/Sm	Zr/Nb	Ti/Y[1]	Mg/Mg+Fe	K/Rb[2]
38206	1.58	16.5	2.0	0.61	457
108	2.19	10.1	1.99	0.56	308
38137	2.66	6.4	2.64	0.68	-
38133	3.09	5.4	2.94	0.56	270
43B	3.23	5.3	2.55	0.60	566
56	3.07	4.9	3.09	0.70	(540)[3]
151	3.12	4.3	3.85	0.67	730
157	4.69	3.0	3.59	0.67	318
38331	6.52	2.76	3.44	0.65	318
3A	6.31	2.03	4.57	0.63	316
64D	8.80	1.53	3.26	0.63	262

[1] $\times 10^{-2}$

[2] for Rb = 0

[3] for 56G: Rb = 4; 56A: Rb = 1 K/Rb = 1910

Table 6.11

La/Sm and La/Yb ratios of Macquarie Island samples grouped by grade of alteration and metamorphism.

	La/Sm	La/Yb
Ocean-floor weathering Group I	4.82-2.56	22.4-8.6
Zeolite facies Group II	1.77-1.46	5.1-4.0
Lower greenschist facies Group III	1.56-0.86	2.96-1.90

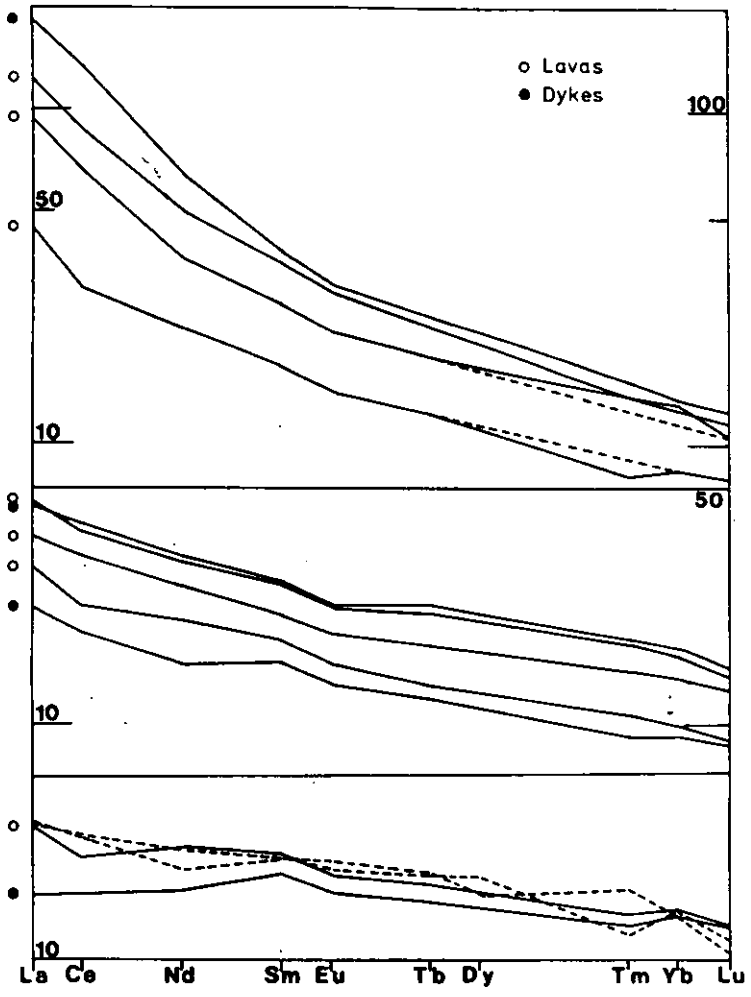

Figure 6.14 Masuda-Coryell REE plot of Macquarie Island basalts and dolerites.

enrichment of the LREE while maintaining relatively constant HREE abundances (Figure 6.14).

In summary these incompatible and hygromagmatophile trace element abundance data show that many of the analyzed Macquarie Island lavas and dykes are extremely similar to "normal" MORB. However, the unbroken trends and variations in both abundances and ratios of these elements progress beyond the "normal" range of values for MORB. Some of the samples (those enriched in these elements) would not be recognized as MORB using recognized basalt discriminant diagrams. This suggests the need for major qualifications to be imposed when using such diagrams. Possible qualifications are discussed later in this chapter.

6.3.6 Implications of incompatible and hygromagmatophile element ratios

It has been shown that the lavas and dykes include samples having wide differences in incompatible and hygromagmatophile element ratios. Specifically La/Sm and Zr/Nb ratios have ranges of 8.8 to 0.86 and 1.53 to 18.0 respectively. The subset of samples for which REE analyses are available almost completely span the range in Zr/Nb ratios of the total data set, ranging from 1.53 to 16.5, and is therefore taken to be representative of the lavas and dykes in the following discussion.

Three main mechanisms have been proposed for observed variations in these element abundances and ratios of basalt suites. Langmuir *et al.* (1977) have invoked a dynamic melting process to explain REE abundances in FAMOUS basalts. In this model a portion of melt is always retained in a zone of melting of continuously upwelling mantle. Providing the melt is on a peritectic or cotectic surface then major element compositions of this melt will be buffered but ratios and abundances of elements with small but differing liquid/solid partition coefficients may alter markedly, depending on the difference in the partition coefficients and the proportion on melt remaining in the melting zone.

Secondly, O'Hara (1977) has proposed a near-surface open-system fractional crystallization process. O'Hara (*op. cit.*) envisaged a magma chamber fed regularly by batches of parental magma in which continuous fractional crystallization occurs. Resultant steady-state liquids could have major element compositions controlled within the liquidus field of a single crystalline phase, or on a cotectic, but potentially large variation in concentrations of incompatible and hygromagmatophile element abundances and ratios. Isotopic variations are considered, in this model, to result from digestion of previously erupted basalts which have been altered through contact with sea water.

The third mechanism assumes that the element abundances and ratios primarily reflect the source mantle characteristics and conseqently variations in the basalts reflect source heterogeneity (Varet & Treuil, 1973; Erlank & Kable, 1976). The concept of a heterogeneous mantle is not new (Green, 1971; Varne & Graham, 1971) but has become established with the recent availability of numerous, precise isotopic and hygromagmatophile element abundance data. Reviews of mantle processes in light of the new geochemical data strongly favour mantle heterogeneity as the prime factor in controlling isotopic and hygromagmatophile element abundances and ratios (Hanson, 1977; Cann *et al.*, 1978; Pearce & Norry, 1979; Sun *et al.*, 1979), although processes akin to dynamic melting may still be significant (Wood, 1979, 1981).

Although isotopic data are not yet available for the Macquarie Island lavas and dykes the extreme ranges in Zr/Nb and La/Sm ratios (of 0.53 to 18 and 8.80 to 0.86) are in favour of a heterogeneous mantle source. Open-system fractional crystallization (O'Hara, 1977) is considered unlikely in view of these extreme ranges, yet relatively thin layer of cumulate rocks (2-3 km; Griffin & Varne, 1980).

In the preceding sections two important geochemical features of the Macquarie Island lavas and dykes have been established. Firstly,

many of the samples are geochemically similar to "normal" MORB. Secondly, those that are not similar differ through a progressive enrichment of incompatible and hygromagmatophile abundances and variations in ratios of these elements. On the basis of the introductory discussion to this section these variations are suggested to represent heterogeneity in the source mantle. Based on the geochemical data the heterogeneity may be in the form of "enriched" veins present in variable but small amounts in a depleted "MORB" mantle peridotite (Wood, 1979).

This could be treated as a two-component model and if correct mixing trends should be identifiable in the data. Langmuir *et al.* (1978) have shown that the isotopic mixing equation (Vollmer, 1976) can be used as a general equation for incompatible/hygromagmatophile element ratios. In the Macquarie Island data suitable ratios are Zr/Nb, and La/Sm. Using the extreme data points (dyke sample 64: La/Sm = 8.80, Zr/Nb = 1.53; dyke sample 38206: La/Sm = 1.58, Zr/Nb = 16.5) the following relationship can be derived:

$$9.65(La/Sm) - 252(La/Sm)(Zr/Nb) + 207.6(Zr/Nb) + 3160.3 = 0.$$

The resultant binary curve matches the intermediary data extremely well (Figure 6.15), supporting a two-component mantle model. Including the complete data set, on the basis of the Zr/Nb ratios, the high Zr/Nb component has a value of 18.0 which leads, by extrapolation, to a La/Sm = 1.52.

Having define end-member ratios for the two components in the *liquids* the next step is to calculate the abundances of the elements. Nb has been selected as the control element for the calculations on the basis of its well documented hygromagmatophile character (Pearce & Norry, 1979), immobile nature (Cann, 1972) and its wide yet coherent range in the sample set.

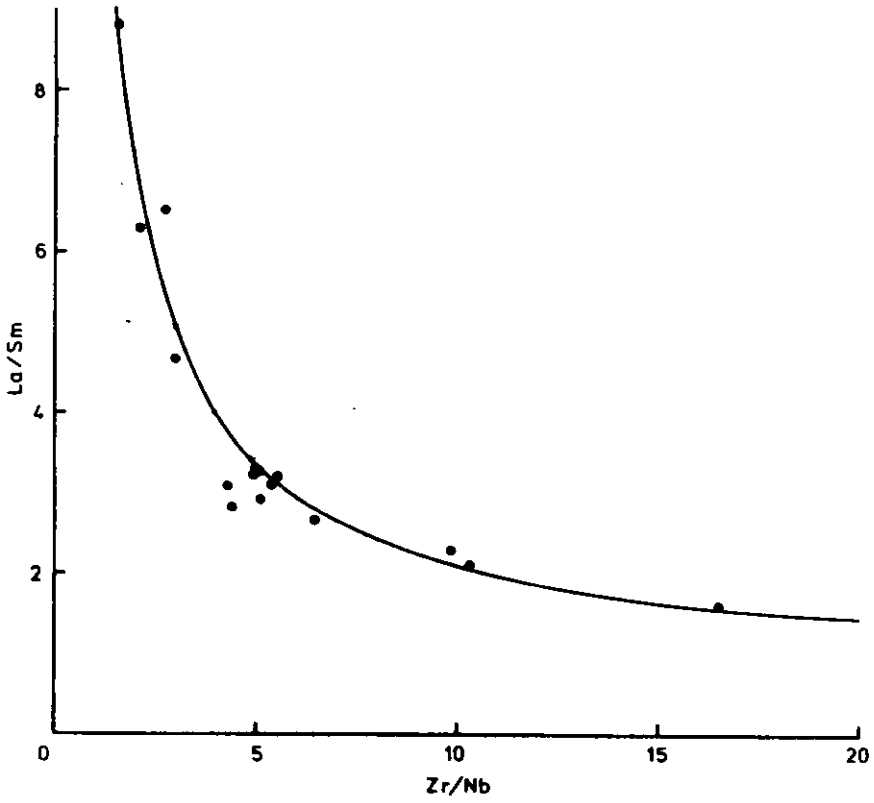

Figure 6.15 La/Sm vs. Zr/Nb with mixing line derived from the extreme data points using the equation of Langmuir *et al.* (1978).

From the data, the low Zr/Nb component in the liquid composition has a Nb abundance of 87 ppm and the high Zr/Nb component has 1 ppm Nb. Abundances in the two components of incompatible and hygromagmatophile elements are given in Table 6.12. These were calculated from the linear regression trends derived from variations of each element with Nb, shown in Figures 6.16 and 6.17, for values of 1 and 87 ppm Nb. The results are presented as geochemical patterns normalized against average MORB (Pearce *et al.*, 1981; Sun, 1980; Wood, 1979) in Figure 6.18. Also included on this figure is a pattern derived using the calculated element trends for a Nb content of 3.5 ppm (Table 6.13). This is to minimize errors resulting from analysis of Nb at the 1 ppm level and to provide a comparison with MORB. The subsequent pattern does not show the pronounced Nb anomaly yet other element abundances, relative to the MORB values, are little changed.

Two major points are reinforced by these geochemical patterns. Firstly, the low Nb or depleted liquid component is similar to MORB in both incompatible and hygromagmatophile element abundances, in support of derivation from a "depleted" mantle. Secondly, the differences between the two components are a function of the incompatibility of the element with possible mantle mineralogies. This feature is in agreement with arguments presented by Hanson (1977) and Wood (1979) for the derivation of the "enriched" ocean-floor basalts from a source containing a component derived through very low degrees of melting of primitive mantle material.

Table 6.12

TRACE ELEMENT ABUNDANCES IN END MEMBER COMPONENTS DEFINED BY Nb VARIANCE IN THE MACQUARIE ISLAND LAVAS AND DYKES.

Nb	Intercept (Nb=0ppm)	Slope	Corr.Coeff.	Comp. A (Nb=1ppm)	Comp. B (Nb=87ppm)
Zr	62.7	1.215	0.709	63.9	168,4
Y	25.9	0.044	0.089	26.0	29.8
TiO_2*	1.11	0.010	0.492	1.12	1.96
P_2O_5*	0.09	0.008	0.934	0.10	0.77
K_2O*	0.25	0.016	0.693	0.27	1.60
Rb	1.5	0.421	0.724	1.9	38.2
Sr	141.4	5.05	0.726	146.4	580.5
La	2.91	0.57	0.986	3.49	52.82
Ce	8.72	1.064	0.978	9.78	101.3
Nd	9.29	0.302	0.960	9.59	35.6
Sm	3.07	0.041	0.897	3.11	6.61
Eu	1.03	0.012	0.866	1.04	2.02
Tb	0.682	0.005	0.661	0.69	1.10
Tm	1.12	-0.055	-3.62	1.12	-
Yb	2.34	0.003	0.20	2.34	2.61
Lu	0.38	0	0.002	0.38	0.38

* wt.%

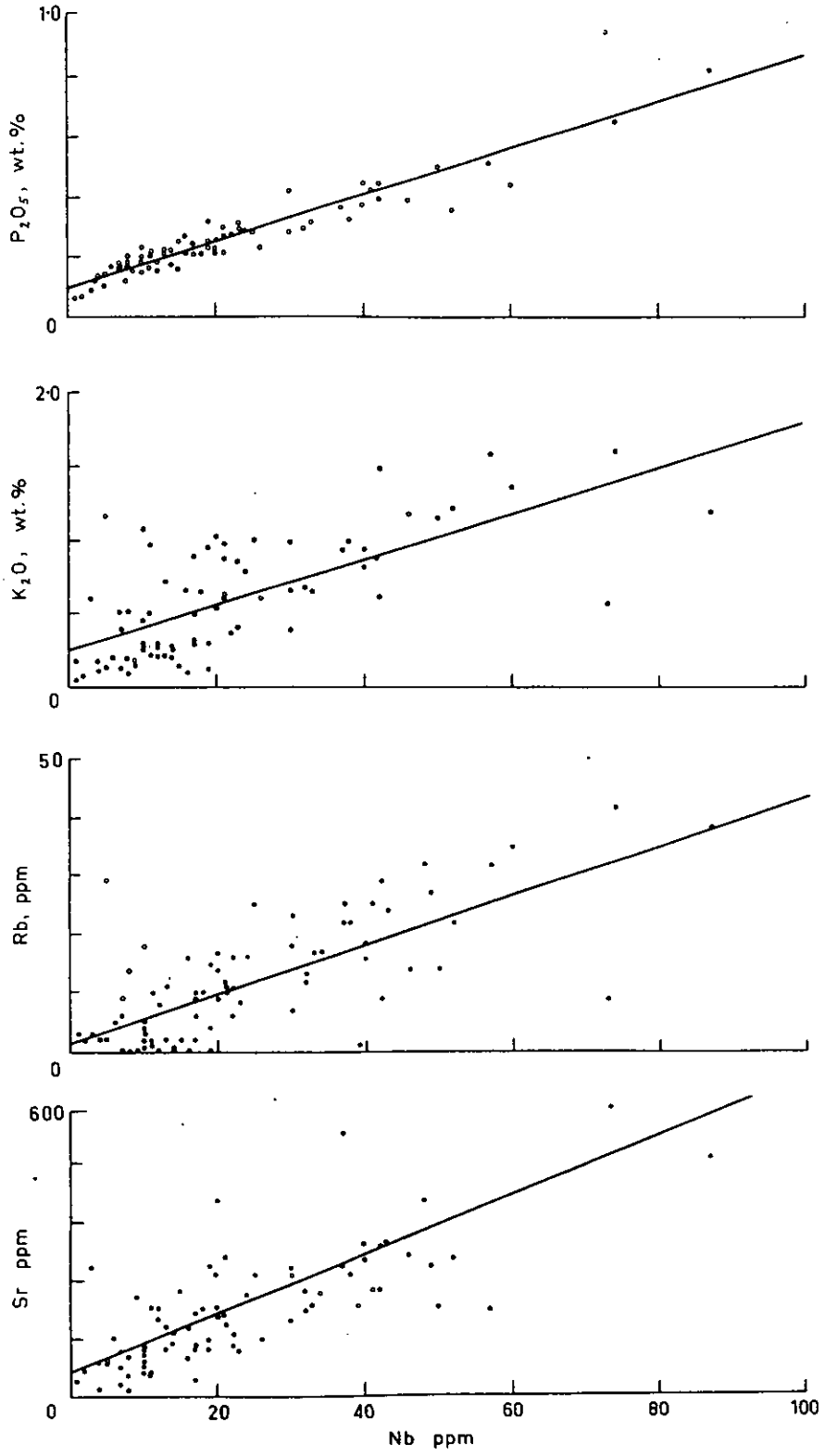

Figure 6·16 Sr, Rb, K_2O and P_2O_5 against Nb for the lavas and dykes with linear regression lines. Intercept, slope and correlation coefficient data are given in Table 6·11.

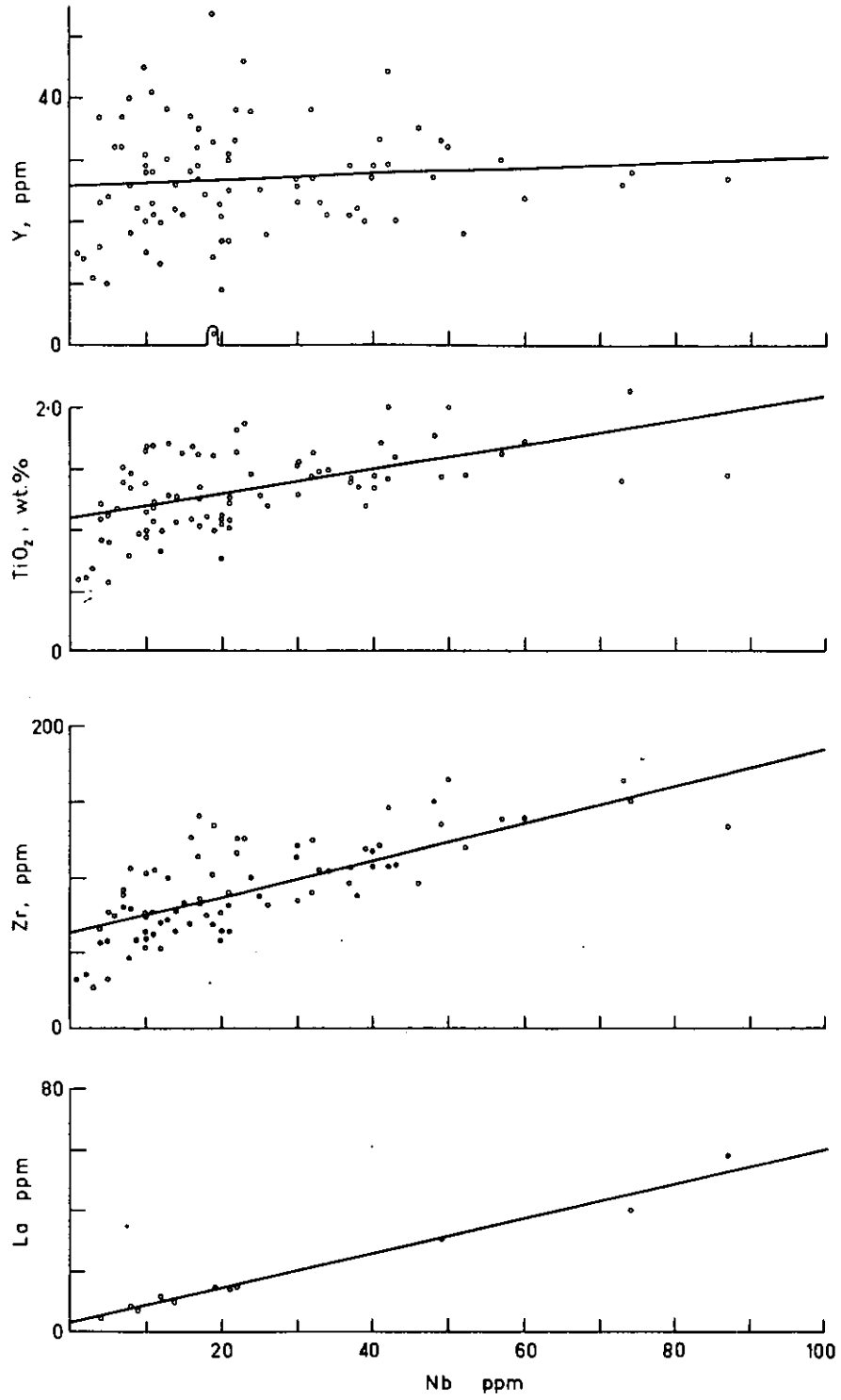

Figure 6·17 La, Zr, TiO_2 and Y against Nb for the lavas and dykes with linear regression lines. Intercept, slope and correlation coefficient data are given in Table 6·11.

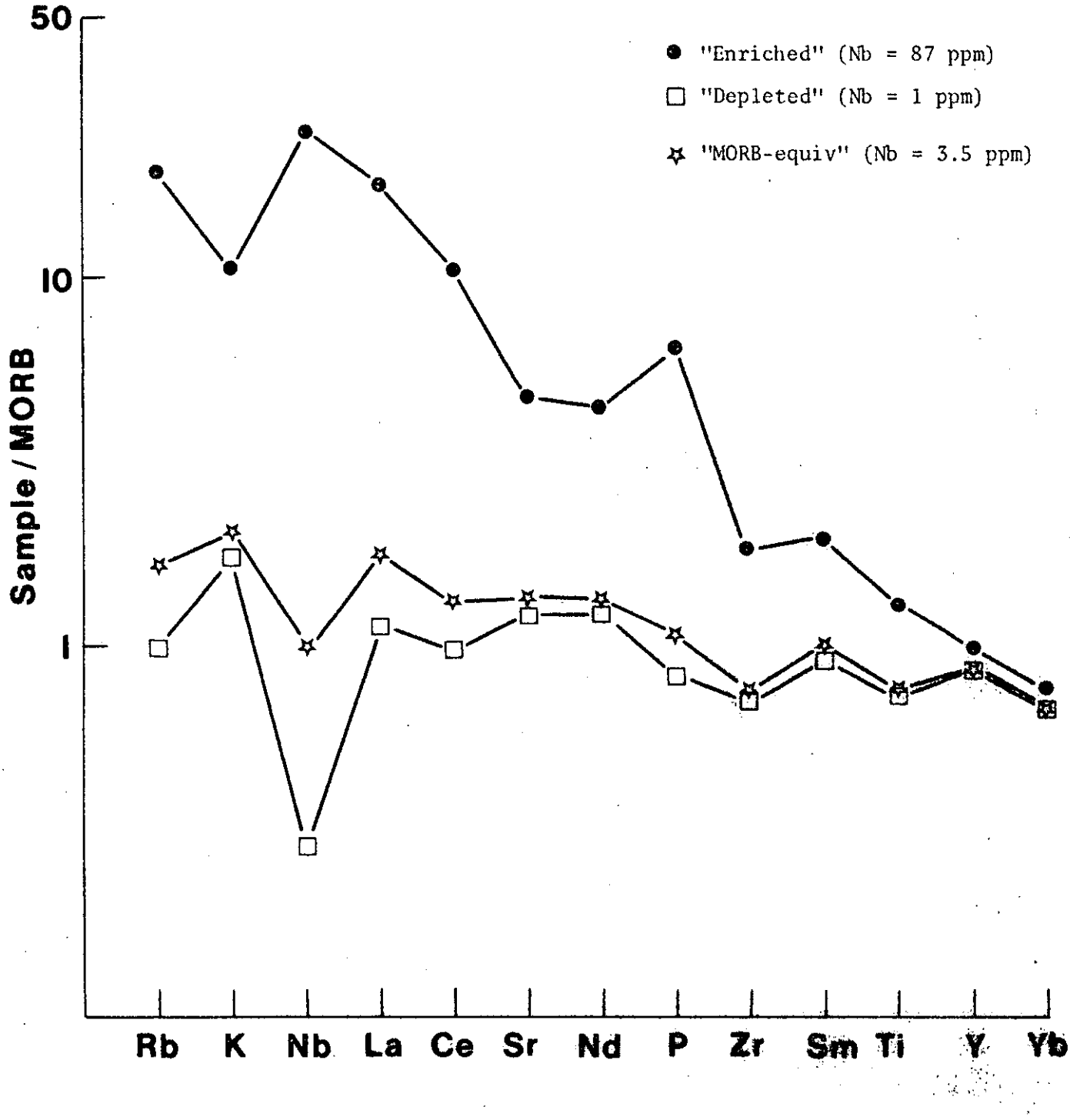

Figure 6.18 Geochemical patterns normalized to MORB abundances for "enriched", "depleted" and "MORB-equivalent" liquids from Macquarie Island.

Table 6.13

"MORB" normalized values of hygromagmatophile elements in the "enriched", "depleted", and "MORB-equivalent" components.

	MORB[1]	Nb=87 Enriched component	Nb=1 Depleted component	Nb=3.5 MORB comp.
Rb[2]	2.0	19.1	0.99	1.68
K	0.15 wt.%	10.7	1.8	2.08
Nb	3.5	24.9	0.29	1.0
La[3]	3.0	17.61	1.16	1.83
Ce	10.0	10.1	0.98	1.35
Sr	120	4.84	1.22	1.37
Nd	7.7	4.62	1.25	1.38
P	0.12 wt.%	6.42	0.83	1.08
Zr	90	1.87	0.71	0.76
Sm	3.3	2.00	0.94	1.0
Ti	1.5 wt.%	1.31	0.75	0.77
Y	30	0.99	0.87	0.87
Yb	3.4	0.77	0.69	0.69

1. Value from Pearce (1981), in ppm unless otherwise shown.
2. Element order from Wood (1979).
3. Sun (1980), values in ppm.

6.3.7 Relationships of the incompatible and hygromagmatophile element abundances to the petrological and normative character of the samples

The preceding sections have established that the variation of the major and compatible trace elements, incompatible elements and hygromagmatophile elements describe a complex petrogenesis involving shallow level fractionation, variations in degree of partial melting, and mantle heterogeneity. Additionally, relevant experimental investigations imply a further process involving olivine fractionation from primary picritic magmas at intermediate depths. Importantly it has been shown that the various processes can be recognized by examining the appropriate sets of element abundances and inter-element relationships.

It is also important to emphasize that although the geochemical behaviour of elements within the particular groups reflect principally the petrogenetic process by which they are most significantly affected, there is within the Macquarie Island data set an overall correlation between the various groups of elements. This can be most clearly seen in a plot of normative ne- or hy-composition against the Nb abundance of the sample (Figure 6.19). The hy-rich samples contain relatively low Nb than the ne-rich samples, which are more variable but generally richer in Nb. Superimposed on this figure is the petrographic nature of each sample, the alkaline variants dominating the Nb-rich samples.

One relevance of this relationship is the use of the basalt discriminant diagrams (Section 6.3.5). It has previously been noted that the Macquarie Island samples which are incorrectly classified using these discriminant diagrams rend to have relatively high Nb contents, low Zr/Nb, Y/Nb, Ti/Zr and K/Rb ratios, to be enriched in K and Sr, and to be ne-normative (Griffin & Varne, 1980). Such ambiguities could be virtually eliminated by applying, therefore, either a petrographic or CIPW normative screen to remove alkaline or ne-normative rocks from the data base being used.

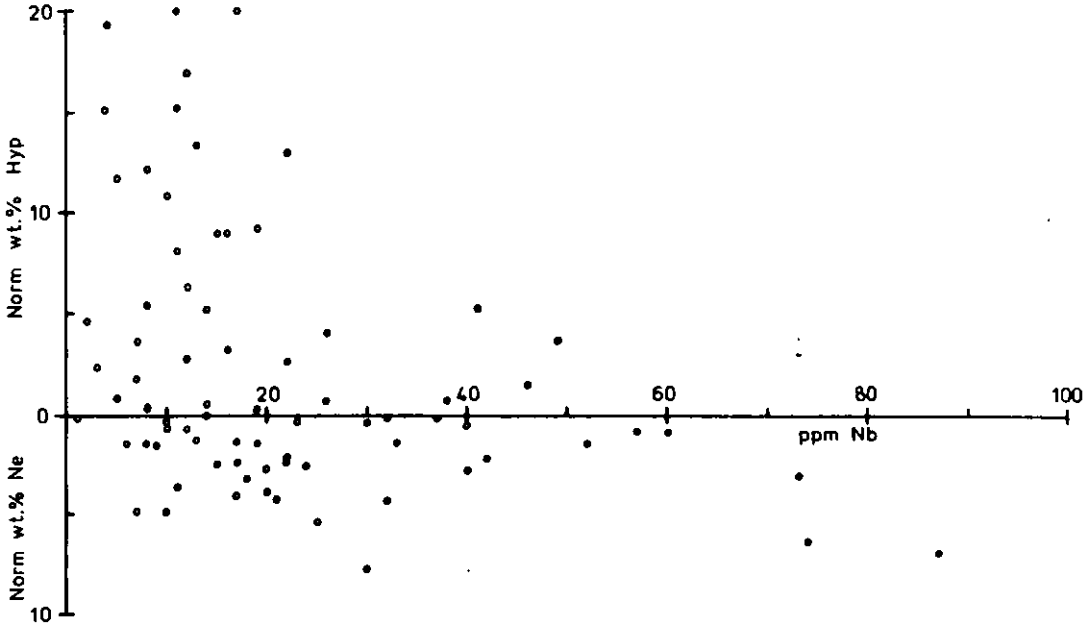

Figure 6.19 Ne- and hy - normative composition content against Nb abundance. Samples recognised petrographically as alkaline variants are denoted by solid circles.

6.3.8 Refinement of partial melting estimates using a two-component mantle

The recognition of a two-component source mantle allows a refinement of estimates of the degrees of partial melting required to produce the observed range of primitive compositions for the Macquarie Island lavas and dykes (Section 6.3.4). The initial discussion was based on the premise that the source mantle was relatively constant. However the ensuing discussion has shown that K_2O and P_2O_5 abundances are primarily source-controlled and that large variations in these elements are present between the two end-member compositions indicated by the lava and dolerite compositions (Sections 6.3.5 and 6.3.6, Table 6.13).

Original estimates of around 20% partial melting for the tholeiitic compositions (Nb = 1 ppm, P_2O_5 = 0.10 wt.%, K_2O = 0.27 wt.%) and subsequent olivine fractionation (15-17%) require a mantle source with 0.017-0.025 wt.% P_2O_5 and 0.045-0.068 wt.% K_2O. These values are within the range of experimentally studied source compositions, i.e. Pyrolite and Tinaquillo lherzolite (Green, 1971; Jaques & Green, 1980) and need no revision. However, the estimates of <18% partial melting for the more alkaline compositions (Nb = 87 ppm, P_2O_5 = 0.77 wt.%, K_2O = 1.60 wt.%) are not valid.

Normative calculations are presented in Table 6.14 for a range of compositions starting from a primitive tholeiite and by the addition of K_2O and P_2O_5 to reach, in the final composition, the observed limiting values for these elements. The normative compositions change from hy-rich (8.75 wt.%) to transitional, with 0.11 wt.% hypersthene. This emphasizes the major influence of K_2O on the normative calculation and the danger of using CIPW normative compositions as a guide to mantle processes where a variable source composition may be involved. From this example it is clear that it is not necessary to appeal to variations in partial melting to explain the range of the Macquarie Island rocks although some variation cannot be excluded.

Table 6.14

Effects of increasing K_2O and P_2O_5 on CIPW normative compositions.

	234		ADD-1		ADD-2		ADD-3		ADD-4	
	WT	C.PC	WT	C.PC	WT	C.PC	WT	C.PC	WT	C.PC
SIO2	50.23	45.832	50.03	45.642	49.84	45.462	49.64	45.267	49.45	45.093
AL203	17.32	18.627	17.25	18.549	17.18	18.471	17.12	18.402	17.05	18.326
FE203	1.25	0.858	1.25	0.858	1.24	0.851	1.24	0.851	1.23	0.844
FEO	6.40	4.884	6.38	4.868	6.35	4.844	6.33	4.828	6.30	4.805
MNO	0.13	0.100	0.13	0.100	0.13	0.100	0.13	0.100	0.13	0.100
MGO	9.45	12.851	9.41	12.794	9.38	12.751	9.34	12.694	9.30	12.639
CAO	10.46	10.227	10.42	10.186	10.38	10.145	10.34	10.103	10.30	10.064
NA2O	2.79	4.936	2.78	4.918	2.77	4.899	2.76	4.880	2.75	4.862
K2O	0.66	0.768	0.91	1.059	1.16	1.350	1.41	1.640	1.66	1.931
TIO2	1.10	0.754	1.10	0.754	1.09	0.747	1.09	0.747	1.08	0.740
P2O5	0.21	0.162	0.35	0.271	0.49	0.379	0.63	0.487	0.77	0.595
TOTAL	100.00	100.00	100.01	100.00	100.01	100.00	100.03	100.00	100.02	100.00
						C.I.P.W. NORM				
OR	3.90	0.007	5.38	0.010	6.86	0.012	8.33	0.015	9.81	0.018
AB	23.61	0.045	23.52	0.045	23.44	0.045	23.35	0.045	23.27	0.044
AN	32.79	0.118	31.90	0.115	31.02	0.111	30.16	0.108	29.28	0.105
DI WO	7.40	0.064	7.31	0.063	7.21	0.062	7.11	0.061	7.01	0.060
EN	4.94	0.049	4.87	0.049	4.81	0.048	4.74	0.047	4.67	0.047
FS	1.92	0.015	1.89	0.014	1.87	0.014	1.84	0.014	1.82	0.014
HY EN	6.30	0.063	4.74	0.047	3.19	0.032	1.62	0.016	0.08	0.000
FS	2.45	0.019	1.84	0.014	1.24	0.009	0.63	0.005	0.03	0.000
OL FO	8.62	0.061	9.68	0.069	10.77	0.077	11.84	0.084	12.90	0.092
FA	3.69	0.018	4.15	0.020	4.61	0.023	5.07	0.025	5.53	0.027
MT	1.81	0.008	1.81	0.008	1.80	0.008	1.80	0.008	1.78	0.008
IL	2.09	0.014	2.09	0.014	2.07	0.014	2.07	0.014	2.05	0.014
AP	0.49	0.001	0.81	0.002	1.14	0.003	1.46	0.004	1.79	0.005
TOTAL	100.00		100.01		100.02		100.04		100.03	

6.4 SUMMARY

The following points briefly summarize the major features and implications of the geochemistry of the Macquarie Island lavas and dykes.

1. Geochemical abundances of both major and trace elements in the analyzed sample set have been little affected by the metamorphic processes that have occurred within this oceanic crust segment. Increases in LOI values and the Fe^{3+}/Fe^{2+} ratios of the samples are the only pervasive effects of the alteration; both effects decreasing in the increasing metamorphic grade.
2. The petrographic variation from tholeiitic to alkaline is matched by the geochemical range in the analyzed sample set. A good correlation between petrography and CIPW normative mineralogy and evidence from pillow rims and core analyses, and variations across a massive lava flow confirm the lack of geochemical alteration of these samples.
3. Three groups of elements have been distinguished on the basis of statistical covariance.
   (i) major and compatible trace elements,
   (ii) incompatible elements, and
   (iii) hygromagmatophile elements.
4. A wide range in Mg/Mg+Fe ratios and Cr and Ni abundance covariance with this ratio define crystal fractionation as a major process in the evolution of these rocks. The spatial association of the lavas and dykes on Macquarie Island with apparently cumulative olivine-plagioclase-rich layered gabbros together with the mineralogical similarity of the phenocryst/megacryst phases of the lavas and dykes and the gabbro phases is good evidence that these two groups of rocks are complementary products of a shallow level crystal fractionation process.

Major element mixing models show that much of the geochemical variations of the analyzed lavas and dykes can be accounted for by such a shallow level process. Plagioclase, olivine and spinel are the major phases involved, but clinopyroxene is also required. If the layered gabbros alone represent the cumulate component then, from the schematic section of Macquarie Island-type oceanic lithosphere (Griffin & Varne, 1980, fig.3) an average of 25% crystal fractionation is required. An overall average fractionation value of 35% is necessary if the recrystallized gabbros, that appear to be between the layered gabbros complex and the basal harzburgites, are also cumulates complementary to the lavas and dykes.

5. K_2O and P_2O_5 show extreme variations and behave, together with Nb, Sr, Rb and the light REE, as completely incompatible elements in these rocks. They have been termed hygromagmatophile to distinguish them from the remaining group of elements - Y, Zr, and TiO_2 - and the heavy REE which show significant correlations with the major and trace elements (Table 6.3).
6. Effects of shallow level fractionation and differences in degree of partial melting of the source mantle are too small to account for the extreme variations in hygromagmatophile element abundances and variations in trace element ratios found in these rocks. Mechanisms involving dynamic melting or open chamber fractionation also appear unlikely to account for the extreme variations although such mechanisms undoubtedly could have had some effect.

The hygromagmatophile element ranges are considered to result primarily from heterogeneity of the source mantle with respect to these elements. Covariants of incompatible/hygromagmatophile element ratios closely match a binary mixing curve (Figure 6.15). Consequently a two-component mantle is envisaged with variations in

proportions of the two components creating the observed heterogeneity. The similarity of major and compatible trace element compositions of the Macquarie Island lavas and dykes to the MORB average composition (Table 6.5) and success of the trace element discrimination diagrams in recognizing the tholeiitic or "depleted" variants as MORB-type rocks is corroborative evidence for an upper mantle essentially homogeneous with respect to these elements. The strong correlation of enrichment and increasing elemental hygromagmatophile nature with respect to likely mantle mineralogies shown in the alkaline or "enriched" variants relative to the tholeiitic variants and to "depleted" MORB (Figure 6.18) supports the presence of an "enriched" mantle component, formed by small degrees of partial melting of, or fluid migration through, a fertile mantle.

7. The petrographic and CIPW normative character has been shown to correlate with the degree of enrichment of the samples in the hygromagmatophile elements. This has raised the question of whether petrographic and CIPW normative variations reflect variations in partial melting or mantle heterogeneity, because of the major control of the latter on K_2O and P_2O_5 abundances in the derived liquids. In view of the major effect of K_2O on CIPW normative compositions (Section 6.3.8) and experimental evidence that the degree of silica saturation of a melt is dependent and inversely related to the alkali content of the source composition (Jaques & Green, 1980), the earlier suggestion that the alkaline variants represent lower degrees of partial melting than the tholeiitic variants seems unlikely. All variants are probably the result of a similar degree of partial melting of the source mantle; the compositional range reflecting source mantle heterogeneity. From the more detailed and extensive experimental studies using tholeiitic compositions, 10-30% partial melting of the source mantle is suggested.

Chapter 7

EVOLUTION OF MACQUARIE ISLAND-TYPE OCEANIC CRUST

7.1 INTRODUCTION

Igneous and metamorphic features of the Macquarie Island lavas and dykes have been described and discussed in the preceding chapters. This concluding chapter integrates the evidence from the various aspects of this study on the formation of Macquarie Island-type oceanic crust. Summaries of individual aspects of this study have been presented at the end of the relevant chapters and are not repeated here. It is important to emphasize that this work is a preliminary investigation. Recommendations for further work are presented in the final section of this chapter.

7.2 METAMORPHIC PROCESSES IN THE OCEANIC CRUST

Various models for ocean-floor metamorphism have been presented based on dredge and drill studies of MORB basalts (Cann, 1970) and derived from studies of ophiolite complexes (Smewing, 1975; Elthon & Stein, 1978; Coleman, 1977; Coish, 1977). However as both Coleman (1977) and Cann (1979) have observed, the similarity between metamorphic (and igneous) models of mid-oceanic ridges and ophiolite sequences is a result of these models drawing heavily on spatial relationships observed for on-land ophiolites. In this sense the data from the oceanic crust exposed on Macquarie Island are unique. They are the connecting link between studies of ophiolites and oceanic crust.

Ocean-floor metamorphism has, from the Macquarie Island example, been recognized to result in a sequence of secondary assemblages ranging from those through cold ocean-floor weathering ("brownstone" facies, Cann , 1979) to zeolite and lower greenschist facies assemblages in

the lava sequence and to greenschist and finally amphibolite facies assemblages in the basal section of the sheeted dyke complex (Chapter 5; Figure 7.1). This provides strong support for the generally accepted metamorphic model reviewed by Cann (1979).

The physical process of this oceanic metamorphism is a more controversial subject, particularly as it addresses the question of chemical interaction and elemental fluxes between the oceans and the oceanic crust during the metamorphic process. Firstly, the metamorphic zonation on Macquarie Island requires a high geothermal gradient, possibly as high as 200°C/km (Section 5.7.2). This value is comparable to estimates from ophiolites (Coleman, 1977) and is strong evidence that the bulk of the metamorphism occurred close to or at the spreading ridge crest.

Fluid penetration appears to involve what may be considered as two discrete albeit interactive processes. One process is fluid flow through the more porous zones of the crust, principally faults and fracture surfaces in the rocks. Rocks in and abutting these zones typically show an extreme degree of alteration both chemically and mineralogically. The second process is a pervasive permeation through the rocks at all scales. Evidence for this is the changes in LOI contents and Fe^{3+}/Fe^{2+} ratios observed in the analyzed samples versus fresh (MORB) basalts (Section 6.2.1), the alteration of interstitial glass in otherwise petrographically fresh rocks (Chapter 5), and regular mineral sequences in amygdules (Section 5.4.2).

The action and interaction of these fluid movement processes must be considered with regard to the following features of the Macquarie Island lavas and dykes:

1. Unaltered volcanic glass, a highly susceptible material with regard to fluid alteration, persists well into the zeolite facies metamorphic zone; commonly present only metres away from strongly altered (zeolitized) rocks;

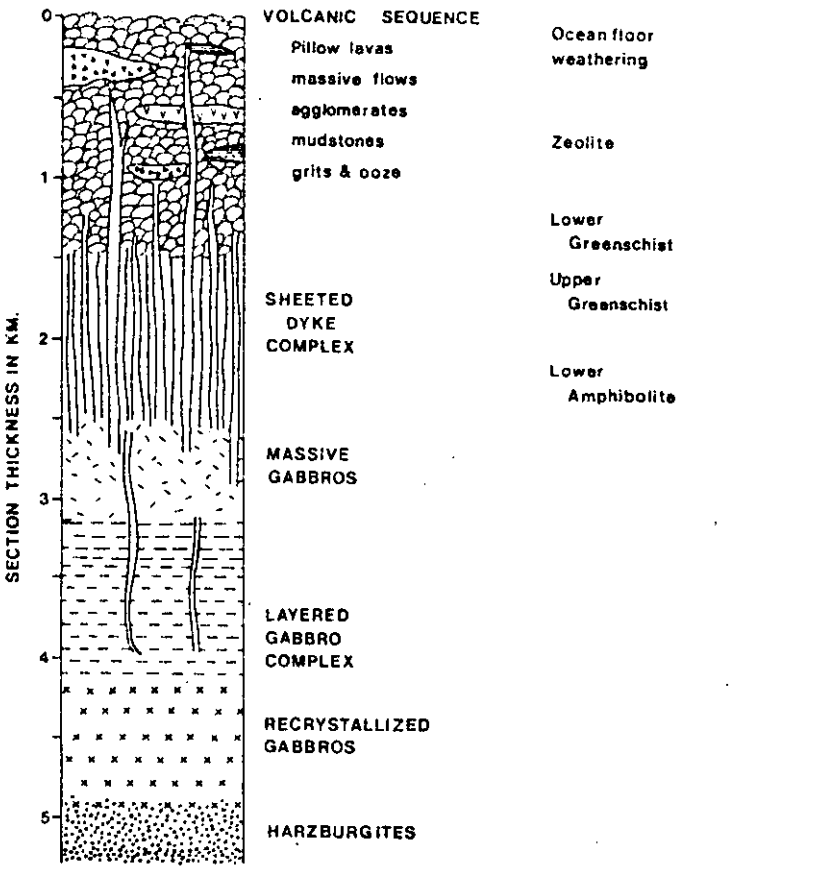

Figure 7.1 A schematic section through Macquarie Island-type oceanic lithosphere. The section is based on the traverse from North Head to Eagle Point via Handspike Point (see Figure 3.2) but is augmented by field data from elsewhere on Macquarie Island. (From Griffin & Varne, 1980.)

2. Only rarely are rocks totally altered. Fresh olivine, plagioclase and clinopyroxene occur in rocks of the brownstone, zeolite and greenschist facies respectively. Areas of extreme alteration appear restricted to fault and shear zones;

3. The geochemistry of petrographically fresh samples show, apart from their LOI contents and Fe^{3+}/Fe^{2+} ratios, no evidence of significant metamorphic alteration from igneous abundances (Chapter 6);

4. Mineral assemblages of quartz, epidote, chlorite and sulphides (principally pyrite with minor sphalerite, galena and chalcopyrite) are in general restricted to veins in the sheeted dyke complex and the lavas that have undergone lower greenschist facies metamorphism, i.e. the lower part of the extrusive sequence;

5. Gypsum deposits present in the top of the sheeted dyke complex may have resulted from the heating of sea water penetrating to this level relatively unaffected by prior rock interaction;

6. Rough heat of reaction calculations demonstrate that the "uralitization" of the rocks of the sheeted dyke complex may be strongly exothermic;

7. Preliminary O and C isotope studies suggest a discrimination between the "brownstone" facies metamorphism and the metamorphism at deeper levels of the oceanic crust. The results also give evidence of penetration of sea water to the base of the gabbroic rocks, a depth of approximately 5 km, although no obvious mineralogical effects of the metamorphism are present; and

8. The greenschist facies vasalts are enriched in ^{18}O whereas the underlying dykes and gabbros are depleted. This may document penetration of sea water to the dykes and gabbros where, through low W/R ratios and high temperatures, the fluid has become enriched in ^{18}O and the rocks correspondingly depleted. Subsequent upwelling of this enriched fluid into the extrusive sequence could have produced the enriched ^{18}O character of these rocks.

On the basis of this evidence the following is suggested for the metamorphism of the Macquarie Island-type oceanic crust. Firstly, this metamorphism is composed of two phases: (i) a relatively short-lived intense hydrothermal phase at or near the ridge crust producing the bulk of the metamorphic effect, and (ii) a relatively cold long-term process resulting in "brownstone" facies alteration of the surface and near-surface lavas. This latter process has been well documented through the results of the Deep Sea Drilling Project (Pritchard *et al.*, 1978; Staudigel & Hart, 1980).

The near-ridge hydrothermal metamorphism results from the interaction of two fluid processes. The first process is a convective circulation. Sea water rapidly penetrates the crust along major fault planes. Sea water that reaches the sheeted dyke zone experiences a rapid temperature rise resulting in precipitation of gypsum. The increase in temperature is a result of both host rock temperature, i.e. the geothermal gradient, and the exothermic heat released during later alteration of the dykes. This results in substantial modification of the fluid, including ^{18}O enrichment and addition of SiO_2. Heavy metal enrichment of the fluid is also probable during this phase.

Subsequent convective upwelling and cooling of the fluid results in the formation of vein and "stockwork" deposits of sulphide-bearing propylitic mineral assemblages. These are concentrated in the top of the sheeted dyke zone and basal zone of the extrusives but may occur higher in the section. If the Troodos massive sulphide desposits are ocean-floor deposits then such fluids may reach the surface, presumably when development of major fault systems occurs at a suitable time.

The second fluid process is one of permeation through the rocks. This may be envisaged as a one-way movement and is essentially a closed system process. Water from a magmatic source (Moore, 1970) is negligible when compared with the large amount of water present in the

altered rocks (2-4 wt.% on average for rocks of the zeolite and lower greenschist facies zones) and the source must be a combination of water trapped during initial eruption of the extrusives, from intercalated sediments, and water entering the sequence along fault and shear zones. This process is physically the dominant process in the extrusive sequence, affecting all rocks to some extent.

To understand the operation of these processes the dynamic nature of the spreading ridge crest must be recognized. The schematic representation of the metamorphism presented in Figure 5.18 is only a scenario of the complete process and represents an ideal end product. The initial lava sequence at the spreading crest is only a thin veneer over the sheeted dyke zone. Penetration of sea water into the underlying "hot" dyke zone is likely to start right at the active spreading area where intense tectonic activity will have provided easy access routes. As the "oceanic crust sequence" develops progressively away from the ridge crest the hot fluid distributes heat away from the basal zone up through the sequence. The final metamorphic zonation thus represents the peak temperature profile through the crustal sequence. A schematic attempting to depict the dynamic nature and evolution is presented in Figure 7.2. This is extremely simplistic because of the lack of specific knowledge about the effects of tectonism at spreading ridge centres; such complications are not likely to alter the fundamental pattern.

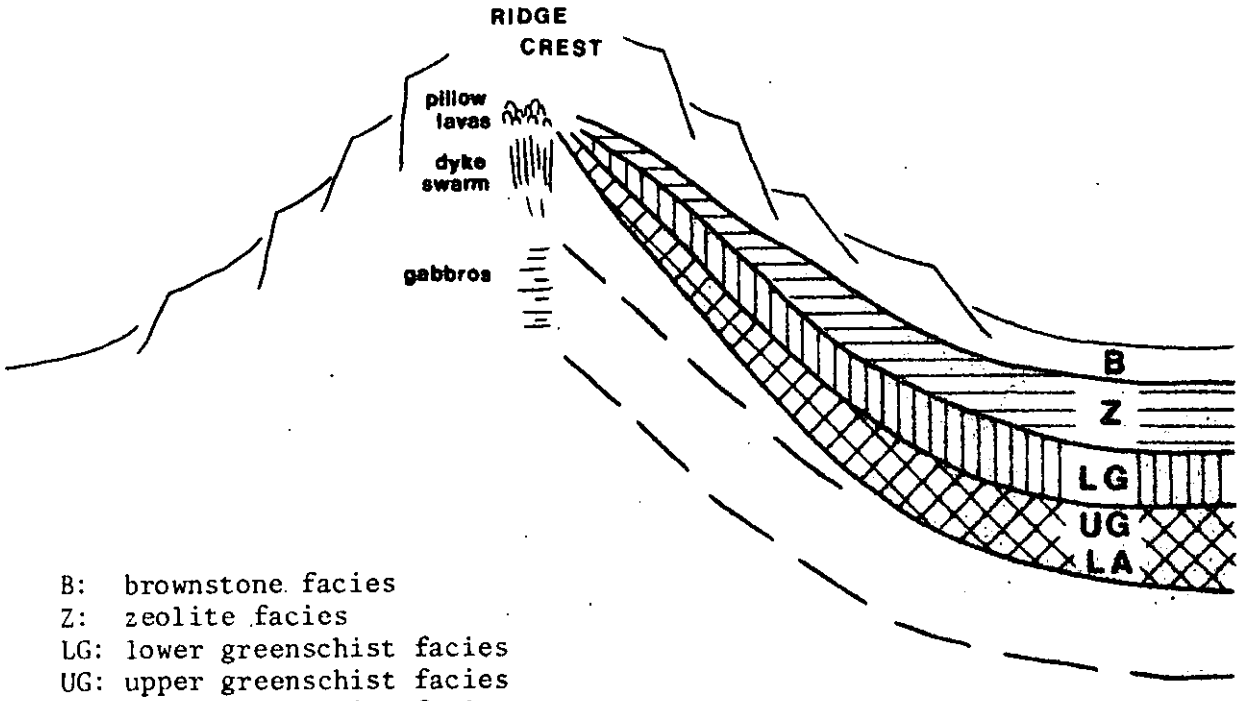

B: brownstone facies
Z: zeolite facies
LG: lower greenschist facies
UG: upper greenschist facies
LA: lower amphibolite facies

Figure 7.2 Dynamic nature and evolution of the oceanic crust sequence of Macquarie Island.

7.3 IMPLICATIONS AND FURTHER STUDIES

1. The distinction between open system fluid movement along fault planes and closed system or one-way fluid movement by permeation through the rocks has major implications for isotopic studies of oceanic crust. Principally, assumptions of fluid compositions for temperature estimates using isolated amygdule phases are clearly made difficult. The fluid will have evolved considerably from a pristine sea water composition and will further fractionate during permeation of the rocks and formation of the amygdule phases.

2. The mechanism of sea water penetration to the sheeted dyke zone and subsequent fractionation has been verified by the preliminary stable isotope studies. These studies are being extended in detail to compare isotopic values of phases formed by the permeating fluid process and to consider the problems raised above.

3. The sheeted dyke swarm and, possibly, the lowest part of the extrusive sequence are, on the basis of these results, the source of metals for the sulphide deposits. This could be examined by base metal analyses of these rocks.

4. S isotopic abundances should be determined for the various sulphate/sulphide occurrences together with ^{18}O isotopic abundances to test the suggested temporal relationships between the various deposits (Figure 5.18).

5. Surface massive sulphide deposits will only occur if tectonic activity creates a fault that penetrates the crust to the level of the sheeted dyke swarms, and allows rapid rise of appropriate solutions to the surface. Also, this must occur during the active initial stages of the metamorphism on or near the spreading ridge crest.

6. Preliminary electron microprobe and petrographic studies of amygdule assemblages have indicated a regular zonation of the phases in

the amygdules. More extensive microprobe studies should be performed to examine this feature and document the chemistry of this process.

7. These results illustrate the importance of the permeation process and the variability of degree of alteration of the rocks throughout the sequence. They further support the problems outlined by Cann (1979) with regard to calculation of element fluxes between oceans and oceanic crust. Until the difficult problem of accurately estimating the relative importance of open system circulation and convection in the overall metamorphic process is overcome, calculations of elemental fluxes will remain crude estimates.

7.4 IGNEOUS PROCESSES AT OCEANIC RIDGE SPREADING CENTRES

The mineralogic and geochemical features of lavas and dykes from oceanic crust exposed on Macquarie Island have been described and discussed in Chapters 4 and 6. Although this thesis is mainly an investigation of ocean crust metamorphism, some aspects of the processes of Macquarie Island crust formation have been explored. The following points constrain magmatic processes at spreading ridges producing Macquarie Island-type oceanic crust:

1. The lava sequence is formed through extrusion of pillow pavas or occasionally minor lava flows. Small lenses of volcaniclastic turbidites are included in the sequences together with occasional block breccias. Hyaloclastite deposits are found as deposits interstitial to lava pillows. None of the sedimentary deposits is spatially extensive and thus they do not appear to record any major temporal breaks in the formation of the approximately 1.5 km thick extrusive sequence;

2. Lavas range from glassy to holocrystalline and are commonly porphyritic. They contain megacrysts of plagioclase, olivine, spinel and rarely clinopyroxene. The plagioclase megacrysts are characterized by reacted cores and the clinopyroxene megacrysts by rounded embayed forms.

Megacryst phase relationships indicate a crystallization sequence of olivine (+ spinel)-plagioclase-clinopyroxene. Dykes both intruding lavas and in the sheeted dyke zone show similar ranges in megacryst contents and form. Plagioclase megacrysts may be more abundant in the dykes. Orthopyroxene is absent;

3. Groundmass mineralogies of the lavas and dykes exhibit a continuous variation from alkaline; with olivine and kaersutitic amphibole present, to tholeiitic. The alkaline variants are most abundant amongst rocks exhibiting "brownstone" facies or ocean-floor weathering alteration. However alkaline lavas are present throughout the extrusive sequence;

4. Microprobe analyses of the megacryst phases give the following compositional ranges:

clinopyroxene	$Ca_{45}Mg_{50}Fe_5$-$Ca_{38}Mg_{50}Fe_{12}$
plagioclase	An_{87}-An_{80}
olivine	Fo_{89}-Fo_{85}.

The spinel is chrome-rich. These compositions have been shown to match those of other ocean-floor basalts and more significantly the compositions of the principal phases of the layered gabbro sequence present on the island (Griffin & Varne, 1980). Magma mixing is evidenced by the presence of Cr-poor clinopyroxene megacrysts in a lava containing Cr-rich groundmass and microphenocryst clinopyroxene;

5. The major elements show variations commensurate with the petrographic variations, ranging from mildly ne-normative to strongly hy-normative. The range from primitive to fractionated compositions can be modelled using the gabbro phase compositions, with clinopyroxene playing a significant role, and a primitive lava composition. Up to 60 wt.% fractionation is required in the extreme cases. K, Nb, P, Rb, Sr and light REE behave as hygromagmatophile elements with respect to the major elements. Zr, Y, Ti and the heavy REE are transitional in behaviour yet still incompatible;

6. The hygromagmatophile element abundances and hygromagmatophile/incompatible element ratios range widely. Trace element discriminant diagrams used for identification of the tectonic environment of basalts incorrectly classify basalts derived from a mantle containing a significant "enriched" component although these diagrams are accurate discriminants for the depleted members of the Macquarie Island lavas and dykes;

7. Two mantle components have been recognized: a dominant "depleted" component comparable to the source of "normal" MORB basalts, and a minor "enriched" component. Geochemical patterns show a strong correlation between degree of enrichment of the hygromagmatophile element and incompatibility with likely mantle mineralogies, relative to MORB. This supports derivation of the second component through an earlier melting event of a "fertile" or undepleted mantle and consequent contamination of the "depleted" MORB mantle with veins of this enriched component. The pronounced effect on K_2O and P_2O_5 abundances in the rocks resulting from this heterogeneity makes estimates of degrees of partial melting based on either the actual elemental abundances or CIPW normative compositions extremely difficult at a specific level; and

8. Two major constraints are provided by these data on the physical nature of the mantle heterogeneity. Firstly, the intercalation of the "enriched" alkaline variants and the "depleted" tholeiitic variants on Macquarie Island define the heterogeneity as a local mantle feature, perhaps on a vertical scale. Secondly, the various mantle sources were accessible at all stages of the formation of the extrusive sequence although the "enriched" mantle source was more dominant in the latter stages.

These brief summarized salient points emphasize that the complex magma processes at spreading ridge centres of the Macquarie Island type can be discussed in terms of both shallow level processes and deeper processes.

7.5 DERIVATION OF PRIMITIVE MAGMAS AND NATURE OF THE MANTLE HETEROGENEITY

Results from the relevant experimental studies have been discussed in the preceding chapter. It was concluded, on the basis of the studies, that primitive tholeiitic liquids parental to the lava and dyke sequences and to the layered gabbro sequence may result from moderate degrees (10-30%) of the partial melting from a peridotitic source mantle, followed by substantial (about 16%) olivine fractionation at deep levels, the initial primary magma being picritic. Depth of segregation of these primary picritic magmas is indicated to be 60-70 km. Arguments that primitive liquids arising from this process could not be parental to the cumulate gabbro sequence (Green *et al.*, 1979) are based on the abundance of orthopyroxene in the gabbro sequences of many ophiolites and the presence of plagioclase more calcic than that predicted from these studies. These have been discounted in view of the lack of orthopyroxene as a major phase in the layered gabbro sequence on Macquarie Island, evidence from other experimental studies (Bender *et al.*, 1978) that plagioclase of compositions similar to those observed in the Macquarie Island rocks is present as a low-pressure liquidus phase for primitive MORB compositions, and the field and mineralogical evidence presented in this thesis from Macquarie Island.

The petrogenesis of the "enriched" alkaline rocks is critical to the overall petrogenetic model and to the nature of the mantle heterogeneity. The constraints discussed earlier (Section 7.4) suggest strongly that the mantle heterogeneity evidenced by the Macquarie Island data is a local feature. Green (1971) and others, have proposed a vertically zoned Low Velocity Zone (LVZ) with hygromagmatophile elements concentrated in a stratified layer (or layers) in the LVZ. Migration of CO_2-rich fluids has been proposed as the method of stratification of this zone (Green & Lieberman, 1976). In the case of Macquarie Island an episodic process would be required; magma derivation tapping the deeper

"enriched" zone progressively more towards the end of the cycle. This could lead to a veneer of alkaline volcanics on the ocean floor. However the complex tectonism at and around mid-ocean ridges would break up this ideal alkaline surface layer, exposing the lower level tholeiitic rocks. In this case the tholeiitic lavas recovered from the ocean floor would be expected to show evidence of having been subjected to higher grades of metamorphism.

An alternative concept discussed by Wood (1979b) is the production of "enriched" mantle pods through veining of "normal" mantle with products of small degrees of partial melting of subducted lithosphere, after an initial dehydration event. Wood (1979b) envisaged that these "enriched" or veined mantle sources became involved in the mantle convection systems and formed enriched pods in a dominantly "normal" mantle. The variation in the Macquarie Island rocks would then reflect migration of one of these "enriched" pods into the zone of magma generation.

Both models have attractive features and the data available at present from the Macquarie Island rocks do not permit an unambiguous solution being identified. Further information is required in two main areas. Firstly, the isotopic characteristics of the lavas and dykes must be identified. Information from Sr, Nd and Pb isotopes should provide mork detailed evidence as to the nature of the two mantle components recognized on the basis of hygromagmatophile and incompatible elements.

Further information is required on the spatial distribution of alkaline rocks in the vicinity of Macquarie Island and other parts of the Australian-Antarctic and Pacific-Antarctic ridge system, the mid-oceanic spreading ridge with which the Macquarie Island oceanic crustal segment is correlated. A traverse from the ridge to the Macquarie Island region would provide information specific to the question of

episodicity of the magma generation. It must be emphasized that systematic drilling of the type performed at the DSDP sites may *fail* to provide accurate information. This is seen by the local variations present in the geology of Macquarie Island. Single drill sites at the southern end of Macquarie Island and at North Head, the northern tip, would yield extremely different information despite being only approximately 37 km apart. Dredge haul studies would appear to offer a better chance of obtaining representative samples from an area.

7.6 NEAR-SURFACE PROCESSES AT A MACQUARIE ISLAND-TYPE MID-OCEANIC RIDGE

Although there is at present a lack of information on the isotropic gabbros and layered gabbros of Macquarie Island the available data in conjunction with the information on the lavas and dykes collected during this study allow a preliminary model to be prepared.

Strong evidence for a series of primitive magmas from different mantle sources reaching a high level in the crust have been presented and discussed in the latter sections of Chapter 6. An important feature of the extrusive section on Macquarie Island is that although there is a gradual change from tholeiitic to alkaline compositions from bottom to top of the section, all variants are present throughout the section as flows interbedded with lavas of contrasting composition. Such relationships could not be achieved in a simple fractionating magma chamber, and presumably at least two chambers would be required. This, however, is extremely unlikely as it would require almost totally discrete paths for the two magma types.

The "infinite leak" model proposed by Nisbet & Fowler (1978) to satisfy constraints suggested by seismic studies of modern mid-oceanic ridges is one which will account for these observed lava relationships. The basic concepts of this model are shown in Figure 7.1 (Nisbet & Fowler, 1978, fig. 6B). Essentially magma batches ascend to the base of the pre-

existing crust and subsequently rise erratically to the surface along tension cracks. The final stage of ascent through this pre-existing crust depends upon the nature of the crack, some magmas becoming trapped and, through fractional crystallization, giving rise to the gabbroic rocks, others ascending rapidly extraining xenocrysts and possibly xenoliths.

The principal feature of the Macquarie Island lavas and dykes summarized in Section 7.4 can be achieved from primitive magmas by selecting appropriate ascent paths for various magma aliquots, like the dynamic melting model of Langmuir *et al.* (1977). This is not a rigorous test of the model as the large number of unconstrained variables including magma volume, rate of ascent, mode of ascent (stepwise or continuous), and pressure and temperature conditions during ascent, allows virtually any desired solution to be reached. It can only be postulated that the mineralogical and geochemical features of the Macquarie Island lavas and dykes are strong evidence against a near-surface single magma chamber model; the following model has been constructed based on this premise and is high speculative in nature.

A schematic model of the near-surface magmatic processes based on the "infinite leak" model (Nisbet & Fowler, 1978) and the schematic section through Macquarie Island-type oceanic lithosphere, based on a field traverse across the northern coast of the island (Griffin & Varne, 1980) is shown in Figure 7.3. A range of magma paths has been imposed on this schematic which would give rise to the observed features of the lavas and dykes.

In addition to the petrological processes depicted in this model it is necessary to consider the physical state of the rocks and the effect of likely geothermal gradients around the propagation zone to understand fully the mechanism and implications of this process. Firstly, it is suggested that the solidus isotherm would occur near the

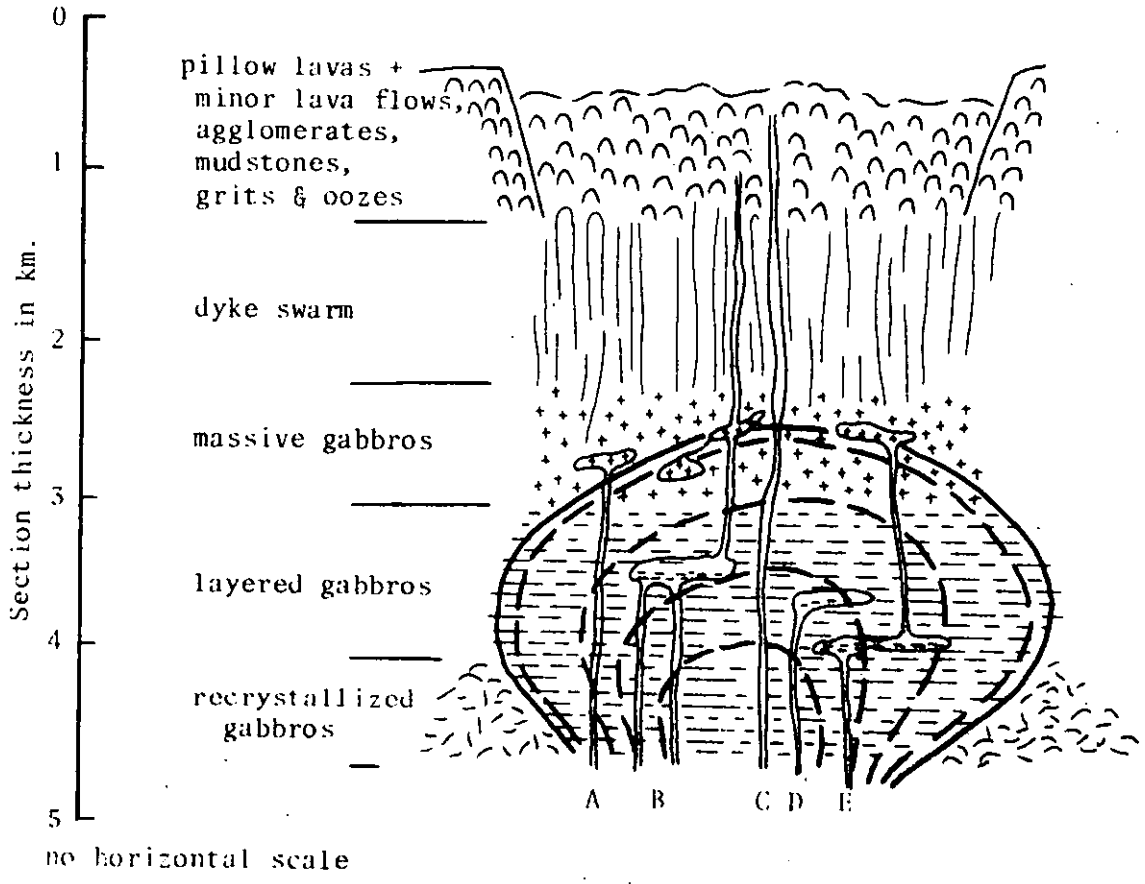

Depicted events:

A: primitive magma → gabbro.

B: mixing of two primitive magmas in small fractionation chamber then rising of "mixed" magma to surface.

C: direct ascent of primitive magma to surface.

D: complete entrapment of primitive magma.

E: primitive magma fractionation → gabbro.

— — possible isotherms ⌒ solidus

Figure 7.3 A schematic model of near-surface magma processes in the formation of Macquarie Island-type oceanic lithosphere.

top of the layered gabbros. [Note that this isotherm, and the others depicted on Figure 7.3, represent the average temperature of the area; localized anomalies will occur around newly arrived magma pockets and the paths of magma which is rising to higher levels in the section.] Secondly, the base of the layered gabbro sequence corresponds to the isotherm above which plagioclase is not a liquidus phase. Low pressure experimental studies of a primitive ocean-floor basalt composition by Green *et al.* (1979) indicate a range of temperatures between these isotherms would be 60°C. Including the recrystallized gabbros, for reasons discussed later, this would give a vertical geothermal gradient in this zone of around 30°C/km. The below-liquidus studies by Green *et al.* (1979) predicted a vertical increase in An content of the plagioclase within the layered gabbro sequence.

The concept of a distinct vertical geothermal gradient in this zone also provides, on the basis of this experimental work, an explanation for two characteristic features of plagioclase megacrysts or xenocrysts in ocean-floor basalts. Magma penetrating the layered gabbro sequence will be hotter than the surrounding material and consequently plagioclase if the host will not be in equilibrium and resorption must occur. If a plagioclase crystal is entrained from the host, reverse zoning will develop around the calcic core, together with resorption of the core until equilibrium is attained. This argument is also applicable to clinopyroxene entrained in ascending magmas but will be more extreme as it has been shown that clinopyroxene is further from the liquidus than plagioclase for liquids of these compositions (Green *et al.*, 1979).

The second implication in this model is that material in the central zone bounded by the solidus isotherm is in a quasi-solid state. This would facilitate penetration of magmas through this zone and also account for slump and drag features observed within the layered gabbro complex on Macquarie Island.

Within this model the recrystallized gabbros at the base of the gabbro section have undergone high temperature subsolidus recrystallization and deformation as the rocks move away from the propagation zone.

The following recommendations for further study would provide further constraints on the near-surface magmatic processes and evaluate the proposed model.

1. Microprobe studies of the mineralogy of layered gabbro sequences in vertical and lateral traverses. Two stages are recommended, firstly a reconnaissance examination of all available material to establish the major variation and a second stage on a local scale, as determined by results of the first stage, to provide information on the fractionation processes. Because the overall sequence is essentially a compositionally buffered system the first-stage results should reflect primarily the geothermal gradients in the propagation path. Second-stage results would be expected to show some evidence of intrusion of individual magma batches. The compatible trace element geochemistry of the phases should detail differences in source magmas even in rocks of similar major element compositions.

2. Low pressure experimental studies of primitive and evolved liquids on and below the liquidus should be performed to provide accurate information with regard to temperature and to test the hypothesis of plagioclase and clinopyroxene resorption and zoning following entrainment.

REFERENCES

Anderson, T.F., and Lawrence, J.R., 1976: Stable isotope investigation of sediments, basalts and authigenous phases from Leg 35 cores. In Hollister, C.D. *et al.* (eds): *Initial Reports of the Deep Sea Drilling Project, 35:* Washington (U.S. Govt Printing Office), 497-505.

Andrews, A.J., 1977: Low temperature fluid alteration of oceanic layer 2 basalts, DSDP leg 37. *Can. Jour. Earth Sci., 14,* 911-926.

_____ , Barnett, R.L., MacClement, B.A.E., Fyfe, W.S., Morrison, G., McRae, N.O., and Starkey, J., 1977: Zeolite facies metamorphism, geochemistry and some aspects of trace element redistribution in altered basalts of D.S.D.P. Leg 37. In Aumento, F., *et al.* (eds), *Initial Reports of the Deep Sea Drilling Project, 35:* Washington (U.S. Govt Printing Office), 795-810.

_____ , and Fyfe, W.S., 1976: Metamorphism and massive sulphide generation in oceanic crust. *Geoscience Canada, 3,* 84-94.

Aumento, F., 1968: The mid-Atlantic Ridge near 45°N. II: Basalts from the area of Confederation Peak. *Can. Jour. Earth Sci., 5,* 1-21.

_____ , Melson, W.G. *et al.*, 1977: Initial reports of the Deep Sea Drilling Project, Volume 37. Washington (U.S. Govt Printing Office), 1008pp.

Ballard, R.D., and van Andel, Tj.H., 1977: Morphology and tectonics of the inner rift valley at lat.36°50'N on the Mid-Atlantic Ridge. *Bull. Geol. Soc. Am., 88,* 507-530.

Baragar, W.R.A., Plant, A.G., Pringle, G.J., and Schau, M., 1977: The petrology of alteration in three discrete flow units of sites 332 and 335. In Aumento, F. *et al.* (eds), *Initial Reports of the Deep Sea Drilling Project, 35:* Washington (U.S. Govt. Printing Office), 811-820.

Bender, J.F., Hodges, F.N. and Bence, A.E., 1978: Petrogenesis of basalts from the Project FAMOUS area: experimental study from 0 to 15 kbars. *Earth Planet. Sci. Lett., 41*; 277-302.

Blount, C.W., and Dickson, F.W., 1969: The solubility of anhydrite ($CaSO_4$) in NaCl-H_2O from 100 to 450°C and 1 to 1000 bars. *Geochim. Cosmochim. Acta, 33*, 227-245.

Bloxam, J.W., and Lewis, A.D., 1972: Ti, Zr and Cr in some British pillow lavas and their petrogenetic affinities. *Nature Phys. Sci., 237*, 134-136.

Boles, J.R., 1977: Zeolites in low-grade metamorphic grades. In Mumpton, F.A., 1977, 103-137.

_____, and Coombs, D.S., 1977. Zeolite facies alteration of sandstone, Southland Syncline, New Zealand. *Am. Jour. Sci., 227*, 982-1022.

Bryan, W.B., and Moore, J.G., 1977: Compositional variations of young basalts in the mid-Atlantic ridge rift valley near 36°49'N. *Bull. Geol. Soc. Am., 88*, 556-570.

Bryan, W.G., Thompson, G., Frey, I.A., and Dickey, J.S., 1976: Inferred geologic settings and differentiation in basalts from the Deep Sea Drilling Project. *Jour. Geophys. Res., 81*, 4285-4304.

Butler, R.F., Banerjee, S.K., and Stout, J.H., 1976. Magnetic properties of oceanic pillow lavas: Evidence from Macquarie Island. *Geophys. Jour. Roy. Astr. Soc., 47*, 179-196.

Cameron, W.E., Nisbet, E.G., and Dietrich, V.J., 1979: Boninites, komatiites and ophiolitic basalts. *Nature, 280*, 550-553.

_____, 1980: Petrographic dissimilarities between ophiolitic and ocean floor basalts. *Proc. Int. Ophiolite Conf., Cyprus, 1979.*

Cann, J.R., 1970: Rb, Sr, Y, Zr, and Nb in some ocean-floor basaltic rocks. *Earth Planet. Sci. Lett., 10*, 7-11.

Cann, J.R., 1971. Major element variations in ocean floor basalts. *Phil. Trans. Roy. Soc. London, A268,* 495.

_____ , 1979: Metamorphism in the ocean crust, in: Deep drill results in the Atlantic Ocean, ocean crust: M. Talwani (Ed.). *Maurice Ewing Ser., Proc. Symp. No.2,* 230-238.

_____, Tarney, J., Varet, J., and Wood, D.A., 1978: Mantle heterogeneity in the North Atlantic: evidence from Leg 49 geochemistry. In: B.P. Luyendyke (Ed.) Deep Sea Drill. Proj., 49, 841-850.

Carmichael, I.S.E., Turner, F.J., & Verhoogen, J., 1974: *Igneous Petrology.* McGraw-Hill, New York.

Cocker, J.D., Griffin, B.J., and Muehlenbachs, K., 1979: Oxygen isotope geochemistry of the Macquarie Island ophiolite. *Trans. Am. Geophys. Union, 58,* 1111.

_____ , in prep.: Oxygen and carbon isotope geochemistry of the Macquarie Island ophiolite.

Coish, R.A., 1977: Ocean floor metamorphism in the Betts Cove ophiolite, Newfoundland. *Contr. Mineral. Petrol., 60.*

Coleman, R.G., 1977: *Ophiolites.* Springer-Verlag, Berlin. 229pp.

Colhoun, E., and Goede, A., 1973: A reconnaissance survey of the glaciation of Macquarie Island. *Pap. Proc. Roy. Soc. Tasm., 108,* 1-19.

Coombs, D.S., 1954: The nature and alteration of some Triassic sediments from Southland, New Zealand. *Trans. Roy. Soc. N.Z., 82,* 65-109.

_____ , 1961: Some recent work on the lower grade of metamorphism. *Aust. J. Sci., 24,* 203-215.

Cullen, D.J., 1969: Macquarie Island, provisional bathymetry, scale 1:200 000. Island Series, N.Z. Oceanogr. Inst., Wellington.

Deer, W.A., Howie, R.A., and Zussman, J., 1966: *An Introduction to the Rock-forming Minerals.* Longman Group Ltd, London.

Elthon, D., 1979: High magnesia liquids as the parental magma for ocean floor basalts. *Nature, 278,* 514-518.

Elthon, D., and Stern, C.R., 1978: Metamorphic petrology of the Sarmiento ophiolite complex, Chile. *Geology, 6,* 464-468.

Engel, A.E.G., Engel, C.G., and Havens, R.G., 1965: Chemical characteristics of oceanic basalts and the upper mantle. *Bull. Geol. Soc. Am., 76,* 719-734.

Erlank, A.J., and Kable, E.J.D., 1976: The significance of incompatible elements in the mid-Atlantic ridge basalts from 45°N with particular reference to Zr/Nb. *Contrib. Mineral. Petrol., 54,* 281-291.

Fehn, V., Cathles, L.M., and Holland, 1978. Hydrothermal convection and uranium deposits in abnormally radioactive plutons. *Econ. Geol., 73,* 1556-1566.

Flanigen, E.M., 1977: Crystal structure and chemistry of natural zeolites. In Mumpton, F.A. (ed.), 1977, 19-52.

Floyd, P.A., and Windchester, J.A., 1975: Magma type and tectonic setting discrimination using immobile elements. *Earth Planet. Sci. Lett., 27,* 211-218.

Foster, M.D., 1965: Studies of the zeolites. *U.S. Geol. Surv. Prof. Pap. 504D-E.*

Fyfe, W.S., 1973: Heats of chemical reactions and submarine heat production. *Geophys. Jour. Roy. Astr. Soc., 37,* 213-215.

_____ , 1974. Burial metamorphism: some thoughts on the present situation. *Canad. Mineral., 12,* 439-444.

_____ , Price, N.J., and Thompson, A.B., 1978: *Fluids in the Earth's Crust.* Elsevier, New York.

Green, D.H., 1970: The origin of basaltic and nephelinitic magmas. *Trans. Leicester Lit. Phil. Soc., 64,* 28-54.

Green, D.H. 1971: Composition of basaltic magmas as indicators of conditions of origin: application to oceanic vulcanism, in: A discussion on the petrology of igneous and metamorphic rocks from the ocean floor, Bullard, S.E., Cann, J.R. and Matthews, D.H. (Eds.), *Phil. Trans. R. Soc. Lond., 268,* 707-721.

_____, Hibberson, W.D., and Jaques, A.L., 1979: Petrogenesis of the mid-ocean ridge basalts. In McElhinny, M.W. (ed.), 1979, *The Earth: Its Origin, Structure and Evolution.* Academic Press, London.

_____ and Liebermann, R.C., 1976: Phase equilibria and elastic properties of a pyrolite model for the oceanic upper mantle. *Tectonophys., 32,* 61-92.

Griffin, B.J., 1978: Energy dispersive analysis system calibration and operation with TAS-SUEDS, an advanced interactive data production package. University of Tasmania, Geology Department Pub. 343, 44pp.

_____, 1980: Erosion and rabbits on Macquarie Island: some comments. *Pap. Proc. Roy. Soc. Tasm., 114,* 81-83.

_____ and Varne, R., 1979: The petrology of the Macquarie Island ophiolite association: Mid-Tertiary oceanic crust of the Southern Ocean. *Proc. Int. Ophiolite Symp., Cyprus, 1979,* 33-35.

_____, 1980: The Macquarie Island ophiolite complex: Mid-Tertiary oceanic lithosphere from a major ocean basin. *Chemical Geology, 30,* 285-304.

Griffiths, J.R., and Varne, R., 1972: Evolution of the Tasman Sea, Macquarie Ridge and Alpine Fault. *Nature Phys. Sci., 235,* 83-86.

Hanson, G.N., 1977: Evolution of the suboceanic mantle. *J. Geol. Soc. London, 134,* 235-253.

Hart, R., 1970: Chemical exchange between sea water and deep ocean basalts. *Earth Planet. Sci. Lett., 9,* 269-279.

Haskin, L.A., Haskin, M.A., Frey, F.A., and Wildeman, P., 1968: Relative and absolute terrestrial abundances of the rare earths, in: Origin and distribution of the elements, ed. L.H. Ahrens. Pergamon Press, New York: p.889.

Hayes, D.E., and Talwani, M., 1972: Geophysical investigation of the Macquarie ridge complex. In Hayes, D.E., (ed.), *Antarctic Oceanology II: The Australian-New Zealand Sector, Antarctic Res. Ser., 19:* A.G.U., Washington, D.C., 211-234.

Hiertzler, J.R., Dickson, G.D., Herron, E.M., Pitman, W.C.,III, and Le Pichon, X., 1968: Marine magnetic anomalies, geomagnetic field reversals and motions of the ocean floor and continents. *J. Geophys. Res, 73,* 2119-2136.

Ivanov, I.P., and Gurevich, L.P., 1975: Experimental studies of T-X_{CO_2} boundaries of metamorphic zeolite facies. *Contrib. Mineral. Petrol., 53,* 55-60.

Jakes, P., and Gill, J.B., 1970: Rare earth elements and the island arc tholeiite series. *Earth Planet. Sci. Lett., 9,* 17-28.

Jaques, A.L. and Green, D.H., 1980: Anhydrous melting of peridotite at 0-15 kb pressure and the genesis of tholeiitic basalts. *Contrib. Mineral. Petrol., 73,* 287-310.

Kay, R., Hubbard, N.J., and Gast, P.W., 1970: Chemical characteristics and origin of ocean ridge volcanic rocks. *J. Geophys. Res., 75,* 227-255.

Keith, T.E.C., Muffler, L.J.P., and Cremer, M., 1968: Hydrothermal epidote formed in the Salton Sea geothermal system, California. *Am. Mineral., 53,* 1635-1644.

Kristmannsdottir, H., and Tomasson, J., 1978: Zeolite zones in geothermal areas in Iceland. In Sand, L.B., and Mumpton, F.A., 1978, 277-284.

La Breque, J.L., Kent, D.V., and Cande, S.C., 1977: Revised magnetic polarity time-scale for Late Cretaceous and Cenozoic time. *Geology, 5,* 330-335.

Langmuir, C.H., Bender, J.F., Bence, A.E., Hanson, G.N., and Taylor, S.R., 1977: Petrogenesis of basalts from the Famous area: mid-Atlantic Ridge. *Earth Planet. Sci. Lett., 36,* 133-156.

Le Pichon, X., Francheteau, J., and Bonnin, J., 1973: *Plate Tectonics.* Elsevier, Amsterdam. 300pp.

Levi, S., Banerjee, S.K., Beske-Diehl, S., and Moskowitz, B., 1978: Limitations of ophiolite complexes as models for the magnetic layer of the oceanic lithosphere. *Geophys. Res. Letters, 5,* 473-476.

Liou, J.G., 1970: Synthesis and stability relations of wairakite, $CaAl_2Si_4O_{12}.2H_2O$. *Contr. Mineral. Petrol., 27,* 259-282.

_____, 1971a: P-T stabilities of laumontite, wairakite, lawsonite and related minerals in the system $CaAl_2Si_2O_8$-SiO_2-H_2O. *Jour. Petrol., 12,* 370-411.

_____, 1971b: Stilbite-laumontite equilibrium. *Contr. Mineral. Petrol., 31,* 171-177.

_____, 1971c: Synthesis and stability relations of prehnite, $Ca_2Al_2Si_3O_{10}(OH)_2$. *Amer. Mineral., 56,* 507-531.

_____ and Ernst, W.G., 1979: Ocean ridge metamorphism of the east Taiwan ophiolite. *Contr. Mineral. Petrol., 68,* 335-348.

Lugg, D.J., Johnstone, G.W., and Griffin, B.J., 1978: The outlying islands of Macquarie Island. *The Geographical Journal, 144,* 277-287.

Malpas, J., 1978: Magma generation in the upper mantle, field evidence from ophiolite suites and application to the generation of oceanic lithosphere. *Phil. Trans. Roy. Soc. London, Ser.A, 288,* 527-546.

Mawson, D., 1943: Macquarie Island, its geography and geology. Australasian Antarctic Expedition 1911-1914. Sci. Rept Sec.A: 5. Govt Printing Office, Sydney.

Melson, W.G., Byerly, G.R., Nelen, J.A., O'Hearn, T., Wright, T.L., and Vallier, T., 1976: A catalog of the major element chemistry of abyssal volcanic glasses. In Mason, B. (ed.), *Mineral Sciences Investigations, 1974-1975: Smithsonian Contrib. Earth Sci., 19,* 31-60.

_____, Thompson, G., and Van Andel, T.H., 1968: Volcanism and metamorphism in the mid-Atlantic Ridge, 22°N latitude. *J. Geophys. Res., 73,* 5925-5941.

Moore, J.G., 1970: Water content of basalt erupted on the ocean floor. *Contr. Mineral. Petrol., 28,* 272-279.

Muehlenbachs, K., 1977: Oxygen isotope geochemistry of rocks from DSDP Leg 37. *Canad. J. Earth Sci., 14,* 771-776.

_____, 1979: Alteration and aging of the basaltic layer of the sea floor: oxygen isotope evidence from DSDP/IPOD Legs 51, 52 and 53. In Donnelly, T., Francheteau, J., Bryan, W., Robinson, P., Flower, M., Salisbury, M., *et al.*, *Initial Reports of the Deep Sea Drilling Project, 51, 52, 53:* Washington (U.S. Govt Printing Office), 1159-1168.

Muir, I.O., and Tilley, C.E., 1964: Basalts from the northern parts of the rift zone of the mid-Atlantic Ridge. *Jour. Petrol., 5,* 409-434.

_____, 1966: Basalts from the northern part of the mid-Atlantic Ridge. II: The Atlantic collections near 30°N. *Jour. Petrol., 7,* 193-201.

Mumpton, F.A., 1977. Mineralogy and geology of natural zeolites. *Mineral. Soc. Am. Short Course Notes, 4,* 1-233.

Myashiro, A., Shido, F., and Ewing, M., 1969: Crystallisation and differentiation in abyssal tholeiites and gabbros from mid-oceanic ridges. *Earth Planet. Sci. Letters, 7,* 361-365.

_____, 1970: Diversity and origin of abyssal tholeiites from the mid-Atlantic Ridge near 24° and 30° north latitude. *Contr. Mineral. Petrol., 23,* 38-52.

_____, 1973. *Metamorphism and Metamorphic Belts.* George Allen and Unwin, London. 492pp.

Nicholls, G.D., 1964: Basalts from the deep ocean floor. *Min. Mag., 34,* 373-388.

Nisbet, E.G., and Fowler, C.M.R., 1978: The Mid-Atlantic Ridge at 37 and 45°N: some geophysical and petrological constraints. *Geophys. J. R. Astron. Soc., 54,* 631-660.

Palache, C., Berman, H., and Frondel, C., 1951: *Dana's System of Mineralogy.* Wiley & Sons, Inc., Washington.

Passaglia, E., 1970: The crystal chemistry of chabazites. *Am. Min., 55,* 1278-1301.

Pearce, J.A., 1975: Basalt geochemistry used to investigate past tectonic environments on Cyprus. *Tectonophysics, 25,* 41-67.

_____, and Cann, J.R., 1971: Ophiolite origin investigated by discriminant analysis using Ti, Zr and Y. *Earth Planet. Sci. Letters, 12,* 339-349.

_____, 1973: Tectonic setting of basic volcanic rocks determined using trace element analyses. *Earth Planet. Sci. Letters, 19,* 290-300.

_____ and Norry, M.J., 1979: Petrogenetic implications of Ti, Zr, Y and Nb variations in volcanic rocks. *Contrib. Mineral. Petrol., 69,* 33-47.

Pearce, J.A., Alabaster, T., Shelton, A.W. and Searle, M.P., 1981: The Oman ophiolite as a Cretaceous arc-basin complex: evidence & implications *Phil. Trans. R. Soc. London, 300,* 299-317.

Piispanen, R., and Alapieti, T., 1977: Uralitisation - an example from Kuusamo, Finland. *Geol. Soc. Finland Bull., 49,* 39-46.

Pineau, F., Javay, M., Hawkins, J.W., and Craig, H., 1976: Oxygen isotope variations in marginal basins and ocean ridge basalts. *Earth Planet. Sci. Letters, 28,* 299-307.

Ploshko, V.V., Bogdanov, Y.A., Emel'yanov, E.M., and Knyazeva, D.N., 1971. Gabbroic rocks from the Romanche Trench (Atlantic Ocean). *Oceanology, 11,* 361-371.

Pritchard, R.G., Cann, J.R., and Wood, D.A., 1979: Low-temperature alteration of oceanic basalts. In Luyendyk, B.D., *et al., Deep Sea Drilling Project Initial Rept, 49,* 709-714.

Quilty, P.G., Rubenach, M., and Wilcoxon, J.A., 1973: Miocene ooze from Macquarie Island. *Search, 4,* 163-164.

Robinson, P.T., Flower, M.F.J., Schminke, H.U., and Ohnmacht, W., 1977: Low temperature alteration of oceanic basalts, DSDP Leg 37. In Aumento, F., *et al.*, 1977, 775-794.

Rodgers, K.A., 1973: Chrome spinels from the Massif du Sud, southern New Caledonia. *Min. Mag., 39,* 326-339.

Rusinov, V.L., 1965: On prehnite finds and the nature of epidote in rocks of some areas of contemporary hydrothermal metamorphism. *Izvest. Akad. Nauk. USSR Geol. Ser., 2,* 33-43.

Sand, L.B., and Mumpton, F.A., 1978. *Natural Zeolites: Occurrence, Properties, Use.* Pergamon Press, Sydney. 546pp.

Schilling, J.G., 1971: Sea-floor evolution: rare-earth evidence. *Phil. Trans. Roy. Soc. London, A268,* 663.

_____ , and Ridley, W.I., 1975: Volcanic rocks from DSDP Leg 29: petrography and rare earth abundances. In Kennet, J.P., Houtz, R.E., *et al., Initial Reports of the Deep Sea Drilling Project, volume 29*: Washington (U.S. Govt Printing Office), 1103-1107.

Schweitzer, E.L., Papike, J.J., and Bence, A.E., 1978: Clinopyroxenes from deep sea basalts; a statistical analysis. *Geophys. Res. Lett., 5,* 573-576.

Seki, Y., 1972: Lower-grade stability limit of epidote in the light of natural occurrences. *J. Geol. Soc. Japan, 78,* 405-413.

Smewing, J.D., 1975: Metamorphism of the Troodos Massif, Cyprus. Unpub. Ph.D. thesis, The Open University.

Spooner, E.T.C., and Bray, C.J., 1977: Hydrothermal fluids of seawater salinity in ophiolitic sulphide ore deposits in Cyprus. *Nature, 266,* 808-812.

Staudigel, H., Hart, S.R. & Richardson, S.H., 1981: Alteration of the ocean crust: processes and timing. *Earth Planet. Sci. Lett., 52,* 311-327.

Steiner, A., 1977: The Wairakei geothermal area, North Island, New Zealand. *Bull. N.Z. Geol. Surv., 90,* 1-136.

Sukheswala, R.N., Avas, R.K., and Gangodadhyay, M., 1974: Zeolite and associated secondary minerals in the Deccan Traps of western India. *Min. Mag., 39,* 658-671.

Summerhayes, C.P., 1974: Macquarie-Balleny Ridge. In Spencer, R.M. (ed.), *Mesozoic-Cainozoic orogenic belts: data for orogenic studies.* Edinburgh: Scottish Academic Press for the Geological Society, London, 381-384.

Sun, S-S., Nesbitt, R.W., and Sharaskin, A.Y., 1979: Geochemical characteristics of mid-ocean ridge basalts. *Earth Planet. Sci. Letters, 44,* 119-138.

Tarney, J., Wood, D.A., Saunders, A.D., Cann, J.R., and Varet, J., 1980: Nature of mantle heterogeneity in the North Atlantic: evidence from deep sea drilling. *Phil. Trans. R. Soc. London, A297,* 179-202

Taylor, H.P., Jr., 1968: The oxygen isotope geochemistry of igneous rocks. *Contrib. Mineral. Petrol., 19,* 1-71.

Thompson, G., 1973: A geochemical study of the low-temperature interaction of seawater and oceanic igneous rocks. *EOS Trans. AGU, 54,* 1015-1018.

_____, Shido, F., and Myashiro, A., 1972: Trace-element distributions in fractionated oceanic basalts. *Chem. Geol., 9,* 89-97.

Tomasson, J., and Kristmannsdottir, H., 1972: High temperature alteration minerals and thermal brines, Reykjanes, Iceland. *Contr. Mineral. Petrol., 36,* 123-134.

Varne, R., Gee, R.D., and Quilty, P.G., 1969: Macquarie Island and the cause of oceanic linear magnetic anomalies. *Science, 166,* 230-233.

_____, and Graham, A.L., 1972: Rare earth abundances in hornblende and clinopyroxene of a hornblende lherzolite xenolith: implications for upper mantle fractionation processes. *Earth Planet. Sci. Lett., 13,* 11-18.

_____, and Rubenach, M.J., 1972: Geology of Macquarie Island and its relationship to oceanic crust. In Hayes, D.E. (ed.), *Antarctic Oceanology. II: The Australian-New Zealand Sector.* Antarctic Res. Ser., A.G.U., Geophys. Mon. 19, 251-266.

Varne, R. and Rubenach, M.J. , 1973: Geology of Macquarie Island in relation to tectonic environment, in: P.J. Coleman (Ed.) The Western Pacific: Island Arcs, Marginal Seas, Geochemistry. University of Western Australia Press, Perth, W.A.

Vollmer, R., 1976: Rb-Sr and U-Th-Pb systematics of alkaline rocks from Italy. *Geochim. Cosmochim. Acta, 40,* 283-296.

Walton, A.W., 1975: Zeolitic sediments, Trans-Peco, Texas. *Bull. Geol. Soc. Am., 86,* 615-624.

Weissel, J.K., and Hayes, D.E., 1972: Magnetic anomalies in the southeast Indian Ocean. In Hayes, D.E. (ed.), *Antarctic Oceanology. II: The Australia-New Zealand Sector.* Antarctic Res. Ser., A.G.U., Geophys. Mon. 19, 165-196.

Williamson, P., 1974: Recent studies of Macquarie Island and the Macquarie Ridge Complex. *Bull. A.S.E.G., 5,* 19-22.

_____ , 1979: The paleomagnetism of outcropping oceanic crust on Macquarie Island. *J. Geol. Soc. Aust., 25,* 387-394.

Wood, D.A., 1979a: Dynamic partial melting: its application to the petrogeneses of basalts erupted in Iceland, the Faeroe Islands, the Isle of Skye (Scotland) and the Troodos Massif (Cyprus). *Geochim. Cosmochim. Acta, 43,* 1031-1046.

_____ , 1979b: A variably veined sub-oceanic upper mantle - genetic significance for mid-ocean ridge basalts from geochemical evidence. *Geology, 7,* 499-503.

Wood, D.A., 1981: Partial melting models for the petrogenesis of Reykjanes Peninsula basalts, Iceland: implications for the use of trace elements and strontium and neodymium isotope ratios to record inhomogeneities in the upper mantle. *Earth Planet. Sci. Letters, 52,* 183-190.

_____, Gibson, I.L., and Thompson, R.N., 1976: Element mobility during zeolite facies metamorphism of the Tertiary basalts of eastern Iceland. *Contrib. Mineral. Petrol., 55,* 241.

_____, Tarney, J., Varet, J., Saunders, A.D., Bougault, H., Joron, J.L., Treuil, M., and Cann, J.R., 1979a: Geochemistry of basalts drilled in the North Atlantic by IPOD Leg 49: implications for mantle heterogeneity. *Earth Planet. Sci. Letters, 42,* 72-97.

_____, Joron, J.L., and Treuil, M., 1979b: A re-appraisal of the use of trace elements to classify and discriminate between magma series erupted in different tectonic settings. *Earth Planet. Sci. Letters, 45,* 326-336.

Yoder, H.S., and Tilley, C.E., 1962: Origin of basalt magmas: an experimental study of natural and synthetic rock systems. *J. Petrol., 3,* 342-532.

Zen, E-an, 1961: The zeolite facies: an interpretation. *Am. Jour. Sci., 259,* 401-409.

_____, 1974: Bunal metamorphism. *Canad. Mineral., 12,* 445-455.

_____, and Thompson, A.B., 1974: Low grade regional metamorphism: mineral equilibrium relations. *Ann. Rev. Earth Planet. Sci., 2,* 179-213.

APPENDIX 1

MAJOR ELEMENT ANALYSES AND C.I.P.W. NORM CALCULATIONS FOR MACQUARIE ISLAND LAVAS AND DYKES

Section A: Major element analyses.

Section B: Major element analyses recalculated volatile-free with Fe^{2+}:total Fe = 0.85, and trace element analyses.

Analytical methods and instrument settings are given in Appendix 6.

Unless marked as below the analyses were performed by the author:

* P. Robinson, analyst, University of Tasmania.

1 J. Cann, University of Newcastle upon Tyne, England.

2 P. Hellman, University of Cambridge, England.

3 J. Cocker, University of Alberta, Canada.

APPENDIX 1: Section A MAJOR ELEMENT ANALYSES OF MACQUARIE ISLAND LAVAS AND DYKES

1. LAVAS

Sample No.	3A	7	35	43B/A	43B/B	56A	56D	56G	56I	60	108C	108E	119
SiO_2	44.84	47.21	44.68	50.20	49.24	48.17	48.58	49.76	47.80	47.52	49.17	50.20	48.79
TiO_2	2.02	1.08	1.45	1.59	1.60	1.03	1.03	1.06	1.05	0.96	1.35	1.30	1.23
Al_2O_3	16.94	17.84	16.00	15.81	16.15	18.68	18.95	18.34	18.51	20.10	15.22	14.79	16.11
Fe_2O_3	3.27	3.74	5.24	4.09	5.09	2.17	1.45	2.27	2.47	2.21	5.05	4.69	3.68
FeO	4.72	3.50	2.85	4.68	4.06	4.45	4.35	4.07	4.46	3.57	5.30	5.95	4.55
MnO	0.14	0.13	0.11	0.19	0.19	0.12	0.12	0.11	0.12	0.10	0.15	0.15	0.16
MgO	7.18	7.27	6.56	6.67	7.31	7.94	7.79	8.07	8.08	7.12	7.29	7.25	7.76
CaO	10.97	10.91	12.29	9.87	10.36	11.72	12.33	11.91	12.25	11.98	11.52	10.85	10.42
Na_2O	3.03	3.38	3.21	3.66	3.27	2.95	2.59	3.19	2.57	2.91	2.85	2.91	3.45
K_2O	1.52	0.53	0.92	0.84	0.63	0.25	0.20	0.25	0.20	0.29	0.51	0.51	0.70
P_2O_5	0.62	0.22	0.39	0.28	0.29	0.17	0.17	0.21	0.17	0.17	0.20	0.18	0.20
L.O.I.	4.50	3.93	5.72	1.81	1.71	2.08	1.63	2.75	1.89	2.61	1.75	1.35	2.75
Total	99.75	99.74	99.42	99.59	99.95	99.71	99.21	100.19	99.58	99.53	100.37	100.13	99.82
$Fe^{2+}/Fe^{2+}+Fe^{3+}$	0.62	0.51	0.38	0.56	0.47	0.70	0.77	0.67	0.67	0.64	0.54	0.59	0.58

Sample No.	139	147	151	157	199	202	206	210	212	214	226	228	233
SiO_2	47.11	51.27	49.55	46.30	48.98	46.95	49.26	49.27	46.85	48.72	49.22	45.85	48.19
TiO_2	0.91	1.63	0.82	0.98	1.63	0.86	1.25	1.46	0.60	1.34	1.45	1.00	1.39
Al_2O_3	20.21	14.65	21.63	18.63	15.43	21.21	16.98	14.91	22.90	14.72	15.15	19.19	16.68
Fe_2O_3	1.99	3.59	0.59	3.89	4.02	2.63	2.24	4.02	2.38	3.81	3.68	2.73	3.30
FeO	4.45	6.77	4.73	2.67	5.86	3.95	5.71	6.92	3.89	6.40	5.81	3.36	4.10
MnO	0.10	0.19	0.11	0.11	0.18	0.11	0.14	0.21	0.11	0.17	0.15	0.10	0.13
MgO	6.92	7.13	6.04	7.19	6.59	6.15	7.35	7.11	6.14	7.27	7.32	6.61	7.20
CaO	9.97	8.46	12.05	11.83	10.31	12.64	10.34	10.31	12.80	10.98	9.71	11.30	10.72
Na_2O	3.92	3.59	2.37	2.64	3.20	2.54	3.41	3.48	2.40	3.49	3.96	2.94	3.54
K_2O	0.45	1.06	0.26	0.83	0.48	0.14	0.27	0.39	0.18	0.25	0.29	0.97	0.90
P_2O_5	0.14	0.19	0.15	0.20	0.21	0.10	0.21	0.17	0.06	0.17	0.19	0.20	0.40
L.O.I.	3.73	2.10	2.29	3.67	1.76	2.14	2.83	2.16	1.95	2.20	2.20	4.52	2.61
Total	99.90	100.65	100.59	98.94	98.65	99.42	99.99	100.40	100.26	99.52	99.11	98.77	99.17
$Fe^{2+}/Fe^{2+}+Fe^{3+}$	0.71	0.68	0.90	0.43	0.62	0.63	0.74	0.66	0.64	0.65	0.64	0.58	0.57

Sample No.	234	235	236	38151	38188	38201	38226	38241*	38265*	38280	38284	38288	38291*
SiO_2	49.15	40.64	47.19	49.55	46.69	46.56	49.30	48.29	46.46	44.69	46.29	46.72	47.69
TiO_2	1.08	0.33	0.68	1.31	1.25	1.00	1.42	1.01	1.65	1.36	1.61	1.34	1.57
Al_2O_3	16.95	5.85	19.44	15.21	15.81	18.95	15.36	18.65	16.37	16.93	16.14	17.45	16.76
Fe_2O_3	3.45	4.58	3.01	4.35	3.36	1.78	5.04	3.57	8.44	3.13	4.68	4.15	7.55
FeO	4.27	5.06	3.20	4.00	4.84	4.95	4.89	3.71		5.99	3.62	3.07	
MnO	0.13	0.14	0.09	0.17	0.14	0.11	0.18	0.14	0.15	0.17	0.13	0.12	0.15
MgO	9.25	29.31	7.71	7.13	10.77	8.12	6.22	7.22	7.89	7.95	8.88	8.59	8.46
CaO	10.23	4.54	11.93	7.45	10.33	8.31	11.05	12.32	11.06	12.23	9.73	10.56	9.63
Na_2O	2.73	0.22	2.79	1.89	2.78	2.90	3.30	3.04	2.46	2.66	2.59	2.66	2.20
K_2O	0.64	0.04	0.58	4.95	0.38	0.20	0.46	0.32	1.30	0.55	0.84	0.90	1.97
P_2O_5	0.20	0.05	0.09	0.24	0.27	0.15	0.28	0.20	0.42	0.92	0.40	0.35	0.44
L.O.I.	2.69	8.68	3.18	3.03	3.39	5.93	2.31	2.19	3.50	3.30	3.85	3.44	3.14
Total	101.24	99.44	99.89	99.28	100.01	98.96	99.81	100.67	99.70	99.88	98.76	99.35	99.56
$Fe^{2+}/Fe^{2+}+Fe^{3+}$	0.58	0.55	0.54	0.51	0.62	0.76	0.52	0.54	-	0.68	0.46	0.45	-

Sample No.	38292	38297	38301	38303	38306*	38307	38310	38314	38315	38325	38331	38335	38336
SiO_2	48.36	46.83	48.99	47.58	46.14	48.10	47.52	47.09	46.85	47.66	49.01	48.84	48.24
TiO_2	1.07	1.16	1.24	1.19	1.40	1.55	1.36	1.50	0.91	1.41	1.41	1.44	1.19
Al_2O_3	19.38	16.63	17.17	18.02	15.39	15.31	16.97	17.43	19.34	15.57	17.62	15.84	17.04
Fe_2O_3	1.68	3.39	2.78	4.46	3.58	4.81	3.95	3.64	2.75	5.62	4.39	3.94	3.88
FeO	4.13	3.56	4.15	2.81	4.62	4.33	3.33	3.94	3.25	3.61	3.06	6.24	4.48
MnO	0.12	0.13	0.13	0.12	0.13	0.18	0.13	0.14	0.10	0.15	0.13	0.20	0.13
MgO	6.39	8.72	7.25	6.02	9.01	6.92	7.52	8.51	6.35	7.37	7.40	7.19	7.13
CaO	10.88	9.52	10.48	10.34	11.34	9.13	10.15	10.25	12.19	10.81	10.64	10.92	10.03
Na_2O	3.70	3.95	4.03	3.77	2.66	3.35	3.09	2.57	2.84	3.35	2.91	3.71	3.71
K_2O	0.63	0.58	0.98	0.86	0.62	1.52	1.42	1.14	0.57	0.76	1.12	0.10	0.94
P_2O_5	0.20	0.24	0.27	0.23	0.29	0.49	0.37	0.38	0.16	0.27	0.49	0.16	0.19
L.O.I.	2.31	4.28	2.83	3.44	3.94	2.98	4.13	3.26	4.74	2.57	0.86	2.02	3.20
Total	99.75	98.99	100.28	98.84	99.12	98.67	99.95	99.85	100.05	99.17	99.05	100.61	100.17
$Fe^{2+}/Fe^{2+}+Fe^{3+}$	0.73	0.54	0.62	0.41	0.59	0.50	0.48	0.55	0.57	0.42	0.44	0.64	0.56

APPENDIX 1: Section A continued

Sample No.	38389	38391	38423	38428*	38434	38462	38473	38478	40434
SiO_2	45.51	47.53	48.81	50.99	47.90	47.00	47.00	46.31	47.68
TiO_2	1.36	1.23	1.66	1.62	1.94	1.13	1.30	0.95	1.14
Al_2O_3	16.25	16.84	17.15	15.33	15.62	19.90	17.15	20.38	18.33
Fe_2O_3	4.70	3.52	4.63	10.30	3.61	4.34	4.40	3.17	2.21
FeO	3.67	4.42	4.76		6.13	2.40	3.28	2.77	5.46
MnO	0.15	0.12	0.17	0.18	0.19	0.11	0.14	0.12	0.15
MgO	8.11	7.67	6.49	5.96	8.63	6.11	7.40	6.71	6.91
CaO	11.73	12.37	11.58	8.90	8.96	11.81	11.29	11.86	10.24
Na_2O	2.91	2.87	3.25	4.14	2.82	3.12	2.54	2.47	3.66
K_2O	0.63	0.59	0.10	0.29	0.58	0.95	0.94	0.91	0.19
P_2O_5	0.27	0.24	0.27	0.22	0.42	0.26	0.31	0.22	0.16
L.O.I.	4.51	2.28	1.18	1.41	3.69	2.98	3.80	3.81	2.87
Total	99.80	99.77	100.03	99.34	100.59	100.11	99.55	99.68	99.00
$Fe^{2+}/Fe^{2+}+Fe^{3+}$	0.46	0.58	0.53	-	0.65	0.38	0.45	0.49	0.73

2. DYKES

Sample No. / Host	53 V	64 V	124 V	139 V	153 V	201 V	220 V	231 V	233 V	38133
SiO_2	48.66	45.98	47.52	48.98	48.27	48.38	46.60	47.81	46.79	48.99
TiO_2	1.84	1.41	1.45	1.36	2.49	1.84	0.78	1.31	1.29	1.54
Al_2O_3	15.16	16.76	15.29	15.34	14.30	15.31	19.79	15.78	17.11	14.64
Fe_2O_3	5.06	2.79	6.16	3.85	1.56	5.34	2.73	3.37	2.32	5.86
FeO	6.03	4.92	4.15	6.33	6.95	5.97	4.36	5.17	4.96	4.17
MnO	0.20	0.14	0.17	0.20	0.11	0.18	0.10	0.13	0.14	0.17
MgO	6.49	7.12	6.45	7.65	6.88	6.98	8.19	7.97	9.05	6.60
CaO	10.35	12.37	10.74	11.45	11.25	10.90	12.49	11.00	10.96	9.40
Na_2O	3.64	3.22	3.92	3.10	3.04	2.79	2.34	3.36	2.61	4.15
K_2O	0.40	1.16	0.49	0.13	0.30	0.53	0.09	0.28	0.79	0.12
P_2O_5	0.30	0.79	0.17	0.16	0.31	0.24	0.12	0.21	0.36	0.24
L.O.I.	1.42	3.68	3.00	1.85	5.03	2.07	2.19	2.47	2.93	2.31
Total	99.73	100.18	99.52	100.40	100.52	99.06	99.78	98.81	98.31	98.21
$Fe^{2+}/Fe^{2+}+Fe^{3+}$	0.57	0.66	0.43	0.65	0.83	0.55	0.64	0.63	0.70	0.44

Sample No. / Host	38136 G	38137 V	38157 V	38206 V	38223* V	38236 DS	38237 DS	38242* DS	38249 G	38273* DS
SiO_2	39.55	48.90	50.13	49.69	46.41	49.84	48.63	47.66	50.19	48.24
TiO_2	0.01	0.93	1.65	1.20	1.37	1.66	0.76	1.02	1.10	1.56
Al_2O_3	22.83	17.74	13.82	15.36	16.74	14.28	20.68	15.48	15.57	15.55
Fe_2O_3	2.83	1.07	2.74	2.98	7.30	1.49	1.29	1.55	1.25	9.55
FeO	2.93	5.18	7.81	6.23		9.03	4.57	7.69	3.14	
MnO	0.07	0.12	0.18	0.16	0.15	0.17	0.12	0.16	0.06	0.18
MgO	11.00	7.14	7.75	7.82	7.17	7.43	6.72	9.43	9.36	6.96
CaO	14.50	10.10	9.27	11.32	12.03	9.41	13.40	11.65	11.45	10.76
Na_2O	0.77	4.02	3.53	2.51	2.42	3.00	2.06	2.44	3.56	3.24
K_2O	0.07	0.18	0.20	0.11	1.16	0.11	0.11	0.12	0.26	0.65
P_2O_5	0.01	0.14	0.21	0.13	0.34	0.28	0.11	0.13	0.17	0.28
L.O.I.	4.50	3.43	2.72	1.20	3.86	3.26	1.82	2.28	2.67	2.38
Total.	99.08	98.94	100.02	98.73	98.95	99.99	100.28	99.61	98.78	99.35
$Fe^{2+}/Fe^{2+}+Fe^{3+}$	0.54	0.84	0.76	0.70	-	0.87	0.80	0.85	0.74	-

Sample No. / Host	38320 DS	38334* DS	38335 V	38337* V	38397* V	38425 DS	38449* DS	38451* DS	38471* V	38493* G
SiO_2	48.73	48.79	48.84	49.37	47.92	49.52	49.74	47.51	44.79	50.15
TiO_2	1.05	1.10	1.44	1.67	1.16	1.74	1.17	0.59	1.15	1.56
Al_2O_3	15.02	16.07	15.84	14.71	16.79	14.86	14.97	21.16	14.95	16.66
Fe_2O_3	1.57	0.27	3.94	4.93	7.95	9.48	9.21	0.48	8.89	8.26
FeO	6.94	8.48	6.24	7.25				5.30		
MnO	0.17	0.17	0.20	0.16	0.18	0.16	0.15	0.11	0.16	0.09
MgO	8.93	9.32	7.19	6.73	8.22	6.89	8.74	6.24	13.50	7.77
CaO	11.44	10.10	10.92	10.87	11.02	10.90	11.75	13.12	10.08	10.22
Na_2O	2.35	2.16	3.71	3.54	2.77	3.03	2.07	2.34	1.91	2.34
K_2O	0.17	1.14	0.10	0.18	0.14	0.36	0.15	0.08	0.57	0.49
P_2O_5	0.12	0.14	0.16	0.21	0.15	0.25	0.16	0.07	0.22	0.20
L.O.I.	2.50	3.39	2.02	1.39	2.91	1.34	0.94	2.42	3.21	1.67
Total	99.00	100.92	100.61	101.01	99.21	98.53	99.05	99.43	99.43	99.41
$Fe^{2+}/Fe^{2+}+Fe^{3+}$	0.83	0.97	0.64	0.62	-		-	0.92	-	-

Host Key:

V = intruding volcanic

DS = in dyke swarm

G = intruding gabbros

Appendix 1: Section B GLASS AND RECALCULATED ROCK MAJOR ELEMENT AND TRACE ELEMENT ANALYSES OF MACQUARIE ISLAND LAVAS AND DYKES

1. GLASSES†

Sample No.	4A	155	157	252	422	38390	40428	47142	47979	47989	47990
SiO_2	48.94	49.05	48.95	50.29	49.16	51.02	50.06	49.25	49.24	48.72	49.08
TiO_2	1.52	1.33	1.38	1.83	1.92	1.71	1.14	1.59	1.06	2.00	1.68
Al_2O_3	18.20	17.28	17.29	17.40	18.08	16.27	16.43	16.27	17.20	18.37	18.05
Fe_2O_3											
FeO	7.37	7.89	8.01	7.72	7.86	9.52	8.53	9.64	8.24	7.06	7.26
MnO	-	-	-	-	-	-	-	-	-	-	-
MgO	7.84	8.41	8.43	7.70	6.51	7.14	8.72	8.68	9.27	6.50	7.31
CaO	11.36	12.53	12.55	10.03	11.15	10.70	12.38	11.19	12.50	11.30	11.62
Na_2O	3.78	2.92	2.77	3.90	4.12	3.06	2.41	3.10	2.50	4.30	3.76
K_2O	0.89	0.59	0.57	1.14	1.21	0.59	0.19	0.29	-	1.77	1.24
P_2O_5	nd	nd	nd	nd	nd	nd	nd	nd	nd	nd	nd
100Mg/Mg+Fe	65.5	65.5	65.2	64.0	59.6	57.2	64.6	61.6	66.7	62.3	64.2
CaO/Al_2O_3	0.624	0.725	0.726	0.576	0.617	0.658	0.753	0.688	0.727	0.615	0.644

† Each glass analysis is an average of at least three microprobe analyses.

2. LAVAS

Sample No.	3A	7	35	43B/A	43B/B	56A	56D	56G	56I	60	108C	108E
SiO_2	47.18	48.56	47.90	50.33	51.43	49.39	49.81	49.28	49.00	49.08	50.03	50.97
TiO_2	2.13	1.11	1.56	1.64	1.63	1.05	1.06	1.08	1.08	1.00	1.37	1.32
Al_2O_3	17.82	20.06	17.15	16.51	16.20	19.15	19.43	18.84	18.97	20.76	15.49	15.02
Fe_2O_3	1.34	1.18	1.35	1.48	1.43	1.09	1.97	1.05	1.15	0.96	1.67	1.72
FeO	6.85	6.01	6.88	7.57	7.27	5.58	4.92	5.35	5.83	4.88	8.53	8.77
MnO	0.15	0.14	0.12	0.19	0.20	0.12	0.12	0.11	0.12	0.10	0.15	0.15
MgO	7.55	7.48	7.03	7.47	6.83	8.14	7.99	8.29	8.29	7.36	7.42	7.37
CaO	11.54	11.22	13.17	10.59	10.11	12.02	12.65	12.24	12.55	12.37	11.72	11.02
Na_2O	3.19	3.48	3.44	3.34	3.75	3.02	2.66	3.28	2.63	3.01	2.90	2.95
K_2O	1.60	0.54	0.99	0.64	0.86	0.26	0.21	0.26	0.21	0.30	0.52	0.52
P_2O_5	0.65	0.23	0.41	0.30	0.29	0.17	0.18	0.22	0.17	0.18	0.20	0.18
100Mg/Mg+Fe	62.5	65.3	60.8	60.0	58.7	69.0	71.0	70.1	68.2	69.5	56.9	56.0
CaO/Al_2O_3	0.648	0.559	0.768	0.641	0.624	0.628	0.651	0.650	0.662	0.596	0.757	0.734
Ti (wt.%)	1.28	0.67	0.94	0.98	0.98	0.63	0.64	0.65	0.65	0.60	0.82	0.79
Ni (ppm)	-	105	189	55	61	87	87	86	92	94	54	49
Cr	-	360	358	142	137	311	294	294	273	405	103	110
Zr	-	63	114	115	117	71	60	68	61	64	78	82
Y	-	23	26	39	38	18	20	23	23	21	40	41
Nb	-	20	30	21	23	14	12	14	14	12	8	8
Rb	-	9	18	12	10	1	0	4	0	3	13	14
Sr	-	239	311	221	197	213	210	207	199	212	145	133
Co	-	-	-	37	37	30	30	32	30	-	40	41
Sc	-	-	-	36	35	34	35	35	35	-	42	42
Zr/Y	-	2.74	4.4	2.95	3.08	3.94	3.0	2.96	2.65	3.05	1.95	2.0
Zr/Nb	-	3.2	3.8	5.5	5.1	5.1	5.0	4.9	4.4	5.3	9.8	10.3

Appendix 1: Section B cont.

Sample No.	119	139	147	151	157	199	202	206	210	212	214	228
SiO_2	50.38	49.03	52.13	50.39	48.74	50.68	48.33	50.75	50.26	47.71	50.17	48.74
TiO_2	1.28	0.95	1.65	0.83	1.02	1.69	0.89	1.28	1.50	0.61	1.38	1.06
Al_2O_3	16.64	21.04	14.89	22.00	19.60	15.97	21.84	17.50	15.21	23.33	15.16	20.40
Fe_2O_3	1.36	1.08	1.69	0.89	1.08	1.64	1.09	1.33	1.80	1.03	1.69	1.03
FeO	6.90	5.51	8.65	4.55	5.53	8.34	5.54	6.77	9.14	5.23	8.61	5.25
MnO	0.17	0.11	0.20	0.11	0.12	0.18	0.11	0.14	0.22	0.11	0.17	0.11
MgO	8.01	7.20	7.26	6.14	7.57	6.82	6.34	7.57	7.26	6.25	7.48	7.02
CaO	10.77	10.38	8.60	12.26	12.45	10.66	13.01	10.65	10.52	13.03	11.31	12.01
Na_2O	3.56	4.08	3.65	2.41	2.78	3.31	2.62	3.51	3.52	2.45	3.60	3.12
K_2O	0.72	0.46	1.08	0.27	0.88	0.50	0.14	0.28	0.40	0.19	0.26	1.03
P_2O_5	0.21	0.15	0.20	0.15	0.21	0.21	0.10	0.22	0.17	0.06	0.17	0.21
100Mg/Mg+Fe	63.7	66.5	56.1	67.2	67.6	55.3	63.4	62.9	54.5	64.4	56.8	67.0
CaO/Al_2O_3	0.647	0.493	0.578	0.557	0.635	0.668	0.596	0.609	0.692	0.559	0.746	0.589
Ti (wt.%)	0.77	0.57	0.99	0.50	0.61	1.01	0.53	0.77	0.90	0.37	0.83	0.64
Ni (ppm)	75	114	72	71	112	77	101	87	52	90	59	94
Cr	175	382	214	276	357	213	354	318	138	270	135	272
Zr	72	58	102	52	63	104	58	78	89	32	74	63
Y	30	20	45	13	17	41	24	26	37	15	29	17
Nb	13	10	10	12	21	11	5	14	7	1	10	20
Rb	11	4	18	0	10	10	2	0	9	3	5	14
Sr	222	186	152	233	339	140	167	192	151	132	145	310
Co	-	-	-	-	33	-	-	-	-	-	-	-
Sc	-	-	-	-	29	-	-	-	-	-	-	-
Zr/Y	2.40	2.9	2.27	4.0	3.71	2.54	2.42	3.0	2.41	2.13	2.55	3.71
Zr/Nb	5.5	5.8	10.2	4.3	3.0	9.5	11.6	5.6	12.7	3.2	7.4	3.2

Sample No.	233	234	235	236	38151	38188	38201	38214	38226	38241	38265	38267
SiO_2	50.03	50.23	44.92	48.89	51.64	48.42	50.08	52.95	50.74	49.17	48.66	48.84
TiO_2	1.44	1.10	0.36	0.70	1.36	1.29	1.07	1.68	1.47	1.03	1.73	1.03
Al_2O_3	17.32	17.32	6.47	20.14	15.85	16.40	20.38	15.92	15.80	18.99	17.15	20.77
Fe_2O_3	1.22	1.25	1.69	1.02	1.37	1.36	1.17	1.48	1.62	1.18	1.33	1.09
FeO	6.24	6.40	8.63	5.21	7.01	6.93	5.99	7.53	8.24	5.98	6.76	5.61
MnO	0.13	0.13	0.16	0.09	0.18	0.15	0.12	0.19	0.19	0.14	0.16	0.13
MgO	7.48	9.45	32.41	7.99	7.43	11.17	8.74	6.19	6.40	7.34	8.26	6.04
CaO	11.13	10.46	5.01	12.36	7.77	10.71	8.94	9.24	11.38	12.54	11.58	13.23
Na_2O	3.67	2.79	0.25	2.90	1.97	2.89	3.12	4.30	3.39	3.10	2.58	2.97
K_2O	0.94	0.66	0.04	0.60	5.16	0.39	0.22	0.30	0.48	0.33	1.36	0.15
P_2O_5	0.44	0.21	0.05	0.09	0.25	0.28	0.16	0.23	0.29	0.21	0.44	0.14
100Mg/Mg+Fe	64.6	69.2	85.1	70.0	61.7	71.0	69.0	55.4	54.0	64.9	64.9	62.2
CaO/Al_2O_3	0.643	0.604		0.614	0.490	0.653	0.439	0.580	0.720	0.660	0.675	0.637
Ti (wt.%)	0.86	0.66	0.22	0.42	0.82	0.77	0.64	1.01	0.88	0.62	1.04	0.62
Ni (ppm)	86	158	1082	164	108	199	79	110	62	98	124	95
Cr	247	652	1292	663	229	514	443	320	143	481	260	350
Zr	117	69	19	27	78	84	62	102	-	140	149	-
Y	29	28	5	11	27	27	21	31	-	35	24	-
Nb	40	16	1	3	15	30	11	10	-	17	60	-
Rb	18	16	2	3	112	7	1	1	-	10	35	-
Sr	358	219	25	322	599	232	139	175	-	130	806	-
Co	-	-	-	-	38	-	-	40	-	46	-	-
Sc	-	-	-	-	34	-	-	-	-	-	-	-
Zr/Y	4.03	2.46		2.45	2.89	3.11	2.95	3.29	-	4.0	6.21	-
Zr/Nb	2.9	4.3		9.0	5.2	2.8	5.6	10.2	-	8.2	2.5	-

Appendix 1: Section B cont.

Sample No.	38280	38284	38288	38291	38292	38297	38299	38301	38303	38306	38307	38310
SiO_2	46.35	48.95	48.86	49.26	50.14	49.43	-	50.35	50.04	48.59	50.46	49.73
TiO_2	1.41	1.71	1.39	1.64	1.11	1.22	-	1.28	1.25	1.48	1.62	1.41
Al_2O_3	17.56	17.07	18.25	17.53	20.10	17.55	-	17.65	18.95	16.21	16.06	17.76
Fe_2O_3	1.52	1.38	1.19	1.10	0.97	1.21	-	1.14	1.20	1.38	1.52	1.20
FeO	7.77	7.03	6.05	6.04	4.97	6.16	-	5.80	6.10	7.02	7.72	6.12
MnO	0.18	0.14	0.13	0.16	0.12	0.14	-	0.14	0.13	0.14	0.19	0.14
MgO	8.24	9.39	8.99	9.38	6.62	9.20	-	7.45	6.34	9.49	7.25	7.88
CaO	12.68	10.28	11.05	10.08	11.27	10.05	-	10.77	10.87	11.94	9.57	10.63
Na_2O	2.76	2.73	2.79	2.30	3.83	4.17	-	4.14	3.97	2.81	3.51	3.24
K_2O	0.57	0.88	0.94	2.06	0.65	0.61	-	1.00	0.90	0.65	1.59	1.49
P_2O_5	0.95	0.42	0.36	0.46	0.21	0.25	-	0.28	0.24	0.31	0.51	0.39
100Mg/Mg+Fe	61.7	66.9	69.2	71.7	67.0	69.3	-	66.0	61.1	67.2	58.7	66.1
CaO/Al_2O_3	0.772	0.602	0.605	0.575	0.561	0.573	-	0.610	0.574	0.737	9,596	0.599
Ti (wt.%)	0.85	1.03	0.83	0.98	0.67	0.73	0.96	0.77	0.75	0.89	0.97	0.85
Ni (ppm)	96	178	131	145	58	138	167	98	68	231	115	88
Cr	135	289	296	343	310	438	365	350	265	552	273	232
Zr	163	121	96	-	75	82	109	88	82	106	138	107
Y	26	33	29	-	24	25	20	25	27	23	30	29
Nb	73	41	37	-	18	21	43	25	17	33	57	42
Rb	9	25	25	-	10	11	24	25	14	17	32	29
Sr	591	283	322	-	251	223	364	307	242	260	249	356
Co	-	-	-	-	37	-	46	-	-	49	-	-
Sc	-	-	-	-	-	-	-	-	-	-	-	-
Zr/Y	6.27	3.7	3.31	-	3.13	3.28	5.45	3.52	3.04	4.61	4.6	3.69
Zr/Nb	2.2	3.0	2.6	-	4.2	3.9	2.5	3.5	4.8	3.2	2.4	2.5

Sample No.	38314	38315	38319	38325	38331	38332	38335	38336	38386	38389	38391	38392
SiO_2	48.88	49.26	-	49.56	50.08	-	49.66	49.88	-	47.92	48.92	-
TiO_2	1.56	0.95	-	1.47	1.44	-	1.46	1.23	-	1.44	1.27	-
Al_2O_3	18.09	20.33	-	16.19	18.01	-	16.11	17.62	-	17.11	17.34	-
Fe_2O_3	1.25	1.00	-	1.50	1.20	-	1.65	1.37	-	1.39	1.30	-
FeO	6.36	5.11	-	7.67	6.09	-	8.45	7.01	-	7.07	6.64	-
MnO	0.15	0.11	-	0.15	0.13	-	0.21	0.14	-	0.16	0.12	-
MgO	8.83	6.65	-	7.67	7.56	-	7.31	7.38	-	8.55	7.88	-
CaO	10.64	12.82	-	11.24	10.88	-	11.10	10.37	-	12.36	12.73	-
Na_2O	2.67	2.99	-	3.48	2.97	-	3.77	3.83	-	3.06	2.96	-
K_2O	1.18	0.60	-	0.79	1.15	-	0.10	0.97	-	0.66	0.60	-
P_2O_5	0.39	0.17	-	0.28	0.50	-	0.17	0.20	-	0.29	0.25	-
100Mg/Mg+Fe	67.8	66.4	-	60.3	65.2	-	56.8	61.6	-	64.7	64.3	-
CaO/Al_2O_3	0.588	0.631	-	0.694	0.604	-	0.689	0.589	-	0.722	0.734	-
Ti (wt.%)	0.94	0.57	0.91	0.88	0.86	0.60	0.88	0.74	0.55	0.86	0.76	0.60
Ni (ppm)	108	82	-	71	154	-	68	101	302	219	142	229
Cr	223	319	-	168	305	-	151	382	403	399	343	428
Zr	96	55	121	100	135	70	79	77	56	90	89	54
Y	35	21	23	38	33	20	26	28	16	38	30	15
Nb	46	-	30	24	49	12	8	11	4	32	21	10
Rb	14	10	23	16	27	8	0	10	2	13	11	3
Sr	345	304	319	278	323	251	114	256	160	249	246	183
Co	37	-	-	-	-	-	-	-	-	40	-	34
Sc	-	-	-	-	-	-	-	-	-	-	-	-
Zr/Y	2.7	2.62	5.26	2.6	4.09	3.5	3.04	2.75	3.5	2.4	2.97	3.6
Zr/Nb	2.1	-	4.0	4.2	2.8	5.8	9.9	7.0	13.3	2.8	4.2	5.4

Appendix 1: Section B cont.

Sample No.	38423	38434	38462	38473	38478	40434
SiO_2	49.51	49.59	48.41	49.26	48.42	49.64
TiO_2	1.68	2.00	1.16	1.36	0.99	1.18
Al_2O_3	17.40	16.17	20.50	17.98	21.31	19.08
Fe_2O_3	1.51	1.62	1.08	1.26	0.99	1.29
FeO	7.70	8.25	5.83	6.44	5.00	6.60
MnO	0.18	0.20	0.12	0.15	0.13	0.16
MgO	6.59	8.94	6.29	7.75	7.02	7.20
CaO	11.75	9.27	12.16	11.83	12.40	10.66
Na_2O	3.30	2.92	3.22	2.66	2.58	3.81
K_2O	0.10	0.61	0.98	0.99	0.95	0.20
P_2O_5	0.27	0.44	0.27	0.32	0.23	0.17
100Mg/Mg+Fe	56.5	62.1	63.4	64.7	67.8	62.4
CaO/Al_2O_3	0.675	0.573	0.593	0.658	0.582	0.559
Ti (wt.%)	1.01	1.20	0.70	0.82	0.59	0.71
Ni (ppm)	89	116	89	103	96	100
Cr	270	202	268	259	236	352
Zr	127	145	83	89	68	75
Y	37	44	31	22	14	32
Nb	16	42	21	38	19	6
Rb	0	9	12	22	15	5
Sr	171	280	338	311	324	202
Co	-	-	-	-	-	-
Sc	-	-	-	-	-	-
Zr/Y	3.43	3.3	2.68	4.05	4.86	2.34
Zr/Nb	7.9	3.5	4.0	2.3	3.6	12.5

3. DYKES

Sample No.	53	64	124	139	153	201	220	231	233	38133	38136	38137	38157
SiO_2	49.53	47.65	49.47	49.81	50.57	49.31	47.83	49.70	48.61	51.33	41.91	51.20	51.58
TiO_2	1.87	1.46	1.51	1.38	2.61	1.88	0.80	1.36	1.34	1.61	0.01	0.97	1.70
Al_2O_3	15.43	17.37	15.92	15.60	14.98	15.61	20.31	16.41	17.77	15.34	24.19	18.57	14.22
Fe_2O_3	1.79	1.28	1.68	1.66	1.46	1.83	1.17	1.42	1.22	1.65	0.97	1.07	1.76
FeO	9.16	6.54	8.58	8.47	7.44	9.34	5.95	7.25	6.22	8.41	4.93	5.47	8.99
MnO	0.20	0.15	0.18	0.20	0.12	0.18	0.10	0.14	0.15	0.18	0.07	0.13	0.19
MgO	6.61	7.38	6.71	7.78	7.21	7.11	8.41	8.29	9.40	6.91	11.66	7.48	7.97
CaO	10.53	12.82	11.18	11.64	11.79	11.11	12.82	11.44	11.39	9.85	15.36	10.57	9.54
Na_2O	3.70	3.34	4.08	3.15	3.19	2.84	2.40	3.49	2.71	4.35	0.82	4.21	3.63
K_2O	0.41	0.20	0.51	0.13	0.31	0.54	0.09	0.29	0.82	0.13	0.07	0.19	0.21
P_2O_5	0.31	0.82	0.18	0.16	0.32	0.24	0.12	0.22	0.37	0.25	0.01	0.15	0.22
100Mg/Mg+Fe	52.2	63.1	54.2	58.2	59.5	53.6	68.2	63.4	69.6	55.5		67.5	57.3
CaO/Al_2O_3	0.682	0.738	0.702	0.746	0.787	0.712	0.631	0.697	0.641	0.642	0.635	0.569	0.671
Ti (wt. %)	1.12	-	0.91	0.83	1.56	1.13	0.48	0.82	0.80	0.97	0.01	0.58	1.02
Ni (ppm)	45	-	68	78	58	67	207	77	107	42	379	117	68
Cr	126	-	292	262	80	208	523	248	330	119	-	332	124
Zr	126	-	89	80	135	113	46	85	107	103	0	58	100
Y	46	-	32	37	53	41	18	29	27	33	1	22	38
Nb	23	-	7	7	19	-	8	17	40	19	0	9	13
Rb	8	-	6	0	0	5	0	2	16	4	2	0	2
Sr	185	-	180	126	199	130	171	192	334	185	307	269	182
Co	-	-	-	-	-	-	-	-	-	-	-	-	-
Sc	-	-	-	-	-	-	-	-	-	-	-	-	-
Zr/Y	2.74	-	2.78	2.16	2.55	2.76	2.56	2.93	3.96	3.12	-	2.64	2.63
Zr/Nb	5.5	-	12.7	11.4	7.1	-	5.8	5.0	2.7	5.4	-	6.4	7.7

Appendix 1: Section B cont.

Sample No.	38206	38220	38223	38236	38237	38242	38249	38250	38273	38285	38289	38295	38320
SiO_2	51.04	-	49.13	51.53	49.41	48.97	52.25	-	50.17	-	-	-	50.51
TiO_2	1.23	-	1.45	1.72	0.77	1.05	1.15	-	1.62	-	-	-	1.09
Al_2O_3	15.78	-	17.72	14.76	21.01	15.91	16.21	-	16.17	-	-	-	15.57
Fe_2O_3	1.53	-	1.16	1.79	0.97	1.56	0.74	-	1.49	-	-	-	1.44
FeO	7.78	-	5.91	9.11	4.95	7.93	3.77	-	7.60	-	-	-	7.36
MnO	0.16	-	0.16	0.18	0.12	0.16	0.06	-	0.19	-	-	-	0.18
MgO	8.03	-	7.59	7.68	6.83	9.69	9.74	-	7.24	-	-	-	9.26
CaO	11.63	-	12.73	9.73	13.62	11.97	11.92	-	11.19	-	-	-	11.86
Na_2O	2.58	-	2.56	7.10	2.09	2.51	3.71	-	3.37	-	-	-	2.44
K_2O	0.11	-	1.23	0.11	0.11	0.12	0.27	-	0.68	-	-	-	0.18
P_2O_5	0.13	-	0.36	0.29	0.11	0.13	0.18	-	0.29	-	-	-	0.12
100Mg/Mg+Fe	61.0	-	66.1	56.1	67.7	64.9	79.6	-	59.1	-	-	-	65.6
CaO/Al_2O_3	0.737	-	0.718	0.659	0.648	0.752	0.735	-	0.692	-	-	-	0.762
Ti (wt.%)	0.74	1.20	0.87	1.03	0.46	0.63	0.69	0.34	0.97	0.46	0.89	0.85	0.65
Ni (ppm)	78	-	100	43	92	116	112	96	72	125	273	171	133
Cr	196	-	230	63	346	451	411	389	89	169	323	327	346
Zr	66	163	119	-	-	-	76	33	124	58	105	107	66
Y	37	32	18	-	-	-	28	10	27	9	21	21	23
Nb	4	50	52	-	-	-	10	5	32	20	34	37	4
Rb	2	14	22	-	-	-	2	2	12	17	17	22	2
Sr	112	253	336	-	-	-	163	163	280	436	278	548	160
Co	-	35	46	-	-	-	-	32	46	26	40	46	46
Sc	-	-	-	-	-	-	-	-	-	-	-	-	-
Zr/Y	1.78	5.09	6.61	-	-	-	2.71	3.3	4.59	6.44	5.0	5.1	2.87
Zr/Nb	16.5	3.3	2.3	-	-	-	7.6	6.6	3.9	2.9	3.1	2.9	16.5

Sample No.	38328	38334	38335	38337	38371	38397	38425	38449	38451	38471	38493	38501
SiO_2	-	49.86	49.66	49.71	-	49.90	51.38	51.11	48.96	46.92	51.68	-
TiO_2	-	1.12	1.46	1.68	-	1.62	1.81	1.20	0.61	1.20	1.61	-
Al_2O_3	-	16.42	16.11	14.81	-	17.49	15.42	15.38	21.80	15.66	17.17	-
Fe_2O_3	-	1.49	1.66	1.96	-	1.24	1.48	1.42	0.98	1.40	1.28	-
FeO	-	7.58	8.46	10.00	-	6.33	7.52	7.24	5.02	7.12	6.51	-
MnO	-	0.17	0.20	0.16	-	0.19	0.17	0.15	0.11	0.17	0.09	-
MgO	-	9.52	7.31	6.78	-	8.56	7.15	8.98	6.43	14.14	8.01	-
CaO	-	10.32	11.10	10.94	-	11.48	11.31	12.07	13.52	10.56	10.53	-
Na_2O	-	2.21	3.77	3.56	-	2.88	3.14	2.13	2.41	2.00	2.41	-
K_2O	-	1.16	0.10	0.18	-	0.15	0.37	0.15	0.08	0.60	0.50	-
P_2O_5	-	0.14	0.16	0.21	-	0.16	0.26	0.16	0.07	0.23	0.21	-
100Mg/Mg+Fe	-	65.5	63.4	50.7	-	67.2	59.0	65.3	66.0	75.0	65.1	-
CaO/Al_2O_3	-	0.629	0.697	0.739	-	0.656	0.733	0.785	0.620	0.674	0.613	-
Ti (wt.%)	1.06	0.67	0.88	1.01	0.66	0.97	1.09	0.72	0.37	0.71	0.97	0.72
Ni (ppm)	68	108	68	46	-	147	65	97	88	102	89	195
Cr	130	392	151	102	-	530	150	180	480	690	430	390
Zr	149	77	79	-	76	84	126	76	36	82	113	118
Y	27	20	26	-	21	21	33	23	14	18	32	20
Nb	48	5	8	-	20	15	22	11	2	26	17	39
Rb	32	29	0	-	1	2	6	2	2	16	6	1
Sr	433	163	114	-	252	280	191	144	148	200	182	253
Co	32	46	-	-	38	42	48	49	35	51	50	52
Sc	-	-	-	-	-	-	-	-	-	-	-	-
Zr/Y	5.52	3.85	3.04	-	3.62	4.0	3.82	3.3	2.57	4.56	3.53	5.90
Zr/Nb	3.1	15.4	9.9	-	3.8	5.6	5.7	6.5	18.0	3.2	6.5	3.0

APPENDIX 2

C.I.P.W. NORMATIVE COMPOSITIONS*† OF MACQUARIE ISLAND LAVAS AND DYKES

Mineral Abbreviations:

Qtz	quartz
Or	orthoclase
Ab	albite
An	anorthite
Ne	nepheline
Di	diopside
Hy	hypersthene
Ol	olivine
Mt	magnetite
Il	ilmenite
H-Ap	hydroxy-apatite

* calculations by method of Kelsey (1960).

† compositions are those given in Section B of Appendix 1.

APPENDIX 2 C.I.P.W. NORMATIVE COMPOSITIONS OF MACQUARIE ISLAND LAVAS AND DYKES

1. GLASSES

Sample No.	4A	155	157	252	422	38390	40428
Qtz	-	-	-	-	-	-	-
Or	5.26	3.48	3.37	6.73	7.14	3.48	1.12
Ab	19.72	20.00	20.26	25.75	19.60	25.85	20.39
An	30.06	32.26	33.04	26.57	27.23	28.87	33.46
Ne	6.64	2.53	1.71	3.90	8.24	-	-
Di	21.17	24.05	23.53	18.63	22.67	19.64	22.61
Hy	-	-	-	-	-	10.55	10.74
Ol	12.49	13.25	13.54	13.09	9.58	6.07	7.45
Mt	1.78	1.90	1.93	1.86	1.90	2.30	2.06
Il	2.89	2.52	2.62	3.47	3.64	3.24	2.17

2. LAVAS

Sample No.	3A	7	35	43B/A	43B/B	56A	56D	56G	56I	60	108C	108E	119
Qtz	-	-	-	-	-	-	-	-	-	-	-	-	-
Or	9.45	3.28	5.83	5.09	3.81	1.51	1.21	1.49	1.21	1.77	3.07	3.06	4.27
Ab	15.28	24.70	14.73	31.73	28.28	25.42	22.47	27.23	22.29	24.03	24.54	25.00	27.74
An	29.60	33.43	28.44	24.83	28.15	37.93	40.51	35.30	39.35	42.29	27.72	26.19	27.28
Ne	6.34	2.83	7.79	-	-	0.09	-	-	-	0.76	-	-	1.31
Di	18.87	17.53	27.71	19.08	18.23	16.52	16.91	18.40	17.56	14.43	23.77	22.31	20.04
Hy	-	-	-	2.42	4.00	-	6.29	0.46	2.82	-	5.37	12.06	-
Ol	12.96	13.81	9.62	11.03	11.61	14.53	8.80	13.10	12.66	13.04	10.04	5.96	14.50
Mt	1.95	1.74	1.96	2.07	2.13	1.59	1.40	1.49	1.66	1.39	2.42	2.50	1.96
Il	4.04	2.15	2.95	3.09	3.11	2.01	2.01	2.03	2.04	1.88	2.61	2.51	2.41
H-Ap	1.54	0.54	0.99	0.68	0.70	0.41	0.41	0.50	0.41	0.41	0.48	0.43	0.49

Sample No.	139	147	151	157	199	202	206	210	212	214	226	228	233
Qtz	-	-	-	-	-	-	-	-	-	-	-	-	-
Or	2.77	6.37	1.56	5.16	2.94	0.85	1.64	2.35	1.08	1.52	1.77	6.09	5.52
Ab	25.59	30.89	20.39	19.37	28.01	22.13	29.72	30.04	20.41	29.15	33.49	19.25	25.81
An	37.71	21.08	48.43	38.47	27.24	47.32	31.15	24.40	52.14	24.48	23.48	38.59	28.00
Ne	4.84	-	-	2.25	-	-	-	-	0.15	0.69	0.62	3.90	2.86
Di	10.35	16.61	9.17	17.68	19.83	13.34	16.43	21.83	9.84	24.89	20.38	15.80	19.77
Hy	-	10.80	16.94	-	8.09	0.77	5.17	1.85	-	-	-	-	-
Ol	15.04	8.19	0.28	13.06	7.82	11.99	11.01	13.71	13.59	13.81	14.67	12.36	12.56
Mt	1.57	2.46	1.29	1.57	2.37	1.57	1.92	2.60	1.48	2.45	2.28	1.49	1.77
Il	1.80	3.15	1.58	1.96	3.20	1.68	2.45	2.83	1.16	2.62	2.85	2.02	2.74
H-Ap	0.34	0.46	0.36	0.50	0.51	0.24	0.51	0.41	0.14	0.41	0.46	0.50	0.98

Sample No.	234	235	236	38151	38188	38201	38226	38241	38265	38267	38280	38284	38288
Qtz	-	-	-	-	-	-	-	-	-	-	-	-	-
Or	3.87	0.26	3.55	30.49	2.33	1.27	2.80	1.93	8.05	0.90	3.37	5.25	5.56
Ab	23.60	2.06	20.21	13.70	23.67	26.39	28.74	23.47	20.17	23.16	17.77	23.17	23.20
An	32.81	16.43	40.22	19.18	30.64	40.99	26.50	36.96	30.20	42.88	33.85	31.66	34.54
Ne	-	-	2.30	1.61	0.39	-	-	1.47	0.88	1.08	3.02	-	0.18
Di	14.25	6.42	16.49	14.36	16.95	1.85	22.97	19.35	18.86	17.68	18.54	13.38	14.34
Hy	8.99	21.67	-	-	-	15.13	4.46	-	-	-	-	5.23	-
Ol	12.29	49.88	14.19	15.49	21.29	10.24	8.75	12.70	14.62	10.43	16.35	15.11	16.94
Mt	1.82	2.45	1.48	1.99	1.97	1.70	2.34	1.70	1.92	1.59	2.21	2.00	1.72
Il	2.10	0.69	1.34	2.59	2.46	2.04	2.78	1.95	3.28	1.95	2.68	3.23	2.66
H-Ap	0.48	0.13	0.22	0.59	0.66	0.38	0.68	0.48	1.04	0.34	2.25	1.00	0.86

Sample No.	38291	38292	39297	38301	38303	38306	38307	38310	38314	38315	38325	38331	38335
Qtz	-	-	-	-	-	-	-	-	-	-	-	-	-
Or	12.16	3.86	3.62	5.95	5.35	3.86	9.42	8.79	6.94	3.54	4.67	6.76	0.60
Ab	19.43	26.59	25.25	25.14	26.02	21.06	28.12	23.14	22.57	21.74	24.72	25.16	29.15
An	31.37	35.68	27.38	26.59	31.25	29.73	23.34	29.57	33.90	40.31	26.21	32.41	26.72
Ne	-	3.18	5.37	5.36	4.08	1.43	0.87	2.29	-	1.91	2.58	-	1.50
Di	12.45	15.24	16.73	20.18	17.13	22.16	16.93	16.61	13.11	17.88	22.52	14.73	22.30
Hy	5.88	-	-	-	-	-	-	-	1.50	-	-	3.66	-
Ol	12.82	11.46	16.89	12.06	11.49	16.25	14.85	14.26	16.25	10.97	13.68	11.65	14.17
Mt	1.71	1.41	1.75	1.65	1.73	2.00	2.19	1.74	1.81	1.45	2.18	1.73	2.40
Il	3.11	2.11	2.32	2.42	2.38	2.80	3.09	2.70	2.96	1.82	2.78	2.74	2.78
H-Ap	1.08	0.49	0.60	0.65	0.57	0.72	1.21	0.91	0.93	0.40	0.66	1.18	0.38

APPENDIX 3

PRIMARY PHASE MICROPROBE ANALYSES.

Section A: Clinopyroxene and kaersutitic amphibole.

Section B: Plagioclase feldspar.

Section C: Olivine.

Section D: Spinel, including recalculations of structure.

Analytical techniques are described in Appendix 6. The tables are coded as below:

As sample number suffix or analysis number prefix -

- P = phenocryst (or xenocryst)
- M = microphenocryst
- G = groundmass.

As analysis number suffix -

- r = rim analysis
- c = core analysis
- m = mid-grain analysis.

Structural formulae have been calculated on the basis of the following numbers of oxygens:

Clinopyroxene	6
Amphibole	23
Plagioclase feldspar	8
Olivine	4

APPENDIX 3: Section A CLINOPYROXENE AND KAERSUTITIC AMPHIBOLE MICROPROBE ANALYSES.

	SiO_2	TiO_2	Al_2O_3	Cr_2O_3	FeO	MgO	MnO	CaO	Na_2O	K_2O	Total	Si	Ti	Al	Cr	Fe	Mg	Mn	Ca	Na	K	Total
163	dyke P																					
A1c	53.30	0.27	2.08	0.45	5.27	17.44	-	21.19	-	-	98.41	1.946	0.007	0.090	0.013	0.161	0.949	-	0.829	-	-	3.995
A2c	52.37	0.17	3.47	1.21	4.02	17.05	-	21.54	-	0.16	97.24	1.910	0.005	0.149	0.035	0.123	0.927	-	9.842	-	0.008	3.997
A3c	52.12	0.29	2.24	0.71	5.36	17.11	-	21.16	-	-	100.55	1.942	0.008	0.097	0.021	0.164	0.932	-	0.829	-	-	3.992
A4c	52.79	0.40	2.29	0.67	5.27	17.26	-	21.15	0.17	-	100.97	1.932	0.011	0.099	0.019	0.161	.941	-	0.829	0.012	-	4.004
A1r	52.75	0.41	2.18	0.25	6.71	16.91	-	20.47	0.32	-	100.57	1.938	0.011	0.094	0.007	0.206	0.926	-	0.805	0.023	-	4.011
A2r	53.19	0.33	2.35	0.36	5.27	17.11	-	21.32	-	0.07	98.60	1.943	0.009	0.101	0.010	0.161	0.932	-	0.835	-	0.003	3.994
A3r	53.28	0.33	1.60	0.20	6.64	17.53	-	20.41	-	-	100.67	1.953	0.009	0.069	0.006	0.204	0.958	-	0.802	-	-	4.000
A4r	53.13	0.46	1.67	0.19	7.22	16.88	-	20.44	-	-	100.16	1.953	0.013	0.072	0.006	0.222	0.925	-	0.805	-	-	3.995
163	dyke G																					
B1	53.08	0.40	1.51	0.11	7.93	17.16	-	19.64	0.17	-	100.26	1.954	0.011	0.065	0.003	0.244	0.941	-	0.775	0.012	-	4.006
B2	52.70	0.46	2.16	0.23	6.79	16.76	-	20.39	-	-	98.70	1.937	0.013	0.094	0.007	0.209	0.918	-	0.823	-	-	4.000
C1	50.86	0.92	2.31	-	12.09	14.80	0.28	18.40	0.34	-	99.67	1.912	0.026	0.102	-	0.380	0.829	0.009	0.741	0.025	-	4.024
C2	52.40	0.34	3.39	0.45	5.26	16.84	-	20.89	0.27	0.16	98.30	1.916	0.009	0.146	0.013	0.161	0.918	-	0.818	0.019	0.008	4.008
C3	52.79	0.41	2.24	0.47	5.70	17.38	-	20.81	0.20	-	99.36	1.933	0.011	0.097	0.014	0.174	0.949	-	0.816	0.014	-	4.008
C4	53.53	0.38	1.46	0.26	6.09	17.44	-	20.85	-	-	99.97	1.959	0.011	0.063	0.007	0.186	0.951	-	0.817	-	-	3.995
159	G																					
C1c	51.61	0.58	3.45	1.18	6.12	16.71	-	19.96	0.38	-	98.13	1.895	0.016	0.149	0.034	0.188	0.915	-	0.785	0.027	-	4.010
C2c	51.27	0.72	3.96	0.81	6.99	17.08	-	18.92	0.25	-	98.56	1.883	0.020	0.172	0.024	0.215	0.935	-	0.744	0.018	-	4.009
C1r	52.97	0.38	2.14	0.78	6.05	17.61	-	19.83	0.24	-	99.02	1.938	0.010	0.092	0.023	0.185	0.960	-	0.777	0.017	-	4.003
C2r	52.12	0.48	2.60	0.75	6.29	17.54	-	20.00	0.21	-	98.03	1.913	0.013	0.112	0.022	0.193	0.960	-	0.786	0.015	-	4.014
A1	49.78	1.39	4.86	0.60	7.55	15.78	-	19.69	0.34	-	98.99	1.841	0.039	0.212	0.018	0.233	0.870	-	0.780	0.024	-	4.017
A2	48.51	1.81	4.29	0.37	11.25	13.26	0.22	19.89	0.39	-	100.72	1.833	0.051	0.191	0.011	0.355	0.747	0.007	0.805	0.029	-	4.029
A3	47.97	1.83	3.77	0.20	15.75	11.71	0.31	18.10	0.36	-	100.21	1.842	0.053	0.171	0.006	0.506	0.670	0.010	0.745	0.027	-	4.030
A4	48.02	1.97	3.67	0.14	15.67	11.16	0.25	18.84	0.29	-	99.93	1.846	0.057	0.166	0.004	0.504	0.640	0.008	0.726	0.022	-	4.022
A5	49.29	1.58	5.36	0.43	8.13	15.02	-	19.95	0.24	-	99.10	1.828	0.044	0.234	0.013	0.252	0.830	-	0.793	0.017	-	4.012
A6	49.34	1.46	5.14	0.41	8.33	15.19	-	19.83	0.29	-	100.30	1.832	0.041	0.225	0.012	0.259	0.841	-	0.789	0.021	-	4.019
A7	49.76	1.31	4.31	0.45	9.06	14.97	-	19.74	0.40	-	99.01	1.854	0.037	0.189	0.013	0.282	0.831	-	0.788	0.029	-	4.023
A8	47.57	2.27	4.44	0.13	14.89	11.50	0.32	18.37	0.42	-	99.98	1.823	0.065	0.201	0.004	0.480	0.657	0.010	0.754	0.031	-	4.025
38178	G																					
A1	49.35	1.73	3.98	0.17	10.26	13.45	-	20.55	0.51	-	99.38	1.854	0.049	0.176	0.005	0.322	0.753	-	0.827	0.037	-	4.025
A2	53.45	0.38	1.71	0.24	5.38	17.11	-	21.59	0.15	-	100.47	1.955	0.010	0.074	0.007	0.165	0.933	-	0.846	0.011	-	4.000
A3	47.69	2.47	3.98	0.25	13.55	11.10	0.32	19.89	0.75	-	100.30	1.827	0.071	0.180	0.008	0.434	0.634	0.010	0.816	0.056	-	4.036
A4	49.50	0.86	1.70	0.26	17.61	8.86	0.42	19.97	0.82	-	101.97	1.927	0.025	0.078	0.008	0.573	0.514	0.014	0.833	0.062	-	4.035
A5	51.97	0.90	2.36	0.17	7.71	15.71	-	20.98	0.21	-	99.13	1.922	0.025	0.103	0.005	0.238	0.866	-	0.832	0.015	-	4.006
A6	53.28	0.43	1.87	0.51	4.87	17.34	-	21.45	0.25	-	99.77	1.946	0.012	0.081	0.015	0.149	0.944	-	0.839	0.018	-	4.003
B1	49.55	1.85	4.03	0.20	9.16	13.97	-	20.83	0.41	-	99.47	1.853	0.052	0.178	0.006	0.286	0.779	-	0.835	0.030	-	4.018
B2	51.82	0.75	3.16	0.20	5.93	16.37	-	21.52	0.24	-	99.64	1.905	0.021	0.137	0.006	0.182	0.897	-	0.847	0.017	-	4.012
B3	52.03	0.67	3.35	0.59	4.78	16.62	-	21.81	0.17	-	98.52	1.904	0.018	0.144	0.017	0.146	0.906	-	0.855	0.012	-	4.003
B4	49.12	1.77	3.97	0.21	10.18	13.58	0.12	20.37	0.07	-	100.63	1.848	0.050	0.176	0.006	0.320	0.761	0.004	0.821	0.049	-	4.036
B5	52.07	0.65	3.35	0.47	5.14	16.56	-	21.49	0.26	-	99.44	1.907	0.018	0.145	0.014	0.158	0.904	-	0.843	0.019	-	4.006
B6	49.89	1.68	3.88	0.16	9.00	14.22	-	20.66	0.52	-	100.05	1.863	0.047	0.171	0.005	0.281	0.791	-	0.827	0.037	-	4.021
B6	50.33	1.29	3.59	0.19	9.14	14.34	-	20.66	0.46	-	100.30	1.878	0.036	0.158	0.006	0.285	0.797	-	0.826	0.034	-	.4020
147A	M																					
A1	50.46	0.96	4.58	0.65	6.80	16.10	-	20.02	0.43	-	99.31	1.860	0.027	0.199	0.019	0.210	0.885	-	0.791	0.030	-	4.020
A2	50.30	1.18	4.71	0.55	6.92	15.42	-	20.76	0.16	-	99.84	1.857	0.033	0.205	0.016	0.214	0.848	-	0.821	0.012	-	4.006
A3	51.20	0.86	3.87	0.42	7.54	16.87	0.13	18.81	0.30	-	99 78	1.884	0.024	0.168	0.012	0.232	0.925	0.004	0.741	0.022	-	4.013
A4	50.99	1.04	3.85	0.60	6.93	15.86	-	20.51	0.22	-	98.94	1.881	0.029	0.167	0.017	0.214	0.872	-	0.810	0.016	-	4.006
C1	50.71	0.98	4.25	0.48	7.22	15.95	-	20.11	0.29	-	99.04	1.871	0.027	0.185	0.014	0.223	0.877	-	0.795	0.020	-	4.013
C2	50.64	0.95	4.21	0.93	6.71	16.31	-	19.86	0.39	-	100.69	1.866	0.026	0.183	0.027	0.207	0.896	-	0.784	0.028	-	4.017
C4	50.11	1.40	4.25	0.47	7.41	14.97	-	20.95	0.43	-	99.67	1.858	0.039	0.186	0.014	0.230	0.828	-	0.833	0.031	-	4.018
C5	50.44	1.13	4.45	0.86	7.25	16.06	-	19.46	0.35	-	99.27	1.861	0.031	0.194	0.025	0.224	0.883	-	0.769	0.025	-	4.011
C6	50.10	1.30	4.75	0.62	7.29	15.70	-	20.23	-	-	99.91	1.850	0.036	0.207	0.018	0.225	0.864	-	0.800	-	-	4.001
147A	amphibole																					
C	56.87	0.76	15.48	0.14	4.72	6.45	-	9.58	5.93	0.68	100.96	7.609	0.077	2.442	0.015	0.460	1.284	-	1.372	1.537	0.115	14.911
38188	G																					
C1	49.31	1.47	8.35	0.10	11.58	8.90	-	17.91	2.02	0.35	100.04	1.848	0.041	0.369	0.003	0.363	0.498	-	0.719	0.147	0.017	4.006
C2	46.29	2.69	8.56	0.25	7.82	11.74	-	22.92	0.36	-	103.71	1.732	0.076	0.378	0.008	0.245	0.655	-	0.894	0.026	-	4.013
C3	46.23	2.54	8.60	0.28	8.23	11.79	-	22.36	-	-	102.00	1.732	0.071	0.380	0.008	0.258	0.658	-	0.897	-	-	4.004
C4	47.90	1.95	5.93	0.16	10.20	11.54	-	21.72	0.58	-	103.00	1.807	0.055	0.264	0.005	0.322	0.649	-	0.878	0.042	-	4.023
E1	46.33	2.80	8.13	0.26	8.18	12.04	-	22.25	-	-	100.89	1.736	0.079	0.359	0.008	0.256	0.672	-	0.893	-	-	4.002
E2	46.10	2.99	7.41	0.28	9.84	11.28	-	21.73	0.36	-	101.88	1.742	0.085	0.330	0.008	0.311	0.635	-	0.880	0.027	-	4.017
D1	45.89	3.45	7.35	0.19	10.52	10.96	-	21.63	-	-	101.70	1.737	0.098	0.328	0.006	0.333	0.618	-	0.877	-	-	3.998
D2	47.30	2.64	5.80	0.20	10.50	11.57	-	21.55	0.44	-	103.13	1.789	0.075	0.259	0.006	0.332	0.653	-	0.873	0.033	-	4.012
64	G																					
D1	46.14	2.12	10.16	0.18	6.53	12.71	-	21.77	0.40	-	99.29	1.712	0.059	0.444	0.005	0.203	0.703	-	0.865	0.029	-	4.019
D2	48.75	1.83	11.05	0.19	5.95	11.96	-	18.71	1.43	0.13	99.77	1.780	0.050	0.475	0.006	0.182	0.651	-	0.732	0.101	0.006	3.983
D3	46.78	2.17	10.40	0.27	6.45	12.07	-	21.01	0.77	0.09	100.04	1.730	0.060	0.453	0.008	0.199	0.665	-	0.832	0.005	0.004	4.008
D4	46.82	2.06	9.15	0.15	7.71	13.52	-	19.57	0.91	0.12	99.84	1.738	0.057	0.400	0.005	0.239	0.748	-	0.778	0.065	0.006	4.037
157	groundmass																					
C1	50.87	0.97	4.43	0.23	6.31	15.41	-	21.56	0.22	-	101.05	1.874	0.027	0.192	0.007	0.195	0.846	-	0.851	0.016	-	4.008
C2	50.90	0.84	4.75	1.14	4.31	16.11	-	21.76	0.20	-	100.53	1.863	0.023	0.205	0.033	0.132	0.879	-	0.853	0.014	-	4.002
C3	51.10	0.64	4.32	1.07	4.42	16.42	-	21.81	0.22	-	99.82	1.871	0.018	0.186	0.031	0.135	0.896	-	0.856	0.016	-	4.010
C4	49.90	1.35	4.41	0.19	7.93	14.64	-	21.16	0.42	-	100.77	1.855	0.038	0.193	0.005	0.247	0.811	-	0.843	0.030	-	4.023
C5	48.70	1.87	4.80	0.16	10.21	13.29	-	20.50	0.47	-	100.37	1.830	0.053	0.212	0.005	0.321	0.744	-	0.825	0.034	-	4.025
C6	50.06	1.23	4.39	0.23	7.71	14.92	-	21.06	0.39	-	100.92	1.858	0.034	0.192	0.007	0.239	0.825	-	0.838	0.028	-	4.022
C7	51.04	0.65	4.45	1.13	4.33	15.96	-	22.19	0.24	-	99.88	1.871	0.018	0.192	0.033	0.133	0.872	-	0.872	0.017	-	4.007
C8	51.09	0.66	4.91	1.08	4.81	16.07	-	21.37	-	-	100.13	1.869	0.018	0.212	0.031	0.147	0.876	-	0.838	-	-	3.991
C9	53.14	0.54	1.91	0.16	6.22	17.06	-	20.75	0.22	-	101.48	1.947	0.015	0.083	0.005	0.190	0.932	-	0.815	0.016	-	4.002
C10	53.35	0.36	2.21	0.56	4.55	17.79	-	21.18	-	-	99.89	1.942	0.010	0.095	0.016	0.139	0.965	-	0.826	-	-	3.993
A	50.98	0.52	5.35	1.87	3.59	16.48	-	21.21	-	-	101.50	1.856	0.014	0.229	0.053	0.109	0.894	-	0.827	-	-	3.987

APPENDIX 3: Section A cont.

	SiO_2	TiO_2	Al_2O_3	Cr_2O_3	FeO	MgO	MnO	CaO	Na_2O	K_2O	Total	Si	Ti	Al	Cr	Fe	Mg	Mn	Ca	Na	K	Total
157	phenocryst																					
C1c	52.86	0.24	3.31	0.48	4.08	17.88	-	20.93	0.22	-	99.21	1.920	0.007	0.142	0.014	0.124	0.968	-	0.814	0.016	-	4.004
C2c	51.62	0.33	4.82	1.38	3.75	16.46	-	21.40	0.24	-	98.97	1.880	0.009	0.207	0.040	0.114	0.894	-	0.835	0.017	-	3.996
C3c	51.71	0.26	4.25	1.36	3.64	16.94	-	21.62	0.23	-	98.25	1.885	0.007	0.182	0.039	0.111	0.920	-	0.844	0.016	-	4.005
C4c	51.52	0.28	4.75	1.38	3.64	16.70	-	21.41	0.31	-	98.41	1.877	0.008	0.204	0.040	0.111	0.907	-	0.836	0.022	-	4.004
C1r	51.81	0.52	3.71	1.08	4.02	16.53	-	22.35	-	-	97.07	1.893	0.014	0.160	0.031	0.123	0.900	-	0.875	-	-	3.997
C2r	50.95	0.64	4.84	0.99	4.21	16.30	-	21.92	0.19	-	98.19	1.864	0.018	0.208	0.029	0.129	0.889	-	0.859	0.013	-	4.007
C3r	50.80	0.39	5.06	1.59	3.82	16.44	-	21.52	0.38	-	100.41	1.857	0.011	0.218	0.046	0.117	0.896	-	0.843	0.027	-	4.014
C4r	51.47	0.72	4.10	0.60	4.66	16.36	-	21.84	0.24	-	100.60	1.884	0.020	0.177	0.017	0.143	0.893	-	0.857	0.017	-	4.008
C5r	51.76	0.50	3.78	1.03	4.12	16.36	-	22.21	0.24	-	98.29	1.893	0.014	0.163	0.030	0.126	0.892	-	0.870	0.017	-	4.005
C6r	50.68	0.50	5.09	1.58	3.90	16.34	-	21.61	0.30	-	100.00	1.854	0.014	0.219	0.046	0.119	0.891	-	0.847	0.021	-	4.011
3A	G																					
A1	45.81	3.11	8.99	0.27	6.27	12.95	0.21	22.30	0.50	0.08	100.51	1.700	0.087	0.393	0.008	0.195	1.716	0.007	0.887	0.036	0.004	4.032
A2	48.75	1.59	5.20	0.28	5.84	15.28	-	21.78	0.31	0.06	99.09	1.820	0.045	0.229	0.008	0.182	0.850	-	0.871	0.022	0.003	4.030
B1	45.97	2.80	8.97	0.42	5.35	13.18	-	22.96	0.35	-	98.05	1.707	0.078	0.393	0.012	0.166	0.729	-	0.913	0.025	-	4.024
B2	48.89	1.02	4.03	0.58	8.10	15.46	-	21.54	0.37	-	102.30	1.829	0.029	0.178	0.017	0.253	0.862	-	0.863	0.027	-	4.058
B3	49.73	1.49	5.33	0.55	4.82	15.13	-	22.60	0.35	-	99.16	1.831	0.041	0.232	0.016	0.148	0.831	-	0.892	0.025	-	4.016
B4	51.31	1.12	4.08	0.52	4.49	15.82	-	22.67	-	-	98.79	1.880	0.031	0.176	0.015	0.138	0.864	-	0.890	-	-	3.994
B5	47.38	2.22	7.83	0.55	5.06	13.75	-	22.84	0.37	-	100.23	1.753	0.062	0.342	0.016	0.157	0.758	-	0.906	0.027	-	4.020
B6	46.48	2.78	8.64	0.44	5.26	13.33	-	22.80	0.26	-	98.35	1.723	0.077	0.377	0.013	0.163	0.737	-	0.905	0.019	-	4.014
D1c	50.16	1.42	4.79	0.34	5.31	15.58	-	22.15	0.24	-	99.05	1.847	0.039	0.208	0.010	0.164	0.855	-	0.874	0.017	-	4.013
D2c	46.25	2.72	9.01	0.36	5.47	13.34	-	22.42	0.32	-	99.28	1.715	0.076	0.394	0.011	0.170	0.737	-	0.890	0.031	-	4.023
D2r	46.33	2.95	8.82	0.24	5.42	13.18	-	22.68	0.38	-	98.71	1.718	0.082	0.385	0.007	0.168	0.728	-	0.901	0.027	-	4.017
C1c	50.71	1.25	4.36	0.50	5.12	15.96	-	21.83	0.28	-	98.86	1.863	0.034	0.189	0.015	0.157	0.874	-	0.859	0.020	-	4.011
C2	46.49	2.48	8.73	0.62	5.10	13.56	-	22.70	0.32	-	99.23	1.722	0.069	0.381	0.018	0.158	0.749	-	0.901	0.023	-	4.021
C4	49.54	1.51	5.14	0.29	5.40	15.39	-	22.33	0.39	-	98.67	1.829	0.042	0.224	0.009	0.167	0.847	-	0.883	0.028	-	4.027
C6	48.06	1.69	7.30	1.04	4.68	14.14	-	22.66	0.43	-	99.93	1.775	0.047	0.318	0.030	0.145	0.778	-	0.897	0.031	-	4.020
E1	47.80	1.90	7.48	0.91	4.61	14.05	-	22.95	0.25	-	98.45	1.765	0.054	0.325	0.027	0.142	0.773	-	0.908	0.018	-	4.014
E2	46.50	2.15	9.05	0.67	6.20	14.07	-	20.93	0.42	-	97.63	1.722	0.060	0.395	0.020	0.192	0.777	-	0.831	0.030	-	4.026
E4	47.00	2.24	8.50	0.88	4.77	13.50	-	22.79	0.30	-	98.44	1.738	0.062	0.370	0.026	0.148	0.744	-	0.903	0.022	-	4.012
E5	48.06	1.64	7.55	1.11	4.43	14.09	-	22.78	0.34	-	99.44	1.772	0.045	0.328	0.032	0.137	0.725	-	0.900	0.024	-	4.014
E6	48.26	1.74	7.28	0.43	5.16	14.19	-	22.73	0.21	-	100.09	1.781	0.048	0.317	0.012	0.158	0.781	-	0.885	0.021	-	4.010
E7	50.91	1.26	4.19	0.40	4.64	15.82	-	22.50	0.29	-	98.89	1.869	0.035	0.181	0.012	0.142	0.865	-	0.885	0.021	-	4.010
3A	Kaersutitic amphibole																					
A2	38.12	5.28	12.89	-	16.88	8.95	0.25	12.00	2.92	1.23	98.52	5.802	0.604	2.313	-	2.149	2.030	0.021	1.957	1.862	0.239	15.977
A3	41.90	4.03	9.79	0.14	8.50	11.55	-	19.94	0.83	0.29	96.52	5.277	0.454	1.728	0.016	1.065	2.578	-	3.128	0.241	0.056	15.544
A5	37.54	6.44	14.05	-	14.07	10.50	-	11.73	2.55	1.08	97.96	5.652	0.729	2.493	-	1.772	2.357	-	1.893	0.745	0.208	15.848
A6	37.14	6.19	13.70	-	15.92	9.20	0.16	11.59	2.83	1.26	97.99	5.659	0.709	2.461	-	2.029	2.089	0.014	1.892	0.836	0.245	15.935
C2	42.49	3.48	10.90	0.14	6.25	11.77	-	22.02	0.41	-	97.97	6.218	0.437	1.878	0.015	0.767	2.568	-	3.454	0.119	-	15.456
C3	37.87	6.09	13.40	0.12	16.82	8.78	0.17	11.57	2.92	1.27	99.01	5.727	0.694	2.388	0.015	2.127	1.978	0.023	1.874	0.855	0.245	15.927
C1	36.66	7.35	14.66	-	13.90	10.31	-	11.88	2.74	1.16	98.65	5.497	0.828	2.590	-	1.743	2.303	-	1.909	0.797	0.221	15.889
3A	G																					
	50.08	1.87	5.56	-	5.60	15.02	-	21.86	-	-	98.10	1.839	0.051	0.240	-	0.171	0.822	-	0.860	-	-	3.987
	45.54	3.50	8.94	-	8.28	12.20	-	20.54	0.97	-	98.10	1.705	0.098	0.394	-	0.259	0.681	-	0.823	0.070	-	4.033
141	dyke G																					
A1	48.30	2.03	4.76	0.17	10.49	13.00	-	20.75	0.51	-	99.84	1.821	0.057	0.212	0.005	0.331	0.731	-	0.838	0.037	-	4.032
A2	50.81	0.99	4.08	0.18	6.91	14.97	-	21.89	0.19	-	89.68											
A3c	49.13	1.76	4.36	0.21	9.85	13.49	0.16	20.57	0.45	-	100.19	1.844	0.050	0.193	0.006	0.309	0.755	0.005	0.827	0.033	-	4.023
A3r	48.15	1.76	4.36	0.17	13.32	11.61	-	20.14	0.48	-	98.38	1.836	0.051	0.196	0.005	0.425	0.660	-	0.823	0.036	-	4.031
A4r	50.79	1.16	3.76	0.14	7.87	14.89	-	21.00	0.38	-	99.39	1.884	0.032	0.165	0.004	0.244	0.823	-	0.834	0.027	-	4.013
A4c	49.87	1.21	5.05	0.30	6.80	14.90	-	21.60	0.28	-	99.02	1.845	0.034	0.220	0.009	0.210	0.822	-	0.856	0.020	-	4.016
A5c	48.15	2.08	4.52	0.15	11.09	12.66	0.16	20.80	0.41	-	99.02	1.822	0.059	0.202	0.004	0.351	0.714	0.005	0.843	0.030	-	4.030
A5r	48.41	1.95	4.24	0.14	11.51	12.21	0.13	20.90	0.51	-	98.60	1.836	0.056	0.190	0.004	0.365	0.690	0.004	0.849	0.038	-	4.030
B1	49.96	1.39	4.21	0.12	8.89	13.96	-	21.03	0.44	-	99.75	1.864	0.039	0.185	0.003	0.278	0.776	-	0.841	0.032	-	4.018
B2	48.60	1.81	4.20	0.17	11.89	11.71	0.13	20.89	0.60	-	99.74	1.845	0.052	0.188	0.005	0.378	0.662	0.004	0.850	0.044	-	4.028
B3	49.41	1.39	5.40	0.46	5.87	15.01	-	22.05	0.42	-	100.38	1.827	0.039	0.235	0.013	0.181	0.827	-	0.873	0.030	-	4.025
B4	50.39	1.33	4.52	0.31	6.74	14.79	-	21.52	0.40	-	99.80	1.863	0.037	0.197	0.009	0.209	0.815	-	0.853	0.028	-	4.011
B5	49.74	1.38	5.34	0.52	6.32	14.80	-	21.72	0.18	-	99.08	1.838	0.038	0.232	0.015	0.195	0.815	-	0.860	0.013	-	4.007
B6	49.93	1.31	5.07	0.38	6.53	14.80	-	21.57	0.39	-	99.72	1.846	0.036	0.221	0.011	0.202	0.816	-	0.855	0.028	-	4.016
B7	49.75	1.61	4.24	0.14	8.89	13.84	-	21.14	0.38	-	100.08	1.858	0.045	0.187	0.004	0.278	0.770	-	0.846	0.027	-	4.015
B8	49.22	1.59	4.40	-	9.31	13.36	-	21.96	0.16	-	99.25	1.846	0.045	0.195	-	0.292	0.747	-	0.883	0.012	-	4.018
B9	50.97	0.78	3.95	0.16	7.17	15.33	-	21.40	0.24	-	99.29	1.885	0.022	0.172	0.005	0.222	0.844	-	0.848	0.017	-	4.014
B10	48.94	1.65	6.19	0.65	5.78	14.74	-	21.74	0.31	-	100.59	1.807	0.046	0.269	0.019	0.179	.811	-	0.860	0.022	-	4.014
B11	50.18	1.27	4.22	0.24	7.55	14.79	-	21.31	0.43	-	100.66	1.863	0.035	0.185	0.007	0.235	0.819	-	0.848	0.031	-	4.022
B12	50.59	0.96	4.44	0.27	6.50	15.17	-	21.63	0.48	-	101.09	1.868	0.027	0.193	0.008	0.201	0.835	-	0.856	0.034	-	4.022
B13c	50.40	1.11	4.25	0.26	7.26	14.82	-	21.38	0.44	0.09	100.04	1.868	0.031	0.186	0.008	0.225	0.819	-	0.849	0.032	0.004	4.022
B13r	48.16	2.00	4.67	0.13	11.04	12.55	0.14	20.63	0.62	0.06	99.55	1.823	0.057	0.208	0.004	0.349	0.708	0.005	0.836	0.045	0.003	4.038
B15c	50.52	1.08	4.39	0.24	7.06	14.96	-	21.48	0.28	-	99.82	1.869	0.030	0.191	0.007	0.218	0.825	-	0.851	0.020	-	4.012
B16c	49.85	1.47	4.89	0.26	7.03	15.03	-	21.20	0.28	-	99.64	1.845	0.041	0.213	0.008	0.217	0.829	-	0.840	0.020	-	4.014
B16c	49.33	1.35	5.60	0.44	6.22	15.07	-	21.65	0.34	-	100.23	1.824	0.037	0.244	0.013	0.192	0.830	-	0.858	0.025	-	4.023
B18r	49.91	1.36	3.94	0.16	8.80	14.07	-	21.43	0.33	-	99.69	1.864	0.038	0.174	0.005	0.275	0.783	-	0.858	0.024	-	4.020
B19r	50.67	1.12	4.15	0.20	6.95	15.25	-	21.48	0.17	-	99.65	1.873	0.031	0.181	0.006	0.215	0.840	-	0.851	0.012	-	4.009
B20r	47.95	1.52	3.31	0.18	15.88	9.92	0.32	20.03	0.77	0.12	99.40	1.858	0.044	0.151	0.005	0.514	0.573	0.010	0.831	0.058	0.006	4.051
B21r	50.65	1.12	4.36	0.25	6.95	15.17	-	21.25	0.25	-	100.68	1.871	0.031	0.190	0.007	0.215	0.835	-	0.841	0.018	-	4.008
B22r	50.05	1.26	5.43	0.42	5.47	15.08	-	22.12	0.17	-	98.83	1.842	0.035	0.235	0.012	0.168	0.827	-	0.872	0.012	-	4.005
B23r	49.82	1.42	4.12	0.21	8.38	14.30	-	21.42	0.34	-	99.66	1.858	0.040	0.181	0.006	0.261	0.795	-	0.856	0.025	-	4.021

APPENDIX 3: Section A cont.

	SiO_2	TiO_2	Al_2O_3	Cr_2O_3	FeO	MgO	MnO	CaO	Na_2O	K_2O	Total	Si	Ti	Al	Cr	Fe	Mg	Mn	Ca	Na	K	Total
425 G																						
D1	53.18	0.58	2.15	-	6.63	18.75	-	18.71	-	-	100.64	1.938	0.015	0.092	-	0.201	1.019	-	0.730	-	-	3.999
D2	53.07	0.45	2.00	0.34	7.47	19.52	-	17.14	-	-	98.94	1.935	0.012	0.086	0.009	0.227	1.061	-	0.669	-	-	4.003
D3	49.39	1.45	5.29	-	8.70	15.06	-	19.57	0.51	-	98.51	1.834	0.040	0.231	-	0.270	0.833	-	0.778	0.036	-	4.026
H1	52.45	0.57	3.04	0.45	6.29	18.31	-	18.90	-	-	99.20	1.913	0.015	0.130	0.013	0.191	0.995	-	0.738	-	-	4.
H2	50.53	1.28	4.80	0.34	6.78	16.35	-	19.91	-	-	99.	1.856	0.035	0.207	0.009	0.208	0.895	-	0.784	-	-	3.998
425 G																						
D4	51.36	0.63	4.01	0.67	5.56	17.29	-	19.99	0.47	-	101.40	1.880	0.017	0.172	0.019	0.170	0.943	-	0.784	0.033	-	4.022
D5	51.81	0.87	3.63	-	8.19	18.02	-	17.48	-	-	99.50	1.897	0.023	0.156	-	0.251	0.984	-	0.685	-	-	4.
D6	51.92	0.60	3.57	0.69	5.36	17.21	-	20.64	-	-	101.	1.897	0.016	0.153	0.019	0.163	0.937	-	0.808	-	-	3.998
E1	53.37	0.38	2.14	0.44	6.29	19.86	-	17.50	-	-	99.90	1.937	0.010	0.091	0.012	0.190	1.075	-	0.680	-	-	3.999
E2	52.97	0.43	2.55	0.53	5.66	18.47	-	19.39	-	-	99.30	1.928	0.011	0.109	0.015	0.172	1.002	-	0.756	-	0	3.997
425 P																						
H1c	52.75	-	3.38	1.08	4.04	17.86	-	20.89	-	-	99.50	1.916	-	0.144	0.031	0.122	0.967	-	0.813	-	-	3.996
H2c	52.24	0.33	3.65	1.05	2.76	18.04	-	20.92	-	-	100.70	1.897	0.009	0.156	0.030	0.114	0.977	-	0.814	-	-	3.999
H3c	52.47	0.30	3.40	0.94	3.77	18.12	-	21.	-	-	100.20	1.905	0.008	0.145	0.026	0.114	0.981	-	0.817	-	-	4.
H1r	50.59	1.18	4.88	-	8.26	15.74	-	19.36	-	-	99.60	1.865	0.032	0.211	-	0.254	0.865	-	0.765	-	-	3.996
H2r	52.00	0.47	4.78	0.53	5.16	16.35	-	20.69	-	-	100.90	1.894	0.012	0.205	0.015	0.157	0.887	-	0.807	-	-	3.981
H3r	51.55	0.72	4.29	0.28	5.93	16.66	-	20.57	-	-	100.30	1.886	0.019	0.184	0.007	0.181	0.909	-	0.806	-	-	3.997
H4r	49.78	1.38	5.05	-	9.92	16.22	-	16.79	0.59	-	101.40	1.845	0.038	0.220	-	0.307	0.896	0.008	0.667	0.042	-	4.027
426 G																						
A1	49.42	1.42	5.78	0.31	7.64	14.97	-	20.43	-	-	99.70	1.827	0.039	0.252	0.008	0.236	0.825	-	0.809	-	-	4.001
A2	49.22	1.45	6.35	0.31	7.11	14.82	-	20.75	-	-	100.20	1.817	0.040	0.276	0.008	0.219	0.816	-	0.821	-	-	4.
A3	49.44	1.70	5.69	-	7.83	14.76	-	20.58	-	-	98.30	1.829	0.047	0.248	-	0.242	0.814	-	0.816	-	-	3.999
427B G																						
1	53.22	0.40	2.17	0.58	5.88	19.60	-	18.15	-	-	101.90	1.933	0.010	0.093	0.016	0.178	1.061	-	0.706	-	-	4.001
B1	51.70	0.63	3.57	0.69	5.63	17.26	-	20.02	0.47	-	101.10	1.893	0.017	0.154	0.019	0.172	0.942	-	0.785	0.033	-	4.019
B2	51.64	0.60	5.67	0.88	5.43	17.03	-	20.76	-	-	101.40	1.890	0.016	0.158	0.025	0.166	0.929	-	0.814	-	-	4.001
D1	51.62	0.75	3.85	0.57	6.00	16.90	-	20.30	-	-	101.20	1.890	0.020	0.166	0.016	0.183	0.922	-	0.796	-	-	3.997
D3	53.01	0.50	2.14	0.29	6.12	18.21	-	19.76	-	-	100.70	1.935	0.013	0.091	0.008	0.186	0.991	-	0.773	-	-	4.001
D4	53.37	0.43	2.23	0.32	6.09	17.96	-	19.63	-	-	100.40	1.945	0.011	0.095	0.009	0.185	0.975	-	0.766	-	-	3.991
427B P																						
D1	51.34	0.58	4.16	1.34	4.99	17.21	-	119.92	0.44	-	101.10	1.877	0.016	0.179	0.038	0.152	0.938	-	0.780	0.031	-	4.014
D2	51.49	0.73	4.02	1.23	5.36	16.91	-	20.23	-	-	100.30	1.883	0.020	0.173	0.035	0.164	0.922	-	0.792	-	-	3.991
D3	51.58	0.82	3.74	0.66	6.21	17.06	-	19.92	-	-	99.	1.889	0.022	0.161	0.019	0.190	0.931	-	0.782	-	-	3.997
E1	53.18	0.38	2.27	0.54	5.96	18.79	-	18.89	-	-	101.	1.935	0.010	0.097	0.015	0.181	1.019	-	0.736	-	-	3.997
E2	52.99	0.42	2.27	0.47	5.85	18.16	-	19.85	-	-	100.50	1.933	0.011	0.097	0.013	0.178	0.987	-	0.776	-	-	3.999
428B G																						
	50.55	1.15	5.14	0.29	5.45	16.22	-	21.20	-	-	100.50	1.852	0.031	0.221	0.008	0.167	0.885	-	0.832	-	-	4.
38189 G																						
B1	50.81	0.55	1.40	-	14.78	9.98	0.39	21.00	1.08	-	97.90	1.953	0.015	0.063	-	0.475	0.572	0.012	0.865	0.080	-	4.038
B2	50.23	1.03	2.80	-	12.75	11.14	0.30	20.90	0.84	-	100.10	1.910	0.029	0.061	-	0.405	0.631	0.009	0.852	0.061	-	4.027
E1	49.01	1.53	5.52	0.66	6.39	14.48	-	21.95	0.46	-	98.60	1.817	0.042	0.241	0.019	0.198	0.800	-	0.872	0.032	-	4.026
E2	48.67	1.73	5.52	0.37	7.38	14.09	-	21.74	0.49	-	99.10	1.812	0.048	0.242	0.010	0.229	0.782	-	0.867	0.034	-	4.029
E3	51.28	1.13	3.06	-	7.96	15.04	-	21.51	-	-	99.20	1.901	0.031	0.133	-	0.246	0.831	-	0.854	-	-	3.999
38190 G																						
1	48.15	1.93	5.16	-	10.50	12.95	-	20.76	0.55	-	100.	1.814	0.054	0.229	-	0.330	0.727	-	0.838	0.040	-	4.036
2	50.12	0.95	5.39	1.02	4.97	15.98	-	21.56	-	-	98.40	1.839	0.026	0.232	0.029	0.152	0.874	-	0.847	-	-	4.003
3	50.42	1.28	2.65	0.28	11.30	13.99	-	20.06	-	-	100.60	1.895	0.036	0.117	0.008	0.355	0.784	-	0.808	-	-	4.005
4	49.24	1.65	4.76	-	9.30	13.83	-	21.21	-	-	99.	1.840	0.046	0.209	-	0.290	0.770	-	0.849	-	-	4.008
38199 G																						
B1	48.17	1.75	7.60	0.34	5.43	14.48	-	22.23	-	-	99.50	1.775	0.048	0.329	0.009	0.167	0.795	-	0.878	-	-	4.005
B2	49.07	1.67	6.67	0.62	5.40	16.10	-	20.44	-	-	100.60	1.799	0.045	0.288	0.018	0.165	0.880	-	0.803	-	-	4.001
B3	47.62	2.52	7.16	0.35	6.60	13.75	-	22.01	-	-	99.	1.767	0.070	0.313	0.010	0.204	0.760	-	0.875	-	-	4.001
38299 G																						
A1	49.82	1.28	5.29	0.38	4.88	15.74	-	22.61	-	-	97.70	1.832	0.035	0.229	0.010	0.149	0.862	-	0.890	-	-	4.012
A2	48.13	2.00	7.10	-	5.79	14.29	-	22.68	-	-	95.60	1.779	0.055	0.309	-	0.178	0.787	-	0.898	-	-	4.010
B	48.15	1.97	7.26	0.48	5.06	14.38	-	22.71	-	-	102.30	1.776	0.054	0.315	0.014	0.155	0.790	-	0.897	-	-	4.005
C	47.68	2.35	7.07	-	6.33	14.06	0	22.49	-	-	100.20	1.768	0.065	0.308	-	0.196	0.777	-	0.893	-	-	4.010
A	47.94	2.55	7.71	-	10.39	10.16	-	19.03	2.21	-	98.70	1.800	0.072	0.341	-	0.326	0.569	-	0.765	0.160	-	4.037

	SiO_2	TiO_2	Al_2O_3	Cr_2O_3	FeO	MgO	MnO	CaO	Na_2O	K_2O	Total	Si	Ti	Al	Cr	Fe	Mg	Mn	Ca	Na	K	Total
204	P																					
A1c	51.90	0.44	3.54	0.89	5.99	17.04	-	19.86	0.33	-	100.56	1.901	0.012	0.153	0.026	0.183	0.930	-	0.780	0.023	-	4.009
A2c	51.74	0.67	3.88	0.73	6.95	17.35	-	18.31	0.38	-	100.77	1.895	0.018	0.167	0.021	0.213	0.947	-	0.718	0.027	-	4.006
A3c	51.68	0.65	3.92	0.49	6.90	16.55	-	19.40	0.41	-	100.92	1.897	0.018	0.170	0.014	0.212	0.906	-	0.763	0.029	-	4.008
A4c	51.74	0.55	4.10	0.76	6.70	16.77	-	19.13	0.25	-	99.49	1.895	0.015	0.177	0.022	0.205	0.916	-	0.751	0.018	-	3.999
A1r	51.69	0.83	3.43	0.42	6.94	17.36	-	19.01	0.34	-	99.60	1.896	0.023	0.148	0.012	0.213	0.949	-	0.747	0.024	-	4.013
A2r	49.63	1.51	5.19	0.22	8.39	15.42	-	19.21	0.43	-	100.34	1.838	0.042	0.227	0.006	0.260	0.852	-	0.762	0.031	-	4.018
A3r	51.72	0.58	3.92	0.39	7.38	17.64	-	18.10	0.26	-	99.61	1.894	0.016	0.169	0.011	0.226	0.963	-	0.710	0.019	-	4.009
A4r	51.33	0.76	4.00	0.42	7.94	17.56	-	18.09	0.35	-	99.52	1.883	0.021	0.173	0.012	0.230	0.961	-	0.711	0.025	-	4.015
A5r	50.20	1.27	5.12	0.36	7.21	16.16	-	19.27	0.41	-	99.76	1.848	0.035	0.222	0.010	0.222	0.887	-	0.760	0.030	-	4.015
A6r	51.40	0.76	3.79	0.36	7.76	17.33	-	18.15	0.38	0.07	99.88	1.889	0.021	0.164	0.010	0.239	0.949	-	0.715	0.027	0.003	4.018
204	M																					
A1	53.73	0.32	1.76	0.63	7.06	19.72	-	16.59	0.20	-	99.88	1.953	0.009	0.076	0.018	0.215	1.069	-	0.646	0.014	-	3.998
C1c	53.32	0.29	1.92	0.64	5.94	18.24	0.11	19.31	0.23	-	99.86	1.946	0.008	0.082	0.018	0.181	0.992	0.004	0.755	0.016	-	4.004
C1r	50.49	1.21	4.78	0.22	7.61	16.31	0.16	18.89	0.34	-	101.23	1.860	0.034	0.207	0.006	0.234	0.895	0.005	0.745	0.024	-	4.012
C2c	53.69	0.30	1.66	0.41	7.56	19.64	-	16.73	-	-	100.39	1.955	0.008	0.071	0.012	0.230	1.066	-	0.653	-	-	3.995
C2r	49.56	1.21	5.49	0.46	7.28	15.57	-	20.02	0.35	0.06	100.82	1.832	0.034	0.239	0.014	0.225	0.858	-	0.793	0.025	0.003	4.022
C5c	51.45	0.68	3.81	0.41	7.42	17.11	-	18.77	0.35	-	100.05	1.890	0.019	0.165	0.012	0.228	0.937	-	0.739	0.025	-	4.015
C3c	51.40	0.69	3.98	0.65	6.95	16.89	-	19.00	0.42	-	100.64	1.887	0.019	0.172	0.019	0.213	0.924	-	0.748	0.030	-	4.013
C3r	50.56	1.00	5.05	0.27	7.17	16.02	-	19.66	0.28	-	99.69	1.860	0.028	0.219	0.008	0.221	0.878	-	0.775	0.020	-	4.009
C4c	51.58	0.56	3.73	0.91	5.85	16.64	-	10.41	0.32	-	99.80	1.892	0.016	0.161	0.026	0.180	0.910	-	0.802	0.023	-	4.010
C4r	51.72	0.64	3.96	0.53	7.30	17.36	-	18.32	0.16	-	99.33	1.895	0.018	0.171	0.015	0.224	0.948	-	0.718	0.011	-	4.000
144	P																					
A1c	53.66	0.11	2.11	0.31	4.79	18.38	-	20.48	0.15	-	100.07	1.950	0.003	0.091	0.009	0.146	0.996	-	0.798	0.011	-	4.002
A2c	54.07	-	2.02	0.21	4.56	18.35	-	20.78	-	-	99.47	1.961	-	0.086	0.006	0.138	0.992	-	0.808	-	-	3.992
A3c	53.55	0.23	2.22	0.22	4.60	18.16	-	21.02	-	-	100.20	1.946	0.006	0.095	0.006	0.140	0.984	-	0.819	-	-	3.997
A1r	52.94	0.48	1.46	0.16	8.76	17.21	-	18.99	-	-	100.08	1.952	0.013	0.063	0.005	0.270	0.946	-	0.750	-	-	4.000
A2r	52.04	0.65	1.46	0.15	10.95	16.15	0.19	18.06	0.35	-	101.07	1.941	0.018	0.064	0.004	0.342	0.898	0.006	0.721	0.025	-	4.019
A3r	51.99	0.73	1.58	-	10.70	15.85	0.24	18.64	0.28	-	100.64	1.939	0.020	0.070	-	0.334	0.881	0.008	0.745	0.020	-	4.016
A4r	51.70	0.66	1.70	0.12	11.36	16.18	0.17	17.77	0.34	-	101.32	1.931	0.019	0.075	0.004	0.355	0.900	0.005	0.711	0.024	-	4.024
A5r	50.77	1.08	1.96	0.15	13.20	13.26	0.18	19.14	0.26	-	99.65	1.922	0.031	0.088	0.004	0.418	0.748	0.006	0.776	0.019	-	4.011
144	G																					
C1	52.27	0.56	2.58	0.28	7.17	16.83	-	19.95	0.35	-	100.01	1.923	0.016	0.112	0.008	0.220	0.923	-	0.787	0.025	-	4.014
C2	51.61	0.79	2.54	0.19	9.87	15.58	-	19.12	0.29	-	99.40	1.919	0.022	0.111	0.006	0.307	0.863	-	0.762	0.021	-	4.011
C3	51.75	0.66	3.16	0.60	6.26	16.43	-	20.85	0.28	-	100.86	1.903	0.018	0.137	0.017	0.193	0.901	-	1.821	0.020	-	4.011
C4	52.33	0.60	2.58	0.18	7.28	16.32	-	20.48	0.23	-	99.51	1.927	0.017	0.112	0.005	0.224	0.896	-	0.808	0.016	-	4.006
C5	53.06	0.43	1.43	0.21	8.50	17.43	-	18.75	0.20	-	98.75	1.954	0.012	0.062	0.006	0.262	0.957	-	0.740	0.014	-	4.007
C6	51.47	0.84	2.32	-	10.77	15.41	0.17	18.74	0.28	-	98.56	1.921	0.025	0.102	-	0.336	0.857	0.005	0.749	0.020	-	4.015
C7	50.90	0.95	2.51	0.14	11.37	15.81	0.17	18.37	0.42	-	99.93	1.907	0.027	0.111	0.004	0.356	0.847	0.005	0.737	0.030	-	4.024
C8	51.37	0.89	2.69	0.15	9.16	15.38	0.14	19.99	0.23	-	99.12	1.910	0.025	0.118	0.004	0.285	0.852	0.004	0.796	0.017	-	4.012
53	G																					
A1c	51.37	0.94	3.65	0.23	7.26	16.23	-	19.89	0.43	-	99.42	1.892	0.026	0.158	0.007	0.224	0.891	-	0.785	0.031	-	4.014
A2c	52.53	0.48	2.91	0.54	6.41	16.96	-	19.89	0.28	-	99.16	1.924	0.013	0.126	0.016	0.196	0.926	-	0.781	0.020	-	4.002
A3	50.93	0.90	4.25	0.33	6.97	16.07	-	20.38	0.35	-	99.52	1.872	0.025	0.184	0.010	0.209	0.882	-	0.804	0.025	-	4.015
A4	50.57	1.14	3.49	0.22	8.60	15.07	0.12	20.31	0.42	0.06	99.72	1.882	0.032	0.153	0.007	0.262	0.836	0.004	0.810	0.030	0.003	4.023
A5	51.33	0.80	3.93	0.31	7.35	15.58	-	20.41	0.29	-	97.80	1.893	0.022	0.171	0.009	0.227	0.856	-	0.807	0.021	-	4.005
A6	50.37	1.30	3.90	0.21	8.36	15.21	-	20.12	0.52	-	99.25	1.870	0.036	0.171	0.006	0.260	0.842	-	0.800	0.038	-	4.024
A7	50.87	1.17	3.73	0.24	7.47	15.24	-	20.89	0.39	-	98.89	1.883	0.033	0.163	0.007	0.231	0.841	-	0.828	0.028	-	4.014
A8	49.03	1.62	3.53	0.14	13.46	11.40	0.27	19.97	0.58	-	100.27	1.870	0.046	0.159	0.004	0.429	0.648	0.009	0.816	0.043	-	4.024
A9	52.61	0.53	1.54	0.18	9.58	17.69	0.21	17.27	0.40	-	99.08	1.944	0.015	0.067	0.005	0.296	0.974	0.007	0.684	0.028	-	4.020
A10	50.85	1.09	3.98	0.20	7.51	15.63	-	20.48	0.26	-	98.45	1.879	0.030	0.173	0.006	0.232	0.861	-	0.811	0.018	-	4.010
A11	49.54	1.40	3.93	0.18	11.05	13.59	0.15	19.64	0.53	-	99.86	1.863	0.040	0.174	0.005	0.348	0.762	0.005	0.791	0.039	-	4.027
A12	49.57	1.38	3.79	-	10.77	13.50	-	20.46	0.52	-	99.24	1.865	0.039	0.168	-	0.339	0.757	-	0.825	0.038	-	4.031
A13	50.92	1.06	3.66	0.22	7.65	15.26	-	20.96	0.27	-	99.52	1.886	0.029	0.160	0.006	0.237	0.843	-	0.832	0.019	-	4.011
A14	49.73	1.47	4.27	-	10.11	14.37	-	19.43	0.61	-	99.39	1.859	0.041	0.188	-	0.316	0.801	-	0.778	0.044	-	4.028
A15	49.64	1.39	3.72	0.23	10.22	14.15	0.16	19.93	0.49	0.07	99.99	1.863	0.039	0.165	0.007	0.321	0.791	0.005	0.802	0.036	0.003	4.032
A16	49.45	1.54	5.57	0.45	7.34	15.31	-	19.92	0.41	-	99.12	1.828	0.043	0.243	0.013	0.227	0.844	-	0.789	0.030	-	4.016
221	M																					
B1	51.15	0.67	4.07	1.22	6.21	16.37	-	20.03	0.27	-	100.43	1.880	0.019	0.176	0.035	0.191	0.897	-	0.789	0.020	-	4.006
B2	51.48	0.67	3.83	0.88	6.61	16.68	-	19.62	0.23	-	100.26	1.890	0.019	0.166	0.025	0.203	0.913	-	0.772	0.017	-	4.004
B3	51.47	0.58	3.84	1.14	5.83	16.45	-	20.30	0.39	-	101.22	1.889	0.016	0.166	0.033	0.179	0.900	-	0.798	0.028	-	4.009
B4	51.09	0.79	3.94	0.75	7.08	16.55	0.15	19.37	0.29	-	101.03	1.881	0.022	0.171	0.022	0.218	0.908	0.005	0.764	0.021	-	4.011
B5	50.74	0.71	4.53	0.91	7.29	16.42	-	19.01	0.38	-	99.54	1.868	0.020	0.197	0.027	0.224	0.901	-	0.750	0.027	-	4.014
B6	51.01	0.78	3.93	1.04	6.10	16.01	-	20.88	0.25	-	100.83	1.878	0.022	0.171	0.030	0.188	0.879	-	0.824	0.018	-	4.009
228	G																					
C1	50.05	0.82	5.44	1.49	4.39	15.62	-	21.93	0.26	-	100.18	1.838	0.023	0.235	0.043	0.135	0.855	-	0.863	0.019	-	4.010
C2	49.10	1.49	6.59	0.57	5.25	15.23	-	21.57	0.20	-	99.82	1.806	0.041	0.286	0.017	0.161	0.835	-	0.850	0.015	-	4.009
C3	48.13	2.16	6.63	-	9.00	12.71	0.12	20.40	0.56	0.28	100.37	1.801	0.061	0.292	-	0.282	0.709	0.004	0.818	0.041	0.013	4.020
C4	48.29	2.15	6.19	0.12	7.30	13.95	-	21.67	0.32	-	101.16	1.796	0.060	0.271	0.004	0.227	0.773	-	0.864	0.023	-	4.018
64	dyke	G																				
B1	47.66	1.74	8.75	0.19	4.83	13.86	-	22.78	0.18	-	98.30	1.755	0.048	0.380	0.006	0.149	0.761	-	0.899	0.013	-	4.010
B2	46.61	1.81	8.16	0.13	7.17	12.69	-	22.92	0.50	-	98.56	1.743	0.051	0.360	0.004	0.224	0.707	-	0.918	0.036	-	4.043
B3	50.06	1.11	4.77	0.17	5.80	14.78	-	23.12	0.19	-	98.49	1.851	0.031	0.208	0.005	0.179	0.814	-	0.916	0.013	-	4.018
B4	51.53	0.69	3.90	0.19	4.34	16.18	-	23.17	-	-	99.01	1.888	0.019	0.169	0.006	0.133	0.883	-	0.910	-	-	4.006
B5	47.04	2.00	8.18	0.13	5.82	13.19	-	23.35	0.28	-	101.62	1.747	0.056	0.358	0.004	0.181	0.730	-	0.929	0.020	-	4.026

APPENDIX 3: Section A cont.

	SiO_2	TiO_2	Al_2O_3	Cr_2O_3	FeO	MgO	MnO	CaO	Na_2O	K_2O	Total	Si	Ti	Al	Cr	Fe	Mg	Mn	Ca	Na	K	Total
64	dyke	Kaersutitic amphibole																				
A1	38.73	5.24	15.20	-	13.72	11.19	-	12.26	2.77	1.10	100.21	5.678	0.578	2.626	-	1.682	2.445	-	1.925	0.786	0.206	15.926
A2	39.26	4.50	14.63	0.10	15.50	10.63	0.24	11.76	3.08	0.95	100.64	5.770	0.498	2.534	0.012	1.905	2.330	0.030	1.852	0.877	0.178	15.986
B1	42.37	3.57	16.20	-	12.76	8.93	0.15	9.86	2.89	0.78	97.50	6.218	0.394	2.802	-	1.566	1.954	0.018	1.550	0.823	0.147	15.472
B2	42.15	4.04	14.65	-	12.60	10.89	-	11.13	3.14	0.81	99.41	6.115	0.441	2.506	-	1.528	2.354	-	1.729	0.883	0.150	15.706
B3	38.30	5.02	15:15	-	15.06	10.47	0.20	11.56	3.01	1.06	99.82	5.674	0.559	2.644	-	1.866	2.312	0.025	1.835	0.864	0.200	15.977
B4	37.49	5.16	14.91	-	13.31	10.99	-	12.13	2.79	1.00	97.79	5.637	0.583	2.642	-	1.674	2.464	-	1.955	0.814	0.191	15.961
214	P-1																					
B1c	52.79	0.31	2.19	0.32	6.61	17.31	-	20.26	0.20	-	99.72	1.937	0.009	0.095	0.009	0.203	0.947	-	0.796	0.014	-	4.010
B2c	52.89	0.33	2.20	0.27	6.72	17.05	-	20.31	0.24	-	99.56	1.941	0.009	0.095	0.008	0.206	0.933	-	0.798	0.017	-	4.007
B1r	53.06	0.32	2.30	0.20	6.83	17.22	-	20.06	-	-	98.50	1.944	0.009	0.099	0.006	0.209	0.940	-	0.787	-	-	3.995
B2r	51.93	0.60	3.52	0.20	6.28	16.94	-	20.35	0.16	-	99.66	1.903	0.017	0.152	0.006	0.192	0.925	-	0.799	0.011	-	4.006
214	P-2																					
B1c	53.09	0.33	2.22	0.28	6.82	17.20	-	19.75	0.31	-	99.39	1.946	0.009	0.096	0.008	0.209	0.939	-	0.775	0.022	-	4.004
B2c	52.93	0.35	2.21	0.29	6.62	17.21	-	20.16	0.23	-	99.92	1.941	0.010	0.095	0.008	0.203	0.940	-	0.792	0.017	-	4.006
B1r	53.82	0.21	1.78	0.36	5.65	18.29	-	19.89	-	-	100.28	1.959	0.006	0.076	0.010	0.172	0.992	-	0.776	-	-	3.992
B2r	53.74	0.32	1.71	0.35	6.49	18.62	-	18.77	-	-	100.01	1.958	0.009	0.073	0.010	0.198	1.011	-	0.773	-	-	3.992
B3r	53.33	0.32	1.82	0.27	6.46	18.46	-	19.06	0.28	-	99.64	1.948	0.009	0.078	0.008	0.197	1.005	-	0.746	0.020	-	4.010
B4r	53.51	0.22	1.56	0.27	7.31	19.16	-	17.74	0.23	-	100.50	1.954	0.006	0.067	0.008	0.223	1.043	-	0.694	0.016	-	4.011
214	M																					
A1	51.10	0.96	4.45	0.25	7.80	15.91	-	19.22	0.31	-	100.47	1.882	0.027	0.193	0.007	0.240	0.873	-	0.758	0.022	-	4.002
A2	54.09	0.26	1.47	0.20	7.10	19.09	-	17.80	-	-	100.94	1.969	0.007	0.063	0.006	0.216	1.036	-	0.694	-	-	3.990
A3	49.85	1.22	4.45	0.23	10.96	14.62	-	18.33	0.34	-	100.89	1.862	0.034	0.196	0.007	0.342	0.814	-	0.734	0.025	-	4.014
A4	51.70	0.65	3.96	0.54	6.57	17.53	-	18.86	0.20	-	100.29	1.891	0.018	0.171	0.016	0.201	0.956	-	0.739	0.014	-	4.005
A5	49.48	1.44	5.21	0.24	8.92	15.01	-	19.26	0.36	0.07	99.88	1.838	0.040	0.228	0.007	0.277	0.831	-	0.767	0.026	0.003	4.018
A6	50.47	1.16	4.73	0.16	8.91	16.14	-	18.22	0.21	-	102.98	1.864	0.032	0.206	0.005	0.275	0.888	-	0.721	0.015	-	4.006
A7	50.19	1.26	4.84	0.16	8.27	15.91	-	18.91	0.46	-	101.10	1.855	0.035	0.211	0.005	0.256	0.876	-	0.749	0.033	-	4.019
A8	50.55	1.14	4.48	0.10	7.96	15.18	-	20.20	0.38	-	100.82	1.870	0.032	0.195	0.003	0.246	0.837	-	0.801	0.027	-	4.012
B1c1	49.70	1.57	4.85	0.18	8.69	14.99	-	19.66	0.36	-	99.73	1.846	0.044	0.212	0.005	0.270	0.830	-	0.782	0.026	-	4.015
B1c2	51.15	0.84	3.67	0.30	8.29	15.85	-	19.53	0.38	-	99.86	1.891	0.023	0.160	0.009	0.256	0.874	-	0.774	0.027	-	4.014
B1r2	51.63	0.67	3.72	0.23	7.16	17.12	-	19.46	-	-	98.92	1.895	0.019	0.161	0.007	0.220	0.937	-	0.765	-	-	4.003
B2c1	52.06	0.43	3.79	0.57	4.61	17.15	-	21.20	0.18	-	99.68	1.899	0.012	0.163	0.016	0.141	0.933	-	0.829	0.013	-	4.006
B2c2	51.44	0.54	4.76	0.46	5.45	16.87	-	20.05	0.43	-	99.83	1.879	0.015	0.205	0.013	0.167	0.918	-	0.785	0.030	-	4.012
B1r1	51.15	0.94	4.58	0.20	6.92	16.55	-	19.47	0.19	-	99.38	1.877	0.026	0.198	0.006	0.212	0.905	-	0.765	0.013	-	4.002
B2r1	51.33	0.83	3.98	0.21	6.97	16.37	-	19.96	0.34	-	99.20	1.888	0.023	0.173	0.006	0.214	0.897	-	0.786	0.024	-	4.012
B2r2	52.52	0.44	3.06	0.33	5.79	16.79	-	21.07	-	-	99.46	1.922	0.012	0.132	0.010	0.177	0.916	-	0.826	-	-	3.995
B2r3	52.33	0.46	3.01	0.34	5.89	16.60	-	21.16	0.19	-	100.08	1.919	0.013	0.130	0.010	0.181	0.907	-	0.831	0.014	-	4.005
B2c3	51.93	0.30	3.97	0.57	4.66	17.20	-	21.08	0.29	-	100.03	1.895	0.008	0.171	0.017	0.142	0.936	-	0.824	0.020	-	4.013
D1	52.62	0.54	1.72	0.18	9.47	18.26	0.18	16.62	0.35	0.07	99.67	1.940	0.015	0.075	0.005	0.292	1.003	0.006	0.656	0.025	0.003	4.020
D2	48.99	1.41	3.89	0.20	13.70	13.41	0.18	17.72	0.49	-	100.89	1.857	0.040	0.174	0.006	0.434	0.758	0.006	0.719	0.036	-	4.031
D4	51.57	0.55	4.67	0.50	5.60	17.32	-	19.79	-	-	100.39	1.881	0.015	0.201	0.014	0.171	0.941	-	0.773	-	-	3.997
D5	52.23	0.46	4.33	0.46	6.41	19.11	-	17.00	-	-	99.60	1.895	0.012	0.185	0.013	0.194	1.033	-	0.661	-	-	3.994
D6	51.55	0.68	3.80	0.13	7.40	16.07	-	20.17	0.19	-	100.28	1.898	0.019	0.165	0.004	0.228	0.882	-	0.796	0.014	-	4.005
D7	51.42	0.77	4.03	0.28	6.65	16.21	-	20.34	0.30	-	100.52	1.890	0.021	0.175	0.008	0.204	0.888	-	0.801	0.022	-	4.009
D8	53.70	0.22	1.58	0.16	7.57	19.39	-	17.20	0.19	-	101.02	1.958	0.006	0.068	0.004	0.231	1.054	-	0.672	0.014	-	4.007
D11	51.79	0.58	4.08	0.40	6.02	16.86	-	20.27	-	-	99.86	1.894	0.016	0.176	0.012	0.184	0.919	-	0.794	-	-	3.996
214	G																					
B1	51.02	0.83	4.36	0.16	7.43	16.36	-	19.84	-	-	98.14	1.877	0.023	0.189	0.005	0.229	0.897	-	0.782	-	-	4.003
B2	52.61	0.54	2.66	-	9.06	18.05	0.13	16.95	-	-	99.83	1.931	0.015	0.115	-	0.278	0.987	0.004	0.666	-	-	3.997
B3	49.82	1.22	4.58	0.26	9.79	15.43	-	18.39	0.50	-	100.42	1.854	0.034	0.201	0.008	0.305	0.855	-	0.733	0.036	-	4.026
B4	50.14	1.26	4.54	0.25	8.29	15.69	0.13	19.28	0.43	-	100.32	1.857	0.035	0.198	0.007	0.257	0.866	0.004	0.765	0.031	-	4.021
C1	49.79	1.35	4.83	-	10.23	14.55	-	18.86	0.39	-	100.39	1.856	0.038	0.212	-	0.319	0.809	-	0.753	0.028	-	4.014
D9	52.75	0.42	2.57	0.28	6.04	17.31	-	20.38	0.26	-	99.91	1.931	0.012	0.111	0.008	0.185	0.944	-	0.799	0.018	-	4.007
D10	49.45	1.40	5.29	0.15	9.05	14.96	0.16	19.01	0.53	-	100.90	1.838	0.039	0.232	0.005	0.281	0.829	0.005	0.757	0.038	-	4.024
D12	52.39	0.40	2.97	0.20	7.89	17.34	-	18.55	0.25	-	99.23	1.923	0.011	0.128	0.006	0.242	0.949	-	0.730	0.018	-	4.007
55A	P																					
A1c	53.29	0.29	2.37	0.39	4.88	17.55	-	21.02	0.21	-	101.04	1.942	0.008	0.102	0.011	0.149	0.954	-	0.821	0.015	-	4.001
A2c	53.39	0.26	2.32	0.33	4.84	17.58	-	20.93	0.36	-	100.09	1.945	0.007	0.100	0.010	0.147	0.955	-	0.817	0.025	-	4.006
A3c	53.44	0.18	2.35	0.32	4.76	17.58	-	21.15	0.22	-	99.42	1.946	0.005	0.101	0.009	0.145	0.954	-	0.825	0.016	-	4.002
A4c	52.39	0.45	3.32	0.38	4.98	17.08	-	21.17	0.22	-	99.88	1.913	0.012	0.143	0.011	0.152	0.930	-	0.828	0.016	-	4.005
A9m	52.29	0.42	3.46	0.38	4.95	16.99	-	21.24	0.28	-	99.10	1.910	0.011	0.149	0.011	0.151	0.925	-	0.831	0.020	-	4.009
A11m	52.36	0.46	3.62	0.42	4.87	16.80	-	21.19	0.28	-	100.56	1.911	0.012	0.156	0.012	0.149	0.914	-	0.829	0.020	-	4.003
A1r	52.26	0.61	2.32	0.40	6.65	16.33	-	21.26	0.17	-	99.32	1.925	0.017	0.101	0.012	0.205	0.897	-	0.839	0.012	-	4.008
A2r	49.59	1.30	4.52	0.81	7.05	15.13	-	21.15	0.45	-	100.41	1.841	0.046	0.198	0.024	0.219	0.837	-	0.841	0.032	-	4.028
A3r	50.71	1.04	3.86	0.76	6.57	15.41	-	21.28	0.37	-	100.13	1.874	0.029	0.168	0.022	0.203	0.849	-	0.843	0.027	-	4.015
A4r	51.50	0.84	3.09	0.75	6.38	15.59	-	21.60	0.24	-	99.52	1.901	0.023	0.135	0.022	0.197	0.858	-	0.854	0.017	-	4.007
A5r	50.34	1.19	3.89	0.81	6.76	15.35	-	21.33	0.34	-	99.85	1.864	0.033	0.170	0.024	0.209	0.847	-	0.846	0.024	-	4.018
55A	G																					
A1	48.88	1.91	5.03	0.13	8.28	14.21	-	21.18	0.37	-	98.73	1.823	0.054	0.221	0.004	0.258	0.790	-	0.847	0.027	-	4.024
A2	48.18	2.15	5.51	0.22	9.59	13.48	0.15	20.23	0.49	-	99.84	1.807	0.061	0.244	0.007	0.301	0.754	0.005	0.813	0.035	-	4.025
A3	47.65	2.56	5.43	0.16	10.71	12.69	-	20.29	0.51	-	100.04	1.798	0.073	0.241	0.005	0.338	0.713	-	0.820	0.037	-	4.025
A4	47.38	2.42	5.22	0.22	10.77	12.68	0.12	20.57	0.62	-	100.18	1.793	0.069	0.233	0.006	0.341	0.715	0.004	0.834	0.046	-	4.041
B1	47.74	2.36	4.84	0.17	11.74	11.77	-	20.78	0.60	-	100.19	1.813	0.067	0.216	0.005	0.373	0.666	-	0.845	0.044	-	4.031
B2	49.87	1.44	4.65	0.87	6.87	14.80	-	21.16	0.35	-	101.06	1.847	0.040	0.203	0.025	0.213	0.817	-	0.840	0.025	-	4.011
B3	50.59	1.24	3.52	0.71	7.71	15.82	-	19.98	0.43	-	101.98	1.874	0.035	0.154	0.021	0.239	0.874	-	0.793	0.031	-	4.020
B4	48.05	2.40	5.85	0.34	8.81	13.76	-	20.46	0.32	-	98.38	1.795	0.067	0.258	0.010	0.275	0.767	-	0.819	0.023	-	4.015
B6	48.32	2.25	5.38	0.24	9.01	13.60	-	20.72	0.49	-	100.33	1.809	0.063	0.237	0.007	0.282	0.759	-	0.831	0.035	-	4.023
B7	48.17	2.55	5.19	0.19	9.18	13.30	-	20.95	0.48	-	100.53	1.807	0.072	0.229	0.006	0.288	0.744	-	0.842	0.035	-	4.021
B8	48.78	2.07	5.03	0.63	7.66	14.15	-	21.33	0.35	-	100.38	1.818	0.058	0.221	0.019	0.239	0.786	-	0.852	0.025	-	4.017
B9	48.27	2.15	5.38	0.24	9.35	13.63	-	20.56	0.43	-	100.61	1.809	0.060	0.237	0.007	0.293	0.761	-	0.825	0.031	-	4.024
B10	47.92	2.53	5.56	0.26	9.33	13.26	-	20.62	0.53	-	100.77	1.798	0.072	0.246	0.008	0.293	0.741	-	0.829	0.038	-	4.024

	SiO_2	TiO_2	Al_2O_3	Cr_2O_3	FeO	MgO	MnO	CaO	Na_2O	K_2O	Total	Si	Ti	Al	Cr	Fe	Mg	Mn	Ca	Na	K	Total
55	P																					
A1c	52.67	0.37	3.41	0.33	4.69	16.90	-	21.14	0.50	-	99.94	1.920	0.010	0.146	0.009	0.143	0.918	-	0.826	0.035	-	4.009
A2c	52.61	0.38	3.39	0.37	4.89	17.07	-	20.95	0.34	-	100.39	1.918	0.010	0.146	0.011	0.149	0.928	-	0.818	0.024	-	4.005
A3c	52.68	0.42	3.29	0.31	4.74	16.99	-	21.25	0.33	-	100.05	1.921	0.011	0.142	0.009	0.144	0.923	-	0.830	0.023	-	4.004
A1r	51.51	0.74	3.78	1.02	5.55	15.86	-	21.18	0.35	-	99.52	1.892	0.020	0.164	0.030	0.171	0.868	-	0.834	0.025	-	4.003
A2r	52.46	0.48	3.30	0.36	4.82	17.09	-	21.15	0.33	-	98.61	1.915	0.014	0.142	0.010	0.147	0.930	-	0.827	0.023	-	4.008
A3r	51.99	0.78	2.95	0.66	6.09	15.89	-	21.26	0.38	-	99.71	1.913	0.021	0.128	0.019	0.187	0.871	-	0.838	0.027	-	4.006
A4r	51.03	0.89	3.96	0.90	6.34	15.38	-	21.10	0.40	-	99.53	1.882	0.025	0.172	0.026	0.196	0.845	-	0.834	0.029	-	4.009
A5r	50.26	1.28	4.31	0.43	6.92	15.18	-	21.06	0.56	-	100.10	1.860	0.036	0.188	0.013	0.214	0.837	-	0.835	0.040	-	4.023
55	G																					
A1	48.01	2.30	5.20	0.26	9.87	13.07	-	20.60	0.62	0.07	98.76	1.807	0.065	0.231	0.008	0.310	0.733	-	0.831	0.046	0.003	4.033
A2	49.54	1.47	4.78	0.69	7.48	14.63	-	20.96	0.47	-	99.76	1.840	0.041	0.209	0.020	0.232	0.810	-	0.834	0.034	-	4.021
A3	49.76	1.48	4.53	0.28	8.37	14.36	-	20.60	0.62	-	99.74	1.853	0.041	0.199	0.008	0.261	0.797	-	0.822	0.045	-	4.025
A4	49.08	1.88	5.04	0.36	7.98	14.20	-	21.02	0.45	-	99.20	1.828	0.053	0.221	0.011	0.249	0.788	-	0.839	0.032	-	4.020
C1	48.02	2.04	4.90	0.20	12.04	11.52	0.20	20.43	0.66	-	100.29	1.824	0.058	0.219	0.006	0.383	0.652	0.006	0.832	0.049	-	4.029
C2	48.38	1.95	5.90	0.44	7.99	14.27	-	20.56	0.50	-	99.91	1.802	0.054	0.259	0.013	0.249	0.792	-	0.820	0.036	-	4.026
C3	48.68	1.78	3.67	0.18	13.77	10.77	0.29	20.12	0.66	0.06	100.30	1.863	0.051	0.166	0.006	0.440	0.614	0.010	0.825	0.049	0.003	4.027
C4	47.30	2.77	4.94	0.21	12.36	11.20	0.16	19.99	0.95	0.08	101.22	1.803	0.080	0.223	0.006	0.394	0.636	0.005	0.817	0.071	0.004	4.039
C5	52.59	0.68	2.15	0.25	8.10	17.28	-	18.69	0.24	-	99.18	1.935	0.019	0.093	0.007	0.249	0.947	-	0.737	0.017	-	4.005
C6	51.17	1.26	2.39	-	10.72	15.25	-	18.76	0.45	-	100.71	1.911	0.035	0.105	-	0.335	0.849	-	0.750	0.032	-	4.017
C7	48.06	2.46	4.91	0.14	10.98	12.48	0.14	20.24	0.59	-	100.73	1.815	0.070	0.219	0.004	0.347	0.703	0.004	0.819	0.043	-	4.025
C8	51.93	1.04	2.41	0.29	8.78	16.22	-	19.00	0.32	-	100.79	1.920	0.029	0.105	0.009	0.271	0.894	-	0.753	0.023	-	4.005
C9	47.22	2.56	6.62	0.36	8.70	13.65	-	20.41	0.47	-	99.50	1.767	0.072	0.292	0.011	0.272	0.761	-	0.818	0.034	-	4.027
C10	48.52	1.95	5.10	0.36	8.35	14.19	-	20.84	0.62	0.07	101.25	1.814	0.055	0.225	0.010	0.261	0.790	-	0.835	0.045	0.003	4.038
C11	48.47	2.27	5.48	0.26	8.90	13.38	-	20.71	0.53	-	100.21	1.813	0.064	0.242	0.008	0.278	0.746	-	0.830	0.039	-	4.018
C12	47.94	2.53	5.25	0.19	10.30	12.81	0.13	20.26	0.58	-	100.82	1.806	0.072	0.233	0.006	0.324	0.719	0.004	0.818	0.042	-	4.024
210	P																					
A1c	53.12	0.29	2.60	0.26	5.45	17.51	-	20.55	0.22	-	99.55	1.938	0.008	0.112	0.007	0.166	0.952	-	0.803	0.016	-	4.002
A2c	53.57	0.28	2.12	0.24	5.58	17.51	-	20.62	-	0.08	97.44	1.954	0.008	0.091	0.007	0.170	0.952	-	0.806	-	0.004	3.991
A3c	53.50	0.25	2.17	0.23	5.15	17.54	-	21.05	0.30	-	100.89	1.945	0.007	0.093	0.007	0.157	0.954	-	0.823	0.021	-	4.008
A4c	53.46	0.20	2.06	0.33	5.63	17.67	-	20.49	0.16	-	100.27	1.951	0.006	0.089	0.009	0.172	0.061	-	0.801	0.011	-	4.000
A3r	52.75	0.47	2.53	0.22	6.71	16.84	-	20.26	0.22	-	100.23	1.935	0.013	0.109	0.006	0.206	0.921	-	0.796	0.016	-	4.002
A4r	53.28	0.21	2.68	0.23	5.08	17.31	-	21.02	0.18	-	100.32	1.942	0.006	0.115	0.007	0.155	0.940	-	0.821	0.013	-	3.998
A5r	53.18	0.29	2.26	0.27	5.37	17.56	-	21.07	-	-	99.34	1.941	0.008	0.097	0.008	0.164	0.955	-	0.824	-	-	3.998
A2r	50.69	1.03	4.31	-	8.43	15.62	-	19.54	0.39	-	99.46	1.875	0.029	0.186	-	0.261	0.861	-	0.775	0.028	-	4.016
A1r	49.04	1.40	4.55	0.11	12.16	13.71	0.16	18.28	0.57	-	100.18	1.847	0.040	0.202	0.003	0.383	0.770	0.005	0.738	0.042	-	4.031
A6r	49.61	1.21	4.20	0.14	12.87	13.81	0.17	17.55	0.44	-	100.42	1.868	0.034	0.186	0.004	0.405	0.775	0.006	0.708	0.032	-	4.019
210	M																					
B1c	51.86	0.73	3.40	0.16	8.39	17.10	0.14	17.77	0.46	-	99.91	1.908	0.020	0.147	0.005	0.258	0.938	0.004	0.700	0.033	-	4.013
B1c2	52.03	0.54	3.09	0.20	7.66	16.49	-	19.74	0.27	-	99.99	1.916	0.015	0.134	0.006	0.236	0.905	-	0.799	0.019	-	4.009
B2c	51.69	0.71	3.59	0.34	6.74	16.56	-	20.06	0.32	-	99.89	1.899	0.019	0.155	0.010	0.207	0.907	-	0.790	0.023	-	4.010
B2r	52.18	0.55	3.42	0.51	6.54	17.02	-	19.50	0.28	-	99.35	1.911	0.015	0.148	0.015	0.200	0.929	-	0.765	0.020	-	4.003
B3c	51.62	0.78	3.30	0.27	7.80	16.06	-	19.81	0.37	-	100.29	1.905	0.022	0.143	0.008	0.241	0.883	-	0.783	0.027	-	4.011
B4c	51.69	0.69	3.51	0.18	7.86	16.34	-	19.47	0.26	-	98.85	1.904	0.019	0.152	0.005	0.242	0.897	-	0.768	0.018	-	4.007
B4r1	52.44	0.53	2.66	0.30	7.04	16.92	-	20.10	-	-	100.12	1.926	0.015	0.115	0.009	0.216	0.926	-	0.791	-	-	3.998
B4r2	50.68	1.08	4.55	0.14	8.44	16.28	-	18.42	0.43	-	100.49	1.869	0.030	0.198	0.004	0.260	0.895	-	0.728	0.030	-	4.015
B5c	51.06	0.77	4.37	0.19	6.75	16.15	-	20.22	0.41	0.08	99.14	1.879	0.021	0.190	0.006	0.208	0.886	-	0.797	0.029	0.004	4.019
B5r	52.10	0.51	3.28	0.27	6.54	17.16	-	19.77	0.30	0.08	100.57	1.910	0.014	0.142	0.008	0.200	0.936	-	0.777	0.021	0.004	4.013
B6c	51.32	0.78	4.24	0.23	8.20	17.15	-	17.72	0.36	-	100.64	1.885	0.022	0.184	0.007	0.252	0.939	-	0.697	0.026	-	4.011
B6r	50.13	1.27	4.88	0.24	8.28	15.34	-	19.34	0.45	-	100.13	1.855	0.035	0.213	0.007	0.256	0.846	-	0.770	0.032	-	4.016
B7c	51.86	0.65	3.47	0.55	6.62	17.54	-	18.92	0.39	-	100.85	1.900	0.018	0.150	0.016	0.203	0.958	-	0.742	0.028	-	4.014
B7r	53.80	0.24	1.59	0.11	7.98	18.73	0.17	17.38	-	-	100.38	1.965	0.007	0.068	0.003	0.244	1.020	0.005	0.680	-	-	3.993
210	G																					
A1	48.23	1.85	3.84	0.21	17.45	11.06	0.32	16.40	0.65	-	100.58	1.857	0.053	0.174	0.006	0.562	0.635	0.010	0.677	0.049	-	4.023
A2	54.19	0.20	1.91	0.26	6.56	18.77	-	18.11	-	-	99.73	1.968	0.005	0.082	0.007	0.199	1.016	-	0.705	-	-	3.982
A3	50.08	1.20	4.73	0.30	7.88	15.53	-	19.82	0.46	-	99.19	1.854	0.033	0.206	0.009	0.244	0.857	-	0.786	0.033	-	4.022
A4	49.17	1.56	4.68	0.19	12.69	14.22	0.18	16.88	0.42	-	100.07	1.848	0.044	0.207	0.006	0.399	0.796	0.006	0.680	0.031	-	4.017
A5	48.59	1.81	3.88	0.13	14.90	12.31	0.22	17.58	0.57	-	99.95	1.853	0.052	0.174	0.004	0.475	0.700	0.007	0.718	0.042	-	4.027
A6	52.98	0.63	3.21	0.13	10.11	17.34	0.12	14.58	0.83	0.08	101.38	1.943	0.017	0.139	0.004	0.310	0.948	0.004	0.573	0.059	0.004	4.000
211	P																					
A1c	53.08	0.23	2.67	0.58	4.54	17.90	-	20.77	0.25	-	98.59	1.932	0.006	0.114	0.017	0.138	0.971	-	0.810	0.017	-	4.005
A2c	52.92	0.22	2.68	0.70	4.46	17.96	-	20.85	0.22	-	99.24	1.927	0.006	0.115	0.020	0.136	0.975	-	0.813	0.015	-	4.007
A3c	52.69	0.28	2.59	0.67	4.53	17.81	-	21.17	0.25	-	102.24	1.923	0.008	0.112	0.019	0.138	0.969	-	0.827	0.018	-	4.013
A4c	53.01	0.27	2.63	0.57	4.45	18.03	-	21.05	-	-	101.00	1.929	0.007	0.113	0.016	0.135	0.978	-	0.821	-	-	3.999
A5r	51.85	0.40	3.66	0.80	5.49	17.21	-	20.29	0.30	-	101.55	1.897	0.011	0.158	0.023	0.168	0.939	-	0.795	0.021	-	4.012
A6r	51.79	0.47	3.71	0.55	6.07	16.99	-	20.06	0.35	-	98.92	1.898	0.013	0.160	0.016	0.186	0.928	-	0.788	0.025	-	4.014
A7r	51.25	0.73	4.05	0.56	5.99	16.75	-	20.34	0.34	-	100.61	1.881	0.020	0.175	0.016	0.184	0.916	-	0.800	0.024	-	4.016
A8r	52.16	0.55	3.39	0.61	5.67	17.14	-	20.22	0.26	-	100.58	1.907	0.015	0.146	0.018	0.173	0.934	-	0.792	0.019	-	4.005
B1c	53.39	0.21	2.52	0.57	4.40	17.73	-	21.18	-	-	99.94	1.941	0.006	0.108	0.016	0.134	0.961	-	0.825	-	-	3.991
B3r	52.86	0.26	2.56	0.62	4.57	17.80	-	21.09	0.25	-	100.51	1.927	0.007	0.110	0.018	0.139	0.968	-	0.824	0.018	-	4.011
B1r	52.29	0.34	3.37	0.72	4.65	17.60	-	20.85	0.17	-	98.21	1.907	0.009	0.145	0.021	0.142	0.956	-	0.815	0.012	-	4.007
B2r	53.02	0.28	2.60	0.50	4.35	17.87	-	21.20	0.17	-	100.85	1.930	0.008	0.112	0.014	0.132	0.970	-	0.827	0.012	-	4.005
D1c	52.41	0.15	3.44	1.38	3.74	17.55	-	21.32	-	-	98.59	1.907	0.004	0.147	0.040	0.114	0.952	-	0.831	-	-	3.995
D2c	52.19	0.19	3.58	1.47	3.56	17.25	-	21.59	0.17	-	99.94	1.901	0.005	0.154	0.042	0.108	0.937	-	0.842	0.012	-	4.002
D3c	53.03	-	2.90	1.00	4.04	17.89	-	21.14	-	-	99.41	1.928	-	0.124	0.029	0.123	0.969	-	0.823	-	-	3.996
D4c	52.18	0.27	3.56	1.43	3.75	17.37	-	21.23	0.23	-	100.63	1.901	0.007	0.153	0.041	0.114	0.943	-	0.828	0.016	-	4.003
D1r	52.18	0.44	3.39	0.39	5.94	17.66	-	19.73	0.27	-	100.08	1.907	0.012	0.146	0.011	0.182	0.962	-	0.773	0.019	-	4.012
D2r	52.26	0.46	3.49	0.38	6.43	18.25	-	18.39	0.35	-	100.41	1.907	0.013	0.150	0.011	0.196	0.992	-	0.719	0.025	-	4.012
D3r	53.01	0.31	2.50	0.42	5.84	18.16	-	19.56	0.20	-	100.59	1.933	0.008	0.107	0.012	0.178	0.987	-	0.764	0.014	-	4.005
D4r	52.14	0.49	3.52	0.77	5.00	17.08	-	20.72	0.28	-	101.02	1.905	0.013	0.151	0.022	0.153	0.930	-	0.811	0.020	-	4.005

	SiO_2	TiO_2	Al_2O_3	Cr_2O_3	FeO	MgO	MnO	CaO	Na_2O	K_2O	Total	Si	Ti	Al	Cr	Fe	Mg	Mn	Ca	Na	K	Total
211	M																					
E1	51.82	0.46	3.55	0.84	5.32	16.84	-	20.93	0.25	-	98.76	1.898	0.013	0.153	0.024	0.163	0.919	-	0.821	0.018	-	4.009
E2	53.66	0.22	1.83	0.54	6.51	19.54	-	17.45	0.24	-	100.13	1.951	0.006	0.079	0.016	0.198	1.059	-	0.680	0.017	-	4.005
E3	51.74	0.42	3.99	1.10	5.56	17.68	-	19.19	0.31	-	99.76	1.889	0.012	0.172	0.032	0.170	0.962	-	0.751	0.022	-	4.009
E4	51.82	0.39	3.72	0.75	5.57	16.94	-	20.39	0.41	-	100.46	1.898	0.011	0.161	0.022	0.171	0.925	-	0.800	0.029	-	4.015
E5	52.25	0.49	3.02	0.31	6.31	17.26	-	20.04	0.32	-	99.92	1.915	0.014	0.130	0.009	0.193	0.943	-	0.787	0.023	-	4.013
E6	52.73	0.47	2.52	0.48	6.18	17.66	-	19.63	0.33	-	100.26	1.929	0.013	0.109	0.014	0.189	0.963	-	0.769	0.023	-	4.009
211	G																					
A1	50.80	0.88	4.33	0.19	8.01	16.71	-	18.82	0.25	-	100.10	1.872	0.024	0.188	0.006	0.247	0.918	-	0.743	0.018	-	4.016
A2	50.54	1.08	4.80	0.27	7.64	16.22	-	19.15	0.29	-	99.58	1.862	0.030	0.209	0.008	0.235	0.891	-	0.756	0.020	-	4.010
A3	50.62	1.09	4.90	0.65	6.69	16.39	-	19.48	0.17	-	99.04	1.859	0.030	0.212	0.019	0.206	0.897	-	0.766	0.012	-	4.001
A4	50.49	1.08	4.91	0.26	7.35	16.17	-	19.46	0.28	-	98.67	1.859	0.030	0.213	0.008	0.226	0.887	-	0.768	0.020	-	4.011
A5	50.15	1.13	4.77	0.13	8.75	15.19	-	19.52	0.37	-	100.32	1.859	0.032	0.209	0.004	0.271	0.839	-	0.776	0.027	-	4.016
A6	51.74	0.33	3.98	1.13	5.29	17.02	-	20.28	0.22	-	99.08	1.892	0.009	0.171	0.033	0.162	0.928	-	0.794	0.016	-	4.005
A7	50.18	1.16	5.15	0.22	7.88	16.02	-	19.09	0.30	-	100.08	1.851	0.032	0.224	0.006	0.243	0.881	-	0.754	0.021	-	4.012
A8	50.76	0.80	3.70	0.30	9.54	15.91	-	18.57	0.43	-	100.29	1.885	0.022	0.162	0.009	0.296	0.880	-	0.739	0.031	-	4.023
A9	49.71	1.29	3.29	-	15.25	13.84	0.18	16.08	0.36	-	100.88	1.884	0.037	0.147	-	0.483	0.782	0.006	0.653	0.027	-	4.019
A10	49.74	1.36	5.30	0.25	7.99	15.64	-	19.40	0.33	-	100.65	1.839	0.038	0.231	0.007	0.247	0.862	-	0.768	0.024	-	4.016
A11	51.51	0.42	3.91	1.38	5.28	16.96	-	20.21	0.34	-	100.95	1.886	0.011	0.169	0.040	0.162	0.926	-	0.793	0.024	-	4.010
A12	51.84	0.51	3.63	0.91	5.46	17.21	-	20.12	0.33	-	100.33	1.896	0.014	0.156	0.026	0.167	0.938	-	0.788	0.023	-	4.010
A13	50.13	1.28	5.10	0.30	7.23	15.95	-	19.54	0.46	-	100.55	1.848	0.036	0.222	0.009	0.223	0.877	-	0.772	0.033	-	4.018
C1	52.17	0.54	3.42	0.74	5.78	17.19	-	20.16	-	-	99.59	1.907	0.015	0.147	0.021	0.177	0.936	-	0.790	-	-	3.994
C2	51.73	0.70	3.63	0.56	6.72	16.92	-	19.45	0.29	-	100.25	1.898	0.019	0.157	0.016	0.206	0.925	-	0.765	0.020	-	4.006
C3	50.38	1.07	4.62	0.14	8.39	15.65	-	19.33	0.41	-	100.70	1.864	0.030	0.201	0.004	0.260	0.863	-	0.766	0.030	-	4.018
C4	49.83	1.42	4.55	-	10.96	15.24	-	17.71	0.28	-	98.52	1.857	0.040	0.200	-	0.342	0.847	-	0.707	0.020	-	4.013
C5	50.12	1.14	3.42	-	12.49	13.80	0.19	18.47	0.36	-	98.71	1.887	0.032	0.152	-	0.393	0.775	0.006	0.745	0.026	-	4.017
C6	50.23	1.26	4.55	0.19	7.74	15.57	-	20.06	0.41	-	100.46	1.858	0.035	0.198	0.006	0.240	0.858	-	0.795	0.029	-	4.020
C7	50.28	1.43	4.89	0.19	8.23	15.91	-	18.68	0.38	-	99.98	1.856	0.040	0.213	0.006	0.254	0.875	-	0.739	0.027	-	4.009
C8	53.57	0.28	2.05	0.20	7.18	19.53	0.12	16.87	0.20	-	100.68	1.949	0.008	0.088	0.006	0.218	1.059	0.004	0.658	0.015	-	4.003
C9	50.53	1.01	4.03	0.15	9.60	15.66	-	18.71	0.31	-	99.78	1.876	0.028	0.177	0.004	0.298	0.867	-	0.744	0.022	-	4.016
C11	53.14	0.37	2.51	0.55	6.18	18.28	-	18.79	0.18	-	99.58	1.936	0.010	0.108	0.016	0.188	0.993	-	0.734	0.013	-	3.998
C10	49.59	1.24	5.48	0.28	8.68	16.16	-	18.20	0.37	-	100.46	1.834	0.035	0.239	0.008	0.268	0.891	-	0.721	0.027	-	4.022
C12	50.49	1.14	4.75	0.22	8.02	16.15	-	18.99	0.23	-	99.60	1.862	0.031	0.207	0.007	0.247	0.888	-	0.750	0.016	-	4.008
235	P																					
A1c	53.19	0.15	3.36	0.42	3.30	17.49	-	21.09	0.19	-	98.79	1.928	0.004	0.144	0.012	0.100	0.945	-	0.850	0.013	-	3.997
A2c	52.99	0.20	3.21	0.40	3.45	17.60	-	22.00	0.16	-	99.80	1.924	0.005	0.137	0.011	0.105	0.952	-	0.856	0.011	-	4.002
A3c	52.89	0.19	3.29	0.47	3.29	17.66	-	22.22	-	-	98.96	1.920	0.005	0.141	0.013	0.100	0.955	-	0.864	-	-	3.998
A4c	53.00	0.16	3.21	0.48	3.32	17.65	-	22.18	-	-	99.53	1.923	0.004	0.137	0.014	0.101	0.955	-	0.862	-	-	3.997
B1c	53.14	0.13	3.26	0.48	3.52	17.62	-	21.86	-	-	99.79	1.927	0.003	0.139	0.014	0.107	0.952	-	0.849	-	-	3.993
B2c	53.02	0.13	3.28	0.48	3.42	17.81	-	21.66	0.20	-	99.75	1.923	0.004	0.140	0.014	0.104	0.963	-	0.842	0.014	-	4.003
	52.95	0.22	3.24	0.50	3.48	17.73	-	21.71	0.16	-	99.81	1.922	0.006	0.139	0.014	0.105	0.959	-	0.844	0.011	-	4.001
	52.91	0.27	3.21	0.66	3.49	17.61	-	21.86	-	-	99.30	1.921	0.007	0.137	0.019	0.106	0.953	-	0.850	-	-	3.994
E1c	52.77	0.20	3.47	0.59	3.47	17.41	-	21.86	0.22	-	98.64	1.917	0.005	0.149	0.017	0.105	0.943	-	0.851	0.016	-	4.003
E2c	52.86	0.21	3.40	0.57	3.52	17.49	-	21.78	0.17	-	98.65	1.920	0.006	0.146	0.016	0.107	0.946	-	0.847	0.012	-	4.000
E3c	52.61	0.26	3.48	0.54	3.44	17.59	-	21.86	0.21	-	99.98	1.912	0.007	0.149	0.016	0.105	0.953	-	0.851	0.015	-	4.006
Cr	50.81	0.72	5.22	-	5.83	15.77	-	21.65	-	-	100.00	1.864	0.019	0.225	-	0.178	0.862	-	0.851	-	-	4.002
235	G																					
F1	52.62	0.39	2.81	0.41	5.39	17.29	-	21.08	-	-	99.13	1.923	0.011	0.121	0.012	0.165	0.942	-	0.825	-	-	3.999
F2	49.91	1.02	5.95	0.54	5.08	14.98	-	22.36	0.16	-	99.01	0.835	0.028	0.258	0.016	0.156	0.821	-	0.881	0.011	-	4.006
F3	48.24	1.51	5.47	0.13	10.50	13.22	-	20.39	0.54	-	100.11	1.815	0.043	0.242	0.004	0.331	0.741	-	0.822	0.039	-	4.038
F4	47.72	2.03	6.03	-	10.27	12.50	0.17	20.78	0.50	-	99.80	1.798	0.057	0.268	-	0.324	0.702	0.005	0.839	0.036	-	4.029
F5	51.35	0.65	3.27	0.21	7.79	15.78	-	20.96	-	-	99.75	1.900	0.018	0.142	0.006	0.241	0.870	-	0.831	-	-	4.008
F6	49.83	1.03	5.35	0.39	6.24	14.83	-	22.12	0.22	-	99.85	1.841	0.029	0.233	0.011	0.193	0.817	-	0.876	0.016	-	4.016
F7	45.97	2.26	7.22	0.12	12.04	12.57	0.16	19.34	0.33	-	98.36	1.743	0.064	0.323	0.004	0.382	0.711	0.005	0.786	0.024	-	4.041
F8	49.71	1.23	5.56	0.33	6.59	14.65	-	21.77	0.16	-	98.66	1.837	0.034	0.242	0.010	0.204	0.807	-	0.862	0.012	-	4.008
1	47.35	2.15	7.16	0.20	8.11	13.25	-	21.48	0.29	-	98.69	1.768	0.060	0.315	0.006	0.253	0.737	-	0.859	0.021	-	4.021
2	47.22	2.23	4.35	0.11	15.54	11.58	0.21	18.22	0.53	-	99.81	1.815	0.064	0.197	0.003	0.500	0.664	0.007	0.750	0.039	-	4.040
B1	49.10	1.10	7.36	0.44	4.83	14.66	-	22.51	-	-	99.46	1.803	0.030	0.319	0.013	0.148	0.803	-	0.886	-	-	4.001
B2	49.13	1.10	7.34	0.51	4.67	14.62	-	22.39	0.22	-	99.67	1.804	0.031	0.318	0.015	0.144	0.800	-	0.881	0.016	-	4.007
B3	50.26	1.04	4.92	0.17	7.00	15.28	-	21.15	0.17	-	98.14	1.856	0.029	0.214	0.005	0.216	0.841	-	0.837	0.012	-	4.011
B4	48.72	1.06	7.66	0.37	4.63	14.61	-	22.71	0.24	-	100.13	1.791	0.029	0.332	0.011	0.142	0.800	-	0.895	0.017	-	4.017
B5	51.17	0.76	4.24	-	6.88	15.86	-	21.08	-	-	99.64	1.884	0.024	0.184	-	0.212	0.871	-	0.832	-	-	4.003
B6	50.09	0.85	5.76	0.26	4.89	15.54	-	22.60	-	-	99.45	1.839	0.023	0.249	0.008	0.150	0.851	-	0.889	-	-	4.009
B7	50.96	0.95	4.89	0.18	7.01	15.57	-	21.08	-	-	99.02	1.857	0.026	0.213	0.005	0.216	0.856	-	0.834	-	-	4.008
	50.96	0.41	5.42	0.67	4.75	15.81	-	21.97	-	-	99.14	1.864	0.011	0.234	0.020	0.145	0.862	-	0.861	-	-	3.998
	50.06	0.93	6.10	0.39	4.91	15.25	-	22.35	-	-	98.98	1.836	0.026	0.264	0.011	0.151	0.834	-	0.878	-	-	4.
C1	50.58	0.75	5.18	0.26	5.05	15.55	-	22.63	-	-	98.95	1.857	0.021	0.224	0.008	0.155	0.851	-	0.890	-	-	4.006
C2	49.76	1.15	5.54	0.15	6.87	14.99	-	21.32	0.21	-	98.76	1.839	0.032	0.241	0.004	0.212	0.826	-	0.844	0.015	-	4.014
C3	50.44	0.71	5.70	0.35	4.80	15.55	-	22.45	-	-	97.95	1.849	0.020	0.246	0.010	0.147	0.850	-	0.882	-	-	4.003
C4	51.20	0.53	4.93	0.30	4.70	15.69	-	22.64	-	-	100.67	1.875	0.015	0.213	0.009	0.144	0.856	-	0.888	-	-	4.
D1	51.24	0.67	3.69	0.14	6.67	15.78	-	21.50	0.29	-	99.62	1.891	0.019	0.161	0.004	0.206	0.863	-	0.850	0.021	-	4.019
D2	50.12	1.14	5.14	0.13	6.34	15.41	-	21.55	0.18	-	99.32	1.848	0.031	0.223	0.004	0.196	0.847	-	0.851	0.013	-	4.013
D3	50.44	0.86	3.66	0.14	9.84	15.65	0.20	18.91	0.30	-	101.41	1.879	0.024	0.161	0.004	0.307	0.869	0.006	0.754	0.021	-	4.025
D4	50.16	1.12	5.17	0.20	7.47	15.94	-	19.94	-	-	99.98	1.849	0.031	0.225	0.006	0.230	0.876	-	0.788	-	-	4.004
D5	53.30	0.38	1.65	0.14	7.81	17.97	-	18.74	-	-	98.81	1.954	0.011	0.071	0.004	0.240	0.982	-	0.736	-	-	3.998

APPENDIX 3: Section A cont.

	SiO_2	TiO_2	Al_2O_3	Cr_2O_3	FeO	MgO	MnO	CaO	Na_2O	K_2O	Total	Si	Ti	Al	Cr	Fe	Mg	Mn	Ca	Na	K	Total
50	G																					
A1	45.33	3.94	7.12	0.45	9.73	10.94	-	22.49	-	-	101.10	1.718	0.112	0.318	0.013	0.308	0.618	-	0.913	-	-	4.003
A2	46.85	3.15	5.99	0.34	10.90	11.24	-	21.52	-	-	100.30	1.774	0.089	0.267	0.010	0.345	0.634	-	0.873	-	-	3.996
A3	45.89	3.55	6.63	0.48	9.66	11.44	-	21.87	0.49	-	101.80	1.737	0.101	0.296	0.014	0.305	0.645	-	0.887	0.035	-	4.024
A4	45.67	3.57	6.90	0.35	11.33	10.93	-	21.25	-	-	98.20	1.735	0.101	0.308	0.010	0.360	0.619	-	0.865	-	-	4.002
7	P and G																					
E1	51.75	0.48	3.91	1.80	3.91	17.11	-	21.03	-	-	96.90	1.886	0.013	0.168	0.051	0.119	0.929	-	0.821	-	-	3.990
E2	51.60	0.50	4.19	1.65	3.83	17.15	-	21.07	-	-	95.90	1.879	0.013	0.180	0.047	0.116	0.931	-	0.822	-	-	3.992
E3	52.99	0.62	3.08	-	5.79	17.88	-	19.64	-	-	100.70	1.928	0.016	0.132	-	0.176	0.969	-	0.765	-	-	3.989
E4	52.13	0.45	3.85	1.58	3.76	17.23	-	21.00	-	-	100.30	1.896	0.012	0.165	0.045	0.114	0.934	-	0.818	-	-	3.986
E5	48.90	2.12	6.41	-	8.99	15.47	-	18.11	-	-	101.60	1.807	0.058	0.279	-	0.277	0.852	-	0.717	-	-	3.993
E7	50.68	0.97	5.03	1.29	4.93	16.18	-	20.95	-	-	100.50	1.855	0.026	0.216	0.037	0.150	0.883	-	0.821	-	-	3.992
	51.51	0.78	4.40	1.23	4.72	16.40	-	20.96	-	-	100.80	1.881	0.021	0.189	0.035	0.144	0.892	-	0.820	-	-	3.985
	49.86	1.68	5.59	0.32	7.89	15.40	-	19.29	-	-	99.90	1.838	0.045	0.243	0.009	0.243	0.846	-	0.762	-	-	3.989
35	G																					
1	46.23	3.53	7.01	0.28	8.54	12.20	-	21.83	0.53	-	98.10	1.738	0.094	0.310	0.008	0.268	0.684	-	0.879	0.038	-	4.024
2	46.12	3.37	6.58	0.29	9.20	12.22	-	21.66	0.54	-	97.80	1.740	0.095	0.292	0.008	0.290	0.687	-	0.875	0.039	-	4.031
3	47.45	1.90	4.01	-	13.97	9.77	0.46	21.63	0.81	-	96.10	1.831	0.055	0.182	0.015	0.450	0.561	0.015	0.894	0.060	-	4.052
4	47.25	2.94	5.56	-	9.82	12.37	-	21.48	0.61	-	99.30	1.783	0.083	0.247	-	0.309	0.695	-	0.868	0.044	-	4.033
60	G																					
1	53.35	0.70	2.31	-	6.12	16.45	-	21.06	-	-	87.20	1.951	0.019	0.099	-	0.187	0.896	-	0.825	-	-	3.979
2	51.51	0.83	4.29	-	5.24	16.23	-	21.90	-	-	97.10	1.885	0.022	0.185	-	0.160	0.885	-	0.858	-	-	3.999
117	G																					
1	49.01	2.00	5.71	0.31	9.06	14.92	-	18.99	-	-	101.90	1.818	0.055	0.249	0.008	0.281	0.825	-	0.755	-	-	3.995
2	49.91	1.47	5.14	0.37	8.31	15.97	-	18.83	-	-	100.60	1.842	0.040	0.223	0.010	0.256	0.878	-	0.745	-	-	3.999
200	G																					
1	47.66	2.50	6.05	0.29	10.54	13.56	-	19.41	-	-	103.70	1.787	0.070	0.267	0.008	0.330	0.758	-	0.780	-	-	4.004
2	41.05	1.73	14.64	0.29	16.30	4.33	-	21.35	-	0.31	97.90											
212	G																					
1	52.05	0.63	3.84	0.31	6.86	18.21	-	18.12	-	-	94.10	1.898	0.017	0.164	0.008	0.209	0.990	-	0.708	-	-	3.997
2	52.43	0.50	3.00	0.32	7.19	19.00	-	17.55	-	-	108.90	1.912	0.013	0.129	0.009	0.219	1.033	-	0.685	-	-	4.004
3	51.00	0.82	4.02	0.64	7.98	16.22	-	19.34	-	-	100.20	1.881	0.022	0.174	0.018	0.246	0.891	-	0.764	-	-	4.
220	G																					
1	51.02	0.62	4.57	1.48	4.80	16.83	-	20.69	-	-	99.60	1.865	0.016	0.197	0.042	0.146	0.914	-	0.810	-	-	3.998
2	52.73	0.35	2.42	0.95	5.15	18.49	-	19.91	-	-	99.30	1.922	0.009	0.103	0.027	0.156	1.004	-	0.777	-	-	4.002
227	G																					
A1	52.52	0.78	2.49	-	5.09	16.93	-	22.19	-	-	101.80	1.922	0.021	0.107	-	0.155	0.923	-	0.870	-	-	4.002
A2	50.81	1.12	2.57	-	9.26	14.34	0.28	21.60	-	-	97.20	1.900	0.031	0.113	-	0.289	0.799	0.008	0,865	-	-	4.010
A3	52.45	0.82	2.57	-	5.24	16.78	-	22.15	-	-	94.	1.921	0.022	0.110	-	0.160	0.916	-	0.869	-	-	4.001
A4	51.60	0.95	2.44	-	8.95	14.41	-	21.65	-	-	102.10	1.921	0.026	0.106	-	0.278	0.799	-	0.863	-	-	3.998
A5	52.97	0.27	0.79	-	11.28	13.20	0.46	20.36	0.66	-	95.10	1.989	0.007	0.035	-	0.354	0.739	0.014	0.819	0.048	-	4.009
B1	51.00	1.18	3.61	-	6.38	15.84	-	22.00	-	-	100.50	1.881	0.032	0.156	-	0.196	0.870	-	0.869	-	-	4.008
D1	51.75	0.80	3.50	0.64	4.37	16.66	-	22.30	-	-	101.70	1.893	0.021	0.150	0.018	0.133	0.908	-	0.874	-	-	4.001
234	G																					
A1	49.29	1.68	5.48	0.29	8.18	14.16	-	20.93	-	-	101.20	1.831	0.047	0.239	0.008	0.254	0.784	-	0.833	-	-	3.999
A2	49.18	1.48	4.74	0.32	9.20	13.90	-	20.47	0.70	-	100.30	1.839	0.041	0.209	0.009	0.287	0.774	-	0.820	0.050	-	4.034
A3	49.76	1.40	4.78	0.37	8.39	14.28	-	21.03	-	-	98.60	1.850	0.039	0.209	0.010	0.260	0.791	-	0.837	-	-	4.
415	P																					
	51.68	0.98	3.57	0.34	5.85	16.61	-	20.43	0.51	-	98.60	1.895	0.027	0.154	0.009	0.179	0.908	-	0.802	0.036	-	4.013
	52.07	0.97	3.38	0.31	5.65	16.58	-	21.04	-	-	96.60	1.905	0.026	0.145	0.008	0.172	0.904	-	0.825	-	-	3.990
	52.13	1.02	3.31	-	5.84	16.57	-	21.14	-	-	99.60	1.908	0.027	0.142	-	0.178	0.904	-	0.829	-	-	3.992
	51.13	0.93	4.55	0.37	6.27	15.75	-	21.	-	-	99	1.877	0.025	0.197	0.010	0.192	0.862	-	0.826	-	-	3.992
415	G																					
1	48.45	1.95	5.14	-	9.69	13.78	-	20.43	0.57	-	98.60	1.816	0.054	0.227	-	0.303	0.770	-	0.820	0.041	-	4.035
2	48.67	2.04	5.20	0.37	9.07	13.68	-	20.97	-	-	96.20	1.819	0.057	0.228	0.010	0.283	0.762	-	0.840	-	-	4.003
3	47.08	2.67	4.89	-	12.05	12.09	0.32	20.09	0.82	-	100.	1.793	0.076	0.219	-	0.384	0.686	0.010	0.820	0.060	-	4.052
419	G																					
I	53.57	0.35	2.10	0.38	6.20	19.83	-	17.57	-	-	98.60	1.943	0.009	0.089	0.010	0.188	1.072	-	0.683	-	-	3.997
423	G																					
A1	52.65	0.50	2.72	0.35	6.37	18.01	-	19.43	-	-	98.70	1.923	0.013	0.117	0.010	0.194	0.980	-	0.760	-	-	4.001
423	P																					
C1c	52.71	0.40	2.68	0.80	4.72	17.92	-	20.74	-	-	99.80	1.920	0.010	0.115	0.023	0.143	0.973	-	0.809	-	-	3.998
C2c	51.17	0.78	4.50	0.56	5.67	16.68	-	20.65	-	-	99.60	1.873	0.021	0.194	0.016	0.173	0.910	-	0.810	-	-	4.
C1r	50.23	1.13	2.97	-	14.27	14.94	0.34	16.13	-	-	100.20	1.893	0.032	0.131	-	0.449	0.839	0.010	0.651	-	-	4.009
C2r	51.40	0.97	2.38	-	11.84	16.03	0.28	17.38	-	-	98.80	1.909	0.027	0.104	-	0.369	0.893	0.008	0.695	-	-	4.010

APPENDIX 3: Section B PRIMARY PLAGIOCLASE MICROPROBE ANALYSES

	SiO_2	Al_2O_3	FeO	MgO	CaO	Na_2O	K_2O	Total	Si	Al	Fe	Mg	Ca	Na	K	Total
211																
P-A-1r	56.06	27.16	0.84	0.56	9.77	5.91	0.24	100.54	2.519	1.439	0.032	0.037	0.470	0.516	0.014	5.026
1-1	49.80	32.19	0.33	-	15.14	2.89	0.10	100.66	2.265	1.726	0.013	-	0.738	0.255	0.006	5.002
1-2	50.79	32.97	0.31	-	15.53	3.01	0.11	102.73	2.260	1.729	0.012	-	0.741	0.260	0.006	5.008
4r	50.91	31.84	0.46	-	14.60	3.51	0.08	101.40	2.293	1.691	0.017	-	0.705	0.307	0.005	5.017
2-1	49.75	32.05	0.28	-	15.11	3.06	0.12	100.38	2.266	1.721	0.011	-	0.737	0.271	0.007	5.012
2-2	49.68	32.14	0.41	-	15.23	3.00	0.17	100.63	2.260	1.723	0.016	-	0.742	0.265	0.010	5.016
2-3	49.09	31.94	0.35	-	15.11	3.01	0.13	99.63	2.255	1.730	0.013	-	0.744	0.268	0.008	5.018
2-4	50.76	32.89	0.30	-	15.36	3.04	0.13	102.49	2.263	1.729	0.011	-	0.734	0.263	0.008	5.007
2-5	48.25	33.71	0.34	-	16.75	2.27	0.14	101.45	2.185	1.800	0.013	-	0.813	0.199	0.008	5.018
2-6	48.65	32.55	0.38	-	15.75	2.48	0.11	99.91	2.230	1.758	0.014	-	0.774	0.220	0.006	5.003
2-7c	47.46	33.75	0.30	-	16.60	2.02	0.15	100.29	2.173	1.822	0.011	-	0.815	0.180	0.009	5.010
2-8c	46.78	34.46	0.31	0.43	17.23	1.34	-	100.94	2.132	1.851	0.012	0.029	0.841	0.154	-	5.019
2-9	48.07	33.00	0.34	-	16.21	2.32	0.12	100.08	2.204	1.784	0.013	-	0.796	0.207	0.007	5.011
3-1	50.63	31.85	0.29	-	14.71	3.19	0.12	100.78	2.292	1.699	0.011	-	0.713	0.280	0.007	5.002
3-2	50.03	31.48	0.35	-	14.66	3.02	0.10	99.64	2.291	1.699	0.013	-	0.719	0.268	0.006	4.997
3-3	53.82	29.75	0.55	-	12.38	4.71	0.16	101.36	2.410	1.570	0.021	-	0.594	0.409	0.009	5.013
3-4	53.17	29.45	0.56	-	12.43	4.63	0.12	100.36	2.406	1.571	0.021	-	0.603	0.407	0.007	5.015
G-A-1	58.28	27.65	0.97	-	9.44	6.42	0.27	103.03	2.551	1.426	0.036	-	0.443	0.544	0.015	5.016
2	54.07	29.53	0.87	-	12.56	4.69	0.19	101.91	2.414	1.554	0.032	-	0.601	0.406	0.011	5.018
3	53.51	29.16	0.76	-	12.20	4.84	0.14	100.61	2.418	1.553	0.029	-	0.591	0.424	0.008	5.022
4	55.14	29.01	0.83	-	11.66	5.01	0.19	101.84	2.454	1.522	0.031	-	0.556	0.432	0.011	5.006
5	53.44	30.35	0.62	-	13.01	4.36	0.19	101.96	2.384	1.596	0.023	-	0.622	0.378	0.011	5.013
6	52.38	30.25	0.61	-	13.18	3.97	0.16	100.56	2.370	1.613	0.023	-	0.639	0.349	0.009	5.003
7	53.50	29.49	0.78	-	12.54	4.45	0.29	101.14	2.408	1.565	0.029	-	0.605	0.389	0.017	5.012
8	54.30	29.66	0.69	-	12.18	4.87	0.17	101.87	2.420	1.558	0.026	-	0.582	0.421	0.010	5.017
P-B-1-1r	50.83	31.25	0.39	-	14.32	3.42	0.15	100.36	2.310	1.675	0.015	-	0.697	0.302	0.009	5.008
2r	51.52	31.52	0.41	-	14.28	3.55	0.14	101.42	2.316	1.670	0.015	-	0.688	0.309	0.008	5.007
3r	51.54	30.97	0.41	-	13.94	3.74	0.14	100.73	2.332	1.651	0.015	-	0.676	0.328	0.008	5.010
4c	50.12	32.10	0.26	-	15.10	2.91	0.06	100.56	2.275	1.718	0.010	-	0.734	0.256	0.003	4.996
5c	49.64	32.01	0.27	-	15.09	3.09	0.16	100.27	2.265	1.721	0.010	-	0.738	0.274	0.009	5.016
6c	50.37	32.36	0.31	-	15.22	3.13	0.12	101.50	2.268	1.718	0.012	-	0.734	0.274	0.007	5.013
7m	49.58	32.00	0.24	-	15.02	3.02	0.13	100.02	2.266	1.723	0.009	-	0.735	0.268	0.008	5.010
8m	49.49	31.83	0.31	-	15.01	3.06	0.10	101.56	2.269	1.717	0.012	-	0.736	0.272	0.006	5.011
2-1r	52.08	30.15	0.57	-	13.18	3.90	0.13	100.84	2.368	1.616	0.022	-	0.642	0.344	0.007	4.999
2r	50.65	30.79	0.51	-	13.94	3.80	0.16	102.22	2.317	1.660	0.020	-	0.683	0.337	0.009	5.027
3c	46.10	34.46	-	-	17.66	1.58	0.08	100.60	2.124	1.872	-	-	0.872	0.141	0.005	5.013
4c	46.21	34.24	0.22	-	17.60	1.60	0.12	100.98	2.129	1.859	0.009	-	0.869	0.143	0.007	5.016
3-1r	47.96	32.93	0.38	-	16.31	2.34	0.08	100.84	2.202	1.782	0.015	-	0.802	0.209	0.005	5.014
2r	48.83	32.18	0.36	-	15.46	2.81	0.17	101.41	2.239	1.739	0.014	-	0.759	0.250	0.010	5.018
3c	47.61	33.26	0.19	-	16.64	2.10	0.08	100.36	2.188	1.802	0.007	-	0.819	0.187	0.005	5.008
4c	48.02	32.95	0.23	-	16.34	2.38	0.08	100.69	2.203	1.782	0.009	-	0.803	0.212	0.005	5.014
M-B-1	51.29	30.76	0.34	-	13.77	3.59	0.12	100.29	2.337	1.652	0.013	-	0.672	0.318	0.007	4.999
2	50.75	31.25	0.36	-	14.12	3.41	0.11	100.29	2.313	1.678	0.014	-	0.689	0.302	0.006	5.002
3	50.73	31.04	0.47	-	14.16	3.45	0.15	101.07	2.315	1.669	0.018	-	0.692	0.305	0.009	5.008
4	51.29	30.89	0.34	-	13.83	3.54	0.11	100.65	2.334	1.657	0.013	-	0.674	0.312	0.006	4.997
5	50.92	30.85	0.50	-	13.99	3.61	0.13	100.76	2.323	1.659	0.019	-	0.684	0.320	0.008	5.012
G-B-1	52.81	29.24	0.74	-	12.71	4.31	0.19	101.29	2.402	1.568	0.028	-	0.619	0.381	0.011	5.010
2	51.43	30.32	0.49	-	13.53	4.04	0.19	100.28	2.346	1.630	0.019	-	0.661	0.357	0.011	5.023
3	56.26	26.68	1.00	-	9.36	6.46	0.23	101.51	2.543	1.422	0.038	-	0.453	0.566	0.013	5.035
I-D-1	48.24	32.68	0.37	-	16.20	2.40	0.11	100.72	2.214	1.768	0.014	-	0.797	0.214	0.006	5.013
2	47.79	33.18	0.23	-	16.52	2.11	0.16	101.37	2.193	1.795	0.009	-	0.812	0.188	0.009	5.008
3	49.81	31.93	0.19	-	15.08	2.83	0.15	101.12	2.274	1.718	0.007	-	0.738	0.251	0.009	4.997
4	47.25	33.34	0.37	-	16.66	2.24	0.13	102.25	2.174	0.808	0.014	-	0.821	0.200	0.008	5.026
M-E-1	51.20	30.62	0.46	-	13.75	3.83	0.15	101.56	2.335	1.645	0.017	-	0.672	0.339	0.009	5.016
2	51.02	30.83	0.36	-	14.02	3.67	0.09	101.67	2.326	1.656	0.014	-	0.685	0.325	0.005	5.011
3	51.63	30.18	0.54	-	13.53	3.94	0.19	101.48	2.353	1.622	0.021	-	0.661	0.349	0.011	5.016
4	51.59	30.65	0.36	-	13.51	3.79	0.09	101.43	2.347	1.643	0.014	-	0.658	0.334	0.005	5.002
3A																
G-B-1	48.46	32.42	0.38	-	15.19	2.74	0.25	99.43	2.233	1.760	0.015	-	0.750	0.244	0.015	5.016
2	48.82	31.91	0.40	-	14.86	2.88	0.26	99.13	2.254	1.736	0.015	-	0.735	0.258	0.015	5.014
P-D-1c	48.61	33.34	0.33	-	16.26	2.40	0.20	101.45	2.199	1.794	0.013	-	0.788	0.211	0.011	5.015
2c	48.81	32.92	0.30	-	15.79	2.68	0.19	100.70	2.222	1.767	0.012	-	0.770	0.236	0.011	5.018
3c	47.86	33.28	0.32	-	16.07	2.37	0.16	100.06	2.195	1.799	0.012	-	0.790	0.211	0.009	5.016
4r	48.77	32.81	0.30	-	15.56	2.84	0.17	100.45	2.225	1.765	0.012	-	0.761	0.251	0.010	5.023
5r	49.68	31.89	0.37	-	14.61	3.25	0.32	100.11	2.270	1.718	0.014	-	0.715	0.288	0.019	5.024
6r	49.31	32.59	0.39	-	15.18	2.97	0.24	100.68	2.243	1.747	0.015	-	0.740	0.262	0.014	5.021
7r	49.47	32.19	0.34	-	14.92	2.91	0.27	100.11	2.260	1.733	0.013	-	0.730	0.258	0.016	5.010
8c	48.33	33.05	0.24	-	15.79	2.55	0.24	100.21	2.211	1.782	0.009	-	0.774	0.226	0.014	5.018
M-E-1	50.00	32.53	0.29	-	15.12	2.80	0.25	101.00	2.262	1.735	0.011	-	0.733	0.246	0.014	5.001
2	50.64	32.40	0.47	-	14.89	3.28	0.27	101.95	2.272	1.714	0.018	-	0.716	0.286	0.015	5.021
3	50.09	32.92	0.47	-	15.49	2.88	0.27	102.13	2.247	1.741	0.018	-	0.744	0.251	0.015	5.016
64D																
G-B-1	48.77	32.61	0.28	-	14.65	3.37	0.30	97.94	2.235	1.761	0.011	-	0.719	0.300	0.018	5.043
3	49.12	33.34	0.50	-	13.03	2.35	1.65	101.16	2.247	1.797	0.019	-	0.639	0.209	0.096	5.007

	SiO_2	Al_2O_3	FeO	MgO	CaO	Na_2O	K_2O	Total	Si	Al	Fe	Mg	Ca	Na	K	Total
157																
P-B-1	48.00	32.78	0.25	-	15.60	2.58	0.14	99.69	2.213	1.782	0 010	-	0.771	0.231	0.008	5.015
2	47.89	33.09	0.22	-	15.96	2.40	0.13	99.69	2.202	1.793	0.009	-	0.786	0.214	0.008	5.012
55A																
G-A-1	53.37	29.00	0.57	-	11.89	4.91	0.26	100.66	2.424	1.552	0.022	-	0.579	0.433	0.015	5.024
2	56.40	27.05	0.74	-	9.18	6.29	0.34	102.80	2.543	1.438	0.028	-	0.444	0.551	0.020	5.023
3	57.38	26.37	0.67	-	8.60	6.52	0.46	102.56	2.582	1.399	0.025	-	0.415	0.570	0.026	5.017
4	56.04	27.22	0.82	-	9.34	6.20	0.38	102.71	2.530	1.449	0.031	-	0.452	0.544	0.022	5.028
G-B-1	57.88	27.72	0.74	-	9.72	6.44	0.34	102.84	2.540	1.434	0.027	-	0.457	0.549	0.019	5.027
2	56.46	27.49	0.66	-	9.72	5.97	0.30	100.60	2.531	1.453	0.025	-	0.467	0.519	0.017	5.011
3	56.16	29.23	0.75	-	11.46	5.43	0.26	103.29	2.464	1.511	0.028	-	0.539	0.462	0.014	5.018
5	53.26	29.15	0.75	-	12.01	4.60	0.22	102.00	2.419	1.561	0.028	-	0.584	0.406	0.013	5.010
38188																
G-A-1	52.24	30.61	0.60	-	13.47	4.07	0.28	101.27	2.352	1.625	0.023	-	0.650	0.356	0.016	5.021
2	51.10	30.86	0.49	-	13.52	3.77	0.25	100.51	2.329	1.659	0.019	-	0.660	0.334	0.015	5.015
G-C-1	50.23	31.56	0.23	-	14.73	2.66	0.12	99.44	2.297	1.702	0.009	-	0.722	0.236	0.007	4.973
G-E-1	56.13	26.21	0.87	-	9.84	5.84	0.42	101.74	2.554	1.406	0.033	-	0.480	0.516	0.024	5.013
204																
G-A-1	53.10	29.07	0.83	-	12.26	4.61	0.14	98.71	2.414	1.557	0.031	-	0.597	0.406	0.008	5.014
2	52.87	29.02	0.86	-	13.32	4.78	0.15	99.88	2.407	1.558	0.033	-	0.601	0.423	0.009	5.030
3	54.58	27.95	0.79	-	11.18	5.36	0.14	98.18	2.474	1.493	0.030	-	0.543	0.472	0.008	5.020
4	53.34	28.83	0.93	-	12.08	4.71	0.11	99.03	2.424	1.545	0.035	-	0.588	0.415	0.006	5.014
5	50.20	30.96	0.48	0.56	13.98	3.71	0.13	99.70	2.294	1.668	0.018	0.038	0.685	0.329	0.008	5.040
P-B-1	48.42	32.88	0.27	-	15.50	2.82	0.11	100.16	2.218	1.776	0.010	-	0.761	0.251	0.006	5.022
2	45.95	34.78	0.20	-	17.58	1.42	0.07	99.54	2.115	1.886	0.008	-	0.867	0.127	0.004	5.007
3	46.10	34.56	0.22	-	17.21	1.79	0.10	100.08	2.123	1.876	0.008	-	0.849	0.160	0.006	5.022
4	46.17	34.63	0.27	-	17.30	1.55	0.08	100.06	2.124	1.878	0.010	-	0.853	0.138	0.005	5.008
53																
G-A-1	52.24	29.81	0.61	-	12.58	4.53	0.22	98.38	2.378	1.600	0.023	-	0.614	0.400	0.013	5.028
2	53.06	29.47	0.72	-	11.79	4.80	0.16	98.97	2.409	1.577	0.027	-	0.574	0.423	0.009	5.019
3	55.07	27.52	1.18	-	10.06	5.86	0.31	98.17	2.497	1.471	0.045	-	0.489	0.515	0.018	5.034
4	53.50	29.10	0.59	-	11.73	4.85	0.23	100.74	2.427	1.556	0.022	-	0.570	0.427	0.013	5.016
144																
G-C-1	52.87	29.59	0.59	-	12.09	4.63	0.21	98.94	2.401	1.584	0.022	-	0.588	0.408	0.012	5.017
2	54.69	28.29	0.50	-	10.87	5.42	0.23	99.79	2.474	1.508	0.019	-	0.527	0.476	0.013	5.016
221																
M-B-1	51.93	29.80	0.65	-	13.43	4.01	0.17	102.05	2.367	1.602	0.025	-	0.656	0.355	0.010	5.014
2	51.84	30.18	0.56	-	13.14	4.11	0.17	102.51	2.361	1.620	0.021	-	0.641	0.363	0.010	5.016
4	52.23	30.01	0.49	-	12.83	4.26	0.17	100.45	2.375	1.608	0.019	-	0.625	0.375	0.010	5.013
5	51.98	30.20	0.59	-	13.31	3.79	0.12	99.67	2.364	1.619	0.022	-	0.649	0.335	0.007	4.997
6	51.64	30.29	0.59	-	13.39	3.98	0.15	100.27	2.353	1.627	0.023	-	0.651	0.351	0.009	5.014
P-B-2	48.12	32.57	0.20	0.48	15.16	2.88	0.19	99.60	2.214	1.767	0.008	0.033	0.747	0.257	0.011	5.037
4	48.22	34.05	0.24	0.52	15.87	2.11	0.42	101.42	2.180	1.815	0.009	0.035	0.769	0.185	0.024	5.017
228																
P-B-1	46.25	34.49	0.19	-	17.27	1.68	0.10	100.61	2.128	1.871	0.007	-	0.852	0.150	0.006	5.014
3	46.53	34.16	0.23	-	17.24	1.70	0.13	100.90	2.141	1.853	0.009	-	0.850	0.152	0.008	5.012
4	46.69	33.98	0.29	-	16.84	2.02	0.17	102.47	2.149	1.844	0.011	-	0.830	0.180	0.010	5.025
64																
P-B-1	46.94	34.00	0.17	-	17.01	1.70	0.17	100.87	2.157	1.842	0.007	-	0.837	0.152	0.010	5.004
2	46.55	34.12	0.18	-	17.09	1.83	0.22	101.32	2.142	1.851	0.007	-	0.843	0.164	0.013	5.020
P-C-1c	46.35	34.32	0.16	-	17.41	1.68	0.08	101.44	2.133	1.862	0.006	-	0.858	0.150	0.005	5.014
2c	48.17	33.07	0.17	-	16.07	2.38	0.13	101.47	2.208	1.786	0.006	-	0.789	0.212	0.008	5.009
3c	48.17	33.00	0.20	-	16.01	2.48	0.13	100.33	2.208	1.783	0.008	-	0.786	0.221	0.008	5.014
4c	47.68	33.45	0.16	-	16.35	2.26	0.10	101.66	2.187	1.809	0.006	-	0.804	0.201	0.006	5.012
5r	53.48	29.06	0.26	-	11.29	5.41	0.49	102.30	2.428	1.555	0.010	-	0.549	0.476	0.029	5.047
6r	48.89	32.42	0.28	-	15.44	2.78	0.20	101.65	2.239	1.750	0.011	-	0.758	0.247	0.012	5.016
7r	51.37	31.37	0.36	-	11.31	3.52	2.08	100.57	2.344	1.687	0.014	-	0.553	0.311	0.121	5.029
8r	49.58	31.72	0.49	-	14.73	3.24	0.24	101.40	2.270	1.712	0.019	-	0.723	0.288	0.014	5.025
G-D-1	51.27	29.97	0.77	-	14.01	3.71	0.26	100.22	2.344	1.616	0.029	-	0.686	0.329	0.015	5.020
2	49.09	32.23	0.49	-	15.10	2.84	0.24	100.82	2.248	1.740	0.019	-	0.741	0.253	0.014	5.015
3	53.01	28.02	1.25	-	13.04	4.25	0.42	98.29	2.424	1.510	0.048	-	0.639	0.377	0.024	5.022
4	50.69	30.61	0.62	-	14.33	3.51	0.24	100.48	2.318	1.650	0.024	-	0.702	0.312	0.014	5.020
38178																
G-A-1	51.41	30.79	0.44	-	13.20	4.03	0.14	98.69	2.340	1.652	0.017	-	0.644	0.355	0.008	5.016
2	52.87	29.68	0.53	-	12.00	4.75	0.17	99.70	2.400	1.588	0.020	-	0.584	0.419	0.010	5.020
3	49.49	32.00	0.34	-	14.82	3.20	0.15	99.87	2.263	1.725	0.013	-	0.726	0.284	0.009	5.021
4	50.24	31.26	0.42	-	14.25	3.71	0.13	100.19	2.296	1.684	0.016	-	0.698	0.328	0.008	5.030
G-B-1	50.60	31.16	0.42	-	13.96	3.75	0.11	99.41	2.309	1.676	0.016	-	0.683	0.332	0.005	5.022
2	52.88	29.85	0.39	-	12.27	4.51	0.10	98.58	2.397	1.595	0.015	-	0.596	0.397	0.006	5.006
P-C-1r	48.91	32.42	0.50	-	14.95	3.04	0.17	100.60	2.240	1.751	0.019	-	0.734	0.270	0.010	5.024
2c	48.59	32.72	0.16	-	15.54	2.86	0.13	99.77	2.226	1.766	0.006	-	0.763	0.254	0.007	5.022
3c	48.31	32.70	0.27	-	15.68	2.92	0.12	100.46	2.216	1.769	0.010	-	0.771	0.260	0.007	5.033

	SiO_2	Al_2O_3	FeO	CaO	Na_2O	K_2O	Total	Si	Al	Fe	Ca	Na	K	Total
38178 cont.														
P-C-4c	48.92	32.53	0.24	15.44	2.77	0.10	99.68	2.238	1.755	0.009	0.757	0.246	0.006	5.011
5c	47.90	33.29	0.23	15.85	2.61	0.13	98.54	2.197	1.799	0.009	0.779	0.232	0.007	5.023
6r	49.91	31.44	0.42	14.77	3.40	0.16	100.52	2.282	1.695	0.016	0.723	0.302	0.009	5.027
159														
P-A-1	46.26	34.53	0.14	17.46	1.50	0.10	99.61	2.128	1.872	0.005	0.861	0.134	0.006	5.006
2	47.43	33.89	0.18	16.41	1.73	0.35	98.07	2.176	1.832	0.007	0.806	0.154	0.021	4.996
3	46.22	34.41	0.12	17.53	1.55	0.16	99.56	2.128	1.867	0.005	0.865	0.138	0.009	5.012
4	46.09	34.58	0.17	17.57	1.48	0.09	99.20	2.122	1.877	0.007	0.867	0.132	0.005	5.009
G-B-1	52.23	30.13	0.33	13.03	4.14	0.14	101.29	2.373	1.614	0.012	0.634	0.365	0.008	5.006
2	52.39	29.71	0.71	12.77	4.26	0.16	101.51	2.384	1.594	0.027	0.622	0.376	0.010	5.012
163 dyke														
P-B-1c	47.10	33.83	0.25	16.58	2.08	0.16	98.20	2.164	1.832	0.010	0.816	0.186	0.009	5.017
2c	50.82	31.17	0.28	14.14	3.49	0.10	99.06	2.315	1.674	0.011	0.690	0.308	0.006	5.004
3r	56.69	27.01	0.50	9.20	6.34	0.25	100.94	2.552	1.433	0.019	0.444	0.544	0.007	5.014
4r	52.57	29.85	0.46	12.51	4.49	0.12	99.12	2.388	1.598	0.017	0.609	0.395	0.007	5.014
5r	54.49	28.33	0.60	10.87	5.49	0.24	99.42	2.467	1.512	0.023	0.527	0.483	0.014	5.025
6r	51.43	30.60	0.38	13.56	3.84	0.19	99.64	2.342	1.643	0.014	0.662	0.340	0.011	5.012
G-C-1	55.69	27.37	0.66	9.92	6.15	0.23	99.49	2.516	1.458	0.025	0.480	0.539	0.013	5.032
2	52.57	29.86	0.48	12.52	4.42	0.16	99.25	2.387	1.599	0.018	0.609	0.390	0.009	5.013
3	54.77	27.91	0.41	10.52	5.64	0.18	101.07	2.488	1.495	0.016	0.512	0.497	0.010	5.018
4	51.82	30.24	0.42	13.02	4.33	0.17	99.65	2.359	1.623	0.016	0.635	0.383	0.010	5.026
141 dyke														
G-A-1	49.27	29.86	0.60	14.10	3.40	0.27	97.50	2.313	1.652	0.024	0.709	0.309	0.016	5.023
2	50.11	31.95	0.36	14.83	3.09	0.20	100.41	2.277	1.712	0.014	0.722	0.273	0.012	5.009
3	51.79	30.73	0.56	13.49	4.23	0.23	100.88	2.339	1.637	0.021	0.653	0.371	0.013	5.034
4	51.30	30.79	0.52	13.78	3.86	0.23	100.49	2.330	1.648	0.020	0.671	0.340	0.014	5.022
G-B-1	54.28	28.70	0.66	11.25	5.37	0.29	100.55	2.449	1.526	0.025	0.544	0.470	0.017	5.031
2	49.79	32.42	0.37	15.21	2.81	0.11	100.71	2.260	1.734	0.014	0.739	0.248	0.006	5.001
3	50.40	31.42	0.38	14.65	3.29	0.19	100.32	2.295	1.686	0.015	0.715	0.290	0.011	5.012
4	50.83	32.03	0.48	14.91	3.36	0.17	101.66	2.284	1.697	0.018	0.718	0.293	0.010	5.019
235														
P-E-B-1	46.81	33.66	0.18	17.15	1.93	0.26	101.44	2.156	1.827	0.007	0.846	0.172	0.015	5.024
2	46.68	34.03	0.17	17.24	1.75	0.13	101.96	2.147	1.845	0.007	0.850	0.156	0.008	5.012
D-1	46.64	34.07	0.22	17.13	1.86	0.07	100.68	2.145	1.848	0.008	0.844	0.166	0.004	5.016
2	46.79	34.12	0.16	17.08	1.78	0.07	100.06	2.150	1.848	0.006	0.841	0.159	0.004	5.008

APPENDIX 3: Section C OLIVINE MICROPROBE ANALYSES.

	SiO_2	Al_2O_3	FeO	MgO	MnO	CaO	Total	Si	Al	Fe	Mg	Mn	Ca	Total	Mg/Mg+Fe
40428	phenocrysts														
1	40.19	-	10.52	49.00	-	0.28	104.98	0.989	-	0.217	1.798	-	0.007	3.011	89.2
2	40.04	-	10.37	49.25	-	0.35	104.30	0.985	-	0.213	1.806	-	0.009	3.015	89.5
3	39.72	-	10.58	49.38	-	0.32	101.95	0.979	-	0.218	1.815	-	0.008	3.021	89.3
4	39.61	-	10.39	49.65	-	0.25	95.55	0.977	-	0.214	1.825	-	0.007	3.023	89.5
5	39.28	-	10.52	49.89	-	0.31	94.95	0.970	-	0.217	1.835	-	0.008	3.030	89.4
6	39.37	-	11.53	48.74	-	0.36	100.01	0.976	-	0.239	1.800	-	0.010	3.024	88.3
38390	phenocrysts														
1	39.52	-	14.20	45.96	-	0.33	107.80	0.989	-	0.297	1.715	-	0.009	3.011	85.2
2	39.34	-	15.03	45.30	-	0.36	109.04	0.989	-	0.316	1.697	-	0.010	3.011	84.3
3	39.44	-	14.14	46.07	-	0.29	107.80	0.988	-	0.296	1.720	-	0.008	3.012	85.3
4	39.30	-	14.39	46.07	-	0.25	106.60	0.985	-	0.302	1.721	-	0.007	3.015	85.1
38189	phenocrysts and quench crystals (B1,B2)														
D1	40.00	-	12.03	47.64	-	0.34	99.20	0.991	-	0.249	1.759	-	0.008	3.009	87.6
D2	40.07	-	12.03	47.62	-	0.28	98.10	0.992	-	0.249	1.758	-	0.007	3.007	87.6
D3	39.94	-	12.13	47.62	-	0.29	98.50	0.990	-	0.251	1.759	-	0.007	3.009	87.5
D4	40.11	-	11.77	47.82	-	0.29	100.80	0.992	-	0.243	1.763	-	0.007	3.008	87.9
D5	40.26	-	11.68	47.80	-	0.25	102.	0.995	-	0.241	1.761	-	0.006	3.005	87.9
B1	37.56	0.42	23.74	37.24	0.61	0.34	100.70	0.986	0.012	0.521	1.462	0.013	0.009	3.007	73.7
B2	37.50	0.40	23.90	37.03	0.48	0.35	102.40	0.989	0.012	0.527	1.456	0.011	0.010	3.005	73.4
E1	40.26	-	11.45	47.99	-	0.31	100.	0.994	-	0.236	1.766	-	0.008	3.006	88.2
E2	40.13	-	11.68	47.85	-	0.34	99.	0.992	-	0.241	1.764	-	0.008	3.008	88.0
E3	39.98	-	11.39	48.35	-	0.27	97.1	0.987	-	0.235	1.781	-	0.006	3.011	88.3
252	phenocrysts														
1	40.52	-	11.94	47.56	-	-	105.8	1.001	-	0.247	1.752	-	-	3.	87.6
2	40.52	-	12.11	47.37	-	-	103.1	1.002	-	0.250	1.746	-	-	2.998	87.5
3	40.43	-	12.13	47.44	-	-	101.89	1.	-	0.251	1.749	-	-	3.	87.5
422	phenocrysts														
2	40.17	-	12.84	46.63	-	0.36	99.6	0.998	-	0.266	1.727	-	0.009	3.002	86.6
3	40.33	-	11.78	47.56	-	0.32	101.3	0.997	-	0.244	1.753	-	0.008	3.003	87.8
3c	40.65	-	11.60	47.74	-	-	99.35	1.003	-	0.239	1.755	-	-	2.997	88.0
5	40.07	-	13.17	46.45	-	0.31	99.5	0.997	-	0.274	1.722	-	0.008	3.002	86.3
6	39.96	-	13.16	46.48	-	0.38	99.7	0.994	-	0.273	1.725	-	0.010	3.004	86.3
47979															
1	40.37	-	11.06	48.57	-	-	100.00	0.994	-	0.228	1.783	-	-	3.006	88.7
47989															
1	40.84	-	11.98	47.17	-	-	103.99	1.008	-	0.247	1.736	-	-	2.991	87.5
47990															
1	41.16	-	11.87	46.96	-	-	100.00	1.015	-	0.245	1.726	-	-	2.985	87.6
2	40.47	-	11.74	47.54	-	0.22	100.00	1.000	-	0.243	1.751	0.006	-	3.000	87.8
3	40.49	-	11.72	47.79	-	-	100.00	1.000	-	0.242	1.759	-	-	3.000	87.9
47142															
1	39.92	-	12.79	47.11	-	-	100.00	0.993	-	0.266	1.747	-	-	3.007	86.6
2	39.98	-	12.29	47.72	-	-	100.00	0.991	-	0.255	1.763	-	-	3.009	87.4
3	40.13	-	12.44	47.42	-	-	100.00	0.995	-	0.258	1.752	-	-	3.005	87.2
4	40.20	-	12.38	47.44	-	-	100.00	0.996	-	0.257	1.752	-	-	3.004	87.3
5	40.22	-	12.34	47.46	-	-	100.00	0.996	-	0.256	1.752	-	-	3.004	87.3
1	39.70	-	13.70	46.58	-	-	100.00	0.991	-	0.286	1.732	-	-	3.009	85.4
2	39.53	-	14.97	45.48	-	-	100.00	0.992	-	0.314	1.701	-	-	3.008	84.4

APPENDIX 3: Section D MICROPROBE ANALYSES OF SPINEL PHENOCRYSTS

	40428		38188							47142		47990			252
	1	2	T1	T2	T3	T4	E1	E2	E3	1	2	1	2	3	1
TiO_2	0.61	0.43	0.67	0.61	0.63	0.66	0.62	0.68	0.62	0.73	0.70	0.82	0.95	0.88	1.03
Al_2O_3	33.04	31.82	33.30	34.79	34.90	36.26	34.99	34.37	35.03	35.50	32.00	36.41	34.61	36.37	31.70
Cr_2O_3	31.31	33.78	31.91	30.26	30.13	28.38	29.58	30.12	29.55	28.66	32.23	28.02	29.58	27.37	36.55
FeO	17.16	16.22	16.71	16.90	16.76	17.87	17.23	17.33	16.84	18.62	19.18	17.97	17.95	18.08	18.97
MgO	17.89	17.73	17.13	17.43	17.58	16.83	17.58	17.56	17.97	16.48	15.89	16.78	16.91	17.05	16.76
MnO	-	-	0.29	-	-	-	-	-	-	-	-	-	-	0.25	-
Mol % ulvospinel	1.71	1.20	1.88	1.71	1.76	0.85	1.74	1.90	1.74	2.04	1.96	2.30	2.66	2.46	2.88
wt.% FeO in ulvosp.	1.10	0.77	1.21	1.10	1.13	1.19	1.12	1.22	1.12	1.31	1.26	1.47	1.71	1.58	1.85
Structure (23 oxygen):															
Al	9.189	8.848	9.274	9.608	9.630	9.999	9.661	9.524	9.652	9.862	9.044	10.069	9.667	10.074	9.007
Cr	5.839	6.299	5.959	5.604	5.575	5.248	5.477	5.597	5.460	5.339	6.109	5.196	5.541	5.084	6.012
Fe^{2+}	3.168	3.048	3.062	3.096	0.060	0.263	0.156	3.167	3.073	3.411	3.593	3.237	3.218	3.242	3.451
Mg	6.290	6.232	6.030	6.085	6.132	5.867	6.136	6.151	6.259	5.787	5.677	5.866	5.971	5.970	6.020
Mn	-	-	0.058	-	-	-	-	-	-	-	-	-	-	0.050	-
Total	24.486	24.427	24.384	24.394	24.397	24.377	24.431	24.439	24.444	24.400	24.423	24.368	24.396	24.421	24.490
Using Rodgers (1973) and recalculating to 24 cations:															
Fe_2O_3	7.30	6.43	5.75	5.96	6.02	5.71	6.52	6.62	6.69	6.01	6.26	5.55	5.93	6.35	7.21
FeO	9.49	9.71	10.33	10.44	10.22	11.55	10.25	10.15	9.60	11.91	12.29	11.50	10.91	10.79	10.63
Al	9.006	8.690	9.128	9.453	9.473	9.844	9.491	9.353	9.483	9.700	8.887	9.917	9.510	9.900	8.827
Cr	5.724	6.187	5.866	5.514	5.484	5.167	5.380	5.497	5.365	5.251	6.003	5.118	5.450	4.996	5.892
Fe^{3+}	1.270	1.121	1.006	1.034	1.043	0.990	1.129	1.150	1.156	1.048	1.110	0.965	1.040	1.103	1.282
Fe^{2+}	1.835	1.881	2.009	1.012	1.968	2.224	1.972	1.959	1.844	2.309	2.421	2.222	2.127	2.084	2.100
Mg	6.165	6.121	5.936	5.987	6.032	5.776	6.028	6.041	6.150	5.692	5.579	5.778	5.873	5.867	5.900
Mn	-	-	0.057	-	-	-	-	-	-	-	-	-	-	0.049	-
Total	24.000	24.000	24.002	24.000	24.000	24.000	24.000	24.000	23.998	24.000	24.000	24.000	24.000	24.000	24.000
Cr/Cr+Al	0.39	0.42	0.39	0.37	0.37	0.34	0.36	0.37	0.36	0.35	0.40	0.34	0.36	0.34	0.40
Mg/Mg+Fe	0.77	0.77	0.75	0.75	0.75	0.72	0.75	0.76	0.77	0.71	0.70	0.72	0.73	0.74	0.74

APPENDIX 4

MICROPROBE ANALYSES OF SECONDARY PHASES IN MACQUARIE ISLAND LAVAS AND DYKES.

Section A: Smectite analyses from zeolite facies samples.

Section B: Phillipsite and smectite analyses from sub-zeolite facies samples.

Section C: Zeolite analyses.

Section D: Smectites and chlorites in lower greenschist facies samples.

Section E: Epidote, prehnite, sphene, K-feldspar, sericite, zeolite and albite analyses from lower greenschist facies samples.

Section F: Amphibole, clinopyroxene and plagioclase analyses from greenschist -lower amphibolite samples.

Analyses names followed by (TPD) were collected using the TPD probe at A.N.U., Canberra. The following table contains the values for the number of oxygens from which the structural formulae for the different phases have been calculated.

Smectite	22	Prehnite	22
Chlorite	28	Epidote	25
Zeolite	72	Sphene	20
Amphibole	23	Feldspar	32

APPENDIX 4: Section A SMECTITE ANALYSES FROM ZEOLITE FACIES GRADE SAMPLES.

	SiO_2	TiO_2	Al_2O_3	FeO	MgO	MnO	CaO	Na_2O	K_2O	Total	Si	Ti	Al	Fe	Mg	Mn	Ca	Na	K	Total
117																				
1	27.49	1.35	14.68	23.92	1.39	-	12.87	-	-	81.70	5.09	0.19	3.20	3.70	0.38	-	2.55	-	-	15.12
2	36.43	-	19.05	10.59	3.23	-	19.63	-	-	88.91	5.67	-	3.50	1.38	0.75	-	3.28	-	-	14.58
3	36.62	-	19.16	10.75	3.28	-	19.50	-	-	89.32	5.68	-	3.50	1.39	0.76	-	3.24	-	-	14.57
4	35.83	-	18.57	10.91	3.42	-	19.17	-	-	87.89	5.66	-	3.46	1.44	0.81	-	3.24	-	-	14.61
157	radiating																			
D1	26.98	-	12.28	29.09	2.01	0.46	13.12	-	-	83.95	5.05	-	2.71	4.56	0.56	0.07	2.63	-	-	15.54
D2	29.84	-	13.32	24.56	2.50	-	14.76	-	-	84.99	5.32	-	2.80	3.66	0.66	-	2.82	-	-	15.28
D3	30.23	-	13.36	23.95	2.62	-	15.11	-	-	85.26	5.35	-	2.79	3.55	0.69	-	2.87	-	-	15.25
	37.01	-	20.84	4.15	15.27	-	5.21	1.33	0.23	84.04	5.65	-	3.75	0.53	3.47	-	0.85	0.39	0.04	14.69
38299	rim																			
B	35.26		17.01	9.87	20.11		0.53	-	-	80.76	5.40	-	3.26	1.34	4.87		0.09	-	-	14.97
C	31.06		20.01	9.44	21.54		0.43	-	-	82.48	4.95	-	3.76	1.26	5.12		0.07	-	-	15.17
1	fibrous rim																			
B1	35.43		16.68	5.80	15.47		3.01	-	0.27	77.81	5.93	-	3.29	0.81	3.86		0.54	-	-	14.43
B2	36.75		17.78	5.21	14.03		3.64	1.77	-	79.19	5.95	-	3.40	0.71	3.39		0.63	0.56	-	14.63
C2	36.28		16.19	6.09	16.98		3.04	0.85	0.24	79.64	5.88	-	3.09	0.82	4.10		0.53	0.27	0.05	14.74
228																				
C1	31.68		14.61	10.43	24.59	0.17	0.74	-	-	81.82	5.16	-	2.81	1.42	5.97	0.02	0.06	-	-	15.44
C2	32.23		15.37	9.24	25.34	0.18	0.38	-	-	83.74	5.15	-	2.90	1.23	6.03	0.02	0.07	-	-	15.40
1	radiating																			
B1	37.41		12.87	8.14	21.41		0.92	-	0.28	81.05	5.99	-	2.43	1.09	5.11	-	0.16	-	0.06	14.83
B2	36.24		12.81	6.96	18.70		1.36	-	0.31	76.38	6.11	-	2.55	0.98	4.70	-	0.25	-	0.07	14.65
C1	36.97		11.17	10.64	22.19		0.81	-	0.31	82.10	5.95	-	2.12	1.43	5.32	-	0.14	-	0.06	15.02
157	green																			
	37.94		12.09	8.94	20.05		2.93	0.15	0.34	82.44	6.04	-	2.27	1.19	4.76	-	0.50	0.05	0.07	14.88

APPENDIX 4: Section B PHILLIPSITES AND SMECTITES IN SUB ZEOLITE FACIES SAMPLES.

252	Phillipsite																			
1	54.12	-	21.05	-	-		2.14	5.73	5.91	88.96	24.81		11.37	-	-		1.05	5.09	3.46	
2	55.62	-	21.77	-	-		1.99	5.36	6.55	91.30	24.84		11.46	-	-		0.95	4.65	3.73	
3	57.37	-	22 43	-	-		2.50	5.38	5.81	93.49	24.88		11.47	-	-		1.16	4.52	3.21	
252	Smectites																			
1	40.43	1.20	13.62	9.69	16.55		1.83	-	0.82	84.16	6.26	0.14	2.49	1.26	3.82		0.30	-	0.16	14.43
2	40.09	1.23	13.79	10.83	15.65		1.99	-	0.72	84.34	6.24	0.14	2.53	1.41	3.63		0.33	-	0.14	14.42
B	45.91	-	15.06	5.89	11.81		2.97	0.65	0.88	80.97	6.82	-	2.77	0.77	2.75		0.50	0.20	0.18	13.98
3	45.91	-	15.51	5.88	12.20		3.02	0.44	0.84	83.80	6.89		2.75	0.74	2.73		0.49	0.13	0.16	13.88
35	radiating beige																			
1	38.40	-	7.61	4.10	20.84		0.69	-	0.35	71.99	6.72		1.57	0.60	5.44		0.13	-	0.08	14.53
2	42.68	-	3.68	0.73	22.26		0.52	-	0.36	70.59	7.39		0.75	0.11	5.84		0.10	-	0.08	14.27
35	massive yellow																			
1	34.33	-	8.18	17.89	20.31		0.78	0.59	0.57	82.68	5.80		1.63	2.53	5.12		0.14	0.19	0.12	15.54
2	24.54	-	8.11	17.23	13.75		1.04	-	0.33	64.96	5.42		2.11	3.18	4.52		0.25	-	0.09	15.57

APPENDIX 4: Section C ZEOLITE ANALYSES.

	SiO_2	Al_2O_3	CaO	Na_2O	K_2O	Total	Si	Al	Ca	Na	K
1	Wairakite										
A1	48.71	21.54	7.23	3.60	0.75	81.83	23.82	12.42	3.79	3.41	0.47
A2	48.39	21.28	7.18	3.38	0.84	81.07	23.89	12.38	3.80	3.24	0.53
A3	47.85	20.84	7.19	3.67	0.75	80.32	23.87	12.26	3.84	3.55	0.48
	Analcite										
A1	53.97	21.96	-	13.09	0.28	89.30	24.34	11.67	-	11.45	0.16
A2	54.61	22.16	-	13.43	0.24	90.45	24.33	11.64	-	11.59	0.14
	Thomsonite - fibrous										
A1	42.91	25.91	8.59	6.23	-	83.64	21.03	14.97	4.51	5.92	-
A2	42.68	25.83	8.63	6.12	-	83.25	21.02	14.99	4.56	5.84	-
A3	43.92	26.09	8.70	6.04	-	84.77	21.20	14.85	4.50	5.65	-
B1	41.97	25.92	8.44	6.15	-	82.48	20.87	15.20	4.50	5.93	-
B2	42.36	25.96	8.54	6.17	-	83.04	20.92	15.12	4.52	5.91	-
	Thomsonite - coarse										
C1	43.13	25.40	8.86	5.51	-	82.89	21.27	14.76	4.68	5.27	-
C2	39.60	27.91	11.04	4.73	-	83.28	19.67	16.34	5.88	4.56	-
	40.54	27.70	10.68	5.14	-	84.05	19.93	16.05	5.62	4.90	-
3A	Thomsonite										
B1	37.63	28.38	11.25	4.27	-	81.54	19.13	17.00	6.13	4.21	-
B2	37.80	27.83	11.00	4.48	-	81.11	19.31	16.76	6.02	4.43	-
C1	38.48	27.87	10.79	4.60	-	81.73	19.48	16.63	5.85	4.51	-
C2	38.98	28.23	10.86	4.52	-	82.58	19.50	16.65	5.82	4.38	-
	Thomsonite (TPD)										
C1	40.46	29.20	10.95	3.96	0.13	84.70	19.66	16.72	5.70	3.73	0.08
C2	39.46	30.37	12.03	4.06	0.08	86.00	19.00	17.24	6.21	3.79	0.05
C4	40.64	29.45	11.61	4.29	0.08	86.07	19.51	16.66	5.97	3.99	0.05
C3	42.73	29.07	8.17	6.39	0.13	86.48	20.25	16.24	4.15	5.87	0.08
	?Mesolite (TPD)										
C1	46.63	22.91	5.62	5.87	3.58	84.72	22.76	13.12	2.93	5.53	2.22
C2	49.15	21.44	5.11	6.93	3.73	86.36	23.47	12.07	2.61	6.42	2.27
A	46.14	23.94	5.30	2.93	6.51	84.80	22.56	13.80	2.78	2.78	4.06
D	49.25	24.72	8.23	5.70	0.89	88.78	22.57	13.35	4.04	5.06	0.52
B1	44.86	22.28	7.36	1.02	7.25	82.80	22.64	13.25	3.98	1.00	4.67
7	Thomsonite-mesolite										
A1	44.56	27.37	8.36	7.37	-	87.68	20.89	15.12	4.2	6.70	-
A2	44.52	26.73	5.83	9.85	-	86.94	21.08	14.91	2.96	9.05	-
A3	45.19	26.40	7.51	7.61	-	86.71	21.34	14.69	3.80	6.97	-
A4	38.71	28.56	11.80	4.39	-	83.46	19.24	16.74	6.29	4.22	-
A5	40.22	28.66	11.20	5.08	-	85.16	19.57	16.43	5.83	4.79	-
C6	38.20	27.08	10.70	4.49	-	80.47	19.63	16.40	5.89	4.48	-
C7	39.49	27.83	10.93	4.84	-	83.09	19.66	16.34	5.83	4.68	-
C8	39.75	28.21	11.20	4.96	-	84.11	19.58	16.38	5.91	4.73	-
D9	37.73	27.99	11.76	4.19	-	81.67	19.18	16.77	6.41	4.13	-
D10	38.28	27.68	11.32	4.32	-	81.60	19.44	16.56	6.16	4.26	-
	Analcite										
B11	54.66	22.57	-	13.36	0.34	90.94	24.23	11.80	-	11.49	0.19
B12	53.83	22.10	-	13.06	0.25	89.25	24.29	11.76	-	11.42	0.14
D13	53.28	22.26	0.48	13.12	0.31	89.46	24.07	11.85	0.23	11.50	0.18
D14	53.32	22.01	-	13.08	0.29	88.71	24.24	11.79	-	11.53	0.17
11	Thomsonite										
1	36.64	27.47	11.05	4.21	-	79.38	19.15	16.92	6.19	4.26	-
2	37.20	27.55	11.25	4.46	-	80.47	19.20	16.76	6.22	4.47	-
3	39.43	27.30	10.84	4.48	-	82.04	19.84	16.20	5.85	4.37	-
	?Mesolite										
4	43.04	24.11	7.88	5.8	-	80.82	21.71	14.33	4.26	5.67	-
60	Thomsonite - fibrous										
A1	42.29	26.81	10.19	5.12	-	84.41	20.59	15.39	5.31	4.84	-
A2	41.71	26.42	10.09	5.18	-	83.39	20.58	15.36	5.33	4.95	-
A3	42.04	26.51	9.99	5.14	-	83.67	20.64	15.34	5.26	4.89	-
C1	41.93	27.08	10.33	5.03	-	84.35	20.45	15.56	5.40	4.75	-
C2	41.16	26.83	10.28	5.05	-	83.34	20.34	15.63	5.45	4.84	-
64D	Thomsonite - fibrous (TPD)										
A1	41.00	30.18	11.56	4.08	-	86.82	19.46	16.89	5.88	3.75	-
A2	40.32	30.37	11.57	4.26	0.15	86.67	19.23	17.08	5.91	3.84	0.09
A3	40.53	30.47	11.77	4.22	-	86.99	19.24	17.06	5.99	3.89	-
	?Mesolite (TPD)										
A1	46.44	26.86	9.54	4.18	0.17	87.20	21.61	14.73	4.76	3.77	0.10
A5	47.04	27.34	9.69	3.85	0.09	88.01	21.63	14.82	4.77	3.43	0.05
A6	46.92	26.74	9.72	3.92	0.25	87.56	21.72	14.60	4.82	3.52	0.15

	SiO_2	Al_2O_3	CaO	Na_2O	K_2O	Total	Si	Al	Ca	Na	K
38189	?Natrolite										
A1	41.31	24.75	2.83	11.84	-	80.74	21.11	14.91	1.55	11.73	-
A2	41.27	25.02	3.76	11.31	-	81.35	20.96	14.98	2.05	11.14	-
A3	41.69	24.60	2.55	12.19	-	81.02	21.23	14.76	1.39	12.03	-
F1	42.10	26.40	4.00	11.55	-	84.05	20.71	15.30	2.11	11.02	-
F2	42.72	26.60	3.57	12.10	-	85.00	20.78	15.25	1.86	11.42	-
F3	41.95	26.32	4.04	11.67	-	84.00	20.67	15.29	2.14	11.15	-
A1	42.57	26.09	3.25	12.43	0.25	84.59	20.85	15.07	1.70	11.81	0.16
A2	43.13	25.94	3.26	12.56	0.25	85.14	20.99	14.88	1.70	11.86	0.16
38190	Natrolite										
C1	43.08	25.40	2.49	12.39	-	83.36	21.28	14.79	1.32	11.87	-
C2	42.51	25.53	3.39	11.75	-	83.19	21.08	14.92	1.80	11.30	-
C1	42.74	25.17	2.77	12.13	-	82.81	21.27	14.76	1.48	11.70	-
	Mesolite										
A1	42.85	26.36	5.85	9.58	-	84.62	20.87	15.13	3.05	9.05	-
A2	42.18	26.32	4.91	10.49	0.25	84.18	20.73	15.25	2.59	9.99	0.16
A3	41.99	25.92	7.44	7.49	-	82.85	20.84	15.17	3.96	7.21	-
C1	43.38	25.23	7.65	6.86	-	83.12	21.36	14.64	4.04	6.55	-
C2	43.32	25.13	7.58	7.10	-	83.13	21.35	14.60	4.01	6.79	-
D1	40.73	25.28	7.12	7.18	-	80.33	20.83	15.24	3.90	7.13	-
D2	41.91	25.89	6.39	8.73	-	82.93	20.82	15.16	3.40	8.42	-
F1	42.36	25.23	6.65	8.16	-	82.39	21.13	14.83	3.55	7.89	-
	Phillipsite										
B1	44.97	20.69	1.33	7.54	5.23	79.74	23.36	12.67	0.74	7.59	3.47
B2	45.52	21.28	1.44	8.44	5.14	81.85	23.13	12.74	0.78	8.31	3.33
B3	45.27	21.41	1.41	8.73	5.34	82.15	22.99	12.82	0.77	8.60	3.46
38191	Analcite										
B1	53.69	21.99	-	13.59	0.30	89.57	24.22	11.69	-	11.88	0.17
B2	53.99	22.20	-	13.43	0.29	89.91	24.23	11.74	-	11.68	0.17
B	53.78	21.73	-	13.10	0.30	88.89	24.38	11.61	-	11.52	0.17
	Natrolite										
B2	45.97	25.74	-	15.62	-	87.33	21.69	14.31	-	14.29	-
	45.74	25.30	0.43	15.29	0.27	87.01	21.71	14.16	0.22	14.07	0.16
	Natrolite (impure)										
B1	45.09	25.75	3.36	11.77	-	85.97	21.54	14.50	1.72	10.90	-
B1	44.75	25.36	2.88	12.44	0.30	85.75	21.52	14.37	1.49	11.60	0.18
B2	44.26	26.28	2.62	13.28	-	86.43	21.15	14.80	1.34	12.30	-
B2	44.50	25.92	1.83	13.87	0.27	86.38	21.30	14.63	0.94	12.88	0.16
	?Mesolite-Natrolite										
A1	43.51	26.53	3.99	11.88	-	85.92	20.92	15.04	2.05	11.07	-
A2	43.32	26.77	4.24	11.82	-	86.16	20.79	15.15	2.18	11.00	-
A3	42.68	26.96	4.87	11.13	-	85.64	20.62	15.35	2.52	10.43	-
	Thomsonite										
A1	40.15	27.93	10.97	4.73	0.28	84.07	19.77	16.21	5.79	4.52	0.17
A2	40.39	27.81	10.45	4.89	0.30	83.83	19.91	16.16	5.52	4.68	0.19
A3	40.28	27.59	10.41	4.91	0.35	83.54	19.94	16.08	5.52	4.71	0.22
38199	Analcite										
C1	54.25	21.24	-	13.02	0.35	88.84	24.59	11.35	-	11.44	0.20
C2	53.50	20.88	-	12.68	0.28	87.32	24.64	11.33	-	11.33	0.16
C3	52.20	21.50	0.52	12.74	0.30	87.29	24.17	11.73	0.26	11.43	0.18
D1	52.90	20.75	-	12.39	0.25	86.30	24.63	11.38	-	11.18	0.15
D2	52.54	20.94	0.38	12.55	0.30	86.70	24.43	11.47	0.19	11.31	0.18
H2	53.14	21.88	0.59	12.59	0.35	88.95	24.12	11.71	0.29	11.08	0.20
I1	54.70	21.18	-	12.58	0.29	88.75	24.73	11.29	-	11.03	0.17
I2	54.29	20.82	-	12.48	0.31	87.92	24.79	11.20	-	11.05	0.18
	Thomsonite - bladed										
F1	39.17	28.14	11.74	4.52	-	83.56	19.44	16.46	6.24	4.35	-
F2	37.48	28.38	11.96	4.25	-	82.07	18.99	16.95	6.50	4.17	-
F3	38.76	27.93	11.61	4.52	-	82.80	19.42	16.49	6.23	4.39	-
F1	38.81	28.44	12.02	4.25	-	83.49	19.29	16.61	6.40	4.09	-
F2	39.70	27.40	10.98	4.73	-	82.83	19.82	16.12	5.88	4.58	-
	?Mesolite - fibrous										
E1	41.52	26.00	8.65	6.30	-	82.46	20.71	15.28	4.62	6.09	-
E2	42.63	26.60	8.87	6.50	-	84.61	20.72	15.24	4.62	6.12	-
E3	41.84	25.79	8.76	6.44	-	82.84	20.79	15.10	4.66	6.21	-
F1	43.49	24.43	8.87	5.50	-	82.29	21.59	14.30	4.72	5.29	-
38299	Analcite										
A1	55.98	21.90	-	12.91	-	90.79	24.70	11.39	-	11.05	-
A2	55.94	21.75	-	12.94	0.28	90.92	24.70	11.32	-	11.08	0.16
	Natrolite										
B	41.61	24.13	1.04	13.44	-	80.20	21.40	14.63	0.57	13.40	-
	Thomsonite - coarse										
B1	37.46	27.76	11.08	4.23	-	80.52	19.27	16.83	6.11	4.22	-
B2	40.37	28.68	10.80	4.92	-	84.78	19.66	16.47	5.64	4.65	-
	?Mesolite										
A1	43.00	24.96	8.28	5.78	-	82.03	21.41	14.65	4.42	5.58	-
A2	40.67	23.71	7.68	5.63	-	77.69	21.38	14.70	4.33	5.74	-
C1	40.94	25.70	8.35	6.21	-	81.22	20.71	15.32	4.53	6.10	-
C2	42.81	26.62	8.63	6.51	-	84.59	20.79	15.24	4.49	6.13	-

Mn 0.40 Mg 0.27

	SiO_2	Al_2O_3	CaO	Na_2O	K_2O	Total	Si	Al	Ca	Na	K
117	Analcite										
B1	53.46	22.15	0.97	12.35	-	88.92	24.19	11.81	0.47	10.84	-
B2	53.46	22.49	0.70	13.03	-	89.95	24.02	11.91	0.34	11.36	0.15
	Natrolite										
1	45.63	25.92	0.50	15.64	0.25	87.95	21.48	14.38	0.25	14.27	0.15
2	45.44	25.83	0.66	15.41	-	87.34	21.50	14.40	0.33	14.13	-
	Thomsonite - fibrous										
1	40.20	27.91	10.93	4.87	-	83.91	19.80	16.20	5.77	4.65	-
2	39.06	28.61	11.28	4.83	-	83.75	19.34	16.69	5.98	4.63	-
3	39.32	28.49	11.40	4.83	-	84.04	19.40	16.57	6.03	4.62	-
A1	38.01	30.04	13.05	4.15	-	85.25	18.60	17.33	6.85	3.94	-
A2	38.10	29.14	12.24	4.07	-	83.54	18.95	17.08	6.52	3.93	-
A3	38.91	28.83	11.81	4.58	-	84.13	19.20	16.77	6.24	4.39	-
157	Thomsonite - coarse (TPD)										
A1	39.88	29.72	11.37	4.10	-	85.07	19.34	16.99	5.91	3.86	-
A2	41.84	30.16	10.89	4.72	-	87.73	19.65	16.70	5.48	4.30	0.07
A3	39.66	30.30	12.18	4.08	0.07	86.28	19.04	17.15	6.27	3.80	0.04
A4	39.81	29.94	11.84	4.02	0.09	85.71	19.21	17.03	6.12	3.76	0.06
B1	41.74	29.13	10.35	4.22	0.09	85.52	20.00	16.46	5.32	3.92	0.06
B2	40.62	29.44	11.07	4.24	0.06	85.43	19.59	16.74	5.72	3.96	0.04
B3	42.12	28.80	10.45	4.00	0.06	85.44	20.18	16.27	5.36	3.72	0.04
	Thomsonite - fibrous (TPD)										
A1	43.19	28.94	10.10	4.19	0.12	86.10	20.39	16.11	5.11	3.84	0.07
A2	43.73	27.99	9.05	4.80	0.15	85.71	20.80	15.69	4.61	4.43	0.09
A3	44.31	27.87	9.30	4.53	0.09	86.10	20.94	15.53	4.71	4.15	0.05
A4	43.28	28.48	10.20	4.71	0.15	86.82	20.43	15.85	5.16	4.31	0.09
A5	43.74	26.92	9.58	4.26	0.10	84.60	21.06	15.28	4.94	3.98	0.06
A6	45.38	27.01	9.06	4.29	0.17	85.91	21.43	15.03	4.58	3.93	0.10
B1	44.39	27.66	8.93	4.38	0.12	85.47	21.08	15.49	4.54	4.03	0.07
B2	43.57	27.84	9.70	4.37	-	85.48	20.77	15.65	4.96	4.04	-
B3	43.27	27.22	7.73	4.03	-	82.25	21.21	15.73	4.06	3.83	-
	?Mesolite										
B1	41.56	26.08	9.30	5.15	-	82.09	20.76	15.35	4.98	4.99	-
B2	41.69	25.58	9.18	5.16	-	81.61	20.93	15.14	4.94	5.02	-
A1	41.59	26.60	9.46	5.22	-	82.87	20.59	15.53	5.02	5.01	-
A2	41.33	25.94	9.33	5.31	-	81.91	20.71	15.32	5.01	5.16	-
A1	40.11	29.36	11.19	5.19	0.13	85.97	19.35	16.70	5.79	4.86	0.08
A2	41.31	29.10	10.35	5.57	-	86.32	19.76	16.41	5.31	5.16	-
	Natrolite										
A1	43.13	27.57	4.34	12.16	-	87.17	20.51	15.45	2.21	11.21	-
A2	42.63	27.40	4.24	12.52	-	86.81	20.40	15.45	2.18	11.63	-
A3	43.36	27.36	4.25	12.31	-	87.29	20.58	15.30	2.16	11.33	-
	Thomsonite - coarse										
A1	38.76	27.29	10.31	4.88	-	81.24	19.72	16.36	5.62	4.81	-
A2	38.74	27.53	10.49	4.95	-	81.71	19.62	16.43	5.69	4.86	-
A3	39.04	27.46	10.35	4.95	-	81.80	19.72	16.35	5.60	4.85	-
A4	38.98	27.12	10.24	4.99	0.30	81.62	19.78	16.22	5.57	4.91	0.19
	Thomsonite - fibrous										
B1	40.82	28.74	10.96	5.36	-	85.88	19.67	16.33	5.66	5.01	-
1	38.40	27.46	10.65	4.69	-	81.18	19.57	16.49	5.81	4.64	-
2	38.74	27.63	10.83	4.89	-	82.08	19.55	16.43	5.86	4.79	-
D1	41.27	26.62	9.86	5.32	-	83.09	20.44	15.55	5.24	5.11	-
D2	42.66	27.44	10.03	5.47	-	85.59	20.49	15.54	5.16	5.10	-
226	Laumontite										
A1	51.06	20.92	10.96	-	0.75	83.70	24.29	11.73	5.58	-	0.45
A2	49.39	20.33	10.68	-	0.71	81.13	24.25	11.77	5.62	-	0.45
A3	50.76	21.03	11.10	-	0.69	83.58	24.20	11.82	5.67	-	0.42
A4	50.14	20.44	11.10	-	0.42	82.09	24.30	11.68	5.76	-	0.26
B1	51.13	20.69	11.19	-	0.57	83.58	24.35	11.61	5.71	-	0.34
B2	49.97	20.52	10.89	-	0.58	81.95	24.27	11.75	5.66	-	0.36
C1	50.93	21.28	11.60	-	0.41	84.22	24.10	11.87	5.88	-	0.25
228	Thomsonite (TPD)										
A1	41.76	25.87	8.71	5.01	0.09	81.44	20.95	15.30	4.68	4.87	0.06
A2	45.13	27.78	10.30	3.57	0.07	86.85	21.11	15.32	5.16	3.24	0.04
B5	43.54	28.64	10.81	4.00	-	86.98	20.46	15.87	5.44	3.65	-
B6	46.46	27.18	9.58	3.93	0.08	87.23	21.57	14.87	4.76	3.54	0.05
C1	44.80	27.46	10.24	3.40	0.11	86.01	21.15	15.28	5.18	3.11	0.07
C2	41.81	30.12	11.50	3.85	0.10	87.39	19.67	16.71	5.80	3.51	0.06

	SiO_2	Al_2O_3	MgO	CaO	Na_2O	K_2O	Total	Si	Al	Mg	Ca	Na	K
235	Thomsonite - fibrous												
E1	38.58	29.28	0.19	12.40	3.22	-	83.66	19.08	17.06	0.14	6.57	3.08	-
E2	38.62	29.50	-	12.43	2.93	-	83.49	19.10	17.20	-	6.59	2.81	-
A1	38.55	29.65	0.26	12.52	3.39	0.09	84.46	18.92	17.16	0.19	6.58	3.23	0.06
A2	38.66	29.77	0.19	12.93	3.28	0.09	84.93	18.89	17.15	0.14	6.77	3.11	0.05
A3	39.15	30.10	0.31	12.67	3.51	0.06	85.81	18.92	17.14	0.23	6.56	3.29	0.04
A4	39.40	30.16	0.27	12.85	3.30	0.08	86.06	18.97	17.12	0.20	6.63	3.08	0.05
A5	38.79	29.83	0.27	12.56	3.37	-	84.82	18.94	17.17	0.19	6.57	3.20	-
A1	39.16	29.12	0.77	12.26	3.14	-	84.44	19.17	16.79	0.56	6.43	2.98	-
A2	39.94	30.11	0.84	12.43	3.27	0.13	86.73	19.05	16.93	0.60	6.35	3.03	0.08

APPENDIX 4: Section D CLAYS AND CHLORITE ANALYSES FROM GREENSCHIST FACIES SAMPLES.

	SiO_2	TiO_2	Al_2O_3	FeO	MgO	MnO	CaO	Na_2O	K_2O	Total	Si	Ti	Al	Fe	Mg	Mn	Ca	Na	K	Total
147A																				
C1	29.39		16.49	24.85	17.27	0.19	0.22	0.29		88.70	6.10	-	4.03	4.31	5.34		0.05	0.12	-	19.95
C2	29.36		16.84	25.20	17.81	0.17	0.23	0.26		89.87	6.01	-	4.06	4.31	5.43	0.03	0.05	0.10	-	20.01
200																				
B1	29.56		15.57	21.42	18.67	0.34	0.38			85.95	6.22	-	3.86	3.77	5.85	0.06	0.09	-	-	19.85
A1	30.93		16.14	21.29	19.88	0.34	0.31		0.29	89.16	6.25	-	3.84	3.60	5.98	0.06	0.07	-	0.07	19.87
E1	33.88		15.55	19.41	20.08	0.66	0.45			90.05	6.67	-	3.61	3.19	5.89	-	0.09	-	0.17	19.61
214																				
A1	31.21		15.15	18.47	21.40	-	0.46			87.68	6.31	-	3.61	3.12	6.75	-	0.10	-	-	19.89
A2	31.15		16.34	20.03	22.01		0.17			89.69	6.19	-	3.83	3.33	6.52	-	0.04	-	-	19.90
C2	31.44		15.49	19.26	22.78	0.19	0.22			89.39	6.26	-	3.63	3.20	6.75	0.03	0.05	-	-	19.93
220																				
A1	29.73		16.04	19.80	19.05	-	0.52			85.13	6.24	-	3.97	3.48	5.96	-	0.12	-	-	19.77
B1	26.78		17.78	19.62	17.78		0.50			78.51	5.84	-	4.57	3.58	5.78	-	0.12	-	-	19.88
41A																				
C1	29.16		15.23	18.94	19.62		0.71			83.68	6.23	-	3.83	3.38	6.25	-	0.16	-	-	19.85
C2	29.09		15.34	18.73	18.87		0.94			83.23	6.26	-	3.89	3.37	6.05	-	0.22	-	-	19.79
C3	30.70		15.51	18.67	19.83		0.73			85.45	6.38	-	3.80	3.24	6.14	-	0.16	-	-	19.72
A1	29.26		15.46	19.57	17.76	0.31	0.55			82.89	6.32	-	3.94	3.54	5.72	0.06	0.13	-	-	19.71
A2	28.73		15.25	18.51	18.16		0.67			81.33	6.30	-	3.94	3.39	5.93	-	0.16	-	-	19.73
212																				
B1	30.53		14.30	21.14	17.79		0.35			84.11	6.53	-	3.61	3.78	5.67	-	0.08	-	-	19.67
B2	30.57		14.47	20.65	17.79		0.41			83.87	6.54	-	3.65	3.69	5.67	-	0.09	-	-	19.64
425																				
C1	28.72		17.27	19.49	19.54	0.43				85.45	6.01	-	4.26	3.41	6.10	0.08	-	-	-	19.86
C2	29.49		15.86	19.50	19.48					84.33	6.24	-	3.96	3.45	6.14	-	-	-	-	19.78
C3	29.38		15.44	18.71	18.71					83.55	6.35	-	3.93	3.38	6.02	-	-	-	-	19.69
D1	28.62		16.80	19.99	20.11	0.40				85.94	5.98	-	4.14	3.49	6.26	0.08	-	-	-	19.95
D2	27.72		17.16	20.03	19.35	0.40				84.66	5.89	-	4.30	3.56	6.13	0.07	-	-	-	19.96
E1	28.60		14.78	20.78	19.05	0.32				83.51	6.19	-	3.77	3.76	6.14	0.06	-	-	-	19.92
I1	28.02		17.08	18.82	18.24	0.35				82.78	6.06	-	4.35	3.40	5.88	0.06	-	-	-	19.76
I2	29.91		18.67	18.89	19.70	0.36				88.25	6.06	-	4.46	3.20	5.94	0.06	-	-	-	19.72
221																				
A1r	32.46		16.80	19.24	20.89	0.27	0.56			90.94	6.37	-	3.89	3.16	6.11	0.04	0.12	-	-	19.69
A2r	31.79		16.95	18.35	19.65	0.12	0.83			88.20	6.40	-	4.02	3.09	5.89	0.02	0.18	-	-	19.59
A3r	31.54		16.83	18.49	20.71	0.16	0.36			88.73	6.32	-	3.98	3.10	6.19	0.03	0.08	-	-	19.69
50																				
C1	31.00		17.12	15.04	22.78		0.67			86.58	6.22	-	4.05	2.52	6.81	-	0.14	-	-	19.75
C2	30.98		16.46	15.22	23.10		0.39			86.14	6.26	-	3.93	2.57	6.95	-	0.08	-	-	19.78
E1	31.00		14.38	15.90	21.97		0.50			83.74	6.48	-	3.54	2.78	6.84	-	0.11	-	-	19.75
E2	31.13		15.02	16.53	22.70		0.34			85.73	6.37	-	3.62	2.83	6.92	-	0.07	-	-	19.82
428B																				
C1	30.16		14.81	10.88	22.92		0.42			79.17	6.49	-	3.75	1.96	7.34	-	0.10	-	-	19.64
C2	31.72		15.66	10.91	23.41	0.36	0.25			82.32	6.54	-	3.81	1.88	7.20	0.06	0.06	-	-	19.55
B1	30.46		15.32	10.86	24.42	0.36				81.41	6.37	-	3.78	1.90	7.62	0.06	-	-	-	19.74
423																				
A1	31.75		14.59	14.25	22.70	0.35	0.29			83.92	6.55	-	3.55	2.46	6.98	0.06	0.06	-	-	19.67
A2	32.62		14.83	14.14	23.31	0.31	0.32			85.52	6.59	-	3.53	2.39	7.02	0.05	0.07	-	-	19.65
	32.24		14.06	14.34	24.82	-	-			85.45	6.53	-	3.36	2.43	7.49	-	-	-	-	19.80
Br	32.17		15.08	13.70	21.61	-	0.43			82.99	6.67	-	3.68	2.37	6.67	-	0.10	-	-	19.49
C	31.21		14.76	13.79	22.22	0.37	0.34			82.70	6.53	-	3.64	2.41	6.93	0.07	0.08	-	-	19.65
55A																				
A1	33.07		15.27	21.41	20.47		0.23			90.46	6.53	-	3.55	3.54	6.02	-	0.05	-	-	19.69
A2	31.78		14.93	23.25	17.85		0.41			88.23	6.52	-	3.61	3.99	5.46	-	0.09	-	-	19.67
A4	33.57		14.99	20.82	18.99	0.15	0.34			88.87	6.72	-	3.54	3.49	5.67	0.03	0.07	-	-	19.51
A3	32.93		14.44	23.55	19.04		0.31			90.27	6.60	-	3.41	3.94	5.68	-	0.07	-	-	19.70
200																				
D1	37.29	1.00	12.02	22.82	1.96		21.18			96.52	7.35	0.15	2.79	3.76	0.58	-	4.47	-	-	19.10
D2	35.79	1.35	8.54	26.37	1.49		20.57			94.11	7.42	0.21	2.09	4.57	0.46	-	4.57	-	-	19.32
C1	41.33		10.43	15.88	17.34		1.57		0.57	87.11	8.13	-	2.42	2.61	5.09	-	0.33	-	0.14	18.73
C2	42.27		10.92	15.41	17.48		2.29		0.67	89.05	8.12	-	2.47	2.48	5.01	-	0.47	-	0.16	18.72
64B																				
A1	41.96		7.45	3.85	23.15		1.00	0.50	0.20	78.11	8.61	-	1.80	0.66	7.08	-	0.22	0.20	0.05	18.62
A2	41.37		7.12	3.72	22.79		1.68	0.44	0.20	77.32	8.60	-	1.74	0.65	7.06	-	0.37	0.18	0.05	18.65

Structure based on 28 oxygens.

APPENDIX 4: Section E EPIDOTE, PREHNITE, SPHENE, K-FELDSPAR, SERICITE, ZEOLITE AND ALBITE ANALYSES FROM LOWER GREENSCHIST FACIES SAMPLES

	SiO_2	TiO_2	Al_2O_3	FeO	MgO	MnO	CaO	Na_2O	K_2O	Total	Si	Ti	Al	Fe	Mg	Mn	Ca	Na	K	Total
50 Epidote																				
A1	37.61	-	25.09	9.57	-	-	23.32	-	-	96.66	6.005	-	4.722	1.278	-	-	3.989	-	-	15.995
A2	37.97	-	25.06	10.75	-	-	23.44	-	-	97.21	6.027	-	4.689	1.284	-	-	3.986	-	-	15.987
A3	36.67	-	24.66	6.13	1.71	-	22.65	-	-	91.82	6.084	-	4.823	0.765	0.423	-	4.027	-	-	16.122
A4	36.30	-	24.90	5.92	1.76	-	22.57	-	-	91.47	6.045	-	4.889	0.742	0.437	-	4.027	-	-	16.140
A5	38.14	-	22.94	14.77	-	-	23.44	-	-	99.27	6.011	-	4.262	1.752	-	-	3.958	-	-	15.983
214 Epidote																				
A1	37.20	-	23.24	11.50	0.90	-	22.27	-	-	95.11	5.995	-	4.415	1.550	0.216	-	3.846	-	-	16.022
A2	36.45	-	22.38	12.25	2.66	-	19.84	-	-	93.57	5.593	-	4.309	1.673	0.647	-	3.472	-	-	16.055
A3	38.09	-	23.99	11.76	0.75	-	22.74	-	-	97.34	5.995	-	4.451	1.548	0.176	-	3.835	-	-	16.005
A4	37.59	-	23.62	11.95	1.37	-	21.95	-	-	96.58	5.967	-	4.420	1.586	0.324	-	3.733	-	-	16.030
C1	37.34	-	23.50	12.74	1.33	-	21.74	-	-	96.66	5.927	-	4.398	1.690	0.315	-	3.698	-	-	16.028
C2	37.89	-	24.01	12.03	0.45	-	22.99	-	-	97.38	5.971	-	4.461	1.586	0.106	-	3.882	-	-	16.006
C3	37.11	-	23.94	11.93	0.84	-	22.37	-	-	96.19	5.919	-	4.502	1.591	0.200	-	3.823	-	-	16.035
C4	38.04	-	24.22	11.69	0.48	-	23.13	-	-	97.55	5.979	-	4.488	1.535	0.112	-	3.895	-	-	16.010
220 Epidote																				
A1	37.65	-	23.75	13.77	-	-	22.36	-	-	97.53	6.003	-	4.464	1.652	-	-	3.820	-	-	15.939
A2	37.33	-	23.22	14.11	-	-	22.35	-	-	97.00	5.998	-	4.398	1.706	-	-	3.848	-	-	15.950
A3	37.39	-	23.54	13.67	-	-	21.79	-	-	96.39	6.023	-	4.471	1.657	-	-	3.761	-	-	15.913
419 Epidote																				
C1	37.33	-	23.66	11.49	-	-	22.65	-	-	95.13	6.21	-	4.64	1.60	-	-	4.03	-	-	16.48
C2	38.23	-	24.02	11.59	-	-	22.54	-	-	96.39	6.06	-	4.49	1.54	-	-	3.83	-	-	15.92
C3	37.63	-	23.60	11.71	-	-	22.09	-	-	95.55	6.06	-	4.48	1.58	-	-	3.81	-	-	15.92
134 Prehnite																				
B1	44.60	-	24.05	0.59	-	-	26.68	-	-	95.94	6.10	-	3.88	0.07	-	-	3.91	-	-	13.96
B2	44.09	-	23.20	1.69	-	-	26.54	-	-	95.51	6.10	-	3.78	0.20	-	-	3.93	-	-	14.01
A1	43.92	-	23.13	1.72	-	-	26.47	-	-	95.24	6.09	-	3.78	0.20	-	-	3.94	-	-	14.01
212 Prehnite																				
A1	45.50	-	22.88	2.61	-	-	26.57	-	-	97.55	6.17	-	3.86	0.30	-	-	3.86	-	-	14.00
A	43.60	-	21.81	3.50	-	-	26.21	-	-	95.10	6.12	-	3.61	0.41	-	-	3.94	-	-	14.08
C1	41.86	-	21.13	3.38	-	-	25.23	-	-	91.60	6.10	-	3.63	0.41	-	-	3.94	-	-	14.08
C2	42.42	-	20.97	4.46	-	-	26.15	-	-	94.02	6.07	-	3.54	0.53	-	-	4.01	-	-	14.16
C	43.00	-	22.84	1.24	-	-	26.26	-	-	93.34	6.08	-	3.81	0.15	-	-	3.98	-	-	14.02
425 Prehnite																				
A1	43.53	-	24.21	0.45	-	-	26.74	-	-	94.92										
A2	44.09	-	24.15	0.98	-	-	27.03	-	-	96.26										
A3	44.20	-	24.05	0.89	-	-	26.92	-	-	96.06										
E1	44.13	-	24.45	0.51	-	-	26.60	-	0.36	96.08										
E2	42.48	-	21.99	3.51	-	-	25.31	-	-	93.30										
F1	41.95	-	22.09	3.23	-	-	25.82	-	-	93.09										
F2	42.40	-	22.13	3.14	-	-	25.82	-	-	93.48										
E?1	41.82	-	22.52	3.82	1.29	-	23.97	-	-	93.43										
E?2	42.06	-	22.86	3.38	0.90	-	24.60	-	-	93.79										
227 Prehnite																				
B1	42.59	-	23.47	1.80	-	-	26.58	-	-	94.45	5.98	-	3.88	0.21	-	-	-	-	-	14.07
50 Sphene																				
D1	32.39	29.64	4.93	2.19	-	-	27.66	-	-	96.79	4.304	2.964	0.773	0.243	-	-	3.941	-	-	12.224
B2	32.39	29.71	5.10	2.12	-	-	27.72	-	-	97.03										
4288 Sphene																				
A	31.92	28.42	6.22	1.74	-	-	27.89	-	-	96.20	4.27	0.98	2.86	0.19	-	-	3.99	-	-	12.29
50 K-feldspar																				
A	63.75	-	18.73	-	-	-	1.23	-	14.80	99.08	11.90	-	4.12	-	-	-	0.25	-	3.53	19.80
C	67.88	-	19.63	-	-	-	1.34	-	15.80	104.66	11.93	-	4.07	-	-	-	0.25	-	3.55	19.80
64 K-feldspar																				
A1	63.17	-	18.31	-	-	-	0.19	0.17	16.13	97.98	11.93	-	4.08	-	-	-	0.04	0.06	3.89	20.00
A2	64.01	-	18.21	-	-	-	0.37	0.13	16.48	99.21	11.96	-	4.01	-	-	-	0.08	0.05	3.93	20.03
147A K-feldspar																				
A1	63.21	-	19.73	-	-	-	0.12	0.78	15.22	99.06	11.77	-	4.33	-	-	-	0.02	0.28	3.62	20.02
A2	64.71	-	18.71	-	0.20	-	-	-	16.71	100.34	11.94	-	4.07	-	0.06	-	-	-	3.93	20.00
B1	63.38	-	19.06	-	-	-	-	-	16.15	98.59	11.88	-	4.21	-	-	-	-	-	3.86	19.95
221 K-feldspar																				
B3	64.09	-	19.21	-	-	-	0.23	0.36	16.11	96.98	2.96	-	1.05	-	-	-	0.01	0.03	0.95	5.00
423 K-feldspar																				
A	65.03	-	18.39	-	-	-	1.34	-	15.13	99.89	11.98	-	3.99	-	-	-	0.27	-	3.56	19.80
B	66.27	-	18.78	-	-	-	1.30	-	15.35	101.70	11.99	-	4.00	-	-	-	0.25	-	3.54	19.78
147A Sericite																				
B	48.38	-	32.71	1.89	1.18	-	-	-	11.23	95.40	6.45	-	5.14	0.21	0.23	-	-	-	1.91	13.94
221 Sericite																				
B1	46.38	-	33.85	1.69	1.06	-	-	0.27	11.43	94.67	6.25	-	5.38	0.19	0.21	-	-	-	0.07	14.07
50 Zeolite																				
A	37.8	-	29.21	-	-	-	12.05	4.00	-	83.07	18.89	-	17.21	-	-	-	6.45	3.88	-	36.10
C1	42.21	-	29.57	-	-	-	11.54	4.80	-	88.11	19.77	-	16.33	-	-	-	5.79	4.36	-	36.10
C2	41.48	-	28.83	-	-	-	11.45	4.66	-	86.43	19.81	-	16.23	-	-	-	5.86	4.32	-	36.04
Av1	37.48	-	29.00	-	-	-	12.17	3.81	-	82.48	18.88	-	17.22	-	-	-	6.57	3.73	-	36.10
Av2	38.76	-	28.63	-	-	-	12.01	4.14	-	83.51	19.25	-	16.78	-	-	-	6.69	3.99	-	36.03
Bv	38.40	-	28.04	-	-	-	11.60	4.12	-	82.16	19.36	-	16.66	-	-	-	6.27	4.03	-	36.02
Cv	38.98	-	29.23	-	-	-	12.08	4.29	-	84.56	19.13	-	16.91	-	-	-	6.35	4.08	-	36.04

Appendix 4: Section E continued

	SiO_2	TiO_2	Al_2O_3	FeO	MgO	MnO	CaO	Na_2O	K_2O	Total	Si	Ti	Al	Fe	Mg	Mn	Ca	Na	K	Total
227	Zeolite																			
D1	50.06	-	21.26	-	-	-	11.32	-	0.43	83.06	24.01	-	12.02	-	-	-	5.82	-	0.27	36.03
D2	51.83	-	21.84	-	-	-	11.52	-	0.54	85.74	24.08	-	11.96	-	-	-	5.74	-	0.32	36.04
D3	52.84	-	21.67	-	-	-	11.45	-	1.14	87.09	24.24	-	11.72	-	-	-	5.63	-	0.67	35.96
D4	50.06	-	21.11	-	-	-	11.40	-	0.58	83.14	24.03	-	11.94	-	-	-	5.86	-	0.35	35.97
D5	39.45	-	28.99	-	-	-	11.50	-	4.35	84.19	19.38	-	16.73	-	-	-	6.06	4.15	-	36.11
D6	39.58	-	28.65	-	-	-	11.24	-	4.54	84.00	19.49	-	16.62	-	-	-	5.93	4.34	-	36.11
C1	39.45	-	29.63	-	-	-	11.95	-	4.45	85.46	19.14	-	16.95	-	-	-	6.21	4.19	-	36.09
C2	39.60	-	29.06	-	-	-	11.50	-	4.49	84.65	19.36	-	16.75	-	-	-	6.03	4.26	-	36.11
Dv1	54.36	-	21.65	-	-	-	0.29	12.58	0.31	89.20	24.50	-	11.51	-	-	-	0.14	10.99	0.18	36.01
Dv2	55.19	-	21.92	-	-	-	0.34	12.68	0.34	90.48	24.53	-	11.48	-	-	-	0.16	10.93	0.19	36.01
419	Zeolite																			
B1	37.74	-	28.23	-	-	-	11.88	4.41	-	82.26	19.08	-	16.82	-	-	-	6.44	4.32	-	35.90
B2	36.94	-	28.80	-	-	-	12.34	4.07	-	82.14	18.74	-	17.22	-	-	-	6.71	4.00	-	35.96
B3	37.20	-	28.68	-	-	-	12.12	4.18	-	82.16	18.85	-	17.13	-	-	-	6.58	4.10	-	35.98
423	Zeolite																			
A1	51.04	-	18.01	-	-	-	6.21	4.44	0.74	80.46	25.49	-	10.60	-	-	-	3.32	0.72	2.83	36.09
A2	52.07	-	19.67	-	-	-	5.27	3.67	0.78	81.46	25.39	-	11.30	-	-	-	2.76	0.74	2.29	36.69
425	Zeolite																			
A1	51.62	-	22.79	-	-	-	0.70	13.48	-	88.59	23.62	-	12.29	-	-	-	0.34	11.96	-	35.91
A2	53.57	-	23.00	-	-	-	0.41	13.97	-	90.92	23.85	-	12.07	-	-	-	0.19	12.05	-	35.92
A3	53.76	-	23.11	-	-	-	0.42	14.22	0.25	91.77	23.78	-	12.05	-	-	-	0.20	12.20	0.14	35.82
D1	52.88	-	21.73	-	-	-	0.27	13.59	-	88.47	24.16	-	11.70	-	-	-	0.13	12.03	-	35.86
I1	52.52	-	22.60	0.42	-	-	0.31	13.71	-	89.55	23.79	-	12.07	0.16	-	-	0.15	12.04	-	35.86
I2	52.71	-	22.39	0.32	-	-	0.35	13.66	0.24	89.69	23.86	-	11.95	0.12	-	-	0.17	11.98	-	35.81
147A	Albite																			
B1	67.89	-	21.12	-	-	-	1.09	11.59	0.14	101.83	11.70	-	4.29	-	-	-	0.20	3.87	0.03	20.10
B2	68.58	-	21.27	-	-	-	1.23	11.57	0.16	102.80	11.71	-	4.28	-	-	-	0.22	3.83	0.04	20.08
221	Albite																			
A	67.43	-	21.59	-	-	-	1.63	10.90	0.40	101.95	2.91	-	1.10	-	-	-	0.08	0.91	0.02	5.01
423	Albite																			
A	67.17	-	20.67	-	-	-	1.08	11.40	0.37	100.71	11.72	-	4.25	-	-	-	0.20	3.86	0.08	20.12
428B	Albite																			
C1	67.62	-	20.80	-	-	-	1.09	11.42	0.49	101.42	11.72	-	4.25	-	-	-	0.20	3.84	0.11	10.12
C2	66.91	-	21.22	-	-	-	1.40	11.59	0.30	101.43	11.62	-	4.34	-	-	-	0.26	3.90	0.07	
A	68.22	-	20.82	-	-	-	0.85	11.79	0.31	102.01	11.75	-	4.23	-	-	-	0.16	3.94	0.07	

APPENDIX 4: Section F AMPHIBOLE, CLINOPYROXENE AND PLAGIOCLASE ANALYSES FROM GREENSCHIST-LOWER AMPHIBOLITE SAMPLES.

	SiO_2	TiO_2	Al_2O_3	Cr_2O_3	FeO	MgO	MnO	CaO	Na_2O	K_2O	Total	Si	Ti	Al	Cr	Fe	Mg	Mn	Ca	Na	K	Total
38493 Uralitised dyke																						
Massive amphibolite																						
D1	48.58	0.82	4.38	-	25.03	10.00	0.50	9.65	1.73	0.29	100.98	7.227	0.091	0.769	-	3.115	2.217	0.063	1.539	0.498	0.055	15.574
D2	49.71	0.82	3.46	-	23.92	10.61	0.39	9.98	1.42	0.29	100.58	7.369	0.091	0.604	-	2.965	2.345	0.049	1.585	0.407	0.055	15.470
D3	48.09	0.85	4.65	-	25.56	9.78	0.43	9.39	1.93	0.35	101.03	7.175	0.095	0.817	-	3.190	2.176	0.054	1.501	0.558	0.066	15.632
B1	50.05	0.67	3.55	-	24.02	11.64	0.34	8.72	1.59	-	100.57	7.378	0.074	0.617	-	2.962	2.559	0.042	1.377	0.455	-	15.464
B2	48.77	1.28	4.55	-	22.60	11.04	0.27	10.23	1.90	-	101.05	7.182	0.142	0.790	-	2.784	2.424	0.034	1.614	0.543	-	15.585
B3	48.02	0.88	4.82	-	22.78	10.63	0.28	9.85	1.63	0.45	99.36	7.197	0.100	0.851	-	2.855	2.374	0.036	1.582	0.474	0.085	15.554
A1	51.30	-	2.76	-	23.25	11.94	0.56	9.53	1.48	-	100.79	7.525	-	0.477	-	2.852	2.611	0.069	1.498	0.422	-	15.454
A2	50.87	0.28	2.74	-	24.64	11.33	0.66	9.28	1.35	-	101.14	7.486	0.031	0.475	-	3.032	2.485	0.082	1.463	0.385	-	15.439
Fibrous actinolite amphibole																						
C1	53.78	0.38	2.36	-	10.68	17.74	-	12.37	-	-	97.33	7.684	0.041	0.398	-	1.276	3.779	-	1.894	-	-	15.072
C2	53.12	-	2.78	-	14.13	15.74	-	12.26	-	-	98.02	7.657	-	0.472	-	1.703	3.381	-	1.893	-	-	15.106
Plagioclase rim analyses																						
D1	59.73	-	24.85	-	0.28	-	-	7.09	8.05	-	90.29	10.676	-	5.235	-	0.042	-	-	1.359	2.789	-	20.101
D2	60.52	-	24.53	-	-	-	-	6.52	8.10	0.34	98.96	10.792	-	5.155	-	-	-	-	1.246	2.801	0.077	20.071
D3	59.26	-	25.34	-	-	-	-	7.70	7.44	0.28	99.53	10.598	-	5.342	-	-	-	-	1.475	2.580	0.063	20.058
38446 Uralitised dyke																						
Relict clinopyroxene																						
D1c	52.54	-	3.70	1.51	3.23	18.01	-	21.02	-	-	99.40	1.905	-	0.158	0.043	0.098	0.973	-	0.817	-	-	3.994
D2c	52.20	0.26	3.68	1.53	3.25	18.19	-	20.88	-	-	99.67	1.894	0.008	0.158	0.044	0.099	0.984	-	0.812	-	-	3.999
D3c	52.32	0.25	3.70	1.56	3.20	18.21	-	20.74	-	-	99.88	1.897	0.007	0.158	0.045	0.097	0.984	-	0.806	-	-	3.994
C1c	53.22	0.28	2.78	0.76	3.78	18.60	-	20.57	-	-	99.93	1.928	0.008	0.119	0.022	0.115	1.005	-	0.798	-	-	3.995
C2c	53.27	-	3.02	0.83	3.99	18.62	-	20.27	-	-	100.31	1.929	-	0.129	0.024	0.121	1.005	-	0.787	-	-	3.995
C3c	53.67	-	1.44	0.82	3.14	17.44	-	23.49	-	-	100.45	1.956	-	0.062	0.024	0.096	0.948	-	0.917	-	-	4.003
Rim amphibole on clinopyroxene																						
C1r	53.61	0.30	3.06	0.95	4.08	18.51	-	20.93	-	-	101.46	7.353	0.031	0.495	0.103	0.468	3.784	-	3.077	-	-	15.311
C2r	52.43	0.47	4.12	0.70	10.07	17.78	-	12.86	0.67	-	99.10	7.397	0.050	0.685	0.078	1.188	3.738	-	1.994	0.184	-	15.264
Fibrous amphibole in totally replaced clinopyroxene sites.																						
B1	50.87	0.58	5.84	-	12.75	16.33	-	11.74	1.17	-	99.31	7.236	0.062	0.979	-	1.517	3.463	-	1.789	0.323	-	15.369
B2	50.10	0.33	6.69	-	12.90	16.33	-	10.68	1.33	-	98.37	7.184	0.036	1.131	-	1.547	3.491	-	1.640	0.371	-	15.400
B3	48.80	0.53	6.58	0.34	13.34	14.96	-	11.39	1.21	-	97.16	7.136	0.059	1.134	0.039	1.632	3.261	-	1.785	0.344	-	15.390
Random amphibole																						
E1	48.05	-	8.22	-	12.67	15.22	-	11.52	1.52	-	97.22	7.005	-	1.412	-	1.545	3.308	-	1.799	0.431	-	15.500
E2	48.20	-	8.13	-	12.36	15.44	-	11.66	1.62	-	97.41	7.008	-	1.393	-	1.503	3.346	-	1.816	0.456	-	15.522
Acicular tremolitic amphibole																						
A1	57.72	-	-	-	4.23	22.78	-	12.22	-	-	96.92	7.997	-	-	-	0.490	4.706	-	1.814	-	-	15.007
A2	56.75	-	0.72	-	7.26	21.29	-	12.15	-	-	98.17	7.882	-	0.118	-	0.843	4.408	-	1.807	-	-	15.058
A3	52.84	-	5.01	-	8.34	19.75	-	11.45	0.96	-	98.33	7.404	-	0.827	-	0.977	4.125	-	1.718	0.260	-	15.311
A4	54.81	-	-	-	4.22	21.39	-	12.13	-	-	92.56	7.976	-	-	-	0.514	4.640	-	1.892	-	-	15.022
Talc centre fill in tremolite patches																						
T1	57.39	-	-	-	1.89	27.81	-	-	-	-	87.09	8.001	-	-	-	0.221	5.778	-	-	-	-	14.000
T2	62.29	-	-	-	2.01	30.16	-	-	-	-	94.47	8.003	-	-	-	0.215	5.777	-	-	-	-	13.995
T3	61.63	-	-	-	1.74	29.81	-	-	-	-	93.18	8.015	-	-	-	0.189	5.760	-	-	-	-	13.983
Relict primary plagioclase																						
D1	53.78	-	28.74	-	0.54	-	-	11.75	5.19	-	101.22	9.753	-	6.143	-	0.082	-	-	2.284	1.825	-	20.087
B1	51.43	-	30.46	-	0.35	-	-	13.98	3.80	-	99.79	9.370	-	6.541	-	0.053	-	-	2.729	1.343	-	20.036
B2	52.99	-	29.27	-	0.49	-	-	12.65	4.58	-	100.04	9.625	-	6.267	-	0.074	-	-	2.462	1.614	-	20.042

APPENDIX 5

XRD RESULTS ON SECONDARY MINERAL SEPARATES

Sample No.	157 vein	228	38478	155	117	41A	119	440	120	11(a)
Dominant Phase	Natrolite + heulandite	Natrolite	Natrolite	Heulandite	Laumontite + natrolite	Laumontite + natrolite	Laumontite	Laumontite	Laumontite	Gyrolite
D (Å)	*6.52	6.51	6.58/*6.54	7.87	*6.55	9.34	9.30/9.15	*9.42	*9.47	11.04
	5.90	5.98	5.89	7.78	*6.49	7.19/*6.57	*6.51	6.83	6.84	9.20
	-	5.82	5.60	6.62	5.90	5.92	5.85	*4.71	4.73	*6.08
	4.66	4.79	-	6.60	5.87	4.66	4.60	4.29	*4.16	5.86
	4.58	4.68	*4.62	6.51	5.61	4.39	4.35	*4.14	3.56	4.20
	-	4.60/4.36	4.39	5.90	5.58	*4.15	*4.11	3.66	*3.50	*4.60
	4.17	4.16	4.13	4.66	4.71	3.51	3.94	3.64	3.27	4.36
	*3.97	4.11	-	4.53	4.61	3.27	3.49	3.50	3.20	4.19
	3.92	3.49	3.51	4.48	4.38	*3.20	3.29	3.26	3.15	*4.12
	-	-	-	4.15	4.19	3.16	3.26	3.14	3.03	3.68
	3.28	3.29	3.27	4.11	4.13	2.95	3.19	3.02	2.88	3.50
	3.19	3.20	3.19	*3.95	3.50	*2.86	3.17		2.44	3.28
	3.15	3.15	3.18	3.89	*3.43	2.68	2.94		2.36	3.21
	3.10	3.08	-	3.57	*3.42	2.18	*2.85		2.15	3.17
	2.94	*2.93	2.95	3.35	3.29	2.18	2.67			3.08
		*2.87	*2.86	3.17	3.27		2.57			3.03
	*2.86	*2.85	2.79	*2.98	3.17		2.56			2.94
	-	2.68	2.68	2.94	2.92		2.43			2.92
	2.58	2.58		2.51	2.88		2.25			2.88
	2.51	2.52		*2.48	2.85					*2.86
	2.45	2.46		2.37	2.69					2.67
	2.41	-			2.67					2.57
	2.32				2.20					2.56
	2.19				2.18					2.43
	2.18									2.25
										*2.18
										2.06

Sample No.	60	199	131	72	129	61	22	111	120	140	157 amyg.
Dominant Phase	Wairakite + natrolite	Prehnite	Prehnite	Quartz	Quartz	Natrolite	Natrolite	Natrolite	Natrolite	Natrolite + wairakite	Natrolite
D (Å)	6.57	5.28	5.25	*4.22	*4.25	*6.49	*6.53	*6.56	*6.58	6.58/*6.51	6.52
	5.87	4.63	4.62	*3.34	*3.34	5.79	5.85	5.85	5.86	5.86	5.86
	*5.57	3.54	3.54	3.28	3.28	5.52	5.58	-	-	5.58	5.81
	4.84	3.48	3.47	2.45	*2.45	4.74	4.70	4.82	4.70	4.72	4.67
	4.60	*3.31	*3.30	*2.28	2.28	4.65	4.60	4.54	4.60	4.60	4.60
	4.39	*3.08	3.27/*3.08	2.24	2.23	4.35	4.35	4.35	4.35	4.35	4.37
	4.13	2.81	2.81	2.13		4.15	4.18	4.19	4.18	4.20	4.33
	3.65	2.63	2.63	1.98		4.10	4.12	4.12	4.12	4.13	4.12
	*3.43	*2.56	*2.56			3.50	3.50	-	3.49	*3.43	3.49
	3.29	2.52	2.36			3.48	*3.42	-	-	*3.42	-
	3.03	2.49	2.31			3.29	3.26	3.28	-	3.29	3.29
	*2.92	2.45				3.20	-	3.21	3.21	3.22	3.19
	2.88	2.43				3.16	3.17	3.16	3.16	3.16	3.16
	2.85	2.36				3.07	-	3.08	3.09	3.09	3.09
	2.79	2.32				2.92	2.92	2.92	2.93	2.93	2.93
	2.69	2.31				*2.88	2.88	*2.88	*2.88	*2.88	*2.87
	2.58	2.07				*2.85	*2.85	*2.85	*2.83	2.86	*2.85
	2.50					2.66	2.67	-	2.70	2.69	2.66
	2.43					2.56		2.57		2.57	2.57
	2.23					2.52		2.50		2.50	2.51
	2.17					2.46		2.47		2.47	2.46
						2.42		2.42		2.42	2.42
						2.24		2.23		2.22	2.25
						2.19		2.20		2.20	2.17
						2.13		2.21		2.13	

* Denotes either three most intense lines or all lines with 100% intensity.

Appendix 6

MAJOR AND TRACE ELEMENT ANALYTICAL TECHNIQUES

Major- and trace-element determinations were largely performed using X-ray fluorescent spectrographic methods based on those of Norrish & Hutton (1969) and Norrish & Chappell (1967), at the Geology Department of the University of Tasmania.

A6.1 Sample preparation

Rock samples of between 0.5 and 2.0 kg weight were chosen for analysis. These were cleaned of all weathered surfaces and initially broken into large fragments with a geological hammer. The sample was then reduced to fragments of 105 mm or less, in a jaw crusher. This crush was then quartered by passing through a stainless steel sample splitter several times to reduce the sample for final grinding to about 200-500 grams. The sample was then ground in a tungsten-carbide swing-mill, in 150 gram lots. Batches of powder from each sample so produced were then recombined and thoroughly mixed.

With the exception of W, C, and Co, the contamination of the sample during crushing and grinding is negligible.

Fused lithium borate glass discs were prepared for major element analysis using the method of Norrish & Chappell (1967). The flux was prepared in bulk prior to the analysis of each batch of samples, the mixture comprising: lithium tetraborate - 38 g, lithium carbonate - 29.6 g, and lanthanum oxide - 13.2 g. This mixture was fused and quenched to a glass coarsely crushed to inhibit the take-up of water from the atmosphere.

Each disc was then prepared from 1.5 g of the above flux, 0.02 g of sodium nitrate and 0.28 g of sample (rock powder). The discs were prepared from unignited rock powders which had been dried at 150°C and loss on ignition was determined separately.

Boric acid-backed, pressed pills were prepared after the method of Norrish & Chappell (1967) for analysis of trace elements and Na. Pills were made with 5-6 g of rock powder as this was the minimum amount of powder required to yield an apparent infinite thickness for Kα radiation of some of the heavier trace elements (e.g. Nb).

A6.2 Major element analysis

The discs and pills were analyzed using a Philips PW1410 vacuum spectrograph. Instrumental settings for major elements are given in Table A6.1. All major elements were determined on the fused glass discs except for Na which was determined on pressed pills. Backgrounds were determined on the peak setting of the element in question using 100% SiO_2 discs. The SiO_2 background was determined on a pure reagent blank disc. Background for Na was taken off-peak and methane gas was used to eliminate interference from the escape peak of K *K*α radiation from the K.A.P. crystal and to reduce backgrounds.

Counting times were 50 seconds (peak) except for SiO_2, MgO, and Na_2O, where 100 seconds (peak) was used. Every Na sample was counted for background as well (50 seconds).

Matrix corrections were made on nominal percentage readings from the XRF using the method of Norrish & Hutton (1969) to yield true percentage values.

Standards prepared from Tasmanian igneous rocks (mainly Jurassic dolerite, TASDOL-1) and calibrated against international standards, were used as "working standards" with known nominal percentage compositions. Discs of several of these were prepared at the same time as the unknown samples, from the same batch of flux. These were checked against international standards and during runs on unknown samples, were counted once every fifth sample to minimise the effects of instrumental drift.

Table A6.1

Instrumental settings for x-ray fluorescent analysis of Major elements

Philips PW1410, Vacuum Spectrograph

Element	Si	Ti	Al	Fe	Mg	Ca	K	P	Mn	Na
Tube	Cr	Cr	Cr	Cr	Cr	Cr	Cr	Cr	Au	Cr
Crystal	P.E.	LiF200	P.E.	LiF200	A.D.P.	LiF200	P.E.	P.E.	LiF200	K.A.P.
Collimator(1)	C	F	C	F	C	F	F	C	F	C
Tube Voltage (KV)	50	35	50	50	50	45	45	50	50	50
Tube Current (ma)	45	12	45	45	45	18	30	50	30	50
Counter E.H.T.(V)	1550	1610	1550	1560	1550	1560	1560	1560	1560	2520
Peak (^{o})	108.79	86.17	144.9	57.45	136.6	113.08	50.17	89.1	62.95	54.2
Background(2) count rate	99 c/s	100 c/s	50 c/s	81 c/s	7 c/s	100 c/s	70 c/s	11 c/s	90 c/s	24 c/s
Analytical Line	Kα	Kα	Kα	Kα	Kα	Kα	Kα	Kα	Kα	Kα
Counter(3) Gas	F+D+V P10	F+D+V P10	F+D+V P10	F+D+V P10	F+D+V P10	F+D+V P10	F+D+V P10	F+D+V P10	F+D+V P10	F+D+V P10
Channel Height(V)	2.10	3.55	2.5	3.6	3.35	2.55	3.0	3.75	2.7	3.0
Lower Level (V)	2	2	2	1	1	1	1	1	2.5	2

Notes: (1) C = coarse, F = Fine; (2) Background determined at peak position for all elements except Na on a pure SiO_2 (+ flux) disc or in the case of SiO_2 on a flux disc. (3) F = Gas Flow Proportional Counter; D = Automatic Discriminator; V = vacuum.

All analyses done on fused glass discs except Na which was determined on pressed powder pellets.

A6.3 Trace element analysis

The instrumental settings used during trace element determinations in this study are given in Table A6.2. The mass absorption coefficients for the trace elements were calculated from the known major element composition of each sample using the method of Champion *et al.* (1968).

Trace elements were determined on boric acid-backed pressed pills. Analytical lines and background positions (see Table A6.2) were chosen to minimize the effects of interfering peaks and sloping backgrounds. Where interferences were unavoidable (e.g. Sr Kα on Zr Kα and Rb Kα on Y Kα) then the extent of interference was measured and corrected for.

Artificial standards were used, largely prepared by mixing measured amounts of trace elements with spec. pure quartz. These standards were checked both for linearity between standards of different concentration of the same element and against international standards (making appropriate correction for the mass absorption of the radiation of the element in question by the silica matrix of the standard).

A6.4 FeO determinations

Samples were dissolved using an HF-H_2SO_4 dissolution and Fe^{2+} was determined using the method of Reichen & Fahey (1962).

In this method, the Fe^{2+}-bearing solution reacts with iodine monochloride in excess HCl. The free iodine thus liberated is titrated against a standard solution of potassium iodate using CCl_4 as an indicator.

The main problem with the method is that there is likely to be some oxidation of Fe^{2+} during the dissolution. This is minimized by digesting the sample cold, overnight.

Table A6.2

Instrument Settings for X-ray fluorescent analysis of trace elements

Philips PW1410, Vacuum Spectrograph

Element	Tube	KV	mA	Coll.	Vacuum	Counter	Crystal	Angle	Background	Counting Time	Comments
Scandium ($K\alpha_1$)	Cr	50	50	coarse	Yes	gfpc	LiF200	97.67	96°	20, 20	Correction for Ca interface made.
Chromium ($K\alpha_1$)	Au	50	50	fine	yes	gfpc	LiF200	69.34	±1°	50, 50, 50	None metalic holders used, correction for $V_{K\beta}$ interference
Nickel ($K\alpha_1$)	Au	50	30	fine	no	gfpc + scint.	LiF200	48.65	49.65°	50, 50	With 3.0 volt window
Rubidium ($K\alpha_1$)	Mo	50	30	fine	no	scint.	LiF200	38.00	±0.6°	20, 20, 20	determined simultaneously with Y
Strontium ($K\alpha_1$)	Au	60	40	fine	no	scint.	LiF220	35.87	±0.7°	20, 20, 20	determined simultaneously with Zr.
Zirconium ($K\alpha_1$)	Au	60	40	fine	no	scint.	LiF220	32.17	±1.0°	20, 20, 20	Correct for Sr $K\beta$ interference
Niobium ($K\alpha_1$)	Mo	50	30	fine	no	scint.	LiF220	30.45	±0.5°	100, 100, 100	5 gram sample
Lanthanum (La_1)	Cr	50	50	coarse	yes	gfpc	LiF220	138.7	±1°	100, 100, 100	2.5 volt window

Notes: All determinations made on pressed powder pellets. gfpc = gas flow proportional counter

Scint. - scintillation counter.

A6.5 References

Kelsey, C.H., 1963: Calculation of the CIPW norm. *Min. Mag., 34,* 276-328.

Norrish, K. and Hutton, J.T., 1969: An accurate X-ray spectrographic method for the analysis of a wide range of geological samples. *Geochem. Cosmochim. Acta, 33,* 431-455.

Norrish, K., and Chappell, B.W., 1967: X-ray fluorescent spectrography. In: *Physical Methods in Determinative Mineralogy.* J. Zussman (Ed.) Academic Press, London.

Reichen, L.E., and Fahey, J.J., 1962: An improving method for the determination of ferrous ozide in rocks and minerals including garnet. *Geol. Surv. Amer. Bull. 1144-B.*

Appendix 7

SAMPLE CATALOGUE

Dept. No.	Field No.	Forms	Description	General Location
60593	4	R	Small glassy pillow lavas.	Eastern flank, Mt. Law
94	4Z	R	Zeolite specimens from 4.	"
95	7	R	Pillow lava.	700m ESE Mt. Ifould.
96	11	R	Coarse lithic wacke.	N end Green Gorge Beach.
97	11Z	R	Veins of zeolites.	"
98	13	R	Massive flow with ropy surface.	100m N Green Gorge Beach.
99	2[illegible]	R	Plag-phyric pillow lava.	200m N Brothers Pt.
60600	23A	R	Massive gabbro.	Pt. N of Sandy Bay.
01	23B	R	Dyke intruding above gabbro.	"
02	24A	R	Dyke/gabbro contact - chilled dyke margin.	2km N Sandy Bay.
03	25B	R	Fine gabbro or dyke in coarse gabbro.	Coast SE Mt. Blair.
04	26B	R	Fine grained dykes cutting porphyritic dyke in dyke swarm.	Isthmus.
05	27	R	Dyke swarm sample.	Perseverance Bluff.
06	29A	R	Dyke from dyke swarm.	Hasselborough Bay.
07	29B	R	"	"
08	29C	R	"	"
09	29D	R	"	"
60610	30	R	Baked sediment in pillow lavas.	ANARE main base.
11	34	R	Glassy selvedge of pillow.	N tip of North Head.
12	34B	R	5cm from rim of pillow.	"
13	34D	R	Core of pillow (15cm from rim).	"
14	35	R	Pillow lava core.	200m S of top of North Head.
15	36	R	Block breccia with red lithic wacke matrix.	S tip Eagle Point.
16	41A	R	Dyke in harzburgite.	Head of bay, S of Eagle Pt.
17	42	R	Pillow lava, chlorite filled vesicles.	1 km ENE Douglas Pt.
18	43C	R	Sheared pillow lava in fault zone.	0.5 km "
19	44	R	Dyke in pillow lavas.	Douglas Pt.
60620	45E	R	Pillow lava rim.	"
21	45C	R	Pillow lava core.	"
22	46A		Coarse red-brown lithic wacke.	50m S of top of Douglas Pt
23	46B		Red-brown mudstone.	"
24	50A		Pillow lava	Unity Pt.
25	50B	R	Red-brown mudstone	"
26	52	R	?Harzburgite	Locality unknown
27	53	R	Dyke in pillow lavas	Bauer Bay
28	53Z	R	Zeolite veins in pillow lavas.	"
29	54	R	Mudstone from lens grading to 60630.	S coast, Bauer Bay

Dept No.	Field No.	Forms	Description	General Location
60630	54B	R	Coarse lithic wacke.	S coast, Bauer Bay.
31	55	R	Baked fine interpillow sediment.	½ way to Mawson Pt, Bauer Bay.
32	55pill	R	Pillow lava.	"
33	56pill	R	Pillow lava underlying massive flow.	Tip of Mawson Pt.
34	56B	R	Massive basalt flow + 75cm from lower edge.	"
35	56C	R	" + 150 cm from lower edge.	"
36	56E	R	" + 300 cm from lower edge.	"
37	56F	R	" + 375 cm from lower edge.	"
38	56H	R	" + 525 cm from lower edge.	"
39	56I	R	" + 600 cm from lower edge.	"
60640	56J	R	" + 675 cm from lower edge.	"
41	56K	R	" + 750 cm = top edge	"
42	60	R	Massive flow within 'ropy' top.	1 km S of Mawson Pt.
43	61Z	R	Zeolite veins in pillow lavas.	1.1 km S of Mawson Pt.
44	63	R	Uralitised? dyke.	1.2 km S of Mawson Pt.
45	64	R	Baked sediment from pillow rim.	1.3 km S of Mawson Pt.
46	64Dy	R	Dyke intruding pillow lavas.	"
47	64pill	R	Pillow lava rim.	"
48	68	R	Baked globigerina ooze.	Comorant Creek.
49	72Z	R	Qtz/calcite/sulphide veins, D.S.	First Gully.
60650	80A	R	Contact between coarse & fine dykes in dyke swarm.	Gadgets Gully.
51	80B	R	Fine plag-phyric dyke, D.S.	"
52	81Z	R	Qtz/calcite/sulphide veins, D.S.	"
53	83	R	Gabbro screen in D.S.	"
54	94	R	Medium grained anorthosite, D.S.	Wireless Hill.
55	97	R	Plag-phyric dyke in gabbro.	1 km E Handspike Pt. on coast.
56	103	R	Dyke intruding gabbro.	Handspike Pt.
57	109	R	Pillow lava.	Caroline Cove.
58	110	R	"	Sodomy Ridge, above Caroline Cove.
59	111Z	R	Zeolite veins and vugs in pillow lava.	"
60660	112	R	Vesicular pillow lava.	Peak, N of Mt. Haswell.
61	115	R	Pillow lava.	Gully, SE of Mt. Haswell.
62	117	R	Pillow lava with zeolites along fractures.	1 km S of Mt. Ainsworth.
63	119	R	"	Peak, Mt. Ainsworth.
64	120	R	"	100m N, Mt. Ainsworth.
65	120Z	R	Zeolite veins in pillow lavas.	"
66	122	R	Aphyric pillow lava.	200m E, Mt. Ainsworth.
67	124	R	Weathered dyke in pillow lavas.	200m N, Mt. Ainsworth.
68	125	R	Mineralised pillow lava (sulphides).	Caroline Cove, at hut.
69	126	R	Pyrite-rich altered basalt.	Caroline Cove, 20 m up creek.
60670	127	R	"	"
71	128	R	Massive pillow lava.	W end, Caroline Cove beach
72	129	R	"	E end, "

Dept. No.	Field No.	Forms	Description	General Location
60673	129Z	R	Zeolites in pillow lavas (60672).	E end, Caroline Cove beach.
74	131A	R	Pillow lava.	Middle of beach, "
75	131Z	R	Prehnite veins in pillow lavas.	"
76	132	R	Palg-phyric pillow lava.	W flank, Petel Peak.
77	133	R	Dyke intruding pillow lavas.	"
78	134	R	Prehnite veins from sheared pillow lavas.	Beach, Caroline Cove.
79	135A	R	Samples from sulphid/quartz/ calcite reef.	S end of quarry, Caroline Cove.
60680	135B	R	"	"
81	135C	R	"	N end of quarry, "
82	135D	R	"	"
83	138	R	Brecciated pillow lava.	300m up creek from Caroline Cove beach.
84	138B	R	Adjacent less disrupted lavas.	"
85	139D	R	Dyke intruding pillow lava.	Hurd Point.
86	139E	R	Pillow lava edge.	"
87	140Z	R	Zeolite veins in pillow lavas.	Coast, 100m N of Hurd Pt.
88	141	R	Pillow lava.	Coast, 1 km N of Hurd Pt.
89	141B	R	Dyke intruding pillow lavas.	"
60690	144	R	Dyke from dyke swarm.	Coast, due E of Mt. Jeffries.
91	145C,E	R	Core and edge pillow lava samples.	Coast, ENE of Mt. Jeffries.
92	146P	R	Pillow lava.	Coast, creek mouth N of Mt. Jeffries.
93	146Dy	R	Dyke cutting pillow lavas.	"
94	147	R	Small aphyric pillow lava (50 cm).	1.2 km S of Lusitania Bay.
95	148	R	Dyke samples from dyke swarm.	N end of beach, Lusitania Bay.
96	149	R	"	1 km N, Lusitania Bay.
97	151	R	Pillow lava.	2 km N, Lusitania Bay.
98	153	R	Dyke sample from dyke swarm.	3 km N, Lusitania Bay.
99	153B	R	Gabbro screen in dyke swarm.	"
60700	155P	R	Pillow lava.	1 km W, Pyramid Peak.
01	155H	R	Hyaloclastite breccia.	"
02	155Z	R	Zeolite veins through pillow lavas.	"
03	156Z,S	R	Loose ooze and zeolite specimens.	Pyramid Peak (W flank).
04	156H	R	Hyaloclastite breccia.	"
05	156P, C,E	R	Core and edge samples of pillow lava.	"
06	157H	R	Hyaloclastite breccia.	E flank, Pyramid Peak.
07	157Z	R	Zeolite specimens in pillow lavas.	"
08	159S	R	Fine to medium grained lithic wackes.	W tip of Southwest Pt.
09	159P	R	Core and edge samples of pillow lava.	"
60710	161	R	Aphyric pillow lava.	S side, Southwest Pt.
11	162	R	Dyke cutting pillow lavas.	+100m S side, S.W. Pt.
12	163	R	Porphyritic pillow lavas.	E tip, S.W. Pt.

Dept. No.	Field No.	Forms	Description	General Location
60713	164	R	Range of mineralised lavas	Field hut, Caroline Cove -
14	165	R	and hyaloclastites.	see map for relative
15	166	R	Dominantly pyrite with minor	localities.
16	167	R	sphalerite, chalcopyrite and	"
17	168	R	rarely galena. X denotes	"
18	169	R	sample of unaltered	"
19	170	R		"
60720	171A	R	"	"
21	171B	R	"	"
22	171C	R	"	"
23	172	R	"	"
24	173	R	"	"
25	174	R	"	"
26	174X	R	"	"
27	175	R	"	"
28	175X	R	"	"
29	176	R	"	"
60730	176X	R	"	"
31	177	R	"	"
32	177X	R	"	"
33	178	R	"	"
34	178X	R	"	"
35	179	R	"	"
36	180	R	"	"
37	180X	R	"	"
38	181	R	"	"
39	181X	R	"	"
60740	182	R	"	"
41	183	R	"	"
42	184	R	"	"
43	185	R	"	"
44	186	R	"	"
45	188	R	"	"
46	189	R	"	"
47	190	R	"	"
48	191	R	"	"
49	191X	R	"	"
60750	192	R	"	"
51	192	R	"	"
52	192X	R	"	"
53	193	R	"	"
54	193X	R	"	"
55	194	R	"	"
56	195	R	"	"
57	196	R	"	"
58	197	R	"	"
59	198	R	"	"
60760	199	R	Pillow lava.	Point NW of Caroline Cove.
61	199Z	R	Prehnite veins in pillow lava.	"
62	200	R	Pillow lava.	S end, Cape Star Bay.
63	201Dy	R	Dyke intruding pillow lava.	200m from S end, Cape Star Bay.
64	202	R	Porphyritic pillow lava.	300m "

Dept. No.	Field No.	Forms	Description	General Location
60765	203	R	Porphyritic pillow lava.	N end, Cape Star Bay.
66	204	R	"	½ way along S side of Cape Star Bay.
67	205	R	Dyke cutting pillow lavas.	3/4 way along S side of Cape Star Bay.
68	207	R	Aphyric pillow lava.	½ way along N sode of Cape Star Bay.
69	208	R	Aphyric dyke intruding pillow lava.	N base of Cape Star Pt.
60770	209	R	Pillow lava.	Coast due W of Waterfall Lake.
71	212	R	"	200 m N "
72	212Dy	R	Dyke intruding pillow lavas.	"
73	215	R	Baked globigerina ooze between pillow lavas.	Coast due W of Mt. Aurora.
74	216	R	Slightly sheared pillow lavas.	+200 M N of Mt. Aurora.
75	217	R	Pillow lava.	Small point N of Precarious Pt.
76	217A	R	Pillow lava with pyrite/qtz/ calcite vein.	"
77	218	R	Plag-phyric pillow lava.	+200 m N along coast
78	219	R	Pillow lava.	+300 m N along coast
79	220	R	Porphyritic dyke cutting pillow lavas.	Creek mouth, SW of Mt. Hamilton.
60780	220P	R	Aphyric pillow lava.	"
81	221	R	Lava block from coarse agglomerate.	Coast due W of Mt. Hamilton.
82	223	R	Globigerina ooze.	500 m S, Pyramid Peak.
83	226	R	Strongly sheared, laumontised basalt.	500 m S, Flat Creek.
84	226B	R	Fresh pillow lava away from fault.	"
85	227	R	Pillow lava.	700 m S of Flat Creek.
86	228	R	Pillow lava, strongly veined.	1 km S of Flat Creek.
87	228B	R	Sheared, highly altered plag-phyric lava.	"
88	230	R	Altered hyaloclastite breccia.	1.5 km S of Flat Creek.
89	230S	R	Baked grey siltstone between lavas.	"
60790	231	R	Dyke intruding agglomerate.	1.5 km N of Aurora Pt.
91	232	R	Pillow lava.	1.2 km N of Aurora Pt.
92	233P	R	"	0.5 km N of Aurora Pt.
93	233Dy	R	Dyke intruding pillow lavas.	"
94	234	R	Pillow lava.	Aurora Pt.
95	235A	R	Greyish chilled edges on Mg-rich pillow lava.	300 m N of Mt. Gwynn.
96	235B	R	Olivine-cpx-phyric Mg-rich pillows.	"
97	235C	R	Weathered-out ol±cpx±plag nodules.	"
98	236	R	Plagioclase-phyric pillow lava.	250 m N of Mt. Gwynn.
99	239B	R	Fresh hyaloclastite breccia.	Location unknown.

Dept No.	Field No.	Forms	Description	General Location
60800	242	R	Dyke swarm sample including sulphide veins.	Isthmus, W side.
01	243	R	Silicified volcanic breccia.	200 m S of Gadgets Gully.
02	245	R	Samples of pillow lavas.	Low plateau on SW section of Bishop Island.
03	245B	R	"	"
04	401	R	Fine grained massive gabbro screen in dyke swarm.	S side Tussock Pt.
05	402	R	Contact between aphyric and plag-phyric dyke swarm sample.	"
06	403	R	Thin gypsum+minor sulphide veins.	Nuggets Beach.
07	404	R	Aphyric dyke.	"
08	405	R	Massive gypsum vein.	"
09	406	R	Plag-phyric dyke with gypsum on fracture surfaces.	"
60810	407	R	Aphyric dyke.	"
11	408	R	Brecciated dykes with gypsum matrix.	"
12	409	R	Fine grained dyke or rhodingite.	Point in Half Moon Bay.
13	410	R	Troctolite (host to 60812).	"
14	411	R	Altered dyke.	N side of Eagle Pt.
15	412	R	Aphyric dyke in gabbros.	Eagle Point.
16	414	R	Pillow lava.	S side Aurora Point.
17	415	R	Dyke intruding lavas.	"
18	416	R	Dyke intruding lavas.	Near creek, middle of Souchek Bay.
19	417	R	"	N side of point S of Souchek Bay.
60820	418	R	Pillow lava.	"
21	419	R	Pillow lava.	Middle of bay S of Souchek Bay.
22	420	R	Aphyric pillow lavas.	Point S of Souchek Bay.
23	421	R	Vesicular pillow lava.	1.5 km S of Mt. Waite.
24	421Z	R	Zeolite specimens from pillow lavas.	"
25	422	R	Hyaloclastite breccia.	E shore of Flynn Lake.
26	423	R	Pillow lava.	Plateau edge W of Flynn L.
27	424	R	"	Coast, mouth of Flynn Creek.
28	425	R	"	N tip of Double Point.
29	426	R	Dyke intruding pillow lavas.	"
60830	427	R	Dyke from dyke swarm.	Davis Point.
31	427B	R	"	"
32	428	R	Pillow lava.	N side of Sandell Bay.
33	428B	R	Pillow lava.	"
34	429	R	Pillow lava.	Coast, middle of Sandell Bay.
35	440	R	Laumontite+ calcite in pillow lava vug.	1/3 way along S coast from Hurd Point.
36	450	R	Red-brown mudstone.	Plateau edge, S side of Jessie Niccoll Creek.
37	452	R	?Malachite staining on gabbro.	On Island track, just S of Red River.
38	454	R	?Malachite staining in pillow lava.	Island track on Windy Ridge, SE Mt. Fletcher.
39	455	R	Pyrite in qtz/calcite reef.	Buckles Bay coast, S end of Isthmus.

THE PETROLOGY OF THE MACQUARIE ISLAND OPHIOLITE ASSOCIATION: MID-TERTIARY OCEANIC CRUST OF THE SOUTHERN OCEAN

B.J. Griffin and R. Varne
Geology Department, The University of Tasmania,
Box 252C, G.P.O. Hobart, Tasmania, Australia, 7001.

The Macquarie Ridge is a narrow arcuate system of submarine ridges that runs south from New Zealand to join the Indian-Pacific ridge system, and marks the boundary between the Indian-Australian and the Pacific plates.

The crest of the Macquarie Ridge is at water depths of less than 200 m in several places, and near 54°S 159°E has emerged to form Macquarie Island. Linear east-west trending marine magnetic anomalies south of Australia have been traced across the ridge to the Macquarie Trough east of Macquarie Island, and geophysically the island represents oceanic crust produced during Tertiary seafloor spreading at the Indian-Pacific ridge system, later uplifted during marginal interactions between the Indian-Australian plate moving north and the Pacific plate moving west.

Most of Macquarie Island is composed of volcanic rocks that are commonly basaltic pillow lavas accompanied by volcanic breccias and more massive lavas, associated with calcareous oozes and lithic wackes. Dolerite dyke swarms, gabbroic masses including a layered complex, and serpentinized peridotites occur mainly in the northern part of the island. The island is made up of fault-bounded blocks with generally northerly tilts, and provides several sections through oceanic crust.

Lavas and dykes are usually porphyritic. Plagioclase (An_{87-70}) is the dominant phenocryst phase, with less abundant olivine (Fo_{89-85}), clinopyroxene ($Ca_{43}Mg_{50}Fe_5$ - $Ca_{38}Mg_{50}Fe_{12}$), and chrome spinel. Little-altered groundmasses of both lavas and dykes exhibit continuous variation from assemblages of subcalcic augite, plagioclase, opaques and glass in subophitic textures to more alkaline assemblages of olivine, titanaugite, kaersutitic amphibole and minor glass in intersertal textures. Gabbros are composed essentially of olivine,

plagioclase and clinopyroxene, similar in composition to some of the phenocrysts of lavas and dykes. Opaques are scarce and orthopyroxene occurs only rarely as thin rims on olivine or remnant cores within clinopyroxene. Peridotites are mainly harzburgite and wehrlite.

Most of the Macquarie Island basalts and dolerites have major and trace element compositions very like those from 45°N and the FAMOUS area on the mid-Atlantic ridge. Altered rocks have high ignition losses, low Fe^{+2} : ΣFe and aberrant Na_2O and K_2O contents. Little-altered rocks vary in normative composition from ol- and hy-bearing to mildly ne-bearing: this normative range from tholeiitic to alkaline character corresponds roughly with their groundmass mineralogy characteristics. Their TiO_2 (1.31±0.28 wt.%) and Al_2O_3 (17.97±2.00 wt.%) contents distinguish the whole group of Macquarie Island lavas and dykes from ocean island and island arc tholeiite series. Preliminary results indicate high La/Sm (1.69±0.24) and La/Yb (4.4±0.9) ratios. The "ocean floor basalt" character of the Macquarie Island rocks extends to the more alkaline compositions: these ne-normative basalts are generally less enriched in LIL elements than ocean island tholeiites and display, for example, low Zr (<150ppm) and Y (<40ppm) but high Nb (20-60ppm) contents.

Four secondary mineral assemblages have been distinguished in the lavas and dykes. Preliminary oxygen and carbon isotope studies show that sea water was the source of much of the fluid involved in the alteration, but the fluid composition appears to have been modified substantially by interaction with the rocks. The lowest grade assemblage is a smectite-carbonate alteration in which olivine and glass are the major phases affected. Lavas that have suffered this ocean floor weathering have been shown to retain the magnetic properties of typical oceanic crust, and were probably at the top of the pile, in the uppermost 200 m. Underlying this is a complex zone of alteration defined by the development of Na and Ca zeolites, particularly natrolite, thomsonite, analcite, wairakite and at the bottom of the zone, laumontite.

The degree of alteration is variable: fresh glass has been found within a few paces of intensively zeolitized lavas. Underlying these zeolite facies assemblages are albite, chlorite, epidote, sphene assemblages that define the lower greenschist facies, attained at the base of the lava pile where about half of the outcrops are composed of basaltic dykes. In contrast, the dykes of the dolerite dyke swarms (sheeted intrusive complex) have suffered a distinctive actinolitic hornblende replacement of primary mafic minerals that has left the plagioclase little-altered. This 'uralitization' is the highest grade of alteration encountered in the fine-grained igneous rocks, and also occurs in the gabbros.

An incomplete section in the south of the island, through zeolite facies volcanics into lower greenschist facies volcanics, is about 1400 m in thickness. Taken together with the ocean floor weathering zone, the Macquarie Island volcanic pile seems to be at least 1600 m, and possibly as much as 2100 m, thick. The dolerite dyke swarms are at least 350 m thick (the elevation above sea level of the island) and if the dykes were vertical when emplaced, they may represent an oceanic crust layer about 1000 m thick derived from oceanic crust underlying the volcanic pile.

Originally deeper levels of the oceanic crust are now exposed in the northern part of the island, where a coastal section has harzburgite at its base, overlain by gabbros that include the layered gabbro complex and form a layer about 2000 m in thickness. Comparison of the phenocrysts of the basalts and dolerites with the mineral compositions of the layered gabbros and wehrlites shows that the basaltic magma compositions may have been derived by low-pressure fractionation and reaction within a zoned crystal-liquid pile that reached the surface and acted as a fractionation column. We also show that the Macquarie Island oceanic crust section puts the "petrological Moho" at a depth of 4000-5000 m, if it is taken to be the transition from harzburgite to gabbro. Last, we note that experimental studies of several ocean floor basalt and

glass compositions show them to be in equilibrium with orthopyroxene only at pressures of at least 8 kb, making the occurrence of harzburgite at shallow depths a difficult feature to explain, and speculate about why this may be so.

Reprinted from
The Geographical Journal,
Vol. 144, Part 2, July 1978

THE OUTLYING ISLANDS OF MACQUARIE ISLAND

D. J. LUGG, G. W. JOHNSTONE AND B. J. GRIFFIN

Close to Macquarie Island (54°30'S, 159°E) there are two groups of outlying islands, the Judge and Clerk group 14 km to the north and the Bishop and Clerk group 33 km to the south. This paper reports on a short visit to the Bishop and Clerk Islands and aerial surveys of the Judge and Clerk Islands and of Anchor Rock (an offshore stack). The field work was carried out in February 1976. The geography and historical records of these islands are summarized, and new information on their geology and biology is presented.

SUB-ANTARCTIC Macquarie Island (54°30'S, 159°E) lies in the South Pacific Ocean 1280 km south-east of Hobart, Tasmania, and 1440 km north of the Antarctic continent (Fig. 1). The island was discovered by Captain F. Hasselburgh during a sealing expedition in 1810. It is about 37 km long by 4·8 km wide and consists mainly of a hilly plateau at about 300 m altitude; the highest point is 433 m. The shores of Macquarie Island are fringed by rock stacks, the most substantial being the 25 m high Anchor Rock 0·4 km offshore, west of the north tip of the island. A submarine ridge, the Macquarie Ridge, extends north and south from the island (Davis, 1919). On this ridge lie two groups of islands (Fig. 2). The Judge and Clerk Islands (Fig. 3) are 14 km north of Macquarie Island, and the Bishop and Clerk Islands (Fig. 4) lie some 33 km off the south coast. Submerged reefs, shoals and banks have been reported near both groups (Antarctic Pilot, 1974) and this together with poor weather has limited observations. Another island was reported some 380 km south-east of Macquarie Island in 1821 but despite its being on charts for 60 years, 'Emerald Island' does not exist (Cumpston, 1968). Judge and Clerk Islands comprise a chain of rocks and reefs, mostly along a north-south line but with the northernmost reef offset to the east. The largest is Judge (19 m high), and the two next largest we called South Rock and North Rock, respectively, for identification purposes only. Bishop and Clerk Islands consist of Bishop Island (highest point *c.* 43 m) surrounded by about twenty smaller islands, stacks and reefs.

In early February 1976, the ANARE relief ship MV *Thala Dan*, with two helicopters on board, spent five days at Macquarie Island. On 6 February, a close inspection of Anchor Rock was made by helicopter, no landing being possible. On the following day, *Thala Dan*, with one helicopter, went south to the Bishop and Clerk Islands. The helicopter, with two of us (DJL and GWJ) aboard, made high and low level circuit flights over the group for oblique photography, and landed on the southern end of Bishop Island. Unfortunately, sea conditions were deteriorating and the visit had to be cut short, with the result that only the period 1340–1415 was spent on the Island. A small collection of rocks was made. On 8 February, a survey was made of the Judge and Clerk Islands with two helicopters from the Macquarie Island station.

This paper presents a review of information on the outlying islands of Macquarie based on these and earlier visits.

Dr D. J. Lugg was Leader of the ANARE Expedition and is Senior Medical Officer with the Antarctic Division, Department of Science; Dr G. W. Johnstone is a Biologist with the Antarctic Division; and B. J. Griffin is a PhD student, Geology Department, University of Tasmania.

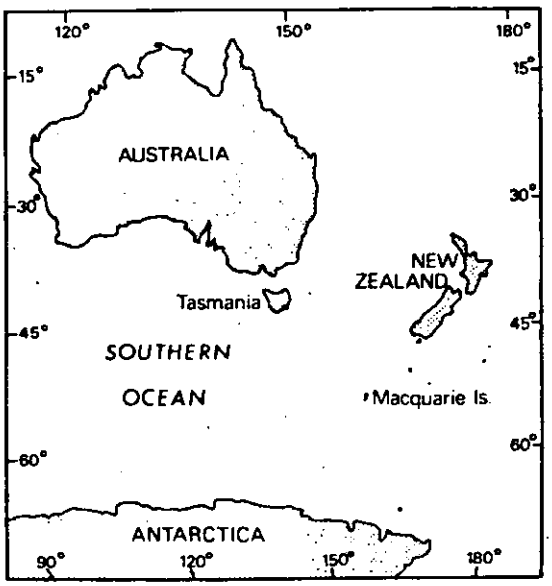

Fig. 1. General location map

General history of Macquarie Island

Mawson (1943), Law and Burstall (1956) and Cumpston (1968) have recorded much of Macquarie Island's history. The island was an important sealing centre in the nineteenth and early twentieth centuries. On 17 May 1933, Macquarie Island was declared a wildlife sanctuary by the Tasmanian Government which is responsible for the administration of the island (Tasmanian Government Gazette, 1923), as politically it is part of the State of Tasmania.

Several Antarctic Expeditions of the 'heroic era' visited Macquarie Island. Bellingshausen (1831), Wilkes (1845) and Scott (1905) spent from a few hours to several days on the island, while members of Shackleton's expedition made collections from the *Nimrod* (Shackleton, 1909).

Scientific study of Macquarie Island has not been neglected and four major phases have occurred. Among visitors to Macquarie Island in the 100 years since its discovery were a number of natural historians who published their observations (Cumpston, 1968). Five members of Mawson's Australasian Antarctic Expedition (AAE) spent from December 1911 until December 1913 on the Island and at the conclusion of this expedition the Commonwealth of Australia established a meteorological station for two years. Mawson's British Australian New Zealand Antarctic Expedition (BANZARE) of 1929–31 visited briefly. Since March 1948 members of the Australian National Antarctic Research Expeditions (ANARE) have maintained a permanently manned station (54°28′S, 158°57′E) on a narrow isthmus at the northern end of the island.

History of the outlying islands

One of the earliest records concerning the outlying islands of Macquarie Island is contained in an account of Macquarie Island by Captain D. F. Smith in the Sydney Gazette, January 1811:

> About 25 miles NNE of the north point of the Island (Macquarie) lies a small isle called the Judge, and a reef called the Judge's Clerk; about 30 miles SSE of the south point of the

Island is an islet and a reef which Captain Smith gave the name of the Bishop and his Clerk. Captain Smith saw several pieces of wreck of a large vessel on this Island, apparently very old and high up in the grass, probably the remains of the ship of the unfortunate de la Perouse. (Cumpston, 1968 p. 15).

In November 1820, Captain Thaddeus Bellingshausen visited Macquarie Island and in describing his arrival from the north comments on 'the Judge' thus:

At 5.0 a.m. I set my course for the northern end of the Island. At 9 o'clock, on approaching closer, we observed rocks, washed by heavy breakers, ahead of us. I recognised them as the rocks which appear on the Arrowsmith chart under the name of 'The Judge'. At 1.0 p.m. passing along the northern side of these rocks ar a distance of about half a mile, we rounded the north-eastern extremity of Macquarie Island . . . .

Cumpston (1968) reports that the Arrowsmith chart of Macquarie Island has not been located despite searches in a number of archives.

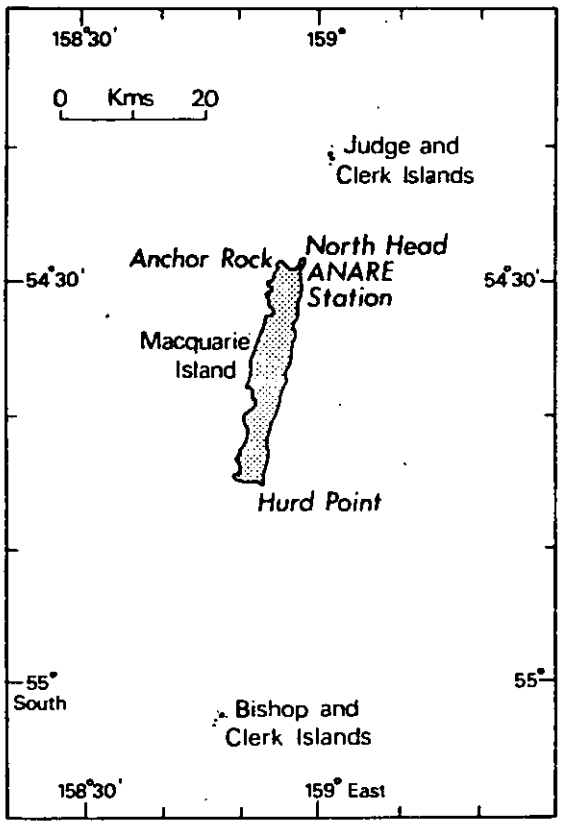

Fig. 2. Macquarie Island and the outlying islands

A further report of the northern islets was made by Captain Daniel Taylor after his ship, the *Caroline*, visited Macquarie Island in 1824:

Caution to Mariners, NW by N (by compass) six leagues from the Northernmost breakers and the Judge's Clerk, lays a very dangerous reef of rocks under the water. The sea broke very heavy on two different parts. I passed close to it with the ship. (Cumpston, 1968 p. 63).

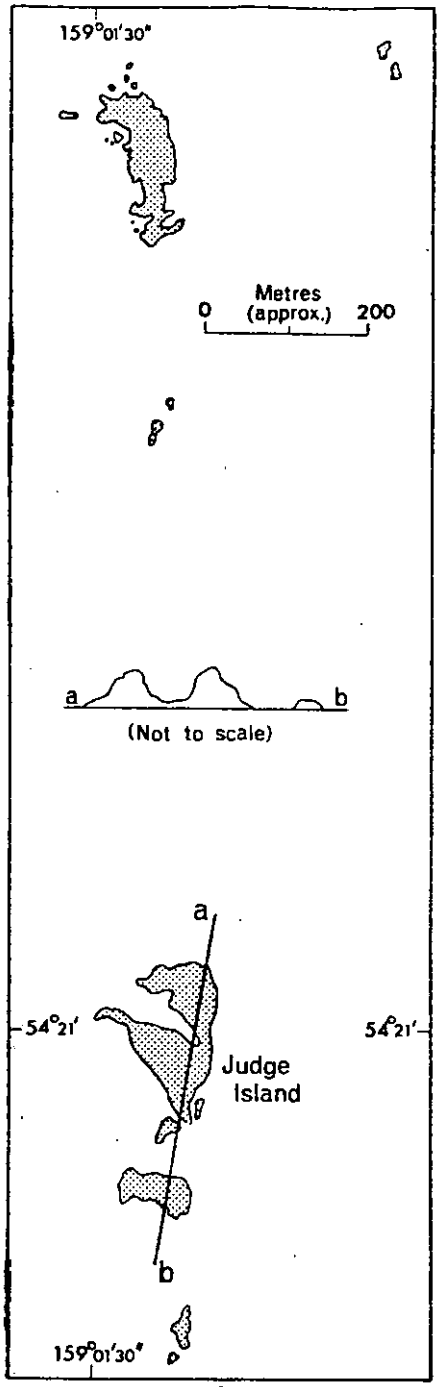

Fig. 3. Sketch map and cross-profile of the Judge and Clerk Islands. (Positions are approximate.)

As late as 1881 there was much confused thought concerning the islets. Professor John Scott read a paper to the Otago Institute in which he stated:

> It (Macquarie) is a solitary island, but it has two outlying rocks. One called the 'Bishop and Clerk' lies 30 miles to the south of the south end; the other called the 'Judge and Clerk' is 7 miles to the north of North Head. (Transactions of the New Zealand Institute, 1882).

Information on these island groups was very limited (Davis, 1919; Falla, 1937; Mawson 1943; Grenfell Price, 1963) up to 1965, when a helicopter from the USS *Glacier* landed for a few minutes on an outlying rock platform (island 'X' in Fig. 4) of the Bishop and Clerk Islands. Six species of birds and one species of seal were reported from that visit (Mackenzie, 1968). Prior to this trip the island groups were considered to be 'mere strings of barren rocks' (Taylor, 1955). Apart from the 1965 landing, no records of other landings are known.

Charts of Macquarie Island and the outlying islands

The earliest extant map of Macquarie Island, drawn by British sealers, was published by Bellingshausen in 1824. The Bishop and Clerk appears on this map. Lieutenant W. Langdon, RN, made a sketch and a plan of Macquarie Island in 1822 and these are in the records of the Hydrographic Department of the Admiralty in London (Cumpston, 1968). Mawson reproduces an Admiralty chart of 1887 in his AAE Report (Mawson, 1943). Captain Neil McDonald of the ketch *Gratitude* made a chart of Macquarie Island in 1899 and this became the official chart of Macquarie Island in 1905. Blake's survey during the AAE resulted in a new chart in 1914 that was published by the Admiralty Hydrographic Department in 1917. A chart which came into the possession of the authorities in Tasmania in

1901 was said to be 'from a survey made by H. Gunderson' but, as Cumpston (1968) reports, it was later found to be traced from a sketch lent to Gunderson by the oil traders Hatch and Fisher. This shows the outlying islets. Mawson (1943) drew a location (Table I) and distribution sketch while aspects of the islands

TABLE I

Reported positions of outlying island groups

Islands	*Reported Lat.*	*and Long.*	*Ship/Expedition*	*Reference*
Bishop and Clerk	—	158°44½'E	Blake from Macquarie Is. AAE 1914	Mawson AAE Report (1943)
	55°03'S	158°46'E	*Discovery*, BANZARE, 1930	Mawson, AAE Report (1943)
	55°04'55"S	158°41'50"E	ANARE, 1958	Admiralty Chart (1958)
	55°05'50"S	158°43'25"E	*Glacier*, 1968	MacKenzie (1968)
	55°04'50"S	158°42'20"E	*Thala Dan* ANARE 1976	This Report
Judge and Clerk	54°21'S	159°01'E	AAE 1911–14, BANZARE 1929–31	Mawson AAE Report (1943)

have been sketched by Davis (Mawson, 1943). The AAE and BANZARE took a large number of soundings from North Head to the Judge and Clerk Islands. As Mawson (1943) states:

> An accurate and complete survey of the Bishop and Clerk group of islets has not yet been achieved. They were too far distant from Macquarie Island for Blake to see any but the highest rocks. On no occasion did the *Aurora* find time to examine and map the group in detail.

The visit by the *Discovery* in 1930 provided more information and a sketch map (Mawson, 1943). The description in Mawson's log (Grenfell Price, 1963) is as follows:

> Friday, 5th December 1930 Bishop and Clerk Islands After clearing Hurd Point course was set to close a reported rock marked (E.D.) about three miles to the south. A good look-out was kept . . . . . However, two miles to the west of the reported position soundings gave a depth of forty fathoms . . . . . C° was then altered for Bishop and Clerk Rocks. Soundings taken frequently were between 40–50 fms. and very regular, proving that a high ridge extends south from Macquarie I. to the Bishop . . . . . the islands appeared in the mist. Although the ship approached to within two or three cables only an occasional glimpse of the island could be seen. The main island appears to be very steep on all sides with a very prominent western summit. A large conspicuous white patch on the eastern side is a Royal and Gentoo penguin rookery. Two or three small islets only were seen; they were about twenty feet high and appeared to run in a N.E. and S.W. direction. There was no indication of the long line of rocks extending to the north as charted (Admiralty Chart). Sights obtained at this position were not accurate but it was estimated that the Bishop and Clerk Rocks lie approximately two miles to the south and one mile to the east of the charted position.

Blake's chart formed the basis of the present day Admiralty Chart No. 1022 and the Australian Division of National Mapping produced a new map of Macquarie Island in 1971. This map resulted from oblique air photography and terrestrial photography by ANARE 1947–1969 with horizontal and vertical control of ANARE surveys 1950, 1958, 1969 and supplementary information from AAE.

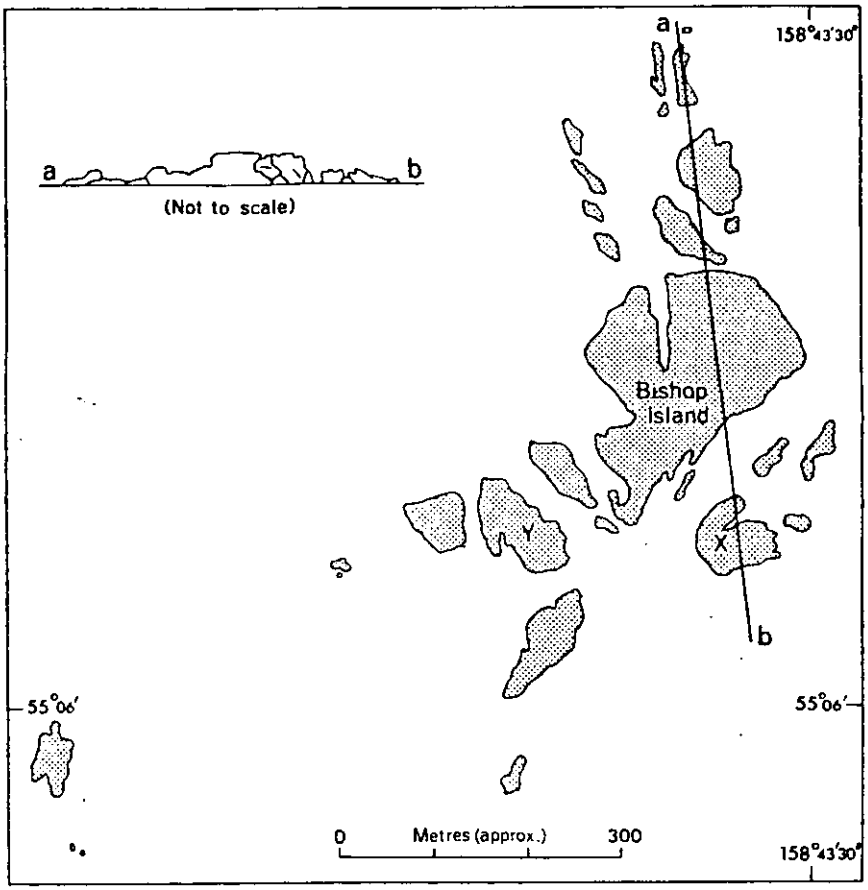

Fig. 4. Sketch map and cross-profile of the Bishop and Clerk Islands. (Positions are approximate.)

In late 1975, a surveyor from the Division of National Mapping made a JMR Doppler satellite position fix and did further tellurometer surveys. During the visit in 1976 further vertical aerial photography was carried out. Table 1 shows the variation in stated position of the Bishop and Clerk. Until a further landing is made and an accurate position found by means of a satellite position fix there will be dispute as to the precise position of the group.

Geology of the outlying island groups

Previous studies.—H. F. Ferrar was the first geologist to visit Macquarie Island. As a member of the British National Antarctic Expedition of 1901, he landed at Lusitania Bay for several hours. L. R. Blake, of the AAE, studied the geology while carrying out a cartographic survey of Macquarie Island. Unfortunately, he was killed on the last day of hostilities of the First World War after serving for several years, and it was left to Mawson (1943) to write up the geology from Blake's work. Mawson recognised three groups of rocks; an older basic group of lavas, in places

intensely folded, intruded by the ultramafic and mafic plutonic rocks of the gabbroid group, with both groups overlain unconformably by a younger basic group of pillow lavas and agglomerates. J. F. Ivanac, of the Bureau of Mineral Resources, Geology and Geophysics, agreed with these observations after spending a few days on Macquarie Island (Ivanac, 1948). From information gathered on the 1968 relief trip to Macquarie Island, Varne *et al.* (1969) suggested that the rocks are oceanic crustal material and that Macquarie Island represents uplifted oceanic crust originally generated at a spreading plate boundary in a mid-oceanic ridge environment. Further evidence supporting this hypothesis has since been presented (Varne and Rubenach, 1972). In these various studies, however, no reference is made to the outlying island groups, and prior to 1976 they represented geologically unknown areas.

Observations—1976.—Bishop Island is entirely composed of pillow lavas with interpillow sediments. The pillows are closely packed and are approximately one metre across. Seven samples were collected: six of these are porphyritic tholeiitic basalts, with coarse plagioclase phenocrysts, and the other sample is an aphyric tholeiitic basalt. All samples were extremely weathered with strong iron discoloration.

The Judge and Clerk Islands group is more variable geologically. The two larger islands are composed of stratified volcanic agglomerate striking approximately SSW, and dipping 25–30° to the ESE. Blocks in the agglomerate are angular and vary in size around an estimated mean of 20 cm. The proportion of blocks in the agglomerate is variable, up to 80 per cent, and this variation defines the stratification. The shelving ridges of Judge Island are bedding plane surfaces; the bounding cliffs are fault scarps. The northernmost island of the group displays, on its northern tip, an apparently conformable contact between agglomerate and pillow lavas. The agglomerate is cut by a series of vertical grey dykes, all striking SSW. The lava pillows are similar in size to those of the Bishop and Clerk Islands group.

The rocks described from the two island groups are very similar to the volcanics and associated rocks on Macquarie Island. Thus it appears that these island groups are geologically extensions of Macquarie Island, and presumably all are subaerial exposures of the Macquarie Ridge.

Biology of the outlying islands

Vegetation.—The ridge of Anchor Rock supports a relatively luxuriant growth of vegetation, including at least a grass and a cushion-forming plant. The latter is presumably *Colobanthus muscoides* which grows commonly on coastal rocks at Macquarie Island where it accounts for up to 10 per cent of the total plant cover (Taylor, 1955). On Anchor Rock it occurs down the north-eastern face to about 10 m below the ridge. The only vascular plant noted on Bishop Island was a cushion-forming one, again probably *C. muscoides*. Cushions of this plant cover much of the summit plateau of Bishop Island, and also occur on the western and northern tops. Two species of lichens were found on the rock specimens collected. They were identified as *Placopsis* aff. *bicolor* and *Caloplaca crozetica* both previously recorded from Macquarie Island. On the Judge group, the only plant life detected was a green coloration, probably algal, on Judge Island beside the white guano of the shag roosts.

Invertebrates.—The rocks collected from Bishop Island and their associated detritus yielded a few invertebrates. Some of these have been identified. All

material has been deposited in the South Australian Museum, Adelaide, except for the dipteran specimens which have been lodged in the Australian National Insect Collection, Canberra.

Annelida.—Some small worms which have not been identified.

Acarina.—Mites were the group best represented in the collection. They included the cryptostigmatid mite *Alaskozetes antarcticus* (Michael), widespread in the far south and present on Heard Island and Macquarie Island (Wallwork, 1963; Watson, 1967); *Parasitiphis jeanneli* (Andre), a littoral gamasine mite widespread in the far south but apparently not previously recorded from Macquarie Island; a prostigmatid mite, possible of the family Penthalodidae; and other unidentified cryptostigmatid, mesostigmatid and gamasine species.

Araneae.—Spider egg sacs and a spiderling, perhaps of the family Lycosidae (wolf spiders).

Collembola.—Several collembolans, most probably *Tullbergia mediantartica* Wise. This species has not previously been found outside the Antarctic continent.

Diptera.—Larvae and pupae of small flies, very probably one of the acalyptrate families.

Birds

Gentoo penguin *Pygoscelis papua*.—This species may have been present in the Bishop Group but was not positively identified. An observer aboard *Thala Dan* reported that many penguins left island 'X' when the helicopter approached and that some of these appeared to be gentoos (N. Brothers, pers. comm.). Mawson (quoted above from Grenfell Price, 1963) reported gentoos among the royal penguins on Bishop Island in 1930. Viewing conditions were very poor, however, and it is possible that shags were mistaken for gentoos; Falla (1937) stated that mist prevented the party from recognising the species with certainty. MacKenzie (1968) reported this species present in small numbers among several hundred royal penguins on island 'X' but implied that they were unlikely to be breeding because this rock would not be safe from high seas. The species is abundant and widespread on Macquarie Island.

Rockhopper penguin *Eudyptes chrysocome*.—Two small groups of breeding rockhopper penguins were noted on Bishop Island between the summit plateau and the albatross colony. There were about 20 half-grown chicks and may well have been more. The species is abundant and widespread on Macquarie Island, but has not been recorded previously from the Bishop group.

Royal penguin *Eudyptes chrysolophus schlegeli*.—There was a group roughly estimated to be in excess of 1000 birds on the upper part of the east side of Bishop Island, and another group, probably smaller, on island 'X'. Some fully grown chicks were noted among the adults on Bishop Island, though most would have gone to sea by this date (Warham, 1971). The presence of this species on Bishop Island was first recorded in 1930 by Mawson as quoted above from Grenfell Price (1963). MacKenzie (1968) recorded approximately 150 on Bishop Island and 700 on island 'X'. This race of the macaroni penguin is abundant and widespread on Macquarie Island where it is endemic.

Black-browed albatross *Diomedea melanophris*.—The southern high area of Bishop Island contains a thriving colony of black-browed albatrosses. There were 44 half-grown chicks present with black flight feathers prominent through the grey down. There were many more adults, and all checked had dark brown eyes confirming that they were the nominate race *D.m.melanophris* which breeds on Macquarie

Island, and not the pale-eyed *D.m.impavida* which is frequently seen between Tasmania and Macquarie Island and breeds on Campbell Island. MacKenzie (1968) recorded 14 chicks and at least 107 adults, counted from the air. It is now certain that, as MacKenzie suggested, the colony on Bishop Island is considerably larger and more productive than the two small colonies at the north and south ends of Macquarie Island, which together have about 30–40 pairs but seldom produce more than 10 chicks in all. However, MacKenzie's suggestion that Macquarie Island was colonized by black-browed albatrosses from Bishop Island sometime between 1911 (AAE) and 1948 when the species was first recorded breeding there by ANARE is based on the assumption that because AAE did not record the species, it was not then breeding. AAE records are notoriously deficient in ornithological information and the lack of mention of a species cannot be taken to imply its absence. The two colonies are in relatively remote and inaccessible places and would easily have been overlooked by other visitors to Macquarie Island.

Cape petrel *Daption capense*.—The status of the cape petrel at Macquarie Island has not been resolved since 1951 when 'a small number' were found 'apparently nesting' on Anchor Rock (Law and Burstall, 1956). The relevant Antarctic Division biology log records that there were either three or five cape petrels sitting on nests and another six or eight flying around on 21 October 1951, but the observer was unable to climb down to the nesting area on the north-east side of the Rock to check for eggs. This is the only record of the species ashore at Macquarie Island. Since then there have been frequent sightings of cape petrels over the sea surrounding Macquarie Island, particularly near the station and North Head and beside relief vessels at anchor east of the station. For example, on 25 November 1975, more than 20 cape petrels attended *Nella Dan* there. Several (three or four) cape petrels seen from *Nella Dan* on 21 November 1971 in the same area had underparts stained brown, suggesting that they had recently left nests (Johnstone, 1974).

The north-eastern and western faces of Anchor Rock cannot be seen from Macquarie Island, but of these only the north-eastern is sheltered from the prevailing westerly winds and seas. During the 1976 inspection by helicopter four cape petrels were occupying three sites on this face, two singly and one pair. The sites with single birds were protected by overhangs and were much whitened with guano and appeared to be suitable for nests. A fourth unoccupied site also had much guano. On the approach of the helicopter the birds flew off. No chicks could be seen; at this date at Heard Island (53°S, 73°30'E) chicks are left unattended, but they do not fledge until March (Downes *et al.*, 1959). Law and Burstall (1956) suggested there might be a colony of cape petrels in the Bishop group, but none were recorded there, nor were any seen in the area from *Thala Dan* during the 1976 visit. The relatively sheltered south-eastern cliffs are steep and creviced like Anchor Rock and may be suitable for this species, but close inspection was not possible. None were seen at the Judge group, and the extreme exposure of these stacks makes it unlikely that any bird could nest there successfully. The cape petrel cannot be regarded as a breeding species at Macquarie Island until it can be demonstrated that the handful of birds on Anchor Rock do actually breed.

King shag *Phalacrocorax albiventer purpurascens*.—This race of the king shag is endemic to Macquarie Island where about 600 pairs breed at 14 colonies, many on offshore rock stacks, all round the island (N. Brothers, pers. comm.). There is a breeding colony on the eastern side of Bishop Island below the royal penguins and separated from them by a deep cleft running across the rock face. About 100 nest sites were counted but most of the season's nests were broken down and an accurate

count would have been impossible even had time been available. No eggs or young chicks were seen but there were many young birds, some still with down but most fledged. There were also a few shags perched on top of the guano-capped island 'Y'. Other prominent crags of Bishop Island were whitened with guano, indicating their use as roosts by shags. Judge Island has two separate tops, both covered with guano; there were more than 100 shags on the southern top and more than 30 on the northern. Most flew off when the helicopters approached, and there was no sign of nests. A single shag was seen on the exposed south-western side of Anchor Rock.

Great skua *Stercorarius skua lonnbergi*.—Near where the helicopter landed on the south-eastern platform of Bishop Island, D. J. Lugg found a nest containing two broken eggs, either a skua's or a southern black-backed gull's. There were some penguin tail feathers beside it which suggest a skua was the more likely. A skua was seen higher up on Bishop Island. MacKenzie (1968) recorded two adults there. One skua was also seen on South Rock in the Judge group during our 1976 inspection.

Southern black-backed gull *Larus dominicanus*.—The only southern black-backed gull seen at any of the outlying islands was a large, but still downy, chick at the eastern end of the summit ridge of Anchor Rock. Earlier in the season, on 28 November 1975, G. W. Johnstone observed two gulls on Anchor Rock sitting on the two main tops of the ridge, as if incubating. Several other nests around Macquarie Island contained eggs at this time. Presumably at least one of these gulls was incubating and the chick was its progeny. MacKenzie (1968) recorded several adult gulls and four downy young among the black-brewed albatrosses on Bishop Island, but none were recorded during the 1976 visit.

Other Species.—Prions *Pachyptila* sp. were common at sea near the Bishop group. The Antarctic prion *P. desolata* is an abundant breeding species at Macquarie Island, where it nests in burrows dug in the peaty soil. (Although the fairy prion has been recorded at Macquarie Island it has not yet been recorded breeding there, *pace* MacKenzie (1968)). The vegetation on Bishop Island is probably too sparse and the terrain too rocky for burrows, but prions could nest in rock crevices as MacKenzie (1968) suggested. Blue petrels *Halobaena caerulea* nest on offshore stacks of Macquarie Island where they are safe from feral cats (N. Brothers, pers. comm.); they also may nest on Bishop Island. Anchor Rock could also support a few of either of these species.

New Zealand fur seals *Arctocephalus forsteri* were recorded at both groups of islands. There were ten on sloping rock near the eastern point of Bishop Island; MacKenzie (1968) recorded two on one of the southern reefs in February 1965. In the Judge group, there were seven fur seals on South Rock. This seal is common on Macquarie Island in summer when about 1000 are present, most non-breeding males which come here from their breeding colonies in New Zealand waters. Breeding has been recorded at Macquarie Island since 1955; the most pups seen were eleven in February 1977. All seals seen on the outlying islands were adult.

Acknowledgements

Messrs. N. Brothers, G. Copson and P. I. Ormay also participated in the surveys and have made their observations freely available to us. We are also grateful to the following for providing identifications and information about material collected: Dr D. H. Colless (Diptera), Messrs D. C. Lee and D. E. Rounsevell (Arachnida), Ms P. Greenslade (Collembola), and Mr R. Filson and Mrs J. Rownrow (lichens).

The assistance of Antarctic Division staff is greatly appreciated: Dr T. Tierney, Miss S. Stallman and Messrs G. McKinnon and B. Hill in the preparation of the sketch maps, and the Photographic Section for the plates.

References

The Antarctic Pilot, 4th edn. 1974. The Hydrographer of the Navy.

Bellingshausen, T. van. 1831. *Two Voyages of Exploration in the Antarctic Ocean and Circumnavigation of the World, 1819–21, in the Vostok and Mirnyi.* St. Petersburg.

Bellingshausen, T. van. 1945. *The Voyage of Captain Bellingshausen to the Antarctic Seas, 1819–21.* Ed. by Debenham, F. Hakluyt Society, p. 364.

Cumpston, J. S. 1968. Macquarie Island. *ANARE Sci. Rep.*, (A) 1. Pub. No. 93. Melbourne: Antarctic Division, Department of External Affairs.

Davis, J. K. 1919. *With the Aurora in the Antarctic 1811–14.* Melrose.

Downes, M. C., Ealey, E. H. M., Gwynn, A. M. and Young, P. S. 1959. The Birds of Heard Island. *ANARE Rep.* (B) 1. Melbourne: Antarctic Division, Department of External Affairs.

Falla, R. A. 1937. Birds. *B.A.N.Z. Antarctic Res. Exped. 1929–31. Rep. Ser.* B. Vol. 11. Adelaide: BANZAR Expedition Committee.

Grenfell Price, A. 1963. BANZARE 1929–31. Geographical Report based on the Mawson Papers. *Rep. Ser.* A. Vol. 1. Adelaide: Mawson Inst. Antarctic Res.

Ivanac, J. F. 1948. Geological Observations at Macquarie Island. *Australian Bureau of Mineral Resources. Rep.* No. 1948/39.

Johnstone, G. W. 1974. Field characters and behaviour at sea of Giant Petrels in relation to their oceanic distribution. *Emu* **74**, 4: 209–218.

Law, P. G., and Burstall, T. 1956. Macquarie Island. *ANARE Interim Rep.* No. 14. Melbourne: Antarctic Division, Department of External Affairs.

MacKenzie, D. 1968. The Birds and Seals of the Bishop and Clerk Islets, Macquarie Island. *Emu* **67**, 4: 241–245.

Mawson, D. 1943. Macquarie Island, its Geography and Geology. *Australasian Antarctic Exped. Sci. Rep.* Ser. A. Vol. V. Sydney: Government Printing Office.

Scott, J. H. 1882. *Transactions of the New Zealand Institute*, p. 484.

Scott, R. F. 1905. *The Voyage of the* Discovery, *1901–04.* Smith Elder.

Shackleton, E. 1909. *The Heart of the Antarctic.* 2 vols. Heinemann.

Tasmanian Government Gazette, 23 May 1933, p. 844.

Taylor, B. W. 1955. The flora, vegetation and soils of Macquarie Island. *ANARE Rep.*, (B) 2. Pub. No. 19. Melbourne: Antarctic Division, Dept. External Affairs.

Varne, R., Gee, R. D. and Quilty, P. G. J. 1969. Macquarie Island and the cause of oceanic linear magnetic anomalies. *Sci.* **166**: 230–233.

Varne, R., and Rubenach, M. J., 1972. Geology of Macquarie Island and its relationship to oceanic crust. *Antarctic Res. Ser.*, **19**: 251–266.

Wallwork, J. A. 1963. The Oribatei (Acari) of Macquarie Island. *Pacific Insects* **5**, 4: 721–769.

Warham, J. 1971. Aspects of breeding behaviour in the Royal Penguin *Eudyptes chrysolophus schlegeli. Notornis* **18**, 2: 91–115.

Watson, K. C. 1967. The Terrestrial Arthropoda of Macquarie Island. *ANARE Sci. Reo.* (B) 1. Pub. No. 99. Melbourne: Antarctic Division, Department of External Affairs.

Wilkes, C. 1845. *Narrative of the U.S. Exploring Exped. 1838–42.* 5 vols. Philadelphia: Lea and Blanchard.

TRANS. AM. GEOPHYS. UN., 58: 1111.

OXYGEN ISOTOPE GEOCHEMISTRY OF THE MACQUARIE ISLAND OPHIOLITE

J.D. Cocker (Dept. of Geology, Univ. of Alberta, Edmonton, Alberta, Canada T6G 2E3)
B. Griffin (Dept. of Geology, Univ. of Tasmania, Hobart, Tasmania, Australia 7001)
K. Muehlenbachs (Dept. of Geology, Univ. of Alberta, Edmonton, Alberta, Canada T6G 2E3)

Macquarie Island is a well preserved Miocene ophiolite with outstanding exposures of weathered pillow basalts, zeolite facies metamorphosed basalts, sheeted dolerite dykes, gabbros and ultramafics. The $\delta^{18}O$ values of basalts and non-uralitized dolerite dykes which intrude the lavas range from +5.7 to +9.6‰; uralitized dykes, gabbros and ultramafics range from +3.2 to +6.0‰. The ^{18}O content of basalts reflects their degree of alteration; basaltic glasses are +5.7‰ whereas the altered basalts are enriched in ^{18}O in proportion to their H_2O content. Uralitized samples from the dyke swarms as well as gabbros and ultramafics have lower $\delta^{18}O$ values indicating hydrothermal alteration. Disseminated and vein calcites from sub-zeolite to high zeolite basalts range in $\delta^{18}O$ from +18 to +33‰ which implies temperatures of 3 to 89°C assuming sea water alteration. Carbonates from intrusive rocks range in $\delta^{18}O$ from +12 to +22‰ corresponding to temperatures of 60 to 150°C. The $\delta^{18}O$ of natrolite, gyrolite, wairakite, laumontite and prehnite range from +8 to +20‰ with prehnite having the lowest $\delta^{18}O$ indicative of higher temperatures of metamorphism. $\delta^{13}C$ values of calcites vary widely (+0.7 to -18.9‰), tending towards lower ratios in the high zeolite basalts and the intrusive rocks. These low $\delta^{13}C$ values in the high temperature rocks suggests that the C was derived from organic sources with alteration occurring in a closed system. The above data indicates that the ^{18}O enriched basalts were altered at low temperatures by sea water in the oceanic crust. The ^{18}O depletion observed in the intrusive rocks must also result from reaction with sea water, but at higher temperatures.

UNIVERSITY OF TASMANIA

Department
of Geology
Publication

ENERGY DISPERSIVE ANALYSIS SYSTEM CALIBRATION AND OPERATION WITH TAS-SUEDS, AN ADVANCED INTERACTIVE DATA-REDUCTION PACKAGE

B.J. Griffin
May 1979

ENERGY DISPERSIVE ANALYSIS SYSTEM CALIBRATION AND OPERATION WITH TAS-SUEDS, AN ADVANCED INTERACTIVE DATA-REDUCTION PACKAGE

B.J. Griffin
Geology Dept.
University of Tasmania

May 1979

CONTENTS

1. Introduction

TAS-SUEDS is a program for rapid quantitative reduction of X-ray spectra collected by an EDAX energy dispersive system attached to a JEOL JXA-50A scanning electron microprobe analyzer. Up to 11 elements may be determined simultaneously and standard data on up to 19 elements may be stored in each of two arrays, this data thus being immediately accessible. Providing suitable standards are available there are no program restrictions on the elements that can be analysed. The program is run on a NOVA 28K minicomputer which is on-line to the EDAX unit. Spectrum transfer from the NOVA to the EDAX is automatic. Rates of twenty analyses per hour are routinely achieved by only minimally trained operators.

Apart from the reduction of unknown spectra, the program also contains options for (i) element calibration using pure or compound standards,

(ii) element background calculations using known spectra, and

(iii) gain and zero calibration of the EDAX analytical system using a pure copper spectrum. Other program options allow input or output of reference standard data, corrections for electron beam drift, changes in major operating conditions of the microprobe (e.g. accelerating voltage), and selection of either of the two arrays of standard data. The last option is of value when the system is used for analysis of materials which require different operating conditions (e.g. silicate analysis is carried out with an accelerating voltage of 15kV, and sulphide analyses with 20kV). The storage of data in separate arrays corresponding to the different conditions eliminates the potential for errors due to the use of inappropriate standard data.

2. Specifications

TAS-SUEDS is a BASIC language program (single-user level) operated on a NOVA 1210 series minicomputer with 28k of RAM. The program requires spectra to be comprised of 800 channels with 20 e.v. per channel, i.e. over a 0-16KeV range. The EDAX analytical system consists of a series 183B detector and amplifier with a series 707B multichannel analyzer. This system is attached on a spectrometer port of a JEOL JXA-50A scanning electron microanalyzer (plate 1) in the Central Science Laboratory at the University of Tasmania.

SUEDS 1 (Nockolds, 1976) was the basis for this program. Major modifications have been made incorporating the data reduction methods of Reed (1975), Reed and Ware (1975), and Ware (pers. comm., 1979). Modifications have also been made to the output format so that it is oriented towards presentation of the analyses of geological materials. These modifications include the calculation of structural formulae on a given number of either oxygen or sulphur atoms and various molecular cation ratios.

Processing of an unknown spectrum for ten elements, plus oxygen by difference, requires about 110 seconds. Spectrum collection with the EDAX takes about 100 seconds but as the program collects all required spectral information from the EDAX unit during the first 15 seconds of data reduction the next spectrum collection can be started after this 15 second period (an "EDAX free" message is displayed). Consequently there is only a 15 second minimum delay between successive spectrum accumulations required by the analytical system and this is virtually always less than operator time required for selection of the next analysis point.

EDAX-NOVA interface routines are included in the BASIC Interpreter system tape supplied with the copy of TAS-SUEDS. These interface routines are controlled by the "CALL" command in BASIC.

3. Software Loading Procedure

TAS-SUEDS is loaded using the normal procedure. Firstly the "bootstrap loader" is entered manually through the data switches on the computer, then the BASIC Interpreter system tape is loaded, and finally, after the "NEW" command, TAS-SUEDS is read in. Once this stage is reached a listing of the program should be obtained and checked against the supplied master listing.

4. System Calibration

4.1. Program Initiation

Once initiated, all options in TAS-SUEDS operate from a central control line (line 7000) and the operating procedure depends upon the option selected by the user. The various options are identified by integer values (table 1) and at the completion of each task the program returns to the central control point. The "RUN" command is only used to start the program for the first time or to clear error conditions in the computer. It resets variable and array values to zero and the operator must re-enter a number of variable values before the program can be used again. If the computer is turned off at the end of each analytical session, it should be reactivated by the command "goto 7000" rather than the "RUN" command.

Default values for the various parameters have been written into the program and these must be checked for each particular system as some are system-dependent. Before initiating the program, the following variables should be checked and redefined if necessary.

4.11. Electron beam current — default value = 3×10^{-9} amps
specified at line 2010 as H8 = 3
change at lines: 2010, 2055, 4515.

Table 1 Options available with TAS-SUEDS

Option Denominator	Function
-1	selection of either of the two standard data arrays
1	quantitative analysis of unknown spectra
2	calculation of element conversion and overlap factors from pure element spectra
3	calculation of element conversion factor from complex spectra
4	calculation of element background values
5	gain and zero calibration of the EDAX system
10	routine to change the defined value of the accelerating voltage in the program
11	lists stored values of variables and standard data
14	routine for variation of the beam current value used in the program.

4.12. Sample tilt — default value = 0^{o}
specified at line 2075 as T1 = 0
change at above line.

4.13. X-ray take off angle — default value = 30^{o}
specified at line 2080 as D1 = 30
change at above line

4.14. System dead time — default value = 16×10^{-6} seconds
specified at line 7233 as 0.000016
change at above.

This 16μs is the effective dead time and is easily calculated by measuring the count rate as a function of beam current using a fixed sample. The count rate is calculated by integrating the whole spectrum and dividing by the displayed time. If the specimen current is used as a rapid measure of beam current it is essential to move to a fresh area of the sample before each reading since build-up of contamination spots can alter the specimen current. Effective dead time should be calculated for both high and low energy X-rays: it is quite common for the dead time to increase at the low energy end where pile-up correction ceases to be effective. If this proves to be the case, the value of the effective dead time calculated for the higher energies should be adopted.

4.15. Interferences on the low energy background position

default values: (Al + Al) = 8.97.E-8
(Mg + Si) = 2.21.E-8

specified at: (Al + Al) line 4051
(Mg + Si) line 4059

change at above lines

Imperfect pulse pile-up correction results in minor (Al K_α + Al K_α) and (Mg K_α + Si K_α) radiation pile-up on the Argon K_α peak position (which is used as the low energy background position). These interferences should be allowed for and the proportion of each interference can be calculated by manual measurement and extrapolation using pure Al and Mg_2 SiO_4 spectra.

4.16. System resolution parameters

default values W7 = 2.392
W8 = 19100

specified at: W7 lines 2022, 6193
W8 lines 2024, 6194

change at above lines

These parameters are fixed during routine system calibration. They are printed out automatically after each calibration check. Initially they do not need to be reset but once the program is operating average values should be obtained and inserted in the program. These parameters set the width of the windows used to measure the counts in each elemental peak and must not be allowed to vary from day to day.

4.17. Calibration target material

A pure copper target is preferred for calibration purposes but other materials, e.g. Ni_2Si, may be used. The only program changes necessary are to reset the values of the calibration peaks.

default values: low energy peak, E3 = 0.930 (KeV)
high energy peak E4 = 8.040 (KeV)

specified at: E3 = line 7091
E4 = line 7092

change at above lines

Once the required alterations have been made the program may be initiated with the "RUN" command (section 5.1). Following this the gain and zero controls of the analytical system must be calibrated with respect to the program.

4.2 Gain and Zero control calibration

The gain and zero of the analytical system will drift and Reed (1975) notes that for accurate results the zero error should be less than ± 2 e.v. between analyses. This program is calibrated using pure copper spectra but as noted

earlier only minor changes are required to allow the use of other materials (section 4.17). Smith (1976) describes zero and gain drift effects in more detail and discusses other potential target materials.

Option 5 is the system calibration routine in the program. Using a spectrum of pure copper, obtained under normal analytical conditions, the program examines the position of the L_α and K_α peaks relative to each other (the gain) and relative to the base channel (the zero). User operation and program flow are described in section 5.2. Written into the program (line 6190) are calibration parameters which are unique to each analytical system and which must be determined. These parameters convert the measured zero and gain errors into clockwise (positive) and anti-clockwise (negative) turns of each adjustment control. They are calculated by holding the gain setting constant and adjusting the zero setting from five turns below its correct setting to five turns above, collecting and processing a new copper spectrum at each zero setting. The change in measured position of the K_α peak (printed out each time) can then be plotted against setting (from +5 to -5) to derive a value for the effect of the zero control, in e.v. per turn. This value can then be inserted instead of the TASUNI system value of 8.5e.v per turn at line 6190 in the program. The zero setting should then be returned to its correct position and the procedure repeated for the gain setting (TASUNI value of 0.09 e.v. per turn at line 6190).

Random variation of ± 1 e.v. in the zero is expected and lies within the tolerances suggested by Reed (1975). Consequently errors of ±0.1 turns (= ±0.85 e.v.) are acceptable for a calibrated system. In practice the gain only shows a minimal drift and rarely requires adjustment whereas the zero drifts by about 0.3 of a turn daily and requires checking at least every six hours. It may be necessary to install an easily adjustable calibrated potentiometer on the zero and gain controls in order to expedite this calibration procedure.

4.3. Background Calibration

Operation of the background value calculation routine (option 4) is described later (section 5.2). However it is useful here to consider briefly the general approach of the routine. Factors affecting spectra are basically either directly dependent or independent of the sample composition. The background calculation used here firstly corrects the spectrum for the compositionally dependent effects (ZAF correction) and then measures the spectrum at the required element peak positions, normalising against measurements at fixed background positions. These background positions are at the Argon K_α and Germanium K_α energies (both of these elements are rare in nature).

The background value takes into account the Brehmstrahlung and the characteristics of the analytical system (e.g. beryllium window absorption). Theoretically the background values derived from different test spectra for an element should be the same but minor errors arise due to the empirical nature of parts of the correction procedures. Some typical examples, shown in table 2, demonstrate the degree of variation commonly encountered. Values selected for use are also shown.

Once the required background values have been derived they can be written into the appropriate data statements in the program (see end of section 4.4).

4.4. Element Conversion factors and Overlap factors

It is also necessary to calculate for each element a conversion factor (which is count per weight percent per second per nanoamp, corrected for matrix absorption effects) and the degree of overlap of each elemental peak on to the peaks of adjacent elements. In dealing with overlaps affecting the element with atomic number Z, this program considers only the elements Z-1 and Z+1. For many analytical systems the degree of low energy tailing of peaks is such that it is necessary to consider the overlap effect on element Z-2. e.g. it may be necessary to consider the overlapping of the Si K_α peak (Z=14) on Mg (Z=12) as well as on Al (Z=13) and P (Z=15). The program must be modified accordingly.

Conversion factors and overlap factors are calculated using options #2 and #3 of the program. Option #2 calculates both conversion and overlap factors from either pure element spectra or from multipeak spectra in which the peak of interest is well removed from other peaks in the spectrum and also the elements which may be affected by overlap from the element of interest are absent. Option #3 calculates the element conversion factor only and is used for processing complex standard spectra, e.g. in the case of using a feldspar as a standard for sodium. Some overlap factors may have to be estimated because of a lack of suitable standards and a guide for estimation is the table of overlap factors presented by Smith (1976).

Machine conditions must be constant during collection of the standard data. Measurements should be repeated during different analytical sessions to obtain representative results. Any values that show significant variations (>±2% relative) should be checked.

Once it has been established that the standard data are accurate and the analytical system is performing consistently then this data can be written into the program in place of the dummy values. The data statements for standards for

Table 2 Background values obtained with Tasuni system at 3 nanoamps and 20 KV

Measured element position	pure Cu			pure Fe			pure Zn		Selected values
	1	2	3	1	2	3	1	2	
S (16)	1.307	1.320	1.319	1.345	1.372	1.357	1.323	1.335	1.335
*Cd (48)	0.943	0.948	0.959	0.947	0.940	0.933	0.925	0.934	0.941
Mn (25)	0.408	0.410	0.409	0.436	0.437	0.433	0.383	0.396	0.410
Fe (26)	(0.523)	(0.517)	(0.506)	-	-	-	0.358	0.366	0.362
Co (27)	0.322	0.317	0.321	-	-	-	(0.460)	(0.478)	0.320
Ni (28)	0.290	0.280	0.282	0.264	0.269	0.265	0.264	0.266	0.273
Cu (29)	-	-	-	0.245	0.252	0.238	0.238	0.253	0.245
Zn (30)	(0.316)	(0.320)	(0.324)	0.204	0.216	0.210	-	-	0.210
As (33)	0.142	0.142	0.143	0.147	0.141	0.141	0.147	0.151	0.144

*Cd — L line is used for analysis rather than K line as with the rest. Bracketed values were rejected because of interferences. Other results were considered in calculating final values.

15 KV analytical work (e.g. silicate phases) are from line 1660 to line 1698 inclusive; and for standards for 20 KV analytical work (e.g. sulphides) are from line 1700 to line 1738 inclusive. Each data statement is structured as below:

```
1600    DATA    12105,    0,    .008,    11,    1.72
```

line number conversion fact overlap-1 overlap+1 atomic number background value

It is useful to then check the system performance on as wide a range of known samples as possible in the first instance. Following this it is usual to include some of the standards and pure copper (or appropriate calibration material) into all specimen holders (plate *2) for easy reference before, during, and after analytical sessions. The standards selected should contain the elements of interest at abundances comparable or higher than those expected in unknowns and at least one of the standards should be a stoichiometric compound. A suitable set of standards for silicate phase analysis is; a magnesian olivine, an augitic clinopyroxene, a plagioclase feldspar, and an amphibole.

When the system has been thoroughly checked and all of the data written into the program a paper tape copy should be obtained. This tape is then the master tape for the system.

The overall system calibration procedure is summarised in figure 1.

Figure 1 Summary of System Calibration Procedure

A. Hardware measurements

1. Measure or check (i) beam current magnitude
   (ii) specimen tilt
   (iii) x-ray take off angle
2. Measure system dead time
3. Measure interferences on Argon Kα position

B. Software loading and calibration

4. Load and check program
5. Replace default values for beam current, specimen tilt, x-ray take off angle, dead time, Argon interferences, and calibration target details where necessary.
6. Activate program with "RUN" command, change accelerating voltage value if necessary (option *10).
7. Measure gain and zero adjustment parameters (ev/turn) and resolution parameters, W7 and W8, insert into the program and calibrate the gain and zero (option *5).
8. Measure all required background values (option *4).
9. Measure all required element conversion and overlap factors (options *2 and *3).
10. Check data reduction on a range of known materials (option *1).
11. Write the collected standard data into the "DATA" statements in the program.

The system should now be calibrated. Regular checks (daily is suggested) should be performed to recognise any short or long term drifts in the system.

5. Program operation and option description

5.1. Program starting, restarting and error correction

For successful quantitative microanalysis three basic conditions must be fulfilled.

(i) A "good" spectrum must be collected, i.e., with the detector properly calibrated, the beam current at the correct magnitude, and the analysis area being a clean, flat, carbon-coated area or spot on the specimen.

(ii) All parameters i.e. background values, standard factors, accelerating voltage, x-ray take off angle, and beam current drift must be correctly specified in the program.

and (iii) The appropriate analysis details must be supplied under option *1, the analysis routine.

When problems are encountered with the analysis results follow the procedure outlined below until the errors have been identified and resolved.

(a) repeat the analysis on a different area of the sample and if still in error check one or more of the standards in the sample holder.

(b) next check that no errors were made in the specific analysis details, as supplied through option *1.

(c) if problems are still encountered, using option *11, obtain a listing of program operating conditions and check these with the reference set of parameters.

(d) then suspend program operation by pressing the "escape" key. A message indicating at which point the program was stopped will be printed out.

(e) enter the "RUN" command. This starts the program again and resets all variable and array values to zero before filling the arrays, etc., from the "DATA" statements at the beginning of the program. It is necessary to enter into the program the current values of the accelerating voltage, beam drift, and number of analyses performed. Values of these parameters are given in Appendix B.

(f) Use option *11 to obtain another listing of the standard data and check that all factors are as given on the reference set. If some are different identify the correct values and insert them into the program. At present no direct input is available for data on standards and consequently standard data must be changed by an external procedure. Stop the program (normally by using the "ESCAPE" key) and then change the appropriate parameter (program variable names are listed in table 3) using the "LET" command (see example in table 3).

Table 3 Internal Variable Names and "LET" Command

Variable	Program variable
Atomic number of standard	Q [3,J]
Element conversion factor	Q [0,J]
Overlap on lower energy element	Q [1,J]
Overlap on higher energy element	Q [2,J]
Background value of element	Q [4,J]

- for standard number J.

To change the element conversion factor for element I (i) stop program using "ESCAPE" key (ii) enter "LET Q [0,I] = xxx"

Normal operation should now be possible. If not then either some part of the program has been corrupted in the computer memory or a hardware problem has been encountered. Reloading the program will overcome the corruption problem but the reasons for the corruption should be identified if possible. Keep a record of the behaviour of the system from just before the trouble commenced as this may be useful in tracing the fault immediately and identifying recurring problems later.

5.2. Option Description

In the following sections the use of each option of the program is described. A briefly annotated flow chart for each option is given in Appendix A and examples of operation and results of each option are given in Appendix B.

5.2.1. Option 1 : Selection of standard data array

It was previously noted that two arrays of standard data are available in the program. Having two arrays avoids potential confusion between standard data for a given element under two sets of operating conditions e.g. Fe at 15 KV for silicates or 20 KV for sulphides. This option is used to define which of the arrays is to be used during the data reduction.

The choice of data array is made through the variable B2 and it may have the value of "Ø" or "9". Normal practice is to store data for analytical work at 15 KV (mainly silicates) in the "Ø" array and for 20 KV work in the "9" array. When the program is started with the "RUN" command the "Ø" array is selected automatically.

5.2.2 Option 1 : Quantitative spectrum reduction

This is the routine through which all unknown spectra are processed. The program counts the number of times this routine is operated, by incrementing the value of the variable J[12] (at line 7026). Thus the number of analyses performed can be determined either by requesting directly the value of J[12] when the program is not in operation ("print J[12]") or through the data listing of option *11.

The result print out routines in this option have been developed particularly with the analysis of silicate phases in mind. For sulphides, etc., the print out formats are acceptable but not optimal at present and these areas of the program could be further developed. The following section is a detailed description of the operator-computer interaction for this routine.

OPTION 1 - ANALYSIS CORRECTION

Computer responses in italics

1. *($)* Call analysis option as below

   $? 1

2. *(SAMPLE=?)* First piece of information is sample identifier - this must contain at least one of: Letter, Blank space, or non-integer symbol (e.g. 1-2) *SAMPLE = ?* DEL. CPX - 1

3. *(?)* After this press RETURN KEY, the response is: ?. If silicates are being analysed the following ratios may be calculated from the analysis:

   0 → No ratios calculated

   1 → Mg/Mg + Fe calculated with all Fe as FeO

   2 → Ca:Mg:Fe with the total normalised to 100

   3 → Ca:Na:K - total 100 as above

   Several options may be selected. End the list with -1.

   NOTE The ratios are calculated from the molecular proportions in the calculated structure.

   i.e. ? 1 - the Mg/Mg + Fe value for the analysis will be calculated.

4. *(OXNO=?)* The next piece of information required is the number of oxygen atoms on which to base the structural formula calculations *(OXNO = ?)*. For samples containing no oxygen obviously this is 0.

   For ANHYDROUS PHASES (e.g. pyroxenes, olivines) the OXNO is the number of oxygens in the ideal structure, (see Deer, Howie, and Zussman, 1966, if you are not sure). However, for HYDROUS PHASES the OXNO is the number of oxygens + ½ the no. of (OH). The number of H_2O molecules is ignored.

e.g.	Name	Formula	Oxno.
	olivine	$(Mg,Fe)_2SiO_4$	4
anhydrous	plagioclase	$(Ca,Na,K)AlSi_3O_8$	8
	augite	$(Ca,Na,Mg,Fe^{2+},Mn,Fe^{3+},Al,Ti)_2[(Si,Al)_2O_6]$	6
hydrous (OH)	hornblende	$(Na,K)_{0-1}Ca_2(Mg,Fe^{2+},Fe^{3+},Al)_5[Si_{6-7}Al_{2-1}O_{22}](OH,F)_2$	23
	muscovite	$K_2Al_4[Si_6Al_2O_{20}](OH,F)_4$	22
hydrous (H_2O)	natrolite (zeolite)	$Na_2[Al_2Si_3O_{10}].2H_2O$	80
	phillipsite (zeolite)	$(\frac{1}{2}Ca,Na,K)_3[Al_3Si_5O_{16}].6H_2O$	32

NOTE 1

In some cases the Oxno. is larger by some multiple of the number of oxygens in the formula (e.g. zeolites). This is done by convention to make the results more easily understood. Check with Deer, Howie and Zussman (1966) if uncertain.

NOTE 2

If you do not know what the phase being analysed is, make an intelligent guess! The output format is best when a structural formula is calculated. Also the structural formula is derived from the analysis and thus does not affect it.

NOTE 3

If glasses are being analysed used an Oxno. of 16. This approximates the Barth cell calculations for a C.I.P.W. Norm. of 160 oxygen atoms.

* NORMALISATION

Finally if you want to normalise the analysis to 100 wt.%, then IF AN OXNO. IS SUPPLIED:- A negative oxno. causes the analysis TO BE NORMALISED AND the PRINTED TOTAL of the oxides is the analysis total BEFORE normalisation.

\- A positive oxno. is used if an unnormalised analysis is required.

i.e. (a) for a normalised analysis of an olivine *OXNO = ?* -4

(b) for an unnormalised analysis of an amphibole *OXNO = ?* 23

NOTE If the mineral being analysed is either hydrous or it contains major elements not included in the analysis e.g. Cl, then the analysis should not be normalised. In this case the beam current should be monitored closely to obtain accurate totals.

These comments also apply to part 6 of this section.

5. If an Oxno. has been used ignore parts 6, 7.

6. *(NORMALISE?)* If the Oxno. is 0 (e.g. for a sulphide analysis) the next question is *NORMALISE ?*. The potential answers are:

0 = yes — the analysis is normalised to 100% and the prenormalisation total is printed out.

9 = no — no normalisation is performed.

i.e. *NORMALISE ?* 0 - yes, normalise the analysis

7. *(SULPH NO.=?)* The program will also calculate structural formulae based on sulphur. If Oxno. = 0 then after 6 the following is asked *SULPH. NO. = ?* Thus if a sulphide is being analysed the number of sulphur atoms in the formula is supplied.

e.g. Name	Formula	Sulphur No.
pyrite	FeS_2	2
sphalerite	(Zn,Fe)S	1
chalcopyrite	$CuFeS_2$	2
bornite	Cu_5FeS_4	4
arsenopyrite	FeAsS	1 *
tennantite - tetrahedrite	$Cu_{12}(As,Sb)_4S_{13}$	13 *
pyrrhotite	FeS_{1-x}	1 *

NOTE 1: Pyrrhotite is non-stoichiometric W.R.T. sulphur and the "Sulph. no." is an approximation only. The other minerals marked * cannot be regarded as combinations of simple sulphides, so the program cannot give accurate structural formulae for these and many similar sulphosalts.

NOTE 2: Again if uncertain make an intelligent guess or check with Berry and Mason (1959) or another appropriate text. It is always useful to use some value if a sulphide is being analysed to get the best format.

i.e. *SULPH. NO. ?* 2 e.g. for chalcopyrite

8. *(AS BEFORE)* Up to this point the information is specific for each analysis and so must be supplied each time. However, the definition of the elements to be analysed for, and the type of sample may often be done once at the start of the analysis session.

Therefore in response to the present question *"AS BEFORE"* the possible answers are:

0 = yes, the other information as previously set

9 = no, if the element analysis list and/or the type of analysis is to be changed.

i.e. *AS BEFORE ?* 0 - yes

* NOTE IF the answer is 0 COMPUTATION STARTS IMMEDIATELY THE "RETURN KEY" IS PRESSED. THUS THE ANALYSIS SPECTRUM MUST BE GATHERED PRIOR TO PRESSING THE RETURN KEY.

9. *(IF SULPHUR OR OX PRESENT (O)?)*

At this stage, before the first analysis or when a change is being made the type of analysis must be declared.

Responses 0 - if sulphur or oxygen is present in the sample

9 - if neither present, e.g. metal alloy

i.e. *IF SULPHUR OR OX PRESENT (O)?* O - an olivine being analysed

10. *(Z, L, Ox, or Z, L)* At this point the elements to be analysed for are defined. Two headings are printed by the computer, depending on the response to part 9 (oxygen or sulphur present or not). as below:

(a) if ox or sulphur present — *? Z, L, Ox/S*

(b) neither present — *? Z, L*

Z = atomic number e.g. Na = 11

L = radiation line to be used in the analysis, where

K - line = 1

L - line = 2

M - line = 3

Ox = no. of atoms of ox or sulph. which combine to form simple sulphides or oxides with the element.

e.g. Na_2O	Ox = 0.5	FeS	Ox = 1
MgO	Ox = 1	CuS	Ox = 1
Al_2O_3	Ox = 1.5		
SiO_2	Ox = 2		

Up to 10 elements may be listed for analysis. If oxygen is present the last data line is "?8 ?O ?O"

Note 1 Any number of elements may be listed up to 10 (not including oxygen if present).

Note 2 After the last "O" is sent computation starts and so a spectrum must be gathered before pressing the "RETURN" Key.

Note 3 Appendix 1-A contains lists of elements for which standard data are available, and the energy lines to be used for analysis.

11. *(EDAX FREE)* The computer only requires the spectrum in the display for the initial calculations. Once these have been completed the message *"EDAX FREE"* is printed out. Following this a new spectrum collection can be started.

Note 1 no response is required from the operator.

Note 2 at present some other information is printed out before the *"EDAX FREE"* message. This information is printed to provide a check on computer operation and does not concern the operator.

12. *(TRACE ELEMENTS?)* After the corrected analysis has been printed out (± ratios) the program checks to see if trace element analyses are being carried out simultaneously. There are two possible responses:

"9" - no, this is the normal case. The program returns to base position and prints $? (see part 1)

"O" - yes,

i.e. *TRACE ELEMENTS?* 9 - no WDS analyses being performed.

The "trace element" question refers to the master version of the program at the University of Tasmania which also has correction routines for dealing with data from wavelength-dispersive crystal spectrometers. These routines are under options 24-30 but are not available with this version of the program.

5.2.3 Options *2 and *3: Calculation of standard data from pure and multi-element spectra

Option *2 calculates the element conversion factor and overlap factors from pure element spectra. Option *3 does not calculate overlap effects and is designed for use with multielement standards. Option *2 can be used on multi-element spectra where there are no interferences present on the target element and the adjacent elements.

Options 2 and 3

1. *($?)* call required option as below
   ? 2 or 3
2. *(STD?)* Firstly the number of the standard must be specified. The list of standard data (from option *11) should be consulted to see which numbers have already been used. If a standard number is duplicated then the previous data will be overwritten by the new values. The range of values for the standard number is 0-40.
3. *(FOR Z = ?)* Give the atomic number of the element which is being calibrated.
4. *(AS BEFORE?)* Does the present target have the same composition as the previous one?

   The possible responses are: Ø = yes
   9 = no

   If a 'yes' response is made the computer starts working on the spectrum without any further operator input.
5. *(IF SULPHUR OR OX PRESENT (O)?)* Is there sulphur or oxygen in the sample, responses: Ø = yes
   9 = no
6. *(Z, L, Ox, K-RAT)* or *(Z, L, K-RAT)* The first if oxygen or sulphur present (part 5).

   This section is where the target composition is defined so that matrix corrections can be made. The composition is supplied one element at a time with Z = atomic number, L = analysis line (K=1, L=2, M=3), ox = number of oxygen atoms per atom of the particular element e.g. Na (Na_2O) Ox .5, Si(SiO_2) Ox=2, and K-FAT is the decimal weight fraction of the oxide or element (if oxygen not present in sample e.g. sulphide). To escape from the input loop once the composition has been defined one of the following

responses may be made:

8, 0, 0, 0 if oxygen present

0, 0, 0, 0 " " not present

If overlap factors are to be calculated (option *2 only) then the elements on which the overlap factors are to be calculated must be specified in the composition list. Their abundance is given as zero. The routine goes into operation after the "return" of the last zero in the composition list. The spectrum must therefore be collected before the zero is "RETURNED".

Results from several runs should be averaged and inserted into the data array (for temporary changes) or written into the appropriate "DATA" statement (for a permanent change).

5.2.4 Option *4: Background value calculation routine

This routine calculates the background values (relative to the measured background at the Argon Kα peak energy) from a spectrum of specified composition. Obviously the spectrum must contain no interfering peaks in the areas of interest and consequently pure metals are commonly used e.g. iron, nickel, zinc.

Background values for up to eight elements can be calculated in any one run of the routine, and because this routine, like all of the routines, does not affect the spectrum in the Video Display Unit, each spectrum can be reprocessed as necessary to obtain all desired background values. At least three measurements should be made to obtain a reliable background measurement result. A set of results obtained with the Tasmanian system is given in table 2. If wide discrepancies occur between results for the same elements derived from spectra of different compositions then it is possible that the value of accelerating voltage, x-ray take off angle, or sample tilt is wrongly specified.

OPTION 4

1. *($?)* call required option

   $?4

2. *(BGD CALCN USING ?)* Any sample description may be given here but it must include a non-numeric character. The response will be (\?), to which any value is given, i.e. FRED \? 2

3. *(AS BEFORE?)* Is the composition of the target the same and do you want background values calculated for the same elements as before? Response:

   Ø = yes

   9 = no

   If "yes" then after "RETURN" of the zero the computer proceeds directly into spectrum processing and so the spectrum must be available at this point.

4. If "9" = NO to part 3 then the program operates as from 5.23 part 5 except

that once the target composition has been given the elements for which background values are required are given in the same list with abundances of zero. Up to 10 elements can be specified overall in the list and so the number of background values that can be calculated depends upon the number of elements in the target, this is another reason for using pure element targets. Once all the elements have been defined the list is finished in the normal manner (5.23-5) and after the "RETURN" of the last zero value the program starts spectrum processing.

5.2.5 Option *5 : System zero and gain calibration

Use and operation of this option has been previously discussed (section 4.2).

1. *($?)* call required option
   $?5

2. *(SPEC CALIBRATION ON PURE Cu)*
   (IS SPECTRUM READY (Ø)?) Enter "Ø" "RETURN" when a copper spectrum has been collected. Data processing then proceeds immediately and on completion the results are printed out. The required adjustments if any, should be made on a new copper spectrum collected. After the results are printed out the following is asked:

4 *(AGAIN?)* responses: Ø = yes - if no spectrum is to be processed
9 = no - if previous results showed that the system was satisfactorily calibrated.

5.2.6 Option *10 : Accelerating voltage input

This option allows changing of the accelerating voltage used in data reduction by the program. It is a routine designed for systems where regular alternation between analytical work at different accelerating voltages occurs.

1. *($?)* 10

2. *(ACC. VOLTAGE=?)* N where N is the new value of the accelerating voltage (in KV).

5.2.7 Option *11 : Standard data print out

This routine prints out current machine conditions and analytical details as well as all of the stored standard data.

1. *($?)* 11

2. *(PROGRAM DATA AT ?)* Three integer values must be given sequentially by the operator at this point. These values are arbitrary as they are not used by the program but they are usually chosen to represent the date.

5.2.8 Option *14 : Electron beam current drift adjustment

For reasons known only to itself an electron microprobe system will often stabilise with a beam current at not quite the set value. An alternative procedure to restabilising the system is to reset the beam current value in the program providing the error is small (≤±5% relative). Because totals are almost directly proportional to beam current the required adjustment can be calculated by analysing a phase with an accurately known analysis total. The required correction can be calculated from several analysis totals.

1. *($?)* 14

2. *(DRIFT?)* give the correction as a fraction of 1 i.e., if analyses are totalling 105 wt % and they should total 100 wt.% then the correction is 1.05. If totals were 96.5 wt.% then the correction would be .965.

3. *(TOTAL DRIFT = xxx)* The program then prints out the total drift factor in use (= new x old) and then returns to the central control line (line 7000).

6. Remarks and Conclusions

Provided that an EDAX system is performing consistently and that it is attached to a stable electron microprobe, it can be calibrated to produce rapid, geologically acceptable quantitative analyses with the procedure outlined here and Tas-sueds. The total procedure should take approximately two weeks and analysis rates of up to 20 analyses per hour should be routinely achieved.

A major problem that was encountered with the Tasmanian system was a gradual build up of contamination on the detector window. The contaminant was oil from the diffusion pump. This has been overcome by the installation of two small heating resistors inside the collimator cap of the detector. These irradiate the outer surface of the Beryllium window and prevent the oil from condensing on it. A check can be made for this type of contamination by manually measuring the ratio of the heights of the copper Kα and Lα peaks during the daily calibration. This ratio is a measure of the efficiency of detection of low energy radiation (Cu Lα) compared to high energy radiation (Cu Kα) and thus is affected by almost any change in detector performance. This ratio should not vary by more than 2% in the short or long term if the background values and conversion factors are to remain correct.

Finally, with the Tasmanian system it has been found that a beam current of three nAnoamps gives a count rate on pure copper of about 7000 counts per second. Dead time at this count rate is about 20%. A live time counting period of 80 seconds is used. The fast discriminator of the EDAX system is set to give a noise rate of 100 counts per second with no incoming signal.

7. Acknowledgements

This report represents investigations and developments that form a necessary part of my Ph.D. thesis. Many people have provided support and encouragement during this work, particularly Dr. R. Varne, R. Lincolne, N.G. Ware, Professor D.H. Green, Dr. A.N. McKee, and Dr. J. Walshe. My fellow postgraduate students showed great tolerance and provided many useful suggestions on this project.

Financial support was provided partly through various research moneys of the University of Tasmania and partly through a Commonwealth Postgraduate Research Award. This support is gratefully acknowledged.

8. References

Berry, L.G., and Mason, B. (1959): "Mineralogy" 630 pp. W.H. Freeman and Company. San Fransisco and London.

Deer, W.A., Howie, R.A., and Zussman, J. (1966): :An introduction to the rock-forming minerals." 528 pp. Longman Press, London.

Dunham, A.C., and Wilkinson, A.C.F. (1978): "Accuracy, precision and detection limits of energy-dispersive electron-microprobe analyses of silicates." J. X-ray Spect., 7(2), 50-56.

Nockolds, C. (1976): "A Program for Quantitative Analysis of Minerals". Edax Editor, 6(4), 34-41.

Reed, S.J.B. (1975): "Electron microprobe analysis." 400pp. Cambridge University Press. Cambridge, England.

Reed, S.J.B., and Ware, N.G. (1975): "Quantitative electron microprobe analysis of silicates using energy dispersive x-ray spectrometry." J. Pet., 16, 499-519.

Smith, D.G.W. (1976): "Quantitative energy dispersive microanalysis." in "MAC short course in microbeam techniques." D.G.W. Smith (Ed.). 186 pp. Co-op Press, Edmonton, Canada.

```
 $ ? -1 SILICATES(0) OR ETCETERA(9)
? 0


 $ ? 1

 Sample=? DELEGATE CPX\? 1? 2? -1 OXNO.=? -6
As before? 9IF SULPHUR OR OX PRESENT (0)? 0

   Z, L, OX/S
? 11? 1? .5
? 12? 1? 1
? 13? 1? 1.5
? 14? 1? 2
? 19? 1? .5
? 20? 1? 1
? 22? 1? 2
? 24? 1? 1.5
?.25? 1? 1
? 26? 1? 1
? 8? 0? 0
*              T1= 9 Time= 80  EDAX free
Tot Int= 524302
ELEM    OX     STRUCT
Na2O    .82    .058
MgO     15.75  .857
Al2O3   5.25   .226
SiO2    51.53  1.88
CaO     21.17  .827
TiO2    .48    .013
Cr2O3   .73    .021
FeO     4.23   .129
 TOTAL 110.27  4.011
 MG/MG+FE=     86.92
 CA: MG: FE = 45.61  47.27  7.12
Trace Elements? 9

 $ ? 14
 DRIFT ? 1.10   TOTAL DRIFT= 1.15556

 $ ? 1

 Sample=? DELEGATE CLINOPYROXENE\? 1? 2? -1 OXNO.=? -6
As before? 0*  T1= 9 Time= 80  EDAX free
Tot Int= 515404
ELEM    OX     STRUCT
Na2O    .63    .045
MgO     15.92  .865
Al2O3   5.22   .224
SiO2    51.49  1.878
CaO     21.31  .833
TiO2    .53    .015
Cr2O3   .72    .021
FeO     4.18   .128
 TOTAL 100.19  4.009
 MG/MG+FE=     87.11
 CA: MG: FE = 45.62  47.37  7.01
Trace Elements? 9
```

```
 $ ? 2
   STD #? 16  FOR Z=? 29
As before? 9IF SULPHUR OR OX PRESENT (0)? 9

   Z, L,K-RAT
? 28? 1? 0
? 29? 1? 1
? 30? 1? 0
? 0? 0? 0
*              T1= 9 Time= 80  EDAX free
Tot Int= 550041
 8965.82       0

OLAP FACTORS 1.75406E-3  0
CONVERSION FACTOR  1877.06
```

```
 $ ? 3
   SUBSTD #? 16  FOR Z=? 29
As before? 9IF SULPHUR OR OX PRESENT (0)? 9

   Z, L,K-RAT
? 28? 1? 0
? 29? 1? 1
? 30? 1? 0
? 0? 0? 0
*              T1= 9 Time= 80  EDAX free
Tot Int= 550041

CONVERSION FACTOR = 1877.06
```

```
 $ ? 4
BGD CALCN USING ?
? PURE CU\? 1
As before? 9IF SULPHUR OR OX PRESENT (0)? 9

   Z, L,K-RAT
? 18? 1? 0 ◄ *  N.B. data for Argon (?18 ?1 ?0) must be given as the first
? 20? 1? 0            element in the list in all cases with option 4.
? 22? 1? 0
? 25? 1? 0
? 26? 1? 0
? 29? 1? 1
? 0? 0? 0
*              T1= 9 Time= 80  EDAX free
Tot Int= 550041
 BACKGROUND FACTORS CALCULATED FOR          15              KV
 Z[I]          BGD FACTOR
 18            1.00092
 20            .737688
 22            .557662
 25            .367205
 26            .417789
 29            4.92978

 $ ?
```

```
 $ ? 5
 SPEC CALIBRATION ON PURE CU
 IS SPECTRUM READY (0)
? 0
 933.609  152.698  8046.86  200.938
EV/CH,ZERO ERROR(EV) 19.9909  3.18323   RES 187.603
W7= 2.39712 W8= 21066.2
G -.101471   Z  -.374497  TURNS
 Again? 0
 936.916  153.435  8049.68  199.617
EV/CH,ZERO ERROR(EV) 19.9922  6.55188   RES 186.812
W7= 2.29143 W8= 21393
G -8.64665E-2   Z  -.770809  TURNS
 Again? 0
 931.105  154.863  8043.82  201.898
EV/CH,ZERO ERROR(EV) 19.9924  .749512   RES 188.867
W7= 2.35829 W8= 21771
G -.084983   Z  -8.81778E-2  TURNS
 Again? 9

 $ ? 10
ACC. VOLTAGE=? 15

 $ ? 11
 Program Data at? 20? 5? 79
Acc. Voltage= 15   Drift Factor= 1.12089  No. Analyses= 200137
 1          11         12105          0      .008     1.72
 2          12         20766          .0352  .0098    1.824
 3          13         28300          .032   .02      1.95
 4          14         31100          .0165  0        2.135
 5          19         19530          0      .015     .843
 6          20         16100          .0075  0        .748
 7          22         12394          0      0        .521
 8          24         8700           0      .1181    .402
 9          25         8235           0      .1105    .333
 10         26         6450           0      .0488    .277
 11         29         3586           0      0        .262
 12         56         11433          0      0        .52
 13         28         3690           0      0        .2
 14         15         27000          0      0        1.62
 15         17         22000          0      0        1.153
 20         32         100            0      0        .1
 ********          *******
 21         16         29463          0      0        1.335
 22         24         0              0      0        .487
 23         25         11484          0      0        .41
 24         26         11500          0      0        .362
 25         27         8215           0      0        .32
 26         26         6786           0      0        .273
 27         29         5436           0      0        .245
 28         30         4213           0      0        .21
 29         33         0              0      0        .144
 30         48         0              0      0        .941
 31         34         0              0      0        .124
 32         47         0              0      0        .993
 33         50         0              0      0        .823
 34         51         0              0      0        .782
 35         75         0              0      0        .207
 36         76         0              0      0        .195
 37         77         0              0      0        .183
 38         79         0              0      0        1.533
 39         82         0              0      0        1.307
 40         32         100            0      0        .162

 $ ?
     14
 DRIFT ? 1.00   TOTAL DRIFT= 1.05051
```

Appendix B PROGRAM FLOW FOR MAJOR OPTIONS

Options 1-4 are dealt with in this appendix. All other options involve only minor computing and do not require any explanation. Comments have been made where necessary and the important variables identified. The following symbols have been used.

xxx
 ¦
 ¦ = program works through from line xxx to line yyy
yyy

xxx
 (= program jumps from line xxx to line yyy
yyy

(A) = brackets indicate operator input data

xxx $ sub yyy = subroutine direction, at line xxx go to sub yyy

Option 1 Quantitative analysis option

7011 $? (1)

C>0 (

7016

7026 J [12] = no. of analyses performed - incremented by 1

7029 Sample = ? (FRED) - input of sample description - not used

7030-33 - input of option choice for molecular rations etc.

7035 - input OXNO = ? - variable M2

M2<>0 (

950 } if M2<0 then M3 (normalisation variable) = 0
 ¦ } M2>0 M3 = 9

958

(otherwise at 7037 input M3

7125 if B2 (silicate (0) or sulphide, etc. (9) control variable <>9

B2<>9 (

(7128 input A9 = no. of sulphur in structural formulae

7130

(2140 } input of details of element list required in analysis.
 ¦ }
2495

(† TASK DEFINITION

↓ RESULT CALCULATION

7140

C>6

7185 – 7203 get spectrum from EDAX U.D.U.

7210 – 7225 add up total integral of spectrum = D9

7233 – 7238 dead time correction = 16×10^{-6} seconds

7240 – 7300 escape peak correction

7310 – 7335 calculation of upper and lower channel numbers for each element window (D[0,I] and D[1,I] respectively)

7337 sub 7740 – 7785 transfers std. data on each required element from permanent data array O[I,J] to temporary array Y[I,J]

7340 – 7360 sums for total integral in window for each element = N[0,I] = N[1,I]

7370 – 7398 - calculation and removal of peak overlaps from window integrals - Also iteration counter variable N3 = -2 on 1st time through and then N3 set at 4 and 7370 used as subroutine block.

7402 – 7408 calculation of nominal wt % C[I]: $\frac{N[1,I]}{Y[0,I] \times H8} * \frac{\text{peak integral}}{(\text{std.factor}) \times \text{beam value}}$

7410 sub 4000 – 4068 calculation of background values at Argon (=Q4) and Germanium (Q3) pos'ns.

7413 sub 2510 – 3113 ZAF correction

7414 - if Ne = 1 → 7531 = escape line from iteration to print out routine

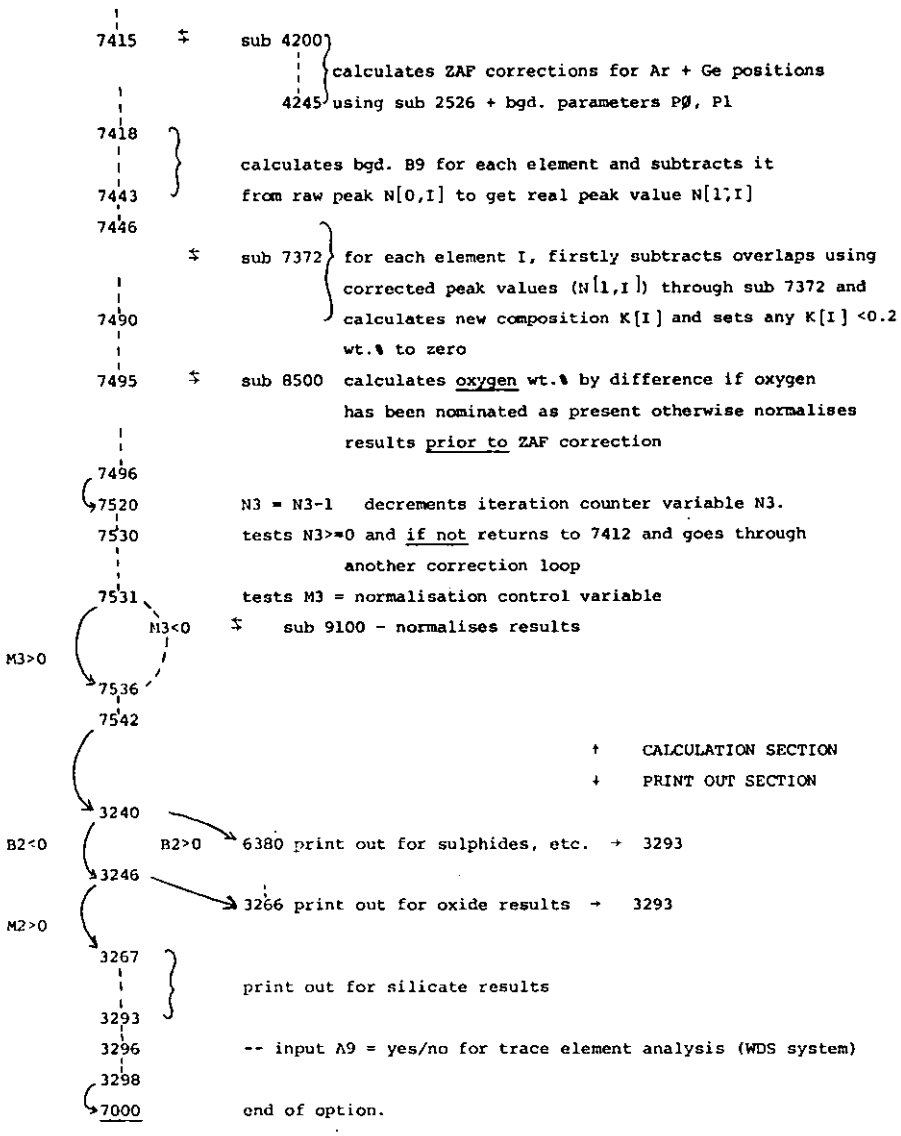
7415 ↕ sub 4200
calculates ZAF corrections for Ar + Ge positions
4245 using sub 2526 + bgd. parameters PØ, P1
7418
calculates bgd. B9 for each element and subtracts it
7443 from raw peak N[0,I] to get real peak value N[1,I]
7446
↕ sub 7372 for each element I, firstly subtracts overlaps using
corrected peak values (N[1,I]) through sub 7372 and
7490 calculates new composition K[I] and sets any K[I] <0.2
wt.% to zero
7495 ↕ sub 8500 calculates oxygen wt.% by difference if oxygen
has been nominated as present otherwise normalises
results prior to ZAF correction
7496
7520 N3 = N3-1 decrements iteration counter variable N3.
7530 tests N3>=0 and if not returns to 7412 and goes through
another correction loop
7531 tests M3 = normalisation control variable
N3<0 ↕ sub 9100 - normalises results
M3>0
7536
7542
↑ CALCULATION SECTION
↓ PRINT OUT SECTION
3240
B2<0 B2>0 6380 print out for sulphides, etc. → 3293
3246
3266 print out for oxide results → 3293
M2>0
3267
print out for silicate results
3293
3296 -- input A9 = yes/no for trace element analysis (WDS system)
3298
7000 end of option.

Options *2 and *3 Standard Factor Calculations

These options are very similar and only differ late in the computational path at line 7617 and so the options are not dealt with individually up to this point.

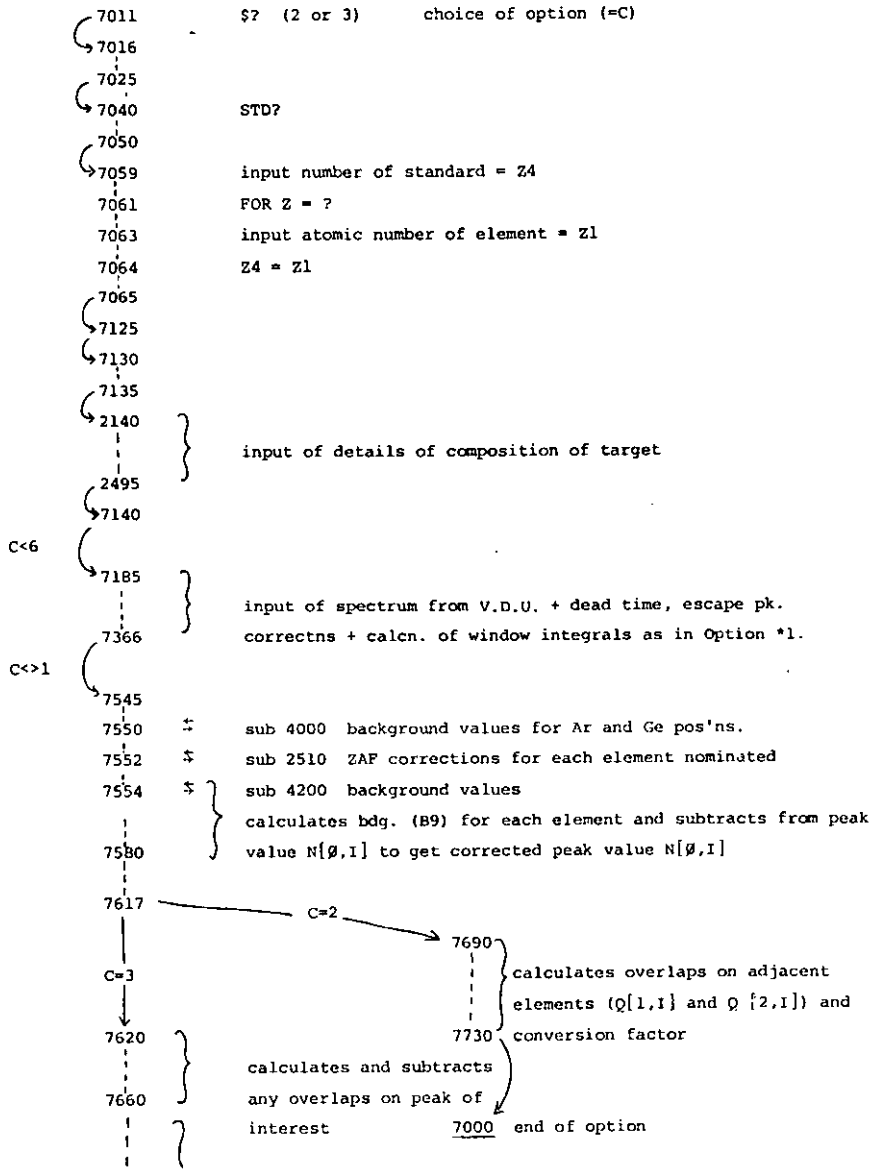

7680 — calculates and prints the element conversion factor.

7000 — end of option.

Option *4 — Background Value Calculations

7011 — $? (4)

C>0 → 7016

7025

C>1 → 7040

C>2 → 7055

C>3 → 7070 — variable N7=9 set by program; BGD CALCN USING? - input of spectrum name- not used.

7080

7125

C<>1 → 7130 — set N3=4

7135

2140 — input of composition details including in element list the elements for which background values are needed

2495

7140

C<6 → 7185 — collection of spectrum, dead time and escape peak corrections, and calculation of element integrals

7364

C=4 → 8180

C=4 → 8200

2510

2791

C=4

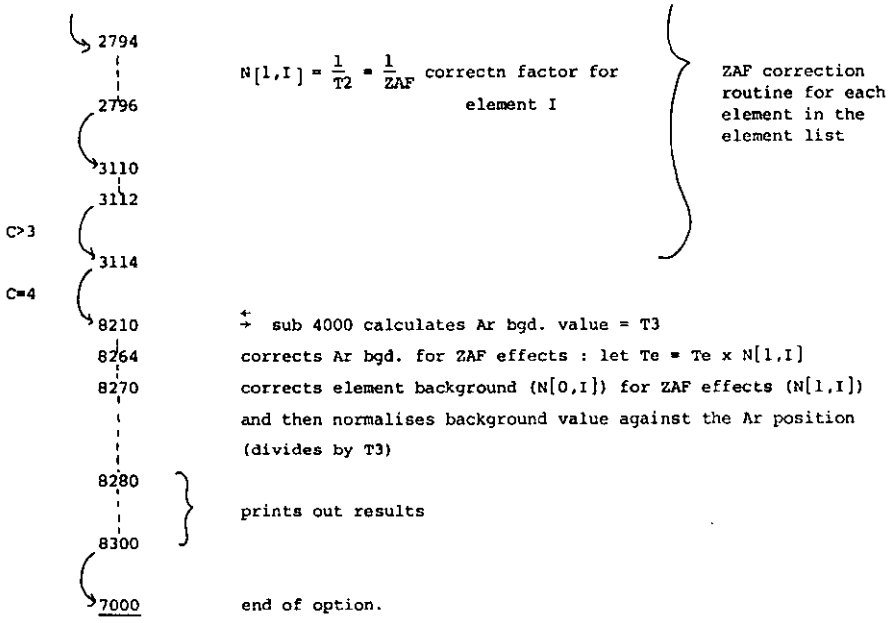
2794
N[1,I] = 1/T2 = 1/ZAF correctn factor for element I
2796
3110
3112
C>3
3114
C=4
8210
sub 4000 calculates Ar bgd. value = T3
8264
corrects Ar bgd. for ZAF effects : let Te = Te x N[1,I]
8270
corrects element background (N[0,I]) for ZAF effects (N[1,I])
and then normalises background value against the Ar position
(divides by T3)
8280
prints out results
8300
7000
end of option.
ZAF correction routine for each element in the element list

TAS SUEDS LISTING

B.J.GRIFFIN 27/4/79
GEOLOGY DEPARTMENT
UNIVERSITY OF TASMANIA
BOX 252CG G.P.O. BD,
HOBART , TASMANIA,
- AUSIRALIA

```
649  GOTO  1005
650  IF Z[I]=11 GOTO  700
651  IF Z[I]=12 GOTO  702
652  IF Z[I]=13 GOTO  704
653  IF Z[I]=14 GOTO  706
654  IF Z[I]=15 GOTO  708
655  IF Z[I]=16 GOTO  710
656  IF Z[I]=17 GOTO  712
657  IF Z[I]=19 GOTO  714
658  IF Z[I]=20 GOTO  716
659  IF Z[I]=22 GOTO  718
660  IF Z[I]=24 GOTO  720
661  IF Z[I]=25 GOTO  722
662  IF Z[I]=26 GOTO  724
664  IF Z[I]=28 GOTO  726
666  IF Z[I]=56 GOTO  728
698  PRINT Z[I];
699  RETURN
700  PRINT "Na2O";
701  RETURN
702  PRINT "MgO";
703  RETURN
704  PRINT "Al2O3";
705  RETURN
706  PRINT "SiO2";
707  RETURN
708  PRINT "P2O5"
709  RETURN
710  PRINT "S";
711  RETURN
712  PRINT "Cl";
713  RETURN
714  PRINT "K2O";
715  RETURN
716  PRINT "CaO";
717  RETURN
718  PRINT "TiO2";
719  RETURN
720  PRINT "Cr2O3";
721  RETURN
722  PRINT "MnO";
723  RETURN
724  PRINT "FeO";
725  RETURN
726  PRINT "NiO";
727  RETURN
728  PRINT " BAO";
730  RETURN
790  GOTO  1005
```

```
792  LET J=1
793  IF I(J)< 0 GOTO  3295
794  LET A9=I(J)
795  GOSUB  800
796  LET J=J+1
797  GOTO  793
800  IF A9>1 GOTO  825
801  FOR I=1 TO N2
802    IF Z(I)<>12 GOTO  804
803    LET A9=J(I)
804    IF Z(I)<>26 GOTO  808
805    IF (A9+J(I))= 0 GOTO  810
806    LET A9=A9/(A9+J(I))
807    LET A9=100*( INT (10000*A9+.5))/10000
808  NEXT I
809  PRINT " MG/MG+FE=",A9
810  RETURN
825  IF A9>2 GOTO  860
826  FOR I=1 TO N2
828    IF Z(I)<>12 GOTO  830
829    LET A5=J(I)
830    IF Z(I)<>20 GOTO  834
832    LET A9=J(I)
834    IF Z(I)<>26 GOTO  850
836    LET A8=J(I)
838    LET M2=A5+A8+A9
850  NEXT I
851  LET A9=( INT (10000*A9/M2+.5)/100)
852  LET A5=( INT (10000*A5/M2+.5)/100)
853  LET A8=( INT (10000*A8/M2+.5)/100)
854  PRINT " CA: MG: FE =";A9;A5;A8
855  RETURN
860  IF A9<>3 GOTO  892
861  FOR I=1 TO N2
862    IF Z(I)<>11 GOTO  864
863    LET A5=J(I)
864    IF Z(I)<>19 GOTO  868
866    LET A8=J(I)
868    IF Z(I)<>20 GOTO  880
870    LET A9=J(I)
874    LET M2=A5+A8+A9
880  NEXT I
882  LET A5=( INT (10000*A5/M2+.5)/100)
884  LET A8=( INT (10000*A8/M2+.5)/100)
886  LET A9=( INT (10000*A9/M2+.5)/100)
888  PRINT " CA: NA: K =";A9;A5;A8
890  RETURN
892  PRINT " NO SUCH OPTION DUMMY!"
894  RETURN
950  IF M2> 0 GOTO  955
951  LET M3= 0
952  LET M2=-1*M2
953  GOTO  958
955  LET M3=9
958  GOTO  7125
1005  PRINT " TAS SUEDS $999"
1012  DIM J(13)
1015  DIM T(25),O(11),I(11)
1020  DIM D(1,11),N(1,11),Q(5,40),Y(3,11)
1040  DIM A(3,3),B(3,9),C(13),E(13),F(13),G(3),H(2,2),K(13),L(13)
1050  DIM M(13,13),P(2,3),U(4),V(2,10),W(12),X(92),Z(13)
1051  DIM R(11),S(4,11)
1080  FOR I=1 TO 3
```

```
1090    FOR J=1 TO 3
1100      READ A[J,I]
1110    NEXT J
1120  NEXT I
1130  DATA -1.88608E-2, 2.21859,-5.17083
1140  DATA -.123941, 3.29533,-9.75836
1150  DATA -.47555, 6.84662,-20.0833
1170  FOR I=1 TO 9
1180    FOR J=1 TO 3
1190      READ B[J,I]
1200    NEXT J
1210  NEXT I
1220  DATA -3.97931E-2, 2.423, 5.5091
1230  DATA -.033916, 2.82526, 9.03526
1240  DATA -8.65397E-2, 3.32315, 10.2505
1250  DATA -.228343, 4.31172, 12.0025
1260  DATA  1.25179,-7.838,-11.5803
1270  DATA  .834903,-4.14925,-3.33802
1280  DATA  .442217,-.979241, 3.15348
1290  DATA  .25141, .931913, 8.03561
1300  DATA  .272951, .688906, 7.4243
1310  FOR I=1 TO 3
1315    READ G[I]
1320  NEXT I
1325  DATA  .88, .75, .5
1340  FOR I=1 TO 11
1342    READ Z[I],L[I],O[I]
1344  NEXT I
1346  DATA  11, 1, .5, 12, 1, 1, 13, 1, 1.5, 14, 1, 2, 19, 1, .5
1348  DATA  20, 1, 1, 22, 1, 2, 24, 1, 1.5, 25, 1, 1, 26, 1, 1, 8, 0,
0
1350  LET O[ 0]= 0
1352  LET N1=11
1354  LET N2=10
1410  FOR I=1 TO 2
1420    FOR J=1 TO 2
1430      READ H[J,I]
1440    NEXT J
1450  NEXT I
1460  DATA  2.373,-8.902
1470  DATA  2.946,-13.94
1550  FOR I=1 TO 2
1560    FOR J=1 TO 3
1570      READ P[I,J]
1580    NEXT J
1590  NEXT I
1600  DATA  1, .24, .02
1610  DATA  4.2, 1, .02
1615  FOR I=1 TO 2
1620    FOR J=1 TO 10
1625      READ V[I,J]
1630    NEXT J
1635  NEXT I
1640  DATA  1, 1, 1.17, 1.63, 1, 1.16, 1.4, 1.621, 1.783, 1
1645  DATA  1, 2, 2, 2, 3, 3, 3, 3, 3, 4
1650  FOR I=1 TO 40
1652    FOR J= 0 TO 4
1654      READ Q[J,I]
1656    NEXT J
1658  NEXT I
1660  DATA  12105, 0, .008, 11, 1.72
1662  DATA  20766, .0352, .0098, 12, 1.824
1664  DATA  28300, .032, .02, 13, 1.95
```

```
1666  DATA  31100, .0165, 0, 14, 2.135
1668  DATA  19530, 0, .015, 19, .843
1670  DATA  16100, .0075, 0, 20, .748
1672  DATA  12394, 0, 0, 22, .521
1674  DATA  8700, 0, .1181, 24, .402
1676  DATA  8235, 0, .1105, 25, .333
1678  DATA  6450, 0, .0488, 26, .277
1680  DATA  3586, 0, 0, 29, .262
1682  DATA  11433, 0, 0, 56, .52
1684  DATA  3690, 0, 0, 28, .2
1686  DATA  27000, 0, 0, 15, 1.62
1688  DATA  22000, 0, 0, 17, 1.153
1690  DATA  0, 0, 0, 0, 0
1692  DATA  0, 0, 0, 0, 0
1694  DATA  0, 0, 0, 0, 0
1696  DATA  0, 0, 0, 0, 0
1698  DATA  100, 0, 0, 32, .1
1700  DATA  29463, 0, 0, 16, 1.335
1702  DATA  0, 0, 0, 24, .487
1704  DATA  11484, 0, 0, 25, .41
1706  DATA  11500, 0, 0, 26, .362
1708  DATA  8215, 0, 0, 27, .32
1710  DATA  6786, 0, 0, 26, .273
1712  DATA  5436, 0, 0, 29, .245
1714  DATA  4213, 0, 0, 30, .21
1716  DATA  0, 0, 0, 33, .144
1718  DATA  0, 0, 0, 48, .941
1720  DATA  0, 0, 0, 34, .124
1722  DATA  0, 0, 0, 47, .993
1724  DATA  0, 0, 0, 50, .823
1726  DATA  0, 0, 0, 51, .782
1728  DATA  0, 0, 0, 75, .207
1730  DATA  0, 0, 0, 76, .195
1732  DATA  0, 0, 0, 77, .183
1734  DATA  0, 0, 0, 79, 1.533
1736  DATA  0, 0, 0, 82, 1.307
1738  DATA  100, 0, 0, 32, .162
1760  FOR I=1 TO 12
1770    READ W[I]
1780  NEXT I
1790  DATA -.232229,-.254471, .256216, 1.35917
1800  DATA  4.07005, 4.76925, 1.15119,-9.49212
1810  DATA -6.22075,-10.3788,-5.68485, 18.6408
1830  FOR I=1 TO 92
1840    READ X[I]
1850  NEXT I
1860  DATA  1.008, 4.004, 6.94, 9.013, 10.82, 12.011
1870  DATA  14.007, 16, 19, 20.18, 22.99, 24.31
1880  DATA  26.98, 28.09, 30.97, 32.06, 35.45, 39.95
1890  DATA  39.1, 40.08, 44.96, 47.9, 50.94, 52
1900  DATA  54.94, 55.85, 58.93, 58.71, 63.54, 65.37
1910  DATA  69.72, 72.59, 74.92, 78.96, 79.91, 83.8
1920  DATA  85.47, 87.62, 88.91, 91.22, 92.91, 95.94
1930  DATA  99, 101.1, 102.9, 106.4, 107.9, 112.4
1940  DATA  114.8, 118.7, 121.8, 127.6, 126.9, 131.3
1950  DATA  132.9, 137.3, 138.9, 140.1, 140.9, 144.2
1960  DATA  145, 50.4, 152, 157.2, 158.9, 162.5
1970  DATA  164.9, 167.3, 168.9, 173, 175, 178.5
1980  DATA  180.95, 183.85, 186.2, 190.2, 192.2, 195.1
1990  DATA  196.97, 200.6, 204.4, 207.2, 209, 210
2000  DATA  210, 222, 223, 226, 227, 232, 231, 238
2002  PRINT
2005  PRINT 'NO. OF ANALYSES=';
```

```
2006  INPUT J[12]
2008  PRINT
2010  LET H8=3
2011  LET B2= 0
2013  FOR I=1 TO N1
2014    LET O[I]=X[Z[I]]/(16*O[I]+X[Z[I]])
2015  NEXT I
2018  LET W3=20
2020  LET W4= 0
2022  LET W7=2.392
2024  LET W8=19100
2030  DEF  FNE(Y)=Y^1.65
2040  DEF  FNF(Y)=1+2*Y+Y*Y
2045  PRINT 'BEAM DRIFT=';
2050  INPUT H9
2055  LET H8=3*H9
2058  PRINT
2060  PRINT 'ACC. VOLTAGE=';
2065  INPUT V9
2075  LET T1= 0
2080  LET D1=30
2085  GOTO  2130
2130  LET D1= COS (1.74533E-2*T1)/ SIN (1.74533E-2*D1)
2132  LET V=V9
2134  LET D=D1
2135  GOTO  7000
2140  IF C<24 GOTO  2146
2141  IF C>30 GOTO  2146
2142  LET D=D0
2144  LET V=V8
2145  GOTO  2150
2146  LET D=D1
2148  LET V=V9
2149  PRINT
2150  PRINT 'As before';
2151  INPUT T1
2152  LET Q5= 0
2154  IF T1= 0 GOTO  2350
2156  PRINT 'IF SULPHUR OR OX PRESENT (0)';
2157  INPUT O[ 0]
2158  PRINT
2159  PRINT
2160  PRINT '   Z, L';
2162  IF C>1 GOTO  2169
2164  IF O[ 0]> 0 GOTO  2179
2166  PRINT ', OX/S'
2168  GOTO  2180
2169  IF O[ 0]> 0 GOTO  2174
2170  PRINT ', OX,K-RAT'
2172  GOTO  2180
2174  PRINT ',K-RAT'
2176  GOTO  2180
2179  PRINT
2180  FOR N1=1 TO 11
2182    LET O[N1]=1
2183    IF C>1 GOTO  2194
2184    IF O[ 0]> 0 GOTO  2190
2185    LET T5= 0
2186    INPUT Z[N1],L[N1],O[N1]
2188    GOTO  2202
2190    INPUT Z[N1],L[N1]
2192    GOTO  2202
2194    IF O[ 0]> 0 GOTO  2200
```

```
2196    INPUT Z[N1],L[N1],O[N1],K[N1]
2198    GOTO  2202
2200    INPUT Z[N1],L[N1],K[N1]
2202    PRINT
2204    IF Z[N1]= 0 GOTO  2290
2206    IF L[N1]= 0 GOTO  2320
2208    IF O[ 0]> 0 GOTO  2270
2210    LET O[N1]=X[Z[N1]]/(16*O[N1]+X[Z[N1]])
2213    IF C=1 GOTO  2270
2214    LET K[N1]=K[N1]*O[N1]
2270  NEXT N1
2280  GOTO  2300
2290  LET N1=N1-1
2300  LET N2=N1
2302  IF B2= 0 GOTO  2310
2303  IF A9= 0 GOTO  2310
2305  LET O[ 0]=9
2310  GOTO  2350
2320  LET N2=N1-1
2350  IF C<24 GOTO  2368
2351  IF C>30 GOTO  2369
2352  IF T1= 0 GOTO  2361
2354  FOR I=1 TO N2
2355    LET C[I]=K[I]
2356  NEXT I
2361  LET I=12
2363  GOTO  2370
2368  PRINT '*',
2369  FOR I=1 TO N2
2370    LET Z= LOG (Z[I])
2380    LET T2=L[I]*L[I]
2390    LET E[I]= EXP (A[1,L[I]]*Z*Z+A[2,L[I]]*Z+A[3,L[I]])
2400    LET F[I]= EXP (B[1,T2]*Z*Z+B[2,T2]*Z-B[3,T2])
2410    LET C[I]=K[I]
2415    FOR J=1 TO N1
2416      LET E=E[I]
2417      LET Z=Z[J]
2418      GOSUB  3310
2419      LET M[I,J]=T3
2420    NEXT J
2423    IF C<24 GOTO  2426
2424    IF C>30 GOTO  2426
2425    GOTO  2530
2426    IF I>11 GOTO  2474
2429  NEXT I
2442  IF C=1 GOTO  2450
2444  GOSUB  8500
2450  IF C>4 GOTO  2495
2454  FOR I=12 TO 13
2458    IF I>12 GOTO  2466
2462    LET Z[I]=18
2464    GOTO  2468
2466    LET Z[I]=32
2468    LET L[I]=1
2470    LET K[I]= 0
2472    GOTO  2370
2474  NEXT I
2495  GOTO  7140
2500  IF N5> 0 GOTO  2505
2502  PRINT
2505  IF N3<>1 GOTO  2510
2510  FOR I=1 TO N2
```

```
2526    REM
2527    REM
2530    LET T6=V/FCI]
2534    IF T6<10 GOTO  2540
2536    LET T6=10
2540    LET T7=.00873*T6^3-.1669*T6^2+.9662*T6+.4523
2550    LET T8=.002703*T6^3-.05182*T6^2+.302*T6-.1836
2560    LET T9=.887-3.44/T6+9.33/T6^2-6.43/T6^3
2565    FOR J=1 TO N1
2570      LET RCJ]=T7-T8* LOG (T9*ZCJ]+25)
2580      LET T2=14*(1- EXP (-.1*ZCJ]))
2585      LET T2=ZCJ]*(T2+75.5/ZCJ]^(ZCJ]/7.5)-ZCJ]/(100+ZCJ]))
2590      LET SC 0,J]=ZCJ]/XCZCJ]]* LOG (583*(V+FCI])/T2)
2640    NEXT J
2700    LET T7= 0
2705    LET T5= 0
2710    LET T8= 0
2720    LET T9= 0
2730    FOR J=1 TO N1
2740      LET T7=T7+CCJ]*SC 0,J]
2750      LET T8=T8+CCJ]*RCJ]
2760      LET T9=T9+CCJ]*MCI,J]
2765      LET T5=T5+CCJ]*1.2*XCZCJ]]/ZCJ]/ZCJ]
2770    NEXT J
2780    IF C>24 GOTO  2808
2784    LET T2=1+T9*D/400000*(V^1.65-FCI]^1.65)
2786    LET T2=(1+T5)/T2/(1+T5*T2)*T8
2787    IF I<12 GOTO  2791
2789    RETURN
2791    IF C=4 GOTO  2794
2792    LET NC1,I]=T2
2793    GOTO  2798
2794    LET NC1,I]=1/T2
2796    GOTO  3110
2798    LET T2=.0000012*( FNE(V)- FNE(FCI]))
2800    LET T4= FNF(T2*MCI,I]*D)
2802    LET T3= FNF(T2*T9*D)
2804    LET T2=RCI]*T3*T7/SC 0,I]/T8/T4
2806    GOTO  2830
2808    LET T2=T3*T7/T8
2830    LET Y= 0
2835    IF CCI]<= 0 GOTO  3061
2840    FOR J=1 TO N1
2850      IF CCJ]<= 0 GOTO  3060
2880      IF ECJ]<FCI] GOTO  3060
2890      IF ECJ]>FCI]+4 GOTO  3060
2900      LET T7=.5* EXP (HC1,LCJ]]* LOG (ZCJ])+HC2,LCJ]])
2910      LET T8= 0
2920      LET T6= 0
2950      LET T8=T8+MCJ,T6]*CCT6]
2955      LET T6=T6+1
2960      IF T6<=N1 GOTO  2950
2970      LET T6=T9*D/T8
2980      LET T5=333000/( FNE(V)- FNE(FCI]))/T8
2990      LET T6= LOG (1+T6)/T6+ LOG (1+T5)/T5
3040      LET T5= FNE((V/FCJ]-1)/(V/FCI]-1))*PCLCJ],LCI]]*GCLCI]]
3050      LET Y=Y+CCJ]*T7*MCJ,I]*T5*T6*XCZCI]]/XCZCJ]]/T8
3060    NEXT J
3061    LET Z2=CCI]/T2*(1+Y)
3063    IF C<24 GOTO  3080
3064    IF C>30 GOTO  3080
3065    LET Z2=(1+Y)/T2
3066    IF C=24 GOTO  9319
```

```
3068    IF C=26 GOTO  9565
3070    IF C=25 GOTO  9565
3080    LET T2=Z2
3085    IF C[I]= 0 GOTO  3110
3090    LET C[I]=(K[I]*C[I]*(1-T2))/(K[I]*(C[I]-T2)+T2*(1-C[I]))
3110  NEXT I
3112  IF C>3 GOTO  3114
3113  RETURN
3114  IF C=4 GOTO  8210
3115  IF N3=1 GOTO  3230
3200  GOSUB  8500
3230  LET N3=N3-1
3235  RETURN
3240  IF B2> 0 GOTO  6380
3241  LET T2= 0
3242  LET T1= 0
3243  LET T4= 0
3244  LET T3= 0
3245  IF O[ 0]> 0 GOTO  3247
3246  IF M2> 0 GOTO  3267
3247  PRINT 'ELEM(Z)','EL%','OX%'
3248  FOR I=1 TO N2
3250    IF O[ 0]> 0 GOTO  3261
3251    LET C[I]= INT (10000*C[I]+.5)/10000
3252    LET T3=C[I]/O[I]
3253    LET T3= INT (10000*T3+.5)/10000
3254    LET T2=T2+T3
3257    PRINT Z[I],100*C[I],100*T3
3258    GOTO  3262
3261    PRINT Z[I],100*C[I]
3262    LET T1=T1+C[I]
3264  NEXT I
3265  PRINT 'TOTAL',100*T1,100*T2,100*Q2
3266  GOTO  3293
3267  PRINT 'ELEM'; TAB (7);' OX'; TAB (13);' STRUCT'
3268  FOR I=1 TO N2
3269    IF C[I]> 0 GOTO  3271
3270    LET J[I]= 0
3271    LET T1=T1+C[I]
3272    LET T3=C[I]/O[I]
3273    LET C[I]=( INT (10000*C[I]+.5))/10000
3274    LET T2=T2+T3
3275  NEXT I
3276  FOR I=1 TO N2
3277    IF C[I]= 0 GOTO  3286
3278    LET T3=C[I]/O[I]
3279    LET J[I]=C[I]/X[Z[I]]*M2*X[8]/(T2-T1)
3280    LET T3=( INT (10000*T3+.5))/10000
3281    LET J[I]=( INT (1000*J[I]+.5))/1000
3282    LET T4=T4+T3
3283    GOSUB  650
3284    PRINT  TAB (6);100*T3; TAB (13);J[I]
3285    LET Q5=J[I]+Q5
3286  NEXT I
3287  IF M3<> 0 GOTO  3290
3289  PRINT ' TOTAL'; INT (10000*Q2+.5)/100;Q5
3290  IF M3= 0 GOTO  3293
3292  PRINT ' TOTAL',100*T2;Q5
3293  IF I[1]> 0 GOTO  792
3295  PRINT 'Trace Elements';
3296  INPUT A9
3297  PRINT
3298  IF A9> 0 GOTO  7000
3299  GOTO  9596
```

```
3310  LET T3= LOG (Z)
3320  LET UC1]= EXP (-.0045522*T3*T3-6.8535E-3*T3+1.07018)
3330  LET UC2]=2.73
3340  LET UC3]=2.6
3350  LET UC4]=2.22
3360  IF Z<42 GOTO  3380
3370  LET UC2]= EXP (-.113159*T3*T3+.836883*T3-.545969)
3380  LET T1=1
3390  IF T1=10 GOTO  3420
3400  LET T0= EXP (BC1,T1]*T3*T3+BC2,T1]*T3-BC3,T1])
3410  IF E<T0 GOTO  3460
3420  LET T0=WCVC2,T1]]*T3*T3+WCVC2,T1]+4]*T3+WCVC2,T1]+8]
3430  LET T0= EXP (T0)/VC1,T1]
3440  LET T3=T0*(12.398/E)^UCVC2,T1]]
3450  RETURN
3460  LET T1=T1+1
3470  GOTO  3390
3602  RETURN
3880  LET U=XCK]
4000  LET Q3= 0
4004  IF B9> 0 GOTO  4010
4006  FOR I=485 TO 503
4008    GOTO  4012
4010    FOR I=489 TO 499
4012      CALL 3,1,I,T2
4014      LET Q3=Q3+T2
4016    NEXT I
4018    IF B9> 0 GOTO  4024
4020    LET Q3=Q3/19
4022    GOTO  4025
4024    LET Q3=Q3/11
4025    LET T3= 0
4030    FOR I=144 TO 152
4035      CALL 3,1,I,T2
4040      LET T3=T3+T2
4044    NEXT I
4046    LET T3=T3/9
4048    LET T2= 0
4049    FOR I=1 TO N2
4050      IF ZCI]<>13 GOTO  4052
4051      LET T2=NC 0,I]*NC 0,I]*8.97E-8
4052    NEXT I
4053    LET JC13]=1
4054    FOR I=1 TO N2
4055      IF ZCI]<>12 GOTO  4057
4056      LET JC13]=NC 0,I]
4057      IF JC13]=1 GOTO  4060
4058      IF ZCI]<>14 GOTO  4060
4059      LET T2=T2+(JC13]*NC 0,I]*2.21E-8)
4060    NEXT I
4062    LET T3=T3-T2
4064    LET Q4=T3
4068    RETURN
4200    LET I=12
4210    GOSUB  2526
4215    LET Q5=T2
4220    LET I=13
4225    GOSUB  2526
4230    LET Z1=T2
4235    LET P0=(Q4-Q3)/(Q5-Z1*QC4,20])
4240    LET P1=Q4-P0*Q5
4245    RETURN
4400    IF C>19 GOTO  5000
4405    IF C>10 GOTO  4415
```

```
4410    GOTO  2060
4415    IF C>11 GOTO  4435
4420    PRINT " Program Data at";
4422    INPUT C,H7,T1
4424    GOTO  9900
4435    IF C>12 GOTO  4455
4455    IF C>13 GOTO  4505
4460    GOTO  7000
4505    IF C>14 GOTO  7000
4510    LET H7=1
4512    PRINT " DRIFT ";
4513    INPUT H7
4514    LET H8=H8*H7
4515    LET H9=H8/3
4516    PRINT "   TOTAL DRIFT=";H9
4520    GOTO  7000
5000    IF C>66 GOTO  9250
5005    GOTO  7000
6000    GOTO  6025
6025    LET T[1]= INT (E3*50+.5)
6030    LET T[2]= INT (E4*50+.5)
6035    FOR J=1 TO 2
6040      LET T2= 0
6045      FOR I=T[J]-5 TO T[J]+5
6050        CALL 3,2,I,T3
6055        IF T3<T2 GOTO  6065
6057        LET T2=T3
6060        LET T4=I
6065      NEXT I
6070      LET T8=-2-2*J
6072      LET T0=T8
6075      FOR I=1 TO 6
6080        LET T[I+2]= 0
6085      NEXT I
6090      FOR I=T4+T0 TO T4-T0
6095        CALL 3,2,I,T3
6100        LET T5= LOG (T3)
6105        LET T[3]=T[3]+T5
6110        LET T[4]=T[4]+T5*T8
6115        LET T[5]=T[5]+T5*T8*T8
6120        LET T[6]=T[6]+1
6125        LET T[7]=T[7]+T8*T8
6130        LET T[8]=T[8]+T8*T8*T8*T8
6135        LET T8=T8+1
6140      NEXT I
6145      LET T2=T[3]-T[6]*(T[3]*T[8]-T[5]*T[7])/(T[6]*T[8]-T[7]*T[7])

6150      LET T[7,1+2*J]=T4-.5*T[4]/T2
6155      LET T[8,1+2*J]=-2.77258*T[7]/T2
6160    NEXT J
6162    PRINT 20*T[9];20* SQR (T[10]);20*T[11];20* SQR (T[12])
6165    LET W3=1000*(E4-E3)/(T[11]-T[9])
6170    LET W4=1000*E3-W3*T[9]
6175    LET W7=W3*W3*(T[12]-T[10])/(E4-E3)/1000
6180    LET W8=T[10]*W3*W3-1000*W7*E3
6185    PRINT "EV/CH,ZERO ERROR(EV)";W3;-W4;"  RES"; SQR (W8+W7*5894)
6187    PRINT "W7=";W7;"W8=";W8
6190    PRINT "G ";(W3-20)/.09;"  Z  ";W4/8.5;" TURNS"
6191    LET W3=20
6192    LET W4= 0
6193    LET W7=2.392
6194    LET W8=19100
6195    PRINT " Again";
```

```
6200    INPUT T1
6202    PRINT
6205    IF T1> 0 GOTO  7000
6210    IF N6= 0 GOTO  7185
6215    CALL 1,2,T
6220    GOTO  6000
6380    LET T1= 0
6425    LET T1= 0
6430    LET T2= 0
6435    LET T3= 0
6440    LET T4= 0
6500    PRINT
6502    LET Q5= 0
6505    PRINT 'ELEM','ELX','SULPHX','STRUCT'
6506    FOR I=1 TO N2
6510      IF Z[I]<>16 GOTO  6525
6512      LET T2=C[I]
6525      LET C[I]=( INT (10000*C[I]+.5))/10000
6530      LET T1=T1+C[I]
6535    NEXT I
6540    FOR I=1 TO N2
6545      IF C[I]= 0 GOTO  6600
6548      IF Z[I]=16 GOTO  6596
6550      LET T3=C[I]*(X[Z[I]]+32.06)/X[Z[I]]
6555      LET J[I]=C[I]/X[Z[I]]*A9*X[16]/T2
6560      LET T3=( INT (10000*T3+.5))/10000
6565      LET J[I]=( INT (10000*J[I]+.5))/10000
6570      LET T4=T4+T3
6590      PRINT Z[I],100*C[I],100*T3,J[I]
6595      LET Q5=J[I]+Q5
6596      IF Z[I]<>16 GOTO  6600
6597      PRINT Z[I],100*C[I],'0','0'
6600    NEXT I
6605    IF M3<> 0 GOTO  6614
6610    PRINT 'TOTAL',100*Q2,'.',Q5
6614    IF M3= 0 GOTO  6625
6615    LET T1= 0
6616    FOR I=1 TO N2
6618      LET T1=T1+C[I]
6619    NEXT I
6620    PRINT 'TOTAL',100*T1,'.',Q5
6625    PRINT
7000    PRINT
7002    LET H5= 0
7003    LET H3= 0
7007    LET N5=1
7010    PRINT ' $ ';
7011    INPUT C
7012    IF C> 0 GOTO  7016
7013    PRINT ' SILICATES(0) OR ETCETERA(9)'
7014    INPUT B2
7015    GOTO  7000
7016    PRINT
7017    IF C=8 GOTO  200
7018    IF C>22 GOTO  9250
7020    IF C>9 GOTO  4400
7025    IF C>1 GOTO  7040
7026    LET J[12]=J[12]+1
7027    PRINT
7028    PRINT
7029    PRINT ' Sample=';
7030    FOR J=1 TO 4
7031      INPUT I[J]
```

```
7032      IF I[J]< 0 GOTO  7034
7033    NEXT J
7034    PRINT " OXND.=";
7035    INPUT M2
7036    IF M2<> 0 GOTO  950
7037    PRINT "NORMALISE";
7038    INPUT M3
7039    GOTO  7125
7040    IF C>2 GOTO  7055
7045    PRINT "   STD #";
7050    GOTO  7059
7055    IF C>3 GOTO  7070
7057    PRINT "   SUBSTD #";
7059    INPUT Z4
7061    PRINT "  FOR Z=";
7063    INPUT Z1
7064    LET Z4=Z1
7065    GOTO  7125
7070    IF C>4 GOTO  7085
7071    PRINT "BGD CALCN USING ?"
7072    LET N7=9
7076    INPUT N7
7077    LET N7=9
7080    GOTO  7125
7085    IF C>5 GOTO  7000
7087    PRINT " SPEC CALIBRATION ON PURE CU"
7088    PRINT " IS SPECTRUM READY (0)"
7089    INPUT N6
7090    LET N6=9
7091    LET E3=.93
7092    LET E4=8.04
7096    PRINT
7097    GOTO  6215
7099    GOTO  7125
7125    IF C<>1 GOTO  7130
7127    IF B2<>9 GOTO  7130
7128    PRINT "SULPHUR NO.";
7129    INPUT A9
7130    LET N3=4
7135    GOTO  2140
7140    IF C<6 GOTO  7185
7145    GOSUB  2500
7150    IF C=7 GOTO  7000
7160    IF N3> 0 GOTO  7145
7165    GOTO  3240
7185    LET X1=399
7188    PRINT " T1=";
7190    CALL 1,1,T1
7192    PRINT T1;
7195    IF T1<8 GOTO  7202
7200    LET X1=799
7202    CALL 3,1, 0,T1
7203    PRINT "Time=";T1;" EDAX free"
7207    IF C>4 GOTO  8180
7210    FOR I=1 TO X1
7215      CALL 3,1,I,T1
7220      LET D9=D9+T1
7225    NEXT I
7230    CALL 3,1, 0,T1
7232    PRINT "Tot Int=";D9
7233    LET D9=1/(1-D9/T1*.000016)
7234    FOR I=1 TO X1
7235      CALL 3,1,I,T1
7236      LET T1=T1*D9
```

```
7237      CALL 4,1,I,T1
7238    NEXT I
7240    FOR I=97 TO X1
7245      IF I>450 GOTO  7310
7250      CALL 3,1,I,T5
7255      LET T3=.001*(W4+W3*I)
7260      LET T6=T5*(.00199/T3+.00976-.00238*T3-1.593E-4*T3*T3)
7265      LET T5=T5+T6
7270      CALL 4,1,I,T5
7275      LET T7=I-87
7285      CALL 3,1,T7,T8
7290      LET T8=T8-T6
7292      IF T8> 0 GOTO  7296
7294      LET T8= 0
7296      CALL 4,1,T7,T8
7300    NEXT I
7310    FOR I=1 TO N2
7315      LET E=1000*E[I]
7320      LET T1= SQR (W8+E*W7)*.5-.5*W3
7325      LET D[ 0,I]= INT ((E-W4-T1)/W3)
7330      LET D[1,I]= INT ((E-W4+T1)/W3+.5)
7335    NEXT I
7337    GOSUB  7740
7340    FOR I=1 TO N2
7344      LET N[ 0,I]= 0
7346      FOR J=D[ 0,I] TO D[1,I]
7348        CALL 3,1,J,T3
7350        LET N[ 0,I]=N[ 0,I]+T3
7352      NEXT J
7356      LET N[ 0,I]=N[ 0,I]/(D[1,I]-D[ 0,I]+1)
7358      LET N[1,I]=N[ 0,I]
7360    NEXT I
7364    IF C=4 GOTO  8180
7366    IF C<>1 GOTO  7545
7368    LET N3=-2
7370    FOR I=1 TO N2
7372      FOR J=1 TO N2
7374        IF Z[J]<>Z[I]-1 GOTO  7380
7376        LET N[1,I]=N[1,I]-N[1,J]*Y[2,J]
7380      NEXT J
7382      FOR J=1 TO N2
7384        IF Z[J]<>Z[I]+1 GOTO  7390
7386        LET N[1,I]=N[1,I]-N[1,J]*Y[1,J]
7390      NEXT J
7392      IF N3=-2 GOTO  7398
7394      RETURN
7398    NEXT I
7400    LET N3=4
7402    FOR I=1 TO N2
7404      LET C[I]=N[1,I]/Y[ 0,I]/H8
7406      LET K[I]=C[I]
7408    NEXT I
7410    GOSUB  4000
7412    REM
7413    GOSUB  2510
7414    IF N3=1 GOTO  7531
7415    GOSUB  4200
7416    IF N3> 0 GOTO  7418
7418    FOR I=1 TO N2
7420      LET E=E[I]
7430      LET B9=Q4/Q5*N[1,I]*Q[5,I]
7431      IF B2=9 GOTO  7440
7432      IF Z[I]<18 GOTO  7440
```

```
7434      LET B9=P1+P0*NC1,I]*QC5,I]
7440      LET NC1,I]=NC 0,I]-B9
7441      IF N3> 0 GOTO  7443
7442      PRINT N3,ZCI],NC 0,I],NC1,I]
7443    NEXT I
7444    IF N3> 0 GOTO  7446
7446    FOR I=1 TO N2
7448      GOSUB  7372
7450      IF N3> 0 GOTO  7471
7471      LET KCI]=NC1,I]/YC 0,I]/H8
7472      IF (KCI]/OCI])>.002 GOTO  7475
7473      LET CCI]= 0
7474      LET NC1,I]= 0
7475      IF N3<3 GOTO  7490
7481      LET CCI]=KCI]
7490    NEXT I
7492    IF N3>-1 GOTO  7495
7493    GOTO  7520
7495    GOSUB  8500
7496    GOTO  7520
7499    IF N3<4 GOTO  7520
7505    FOR I=1TON1
7510      LET KCI]=CCI]
7515    NEXT I
7520    LET N3=N3-1
7521    FOR I=1 TO N2
7523    NEXT I
7530    IF N3>= 0 GOTO  7412
7531    IF M3> 0 GOTO  7536
7532    GOSUB  9100
7536    LET Q5= 0
7538    FOR I=1 TO N2
7541    NEXT I
7542    GOTO  3240
7545    IF C=4 GOTO  8180
7550    GOSUB  4000
7552    GOSUB  2510
7554    GOSUB  4200
7556    FOR I=1 TO N2
7558      LET B9=Q4/Q5*NC1,I]*QC5,I]
7560      IF ZCI]<18 GOTO  7564
7562      LET B9=P1+P0*NC1,I]*QC5,I]
7564      LET NC 0,I]=NC 0,I]-B9
7566      IF NC 0,I]>= 0 GOTO  7572
7568      LET NC 0,I]= 0
7572    NEXT I
7580    FOR I=1 TO N2
7582      IF ZCI]=Z4 GOTO  7586
7584    NEXT I
7586    LET Z3=I
7617    IF C=2 GOTO  7690
7620    FOR J=1 TO 3
7625      FOR I=1 TO N2
7630        IF I=1 GOTO  7645
7635        IF ZCI-1]<>ZCI]-1 GOTO  7645
7640        LET NC 0,I]=NC 0,I]-NC 0,I-1]*YC2,I-1]
7645        IF ZCI+1]<>ZCI]+1 GOTO  7655
7650        LET NC 0,I]=NC 0,I]-NC 0,I+1]*YC2,I+1]
7655      NEXT I
7660    NEXT J
7670    LET QC 0,Z4]=NC 0,Z3]/(CCZ3]/NC1,Z3])/H8/(H9*H9)
7675    PRINT
```

```
7680    PRINT "CONVERSION FACTOR =";Q[ 0,Z4]
7685    GOTO  7000
7690    IF Z3=1 GOTO  7700
7692    IF Z[Z3-1]<>Z[Z3]-1 GOTO  7700
7695    LET Q[1,Z4]=N[ 0,Z3-1]/N[ 0,Z3]
7700    IF Z[Z3+1]<>Z[Z3]+1 GOTO  7710
7705    LET Q[2,Z4]=N[ 0,Z3+1]/N[ 0,Z3]
7710    LET Q[ 0,Z4]=N[ 0,Z3]/(C[Z3]/N[1,Z3])/H8/(H9*H9)
7712    PRINT N[ 0,Z3],Z2
7715    PRINT
7720    PRINT "OLAP FACTORS";Q[1,Z4];Q[2,Z4]
7725    PRINT "CONVERSION FACTOR ";Q[ 0,Z4]
7730    GOTO  7000
7740    FOR I=1 TO N2
7742      IF B2= 0 GOTO  7745
7743      FOR J=21 TO 40
7744        GOTO  7750
7745        FOR J=1 TO 20
7750          IF Z[I]<>Q[3,J] GOTO  7775
7755          LET Y[ 0,I]=Q[ 0,J]
7760          LET Y[1,I]=Q[1,J]
7765          LET Y[2,I]=Q[2,J]
7768          LET Q[5,I]=Q[4,J]
7770          GOTO  7780
7775        NEXT J
7780      NEXT I
7785      RETURN
7900      FOR I=40 TO 200 STEP 2
7905        LET E=.02*I
7910        GOSUB  4200
7915        CALL 4,2,I,B9
7920      NEXT I
7925      CALL 2,2
7930      GOTO  7000
8180      GOTO  2510
8210      GOSUB  4000
8240      PRINT " BACKGROUND FACTORS CALCULATED FOR",V," KV"
8250      PRINT " Z[I]"," BGD FACTOR"
8260      FOR I=1 TO N2
8262        IF Z[I]<>18 GOTO  8266
8264        LET T3=T3*N[1,I]
8266      NEXT I
8268      FOR I=1 TO N2
8270        LET N[ 0,I]=N[ 0,I]*N[1,I]/T3
8280        PRINT Z[I],N[ 0,I]
8290      NEXT I
8300      GOTO  7000
8500      LET Q= 0
8505      LET V1= 0
8510      FOR J=1 TO N2
8515        LET V1=V1+C[J]/Q[J]
8520      NEXT J
8525      IF N1=N2 GOTO  8560
8530      IF Q[ 0]= 0 GOTO  8560
8535      LET Q=V1
8540      IF Q<=1 GOTO  8550
8545      LET Q=1
8550      LET C[N1]=1-Q
8555      RETURN
8560      FOR J=1 TO N2
8565        LET C[J]=C[J]/V1
8570        LET Q=Q+C[J]
8575      NEXT J
8580      IF Q[ 0]= 0 GOTO  8540
```

```
8585      RETURN
9000      LET E=1.739
9010      GOSUB  3600
9100      LET Q2= 0
9102      FOR J=1 TO N2
9103        IF M2= 0 GOTO  9106
9105        LET Q2=Q2+C[J]/Q[J]
9106        IF M2> 0 GOTO  9110
9107        LET Q2=Q2+C[J]
9110      NEXT J
9112      FOR J=1 TO N2
9114        LET C[J]=C[J]/Q2
9116      NEXT J
9120      RETURN
9150      LET C[I]= INT (10000*C[I]+.5)
9155      LET C[I]=C[I]/10000
9160      RETURN
9170      LET T3= INT (10000*T3+.5)
9175      LET T3=T3/10000
9180      RETURN
9200      FOR I=1 TO N2
9205        IF O[ 0]> 0 GOTO  9220
9210        LET C[I]=C[I]*100/T2
9215        GOTO  9225
9220        LET C[I]=C[I]*100/T1
9225      NEXT I
9230      RETURN
9250      PRINT
9255      IF C>23 GOTO  9287
9260      FOR L=1 TO N2
9265        LET C[L]= INT (100*C[L]+.5)
9270        LET C[L]=C[L]/100
9275        LET J[L]= INT (10000*J[L]+.5)
9280        LET J[L]=J[L]/10000
9285      NEXT L
9286      RETURN
9287      IF C>30 GOTO  9800
9288      LET A8= 0
9289      LET A9= 0
9291      IF C>30 GOTO  9800
9292      GOTO  9596
9596      PRINT ' No trace elements routines loaded. '
9597      GOTO  7000
9800      PRINT
9801      GOTO  7000
9900      PRINT
9904      PRINT 'Acc. Voltage=';V9;'  Drift Factor=';H9;' No. Analyses
='; J[12]
9934      FOR J=1 TO 20
9935        IF Q[3,J]= 0 GOTO  9940
9936        PRINT J; TAB (10);Q[3,J]; TAB (19);Q[ 0,J]; TAB (32);Q[1,J
];
9937        PRINT  TAB (38);Q[2,J]; TAB (46);Q[4,J]
9938        IF J>21 GOTO  9952
9940      NEXT J
9942      PRINT ' ********       *******'
9948      FOR J=21 TO 40
9949        IF Q[3,J]= 0 GOTO  9952
9950        GOTO  9936
9952      NEXT J
9960      GOTO  7000
9974      END
```

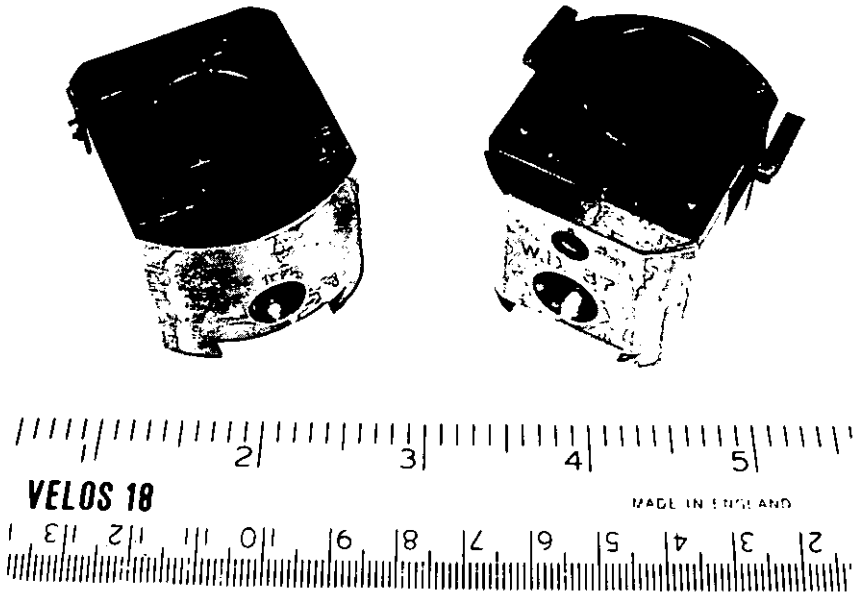

PLATE 1 The Jeol JXA-50A scanning electron microanalyses and EDAX energy dispersive analysis system at the Central Science Laboratory, University of Tasmania. The EDAX MCA console and V.D.U. are at left in the photograph.

PLATE 2 Sample holders used in microanalysis work. The standards are mounted in the replaceable brass strips in the surface of the holders. The holder on the left is used for work with polished thin sections and other glass slide mounts, the other holder is used with one inch diameter araldite mounts containing surface embedded specimens, e.g. experimental charges, ore samples.

IN PRESS:

Oxygen and carbon isotope evidence for seawater-hydrothermal alteration of the Macquarie Island Ophiolite

by

J.D. Cocker
Department of Geology
Oregon State University
Corvallis, Oregon 97331

B. J. Griffin
Geology Department
University of Tasmania
Hobart, Tasmania
Australia 7000

K. Muehlenbachs
Geology Department
University of Alberta
Edmonton, Alberta
Canada T6E 2E3

ABSTRACT

Rocks of the Miocene Macquarie Island ophiolite, south of New Zealand, have oxygen and carbon isotopic compositions comparable to those of seafloor rocks. Basalt glass and weathered basalts have $\delta^{18}O$ values at 5.8 to 6.0‰ and 7.9 to 9.5‰, respectively, similar to drilled seafloor rocks including samples from the Leg 29 DSDP holes near Macquarie Island. Compared to the basalt glass the greenschist to amphibolite facies metaintrusives are depleted in ^{18}O ($\delta^{18}O$ = 3.2 to 5.9‰) similar to dredged seafloor samples, whereas the metabasalts are enriched ($\delta^{18}O$ = 7.1 to 9.7‰). Although the gabbros are only slightly altered in thin-section they have exchanged oxygen with a hydrothermal fluid to a depth of at least 4.5 km. There is an approximate balance between ^{18}O depletion and enrichment in the exposed ophiolite section. The carbon isotopic composition of calcite in the weathered basalts ($\delta^{13}C$ = 1.0 to 2.0‰) is similar to those of drilled basalts, but the metamorphosed rocks have low $\delta^{13}C$ values (-14.6 to 0.9‰).

These data are compatible with two seawater circulation regimes. In the upper regime basalts were weathered by cold seawater in a circulation system with a high water/rock ratio (>>1.0). Based on calcite compositions weathering temperatures were less than 20°C and the carbon was derived from a predominantly inorganic marine source. As previously suggested for the Samail ophiolite, it is postulated that the lower hydrothermal regime consisted of two coupled parts. At the deeper levels, seawater circulating at low water/rock ratios (0.2 to 0.3) and high temperatures (300-600°C) gave rise to ^{18}O depleted gabbro and sheeted dikes via open system exchange reactions. During reaction the seawater underwent a shift in oxygen isotopic compositon ($\delta^{18}O$ = 1 to 5‰) and subsequently caused ^{18}O enrichment of the overlying metabasalts. In the shallower part of the hydrothermal regime the metabasalts were altered at relatively high water/rock ratios (1 to 10) and temperatures in the range 200-300°C. The relatively low seawater/rock ratios in the hydrothermal regime are supported by the low $\delta^{13}C$ values of calcite, interpreted as evidence of juvenile carbon in contrast to the inorganic

marine carbon found in the weathered basalts.

The similarity in stable isotopic composition between the Macquarie Island ophiolite, especially the weathered basalts, and seafloor rocks is added to the growing list of characteristics which indicate Macquarie Island is an uplifted section of oceanic crust. Consequently the hydrothermal model developed for this exposed crust, although simplified and in need of refinement, may be used to constrain hydrothermal processes at slow spreading ridges.

1. Introduction

The Macquarie Island ophiolite presents several advantages compared to other ophiolites to model alteration processes of the oceanic crust. Primarily the well-exposed ophiolite, which includes a pillow basalt sequence, sheeted dike complex, layered and massive gabbros, and a basal harzburgite section, is still in an oceanic rather than a continental environment [1,2]. The island is an emergent section of the central portion of the Macquarie Ridge which marks the dominantly transform boundary between the Pacific and Indian-Australian plates [3,4]. A compressional component of the movement along the ridge [5] and the tendency for buckling of the Indian-Australian Plate [6] may have caused the emergence of the island in middle or late Pleistocene time [7]. The ophiolite is Miocene in age [1,8] and formed on the Indian-Australian - Antarctic Ridge to the south of its present position. Also, several studies have shown that the rocks of this complex resemble ocean floor rocks petrographically [2,9] and chemically. The Macquarie Island basalts and dikes range compositionally from typical ocean-floor basalts to more alkaline varieties, enriched in some incompatible trace elements, particularly Nb (20-60ppm), similar to ocean-floor basalts from the "abnormal" ridge segments near 45°N and 36°N (FAMOUS area) on the Mid-Atlantic Ridge [2]. The strontium, isotopic composition (0.70229-0.70276) of minimally altered rocks [10,11] is also comparable to the isotopic composition of seafloor rocks. The magnetic properties [11,12,13] of the upper level extrusives as well as the seafloor magnetic anomaly pattern [4,13] traced across the island, indicate that the ophiolite is an exposed section of oceanic crust. With these considerations in mind we examined the oxygen and carbon isotope geochemistry of the ophiolite, anticipating similarities with the seafloor and lack of emplacement or post-emplacement disturbance to the isotopic systems.

Stable isotope studies have contributed substantially to our understanding of the nature and extent of alteration of the oceanic crust. Drilled and dredged samples of layers 2 and 3 of the oceanic crust indicate extensive exchange between the crust and sea water [14-19]. Cold seawater weathered, pillow basalts are enriched in ^{18}O compared to unaltered basaltic glass as a result of non-equilibrium replacement of the basalt by smectites, iron oxides and calcite. At deeper levels, relatively high temperature hydrothermal alteration (>300°C) and metamorphism gives rise to a decrease in ^{18}O in dredged greenschist and amphibolite facies metabasalts, metagabbros, and serpentinites. As our understanding of alteration processes is restricted by lack of exposure of the deeper levels of oceanic crust, the Macquarie Island ophiolite provides constraints for a model of crustal alteration especially as the complex has not experienced any continental geochemical influences such as groundwaters equilibrated with silicic rocks.

Although the Macquarie Island ophiolite is strongly faulted, all the components of an ophiolite (Figure 1) are exposed [1,2]. Over most of the island pillow basalts and minor volcanic breccias, massive lavas, oozes and interpillow sediments crop out. The extrusives range from fresh tholeiitic glass among cold temperature, seawater weathered pillow lavas and breccias through zeolite to lower greenschist facies metabasalts. The extrusives are intruded by dolerite dikes and some fault bounded blocks are entirely composed of uralitized dolerite dike swarm. Dolerite dikes also intrude layered and massive gabbros and partially serpentinized harzburgite. The gabbros which are remarkably unaltered comprise some 15% of the area of the island. Most basalt and dike outcrops are cut by narrow veins with calcite, clay, zeolite and prehnite being common vein phases.

2. Analytical Procedures

The silicate samples were analyzed by the BrF_5 method [20] and the carbonate from veins and disseminated grains in whole rock samples by H_3PO_4 decomposition [21].

The data are reported with respect to the SMOW and PDB Standards for $\delta^{18}O$ and $\delta^{13}C$, respectively, in the usual δ notation. The fractionation factor between CO_2 and water was taken to be 1.0407 [22]. Reproducibility of replicate oxygen analysis is ± 0.1‰ and ± 0.3‰ for disseminated carbonate (1σ). During the period of this study the $\delta^{18}O$ value of NBS-28 was 9.6 ± 0.1‰ (1σ, 7 analyses).

3. Results

Glass is preserved as pillow selvedges and hyloclastite breccias in pillow sequences which have been weathered and partially replaced by calcite and smectite. Representative analyses of glasses, including two samples whose $\delta^{18}O$ values (Table 1) have been determined, are given in Table 2. The oxygen isotopic composition of three basaltic glass samples is in the range $\delta^{18}O$ = 5.8 - 6.0‰ (Figure 2A) and is identical to glass and phenocryst mineral compositions for basalts from the sea floor [17,18,23,24,25,26]. $\delta^{18}O$ values in this range are considered to be representative of the unaltered composition of magmas from the oceanic mantle and this appears to be the case for the Macquarie Island basalts which are relatively alkali-rich.

The low temperature weathered basalts with secondary phases smectite, calcite and iron oxides are enriched in ^{18}O compared to unaltered glass. $\delta^{18}O$ values range from 7.9 to 9.5‰ (Table 1) reflecting the progressive alteration of fresh basalt ($\delta^{18}O$ = 5.8‰) to smectite ($\delta^{18}O \simeq 21$-25‰), calcite ($\delta^{18}O \simeq 30$-32‰) and iron oxides ($\delta^{18}O \simeq 15$-20‰). This alteration is pervasive although variable throughout the drilled oceanic crust and has been shown to occur to a depth of at least 600 m [17,18,26,29]. Enrichments in ^{18}O ($\delta^{18}O$ = 7.0 to 8.4‰), similar to those for the ophiolite, were found in DSDP Holes 278, 279, and 279A (Leg 29) of Oligocene-Miocene age to the south and north of Macquarie Island in the South Emerald Basin and on the Macquarie Ridge, respectively. Comparisons with other ophiolites cannot be made for the cold, seawater weathered basalts because basalts altered at less than 100-200°C are not preserved.

The weathering by cold seawater of the upper level basalts from Macquarie Island is shown by the isotopic composition of disseminated calcite. Calcite from the weathered basalts has $\delta^{18}O$ values in the range 29.6 to 33.0‰ (Table 1) and is similar to calcite found in the Leg 29 samples (34.0-35.1‰) (Figure 2B) and disseminated and vein calcite in many sections of the upper basaltic oceanic crust [15,18,19,26,27,28,29]. An alteration temperature of 3-17°C (Table 1) can be calculated from the $\delta^{18}O$ analyses of the calcite [30] on the assumption the carbonate was precipitated in equilibrium from normal seawater ($\delta^{18}O$ - 0‰). The $\delta^{13}C$ values, +0.7 to -2.2‰ indicate that the source of carbon in these basalts was largely dissolved inorganic carbon in seawater, again comparable to the Leg 29 data (+1.0 to -0.8‰) and the drilled basalts elsewhere. A small component of oxidized organic carbon may be expected in the relatively shallow upper levels of the basalt sequence and may give rise to the slightly negative $\delta^{13}C$ values [29].

Calcite from a natrolite-gyrolite-calcite vein cutting zeolite facies basalts has a $\delta^{18}O$ value of 28.1‰ indicating an apparently low temperature (24°C), but the depleted $\delta^{13}C$ value (-18.9‰) of this calcite suggests organic carbon or juvenile sources. Similar carbon isotopic compositions have rarely been observed in DSDP basalts and have been attributed to closed vein fluid circulation in contact with oxidized organic-rich sediment [18]. If the carbon isotopic composition reflects a closed system, then the assumption of $\delta^{18}O$ = 0‰ for the fluid is incorrect and the apparent temperature of calcite formation is probably higher in this sample. Relatively depleted $\delta^{13}C$ values of the deeper levels metamorphosed rocks are discussed below.

Using oxygen isotope compositions, the metamorphosed rocks are divided into two groups. The intrusive rocks including sheeted dike swarms, gabbros, and serpentinized harzburgites are depleted in ^{18}O whereas the extrusive zeolite to lower greenschist facies metabasalts are enriched in ^{18}O relative to basaltic

glass (Table 1, Figure 2A). The greenschist and amphibolite facies metaintrusive rocks have δ^{18} values in the range 2.6 to 5.9‰. Similar depletions occur in gabbros and serpentinites dredged and drilled from the oceanic crust [16,26,32,33]. The ^{18}O depletion of these deeper level rocks has been attributed to high temperature (>300°C) exchange with seawater ($\delta^{18}O$ 0‰) [16,32,33,39].

To further understand the nature of the hydrothermal alteration a preliminary study has been made of the oxygen isotopic composition of clinopyroxene and plagioclase in the gabbro section on Macquarie Island. For rocks which are clearly depleted in ^{18}O there is relatively little petrographic evidence for subsolidus alteration. The clinopyroxene is rarely replaced along margins by hornblende and plagioclase is replaced by less than 2% calcite and talc. Olivine is partially replaced by talc, magnetite, actinolite, and serpentine (30-60%). The talc + magnetite assemblage is indicative of high alteration temperatures in accord with the whole rock oxygen isotopic compositions. Also, there is clear isotopic disequilibrium between clinopyroxene and plagioclase in most samples with plagioclase depleted by up to 2.5‰ from igneous values of 6.0‰. In three gabbros the clinopyroxene is also depleted and in one sample (38357) has a $\delta^{18}O$ value similar to the coexisting depleted plagioclase. This disequilibrium exchange pattern is characteristic of open rather than closed system conditions [35]. As the clinopyroxene and plagioclase are virtually pristine, lacking hydrous replacement phases, the hydrothermal alteration evident from the depleted ^{18}O compositions must have occurred at high temperatures (probably greater than 400°C) and relatively low water/rock ratios. Under these conditions plagioclase and clinopyroxene are stable, but exchange oxygen with the hydrothermal fluid. This pattern of alteration and degree of depletion are similar in both the massive and layered gabbro on Macquarie Island and are similar to that found in gabbro of the Skaergaard intrusion [36] and especially the Samail ophiolite [35].

In contrast, the metabasalts whose metamorphic grade overlaps with the metaintrusives are enriched with $\delta^{18}O$ values in the range 6.9 to 9.6‰ (Figure 2A). In fact, the degree of enrichment is similar to that found in the low temperature weathered basalts. Included in this group are three sub-greenschist facies dikes which intrude zeolite to lower greenschist facies metabasalts. Zeolite to greenschist facies metabasalts in the E. Liguria [31], Pindos [31], Troodos [31,32] and Chilean [37,38] ophiolites also show ^{18}O enrichment in contrast with dredged submarine greenstones which are commonly depleted to only slightly enriched ($\delta^{18}O$ - 2.8 to 6.8‰) [33,39,40]. Although the metabasalts are ^{18}O enriched compared to the metaintrusives, the isotopic compositons of disseminated calcite in both groups are similar. The carbonates have $\delta^{18}O$ and $\delta^{13}C$ values in the range 12 to 26‰ and 0.9 to -14.6‰, respectively (Figure 2B). Such a wide range in $^{13}C/^{12}C$ ratios of carbonates in the metamorphosed rocks has not been found in sea floor rocks, the most depleted composition being -6.6‰ [33]. The calcite isotope compositions of the metamorphics are clearly different to those of the low temperature weathered basalts at higher levels in the oceanic crust.

4. Discussion

The Macquarie Island ophiolite has a range in oxygen isotopic composition comparable to that known for the oceanic crust. The basaltic glass, cold, seawater weathered basalts and secondary calcite have oxygen and carbon isotopic compositions comparable to those of drilled layer 2 of the oceanic crust, including nearby DSDP holes. These data are another important link in establishing the "pedigree" of the ophiolite as oceanic crust and providing evidence necessary to use the deeper units of the ophiolite to model the lower oceanic crust. The deeper level metamorphosed dikes, gabbro and harzburgite bodies also have isotopic compositions comparable to those of rocks dredged from the sea floor, further linking the ophiolite to the ocean crust.

Based on this relatively small number of oxygen isotope results and the preliminary stratigraphic section through the ophiolite, there is a balance between rocks depleted and enriched in ^{18}O. Assuming a simple and regular stratigraphy, there is a 1.5 km basalt sequence with an average $\delta^{18}O$ value of 8.3‰, enriched by 2.5‰ from a pristine mantle composition of 5.8‰. The intrusives are estimated to be 3.5 km thick and with an average $\delta^{18}O$ value of 4.5‰, depleted by 1.3‰. Although the overall balance in oxygen isotopic composition is strongly dependent on the stratigraphic thickness, these data support Muehlenbachs and Clayton's [17] model for the alteration of the oceanic crust and the constant $\delta^{18}O$ composition of seawater. This balance is established for the ophiolite despite the evidence for isotopic aging of fluids and possible successive alteration events to be discussed below. A similar balance has been found in the Samail ophiolite [35] in which there is evidence for evolution of the hydrothermal fluid isotopic composition.

The oxygen isotopic depletion of the intrusives in the ophiolite is contrasted with the enrichment of the greenschist facies metabasalts. For metabasaltic rocks enrichment or depletion will depend on the temperature, the modal mineralogy of the altered rock, the isotopic composition of the hydrothermal fluid and the water/rock (W/R) ratio. Without isotopic results for minerals or other independent geothermometry, specific models for the hydrothermal alteration are difficult to construct and involve several assumptions. The model developed below for the deeper hydrothermal circulation links the alteration of the metabasalts to the reaction of the intrusives with seawater at relatively low W/R ratios. This is in contrast to the upper circulation regime in which cold seawater reaction gave rise to the weathered basalts.

For a closed system exchange between seawater and basalt rock the W/R ratio (atomic percent) is given by [41]:

$$W/R = \frac{\delta^{f}_{rock} - \delta^{i}_{rock}}{\delta^{i}_{seawater} - (\delta^{f}_{rock} - \Delta)} \qquad (1)$$

where i = initial value, f = final value and the ^{18}O fractionation factor $\Delta = \delta^{18}O^{f}_{rock} - \delta^{18}O^{f}_{water}$. Δ is a function of temperature and for basaltic rocks can be approximated by plagioclase (An_{60})-water isotopic exchange [42]:

$$\Delta = \frac{2.3}{T^{2}} \times 10^{6} - 3.74 \qquad (2)$$

where T is temperature (°K). Using these relationships, metabasalts reacting to equilibrium at approximately 250°C will undergo little change in $^{18}O/^{16}O$ ratios from the primary composition (5.8‰) if the hydrothermal fluid is seawater. However, at higher temperatures in the range 300-600°C altered rocks of basaltic composition would be depleted and the hydrothermal fluid enriched assuming a closed system, equilibrium rock-seawater reaction. Using equations (1) and (2) the degree of enrichment can be calculated for varying W/R ratios. For low W/R ratios (0.2 to 0.3) at equilibrium, the depleted intrusive sequence would have $\delta^{18}O$ values in the range 5.3 to 4.5‰, whereas the seawater would be enriched with $\delta^{18}O$ values of 1.6 to 5.3‰ for temperatures of 300 to 600°C. For higher W/R ratios (W/R = 1.0) the seawater is not as strongly enriched ($\Delta^{18}O$ = 1.3 to 1.2‰). The evolution in the fluid composition is little changed if an open system [41] circulation pattern which is indicated by the plagioclase-pyroxene data from the gabbroic rocks, is used in the calculation. The isotopically shifted seawater is then able to react with overlying rocks and also exit to the seafloor.

The reaction between the isotopically shifted seawater and the metabasalts can be modelled using equations (1) and (2) for varying W/R ratios and temperatures in the range 200 to 300°C. Assuming the seawater reacting with the lower greenschist metabasalts is shifted to a $\delta^{18}O$ value of 5‰, the metabasalts are enriched to 7.2 to 11.2‰ at W/R ratios in the range 1-10. Lower W/R ratios

and higher temperatures would not give rise to the measured enrichments in the metabasalts ($\delta^{18}O$ = 7.1-9.7‰). If the seawater on reaction with the intrusives is only enriched to 4‰, the metabasalts are enriched to $\delta^{18}O$ values of 8.4 to 10.3‰ only at the lower end the considered temperature range (200°C). Using plagioclase compositions similar to those in the metabasalts and allowing plagioclase to reequilibrate to low temperatures (100°C) in the presence of the hydrothermal fluid increases the degree of enrichment in the model calculations. The greater enrichment of the zeolite facies metabasalts is consistent with lower temperature metamorphism compared to the lower greenschist facies rocks. Also in some areas there is mineralogical evidence for retrograde zeolite facies conditions after the formation of greenschist facies phases. Such retrograde metamorphism would be consistent with relatively high $\delta^{18}O$ values.

The model for the hydrothermal alteration of the Macquarie Island ophiolite links the metamorphism of the basalts to that of the intrusive rocks. The metabasalt oxygen isotope compositions require reaction with an enriched fluid ($\delta^{18}O$ = 3 to 5‰) at relatively high W/R ratios (W/R = 1 to 10) and low temperatures (200 to 300°C). Two sources for hydrothermal fluid with $\delta^{18}O$ > 0‰ in the oceanic crust are seawater which has an isotopically shifted composition after high temperature reaction with rocks of basaltic composition, and magmatic water. Although there is evidence for magmatic volatiles from the carbon isotopic composition (discussed below) magmatic water is considered to be a minor component in the hydrothermal fluid because of the pervasive isotopic depletion of the intrusive rocks. It is postulated that isotopically shifted seawater is generated by reaction of seawater ($\delta^{18}O$ = 0‰) with the intrusives at high temperatures (300-600°C) and low W/R ratios (0.2 to 0.3). The W/R ratios used in this calculation are low in order to give rise to a strongly ^{18}O shifted fluid and still cause a decrease in the $\delta^{18}O$ value of the intrusives, comparable to that measured for the ophiolite. The isotopically shifted seawater from deeper levels of the

hydrothermal system rises to interact with the overlying basalts. Evolution in the isotopic composition of seawater is supported by recent data from active seafloor systems [48] with enriched fluids ($\delta^{18}O$ = 1.6‰). The model discussed above is based on relatively low W/R ratios. Although calculated ratios are minimum values it is clear that the hydrothermal system was rock-dominated [43]. However, evidence for seawater dominated alteration may be expected among strongly veined areas in both dike swarms and metabasalts on Macquarie Island.

The relatively depleted carbon isotopic compositions from the deeper hydrothermal regime effectively distinguishes this regime from that which characterized the weathered basalts. The calcite in cold, seawater weathered basalts has both oxygen and carbon isotopic compositions comparable to those of drilled layer 2 and is compatible with a relatively high water/rock ratio (>1.0), seawater circulation system. However, the carbon isotopic composition of metamorphosed rocks ($\delta^{13}C$ = -14.6 to 0.9‰) suggests either several carbon sources or variable pH, fO_2 and carbon species in solution. Three carbon sources are plausible for this range in isotopic composition - inorganic carbon in seawater ($\delta^{13}C$ = 0.0 to 3.0‰) [44,18,29], organic carbon ($\delta^{13}C$ = -27.0 to -19.0‰) [44,45] and juvenile carbon ($\delta^{13}C$ = -9.0 to -2.0‰) [46,47]. It is clear that inorganic seawater carbon has not been the major carbon source in the metamorphosed rocks. It may be significant that the deeper level intrusives have an average $\delta^{13}C$ = -6.0‰, similar to the composition of trapped CO_2 in seafloor basalts [46] and CO_2 discharged at submarine hot springs [48]. Juvenile carbon, as CO_2 exsolved from magmas, could contribute to a hydrothermal fluid precipitating calcite in the $\delta^{13}C$ range -10.0 to 0.0‰ over a wide temperature interval (500-50°C) based on CO_2-calcite fractionation [49]. Also, CH_4-calcite fractionation [49] could give rise to depleted calcite in a hydrothermal system and CH_4 has been found in submarine hot springs ($\delta^{13}C$ = -18.0 to -20.0‰ [50]). The light carbon isotopic compositions may also reflect a partly organic source

although this is unlikely for rocks deep in the hydrothermal system. Variable pH and fO_2 will also influence the carbon isotopic composition and require assessment for different components of the circulation system. Although tentative, this carbon isotope data is supportive of the relatively low W/R ratios inferred from oxygen isotopic compositions as the deeper levels have not seen predominantly inorganic seawater carbon. Also the low $\delta^{13}C$ values indicate pervasive low temperature seawater circulation has not accompanied the emplacement of the island or contributed to the ^{18}O enrichment of the metabasalts.

If our interpretation of the oxygen isotopic composition of the calcite is correct, the temperatures shown in Figure 2B must be considered with caution. They are calculated on the assumption that the hydrothermal fluid was seawater ($\delta^{18}O$ - 0‰). This assumption is probably valid for the weathered basalts and the ^{18}O-depleted intrusives, but for the ^{18}O-enriched metabasalts the fluid may have been enriched relative to seawater. A few permil (2-3‰) enrichment of the fluid increases temperatures by approximately 20°C over the 50-100°C temperature range shown in Figure 2B. In that case the calculated temperatures in the metabasalts ranges from 70 to 110°C. The estimated temperatures are less than those expected for the greenschist and amphibolite facies indicating that the calcite either reequilibrated during translation away from the ridge and subsequent uplift, or was deposited during the waning stages of hydrothermal activity in the crust.

Although the model presented above is based on a number of assumptions which need refinement there is evidence that broadly similar hydrothermal systems existed in other ophiolites. A comprehensive oxygen isotope study of the Samail ophiolite [35] presents evidence for the evolution of the oxygen isotopic composition of seawater and the ^{18}O enrichment of greenschist facies dike rocks. The enrichment of the metabasalts rather than the dike swarm on Macquarie Island may reflect the different tectonic environment and hence different hydrothermal

systems along slow-spreading ridges with relatively small magma chambers [2,35]. There is evidence for enrichment in ^{18}O of the hydrothermal fluid in the Troodos ophiolite and although uncommon, enriched greenschist facies diabase dike rocks have been analyzed [32]. Several other ophiolites [32,37,38] have greenschist facies metabasalts with $\delta^{18}O$ values greater than 6.0‰, possibly reflecting shifts in isotopic composition of the hydrothermal fluid similar to those postulated for the Macquarie Island ophiolite. The ophiolite data for greenschist facies metabasalts is contrasted with that of dredged metabasalts which are depleted to slightly enriched. We have no clear explanation for this contrast. It is unlikely to be related to modal differences, but it may reflect higher temperatures and/or W/R ratios for hydrothermal systems sampled by dredge hauls mainly from transform fault scarps. These characteristics of the hydrothermal system may be in response to thinner oceanic crust along some transform faults [51].

The coupled hydrothermal model presented above for the deeper sections of the Macquarie Island ophiolite is not related to the cold, seawater weathering of the upper level basalts. The weathered assemblage is distinctive and the rocks have isotopic compositions compatible with low temperature (less than 20°C) replacement of igneous phases by ^{18}O enriched minerals [17,18,52]. The degree of replacement is markedly irregular and is a non-equilibrium process in contrast to the deeper metamorphic reactions.

5. Conclusions

The oxygen and carbon isotope geochemistry and postulated alteration patterns of the Macquarie Island ophiolite further confirm the oceanic origin of the ophiolite. The exposed crustal section has isotopic compositions comparable to those of drilled and dredged oceanic crust. The lower hydrothermal circulation system in operation when the ophiolite was formed penetrated to the base of the gabbro section and this pervasive alteration would not be detected without oxygen isotope analysis. There is an approximate overall balance between ^{18}O depleted

and enriched rocks in the ophiolite as is postulated for the oceanic crust [17] and has occurred despite inferred variations in W/R ratios and evolution of the fluid isotopic composition.

Two alteration regimes are evident at Macquarie Island. The upper circulation system with high seawater/rock ratios (>>1.0) gave rise to cold, seawater weathered basalts, which were strongly enriched in ^{18}O. This enrichment is similar to that found for the drilled oceanic crust, further substantiating the oceanic-ridge origin for the ophiolite. It is postulated that in the lower hydrothermal circulation system the metamorphism of the ^{18}O enriched greenschist facies metabasalts is coupled with the alteration of the ^{18}O depleted dikes and gabbros. Seawater reaction with the intrusives at low W/R ratios (>0.5) and high temperatures (300-600°C) in an open system gave rise to an enriched fluid ($\delta^{18}O$ = 2 to 5‰) which then caused the enrichment at lower temperatures (200-300°C) of the metabasalts. The carbon isotope data for calcite in the lower hydrothermal system indicates a juvenile source for carbon rather than inorganic marine carbon and is consistent with low W/R ratios inferred from the oxygen isotope data.

The metamorphosed rocks of the Macquarie Island ophiolite have oxygen isotopic compositions comparable to dredged seafloor rocks and other ophiolites. Among ophiolites broadly similar hydrothermal systems were operative and there is evidence for isotopically shifted seawater in ophiolites formed at both slow (Macquarie Island) and fast (Samail - [35]) spreading ridges. A point of contrast between Macquarie Island and the seafloor is the ^{18}O enrichment of the ophiolite metabasalts. Lack of ^{18}O enrichment among seafloor metabasalts may be attributable to sampling bias along transform faults where most dredged samples have been collected. Transform fault zones may have hydrothermal systems characterized by higher W/R ratios and temperatures reflecting the structure and possibly thinner, oceanic crust. Similar variations may well be found among ophiolites,

including Macquarie Island, especially in intensely veined sections. The advantage which the Macquarie Island ophiolite brings to the discussion of ophiolites and their relevance for modelling oceanic crust processes is the link between the drilled seafloor and weathered basalts of the ophiolite. With this link established the hydrothermal model deduced for the ophiolite may be used to constrain hydrothermal processes at slow-spreading ridges.

Acknowledgements

This work was supported by the National Science Foundation (EAR-8011411, to JDC), the National Research Council of Canada (to KM), and the Australian Department of Science (to BJC and JDC). Mrs. E. Toth's assistance with analytical work is gratefully acknowledged. We thank R. Varne for stimulating discussions.

REFERENCES

1. R. Varne and M. J. Rubenach, Geology of Macquarie Island and its relationship to oceanic crust, in: Antarctic Oceanology II: The Australian-New Zealand Sector, D. E. Hayes, ed., Am. Geophys. Union, Antarctic Res. Ser. 19 (1972) 251-266.

2. B. J. Griffin and R. Varne, the Macquarie Island Ophiolite complex: Mid-Tertiary oceanic lithosphere from a major ocean basin, Chem. Geol. 30 (1980) 285-308.

3. P. Williamson and B. D. Johnson, Crustal structure of the central region of the Macquarie Ridge Complex from gravity studies, Mar. Geophys. Res. 9 (1974) 127-132.

4. P. Williamson, Recent studies of Macquarie Island and the Macquarie Ridge Complex, Bull. Aust. Soc. Explor. Geophys. 5 (1974) 19-22.

5. T. Johnson and P. Molnar, Focal mechanisms and plate tectonics of the Southwest Pacific, J. Geophys. Res. 77 (1972) 5000-5032.

6. J. B. Minster and T. H. Jordan, Present-day plate motions, J. Geophys. Res. 83 (1978) 5331-5354.

7. E. A. Colhoun and A. Goede, Fossil penguin bones, ^{14}C dates and the raised marine terrace of Macquarie Island, some comments, Search 4 (1973) 499-501.

8. P. G. Quilty, M. Rubenach and J. A. Wilcoxon, Miocene ooze from Macquarie Island, Search 4 (1973) 163-164.

9. W. E. Cameron, E. G. Nesbit and V. J. Dietrich, Petrographic dissimilarities between ophiolite and ocean floor basalts, in: Ophiolites, A. Panayiotou, ed., Ministry of Agriculture and Natural Resources, Republic of Cyprus (1979) 182-192.

10. S. Williams and V. R. Murthy, Sr-isotopic and trace element geochemistry of the Macquarie Ridge Ophiolite Complex (abstr.), Trans. Am. Geophys. Union 58 (1977) 536.

11. S. K. Banerjee, Magnetism of the oceanic crust: evidence from ophiolite complexes, J. Geophys. Res. 85 (1980) 3557-3566.

12. S. Levi, S. K. Banerjee, S. Keske-Diehl and B. Moskowitz, Limitations of ophiolite complexes as models for the magnetic layer of the oceanic lithosphere, Geophys. Res. Lett. 5 (1978) 473-476.

13. P. Williamson, The paleomagnetism of outcropping oceanic crust on Macquarie Island, J. Geol. Soc. Aust. 25 (1979) 387-394.

14. D. G. Garlick and J. R. Dymond, Oxygen isotope exchange between volcanic materials and ocean water, Bull. Geol. Soc. Am. 81 (1979) 2137-2143.

15. K. Muehlenbachs and R. N. Clayton, Oxygen isotope studies of fresh and weathered submarine basalts, Can. J. Earth. Sci. 9 (1972) 172-184.

16. D. B. Wenner and H. P. Taylor, Oxygen and hydrogen isotope studies of the serpentinization of ultramafic rocks in oceanic environments and continental ophiolite complexes, Am. J. Sci. 273 (1973) 207-239.

17. K. Muehlenbachs and R. N. Clayton, Oxygen isotope composition of the oceanic crust and its bearing on seawater, J. Geophys. Res. 81 (1976) 4365-4369.

18. K. Muehlenbachs, The alteration and aging of the basaltic layer of the sea floor: oxygen isotope evidence from DSDP/IPOD Legs 51, 52 and 53, in: T. Donnelly, J. Francheteau, W. Bryan, P. Robinson, M. Flower, M. Salisbury, et al., eds., Initial Reports of the Deep Sea Drilling Project, 51, 52, 53 Part 2 (1979) Washington (U.S. Government Printing Office) 1159-1167.

19. J. R. Lawrence, J. I. Drever, T. F. Anderson and H. K. Brueckner, Importance of alteration of volcanic material in the sediments of Deep Sea Drilling Site 323: chemistry, $^{18}O/^{16}O$ and $^{87}Sr/^{86}Sr$, Geochim. Cosmochim. Acta 43 (1979) 573-588.

20. R. N. Clayton and T. K. Mayeda, The use of bromine pentafluoride in the extraction of oxygen from oxides and silicates for isotopic analysis, Geochim. Cosmochim. Acta 27 (1963) 43-52.

21. J. M. McCrea, On the isotopic chemistry of carbonates and a paleotemperature scale, J. Chem. Phys. 18 (1950) 849-857.

22. J. R. O'Neil, L. H. Adami and S. Epstein, Revised value for the ^{18}O fractionation between CO_2 and H_2O at 25°C, J. Res., U.S. Geol. Surv. 3 (1975) 623-6.

23. H. P. Taylor, The oxygen isotope geochemistry of igneous rocks, Contr. Mineral. Petrol. 19 (1968) 1-71.

24. F. Pineau, M. Javoy, I. W. Hawkins and H. Craig, Oxygen isotope variations in marginal basins and ocean-ridge basalts, Earth Planet. Sci. Lett. 28 (1976) 299-307.

25. T. K. Kyser and J. R. O'Neil, Oxygen isotope relations among oceanic tholeiites, alkali basalts, and ultramafic nodules, U.S. Geol. Surv. Open-File Rept. 78-701 (1978) 237-240.

26. H. Friedrichsen and S. Boernes, Oxygen and hydrogen isotope exchange reactions between sea water and oceanic basalts from Legs 51 through 53, in: T. Donnelly, J. Francheteau, W. Bryan, P. Robinson, M. Flower and M. Salisbury et al., eds. Initial Reports of the Deep Sea Drilling Project, 51, 52, 53 Part 2 (1979) Washington (U.S. Government Printing Office) 1177-1181.

27. J. R. Lawrence, J. J. Drewer and M. Kastner, Low temperature alteration of basalts predominates at DSDP site 395, in: W. G. Melson and P. D. Robinowitz, et al., eds., Initial Reports of the Deep Sea Drilling Project, 45 (1978) Washington (U.S. Government Printing Office) 609-612.

28. M. Javoy and A. M. Fouillac, Stable isotope ratios in Deep Sea Drilling Project Leg 51 basalts, in: T. Donnelly, J. Francheteau, W. Bryan, P. Robinson, M. Flower and M. Salisbury, et al., eds., Initial Reports of the Deep Sea Drilling Project, 51, 52, 53 Part 2 (1980) Washington (U.S. Government Printing Office) 1153-1157.

29. T. F. Anderson, Stable isotope evidence for the origin of secondary carbonate veins in Deep Sea Drilling Project Leg 58 basalts, in: G. de Vries Klein and K. Kobayashi, et al., eds., Initial Reports of the Deep Sea Drilling Project 58 (1980) Washington (U.S. Government Printing Office) 905-911.

30. J. R. O'Neil, R. W. Clayton and T. K. Mayeda, Oxygen isotope fractionation in divalent metal carbonates, J. Chem. Phys. 51 (1969) 5547-5558.

31. E. T. C. Spooner, R. D. Beckinsale, W. S. Fyfe and J. D. Smewing, ^{18}O enriched ophiolitic metabasic rocks from E. Liguria (Italy), Pindos (Greece), and Troodos (Cyprus), Contr. Mineral. Petrol. 47 (1974) 41-62.

32. T. D. Heaton and S. M. F. Sheppard, Hydrogen and oxygen isotope evidence for sea-water-hydrothermal alteration and ore deposition, Troodos complex, Cyrpus, in: Volcanic Processes in Ore Genesis, Geol. Soc. London, Spec. Paper 7 (1977) 42-57.

33. K. Muehlenbachs and R. N. Clayton, Oxygen isotope geochemistry of submarine greenstones, Can. J. Earth Sci. 9 (1972) 471-478.

34. K. Muehlenbachs, Oxygen isotope geochemistry of DSDP Leg 36 basalts, in: R. S. Yeats and S. R. Hart, et al., eds., Initial Reports of the Deep Sea Drilling Project 34 (1976) Washington (U.S. Government Printing Office) 337-339.

35. R. T. Gregory and H. P. Taylor, An oxygen isotope profile in a section of Cretaceous oceanic crust, Samail ophiolite, Oman: Evidence for $\delta^{18}O$ buffering of the oceans by deep (>5km) seawater-hydrothermal circulation at mid-ocean ridges, J. Geophys. Res. 86 (1981) 2737-2755.

36. H. P. Taylor and R. W. Forester, An oxygen and hydrogen isotope study of the Skaergaard Intrusion and its country rocks: A description of a 55 my old fossil hydrothermal system, J. Petrol. 20 (1979) 355-420.

37. C. Stern, M. J. DeWit and J. R. Lawrence, Igneous and metamorphic processes associated with the formation of Chilean ophiolites and their implication for ocean floor metamorphism, seismic layering and magnetism, J. Geophys. Res. 81 (1976) 4370-4380.

38. D. Elthon and C. Stern, Vertical variations in the effects of hydrothermal metamorphism in Chilean ophiolites: their implications for ocean floor metamorphism, Tectonophysics 55 (1979) 179-213.

39. K. Muehlenbachs, Oxygen isotope geochemistry of rocks from DSDP Leg 37, Can J. Earth Sci. 14 (1977) 771-776.

40. D. S. Stakes and J. R. O'Neil, Stable isotope composition of hydrothermal minerals from altered rocks from the East Pacific Rise and Mid-Atlantic Ridge (abstr.), Trans. Am. Geophys. Union 58 (1977) 1151.

41. H. P. Taylor, Water/rock interactions and the origin of H_2O in granitic batholiths, J. Geol. Soc. London 133 (1977) 509-558.

42. J. R. O'Neil and H. P. Taylor, The oxygen isotope and cation exchange chemistry of feldspars, Am. Mineral. 52 (1967) 1414-1437.

43. M. J. Mottl and W. E. Seyfried, Sub-seafloor hydrothermal systems rock-vs. seawater-dominated, in: P. A. Rona and R. P. Lowell, eds., Seafloor Spreading Systems (1980) Dowden, Hutchinson and Ross, Inc., Stroudsburg 66-82.

44. P. Kroopnick, The dissolved O_2-CO_2-^{13}C system in the eastern equatorial Pacific, Deep Sea Res. 21 (1978) 211-227.

45. B. J. Eadie, L. M. Jeffrey and W. N. Sackett, Some observations on the stable carbon isotope composition of dissolved and particulate organic carbon in the marine environment, Geochim. Cosmochim. Acta 42 (1978) 1265-1269.

46. F. Pineau, M. Javoy and Y. Bottinga, $^{13}C/^{12}C$ ratios of rocks and inclusions in popping rocks of the Mid-Atlantic ridge and their bearing on the problem of isotopic composition of deep-seated carbon, Earth Planet. Sci. Lett. 29 (1976) 413-421.

47. M. Javoy, F. Pineau and I. Iyama, Experimental determination of the isotopic fractionation between gaseous CO_2 and carbon dissolved in tholeiitic magma: A preliminary study, Contribs. Mineral. Petrol. 67 (1978) 35-40.

48. H. Craig, J. A. Welhan, K. Kim, R. Poreda and J. E. Lupton, Geochemical studies of the 20°N EPR hydrothermal fluids (abstr.), Trans. Am. Geophys. Union 61 (1980) 992.

49. Y. Bottinga, Calculated fractionation factors for carbon and hydrogen isotope exchange in the system calcite-carbon dioxide-graphite-methane-hydrogen-water vapor, Geochim. Cosmochim. Acta 33 (1969) 49-64.

50. J. Welhan, Gas concentrations and isotope ratios at the 21°N EPR hydrothermal site (abstr.), Trans. Am. Geophys. Union 61 (1980) 996.

51. P. J. Fox, R. S. Detrick and G. M. Purdy, Evidence for crustal thinning near fracture zones: implications for ophiolites, in: Ophiolites, A. Panayiotou, ed., Ministry of Agriculture and Natural Resources, Republic of Cyprus (1979) 161-168.

52. H. Staudigel, K. Muehlenbachs, S. H. Richardson, and S. R. Hart, Agents of low temperature ocean crust alteration, Contribs. Mineral. Petrol. (1981) in press.

Table 1

Oxygen and carbon isotopic results for rocks and minerals of the Macquarie Island Ophiolite and DSDP Leg 29 Holes 278, 279, 279A.

Sample	H_2O^+ (wt %)	$\delta^{18}O$ (Whole Rock)	$\delta^{18}O$ Plagioclase	$\delta^{18}O$ Clinopyroxene	$\delta^{18}O$ Calcite	$\delta^{13}C$ Calcite	T°C*
Glass							
BG 348		5.8					
BG 157		5.8					
BG 256		6.0					
Weathered basalt							
BG 35	2.14	8.8			29.6	0.4	17
38265	4.03	9.5			31.0	+ 2.2	11
38391	1.54	7.9			31.0	0.7	3
Zeolite facies basalt							
BG 157	3.36	9.0			21.0	0.2	65
38188	3.55	8.2			22.0	- 7.3	58
38310	4.06	9.7			19.6	- 3.7	75
BG 11 (calcite vein)					28.1	-18.9	24
Lower greenschist facies basalt							
BG 43		8.8			22.9	-10.7	52
BG 56D	1.76	7.1			21.9	0.9	59
BG 56G	2.08	7.7			22.4	- 2.0	55
BG 108C	1.43	7.2			19.0	- 9.1	79
BG 119	2.50	8.8			17.8	-12.4	89
BG 199	1.43	8.3			19.5	-14.6	75
BG 340 (calcite vein)					16.8	- 3.2	98
Weathered dolerite dike							
BG 231	1.93	8.3			23.0	- 3.3	51
38337	1.10	6.9					
38471	3.44	8.8			23.1	- 6.0	51
Uralitized dolerite dike							
BG 153	1.87	6.0			20.6	- 9.2	67
38157	2.29	5.9			21.6	- 7.0	60
38236	2.43	6.0			12.5	- 5.9	145
38451	2.07	6.1			18.5	+ 5.5	83
Gabbro							
massive upper							
38375		3.6	3.5	5.0	18.4	-11.1	94
38345	1.82	5.7			18.1	- 3.8	87
38374		5.3	5.7	5.2	17.5	- 6.8	92
3774) (xenolith in dike)		2.6	3.6	5.5	17.2	-13.0	94
layered							
38365	4.48	6.2			20.2	- 0.8	70
38357		6.3	4.4	6.3	18.8	- 8.5	81
38368		5.3	6.0	5.5	25.1	- 0.8	37
38394		4.7	5.1	5.6			
38484		6.1			25.3	0.2	36
massive lower							
38381		4.6			25.6	- 3.6	37
Serpentinized harzburgite							
38492	10.00	6.9			19.8	- 6.5	71
38498	13.08	3.2			17.1	- 5.0	92
Leg 29 weathered basalt							
Hole 278/31-33		8.4			34.0	0.4	-0.3
Hole 278/133-136		8.4			34.1	1.0	-0.6
Hole 279A/98-101		7.0			35.1	- 0.8	-3.2
Hole 279A/116-120		8.1					
Hole 279A/121-124		7.0					
Hole 279/0-2		7.8					

*Temperatures calculated using calcite-water fractionation curve (30) and $\delta^{18}O=0$‰ for hydrothermal fluid (seawater).

Table 2

Composition of typical glasses from weathered and zeolite facies basalts, Macquarie Island ophiolite (energy dispersive electron microprobe analyses).

Sample	40428	BG 157	BC 4A	BF 256
SiO_2	50.06	48.95	48.94	50.29
TiO_2	1.14	1.38	1.52	1.83
Al_2O_3	16.43	17.29	18.20	17.40
FeO_T	8.53	8.01	7.37	7.72
MgO	8.72	8.43	7.84	7.70
CaO	12.38	12.55	11.36	10.03
Na_2O	2.41	2.77	3.78	3.90
K_2O	0.19	0.57	0.89	1.14

T - Total Fe as FeO

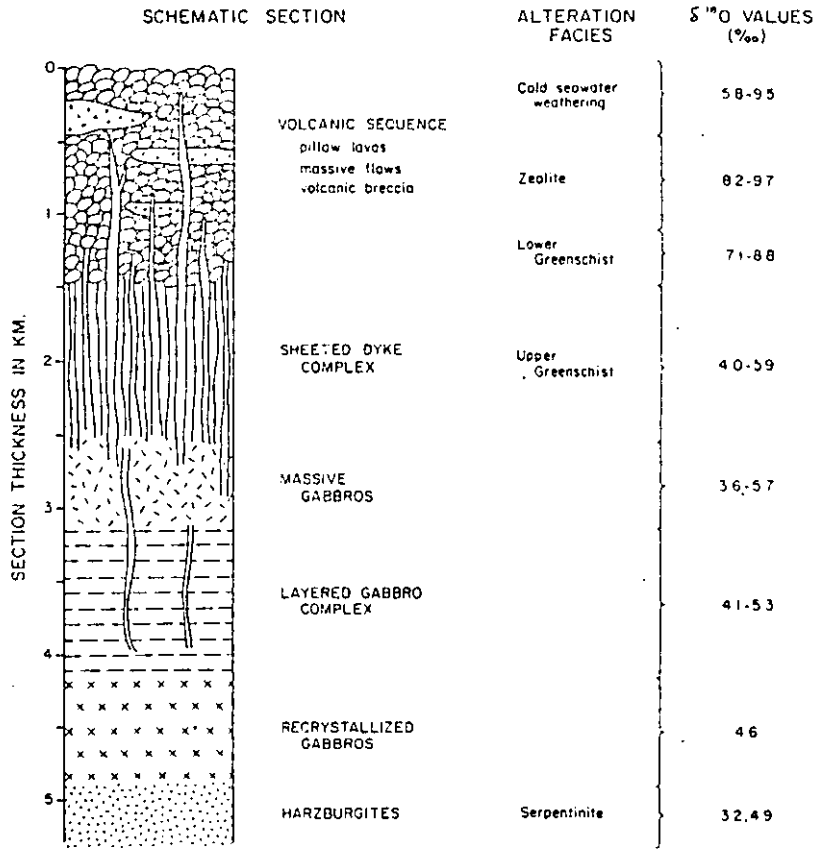

Figure 1. Schematic section and alteration facies of the Macquarie Island ophiolite [2]. The whole-rock oxygen isotope composition of each metamorphic assemblage is given as a range of values. The common alteration assemblages are: Cold, seawater weathering - smectite, calcite; Zeolite facies - natrolite, thomsonite, analcite, wairakite, laumontite; Lower Greenschist facies - albite, chlorite, epidote, sphene; Upper Greenschist facies - plagioclase, actinolite, epidote, chlorite, sphene. Hydrothermal phases in the gabbro section rarely exceed 5% (vol) and include talc, magnetite, actinolite, hornblende, and minor serpentine and calcite.

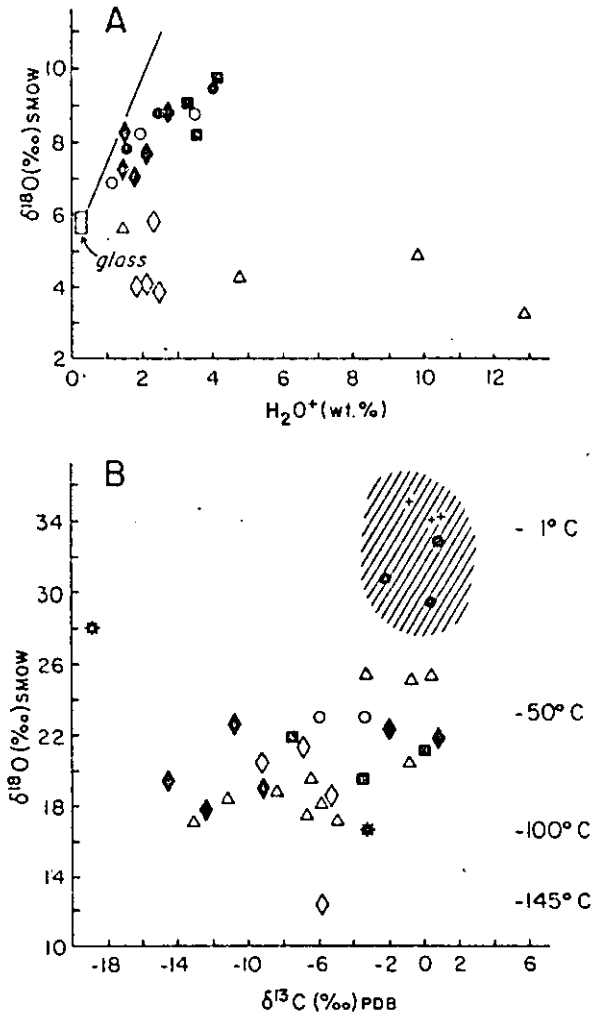

Figure 2. A. Oxygen isotope composition for whole-rocks of the Macquarie Island ophiolite versus H_2O^+ content. The line is the locus of DSDP weathered basalts for relatively low degrees of weathering. Symbols: (◉) weathered basalt, (■) zeolite facies basalt, (◆) lower greenschist facies basalt, (○) weathered dolerite dike, (◇) uralitized dolerite dike, (△) gabbro and serpentinized harzburgite.

B. Oxygen and carbon isotope composition for calcite in the Macquarie Island ophiolite. Symbols are the same as in A except for two calcite vein samples (✱) and DSDP Leg 29 disseminated calcite (+). The shaded area shows the composition of DSDP basalt calcite. The temperature scale is based on calcite-water fractionation [30] and the assumption that calcite was deposited in equilibrium with seawater ($\delta^{18}O$ = 0‰).

INTERNATIONAL UNION GEODESY MEETING ABSTRACTS, AUSTRALIA (1979).

THE MACQUARIE ISLAND OPHIOLITE ASSOCIATION: MID-TERTIARY OCEANIC CRUST OF THE SOUTHERN OCEAN

B.J. Griffin and R. Varne

Department of Geology, University of Tasmania

The Macquarie Ridge runs south from New Zealand to join the Indian-Pacific ridge system, and emerges near 54°S 159°E to form Macquarie Island. The island represents Tertiary oceanic crust produced during seafloor spreading at the Indian-Pacific ridge system, later uplifted during marginal interactions between the Indian-Australian and Pacific plates.

Most of the island is composed of basaltic pillow lavas accompanied by volcanic breccias and more massive lavas, associated with calcareous oozes and lithic wackes. The volcanics have suffered some metamorphism and alteration. A composite section passes from an "ocean floor weathering" zone through zeolite facies into lower greenschist facies volcanics and is about 1600 m thick. Deeper levels of the oceanic crust section are exposed in the north of the island, where a coastal section about 2000 m thick has harzburgite at the base, overlain by gabbros that include a layered gabbro complex. Dolerite dyke swarms form a sheeted intrusive complex perhaps 1000 m in thickness derived from oceanic crust underlying the volcanic pile.

Macquarie Island basalts and dolerites are very like those from 45°N and 36°N (FAMOUS area) on the Mid-Atlantic Ridge. Usually porphyritic, they carry plagioclase (An_{87-70}) as the dominant phenocryst phase, with less abundant olivine (Fo_{89-85}), clinopyroxene ($Ca_{45}Mg_{50}Fe_5$ - $Ca_{38}Mg_{50}Fe_{12}$), and chrome spinel. Groundmasses of little-altered lavas and dykes exhibit continuous variation from assemblages of subcalcic augite, plagioclase, opaques and glass in subophitic textures to more alkaline assemblages of olivine, titanaugite, kaersutitic amphibole and minor glass in intersertal textures. Gabbros are composed essentially of olivine, plagioclase and clinopyroxene. Opaques are scarce and orthopyroxene occurs only rarely as thin rims on olivine or remnant cores within clinopyroxene. Peridotites are mainly harzburgite (Fo_{91}) and wehrlite (Fo_{85-81}).

TiO_2 (1.31±0.28 wt %) and Al_2O_3 (17.97±2.00 wt %) contents distinguish the whole group of Macquarie Island lavas and dykes from ocean island and island arc tholeiite series. Normative variation from *ol*- and *hy*- bearing to mildly *ne*-bearing types corresponds roughly with groundmass mineralogy assemblage. The "ocean floor basalt" character of the volcanics is also apparent in the most alkaline *ne*-bearing compositions which are generally less enriched in LIL elements than ocean island tholeiites and display, for example, low Zr (<150 ppm) and Y (<40 ppm) but high Nb (20-60 ppm) contents.

Mixing calculations using observed phenocryst and rock compositions suggest that much of the compositional variation in the volcanics could have arisen by low-pressure crystal fractionation. Some compositions of olivine, plagioclase and clinopyroxene from the layered gabbro complex can be closely matched with phenocrysts from lavas and dykes. The lavas are generally less fractionated than the dykes; the most primitive compositions have Mg/Mg+Fe = 0.71 with high Ni and Cr contents. Low-pressure fractionation processes are inadequate to account for all of the variation in the 'incompatible elements': some may arise from different degrees of partial melting of a possibly inhomogeneous source.

Chemical Geology, 30 (1980) 285—308
Elsevier Scientific Publishing Company, Amsterdam — Printed in The Netherlands

THE MACQUARIE ISLAND OPHIOLITE COMPLEX: MID-TERTIARY OCEANIC LITHOSPHERE FROM A MAJOR OCEAN BASIN

B.J. GRIFFIN* and R. VARNE

Department of Geology, The University of Tasmania, Hobart, Tasmania 7001 (Australia)

(Accepted for publication June 5, 1980)

ABSTRACT

Griffin, B.J. and Varne, R., 1980. The Macquarie Island ophiolite complex: mid-Tertiary oceanic lithosphere from a major ocean basin. In: R.W. Le Maitre and A. Cundari (Guest-Editors), Chemical Characterization of Tectonic Provinces. Chem. Geol., 30: 285—308.

The rocks of Macquarie Island are part of the mid-Tertiary oceanic lithosphere from a major ocean basin. They were probably created at the Indian—Australian—Pacific spreading ridge.

The basalts and dolerites are usually porphyritic, carry plagioclase (An_{67-80}) as a dominant phenocryst phase with less abundant olivine (Fo_{89-85}), chrome spinel and rare clinopyroxene ($Ca_{45}Mg_{50}Fe_5$—$Ca_{38}Mg_{50}Fe_{12}$) phenocrysts. Normatively the rocks range from *ne*- to *Q*-bearing, with most falling near the critical plane of normative silica undersaturation. Dykes tend to be more Fe-rich than lavas, and to include the more *di*-poor rocks. The rocks also range compositionally from typical ocean floor basalts through to varieties relatively enriched in some incompatible trace elements, particularly Nb (20—60 ppm), that otherwise retain ocean-floor basalt phenocryst assemblages, major-element compositions and Ti, Ni, Cr and Zr contents. This enrichment, also characteristic of ocean-floor basalts from the "abnormal" ridge segments near 45°N and 36°N (FAMOUS area) on the Mid-Atlantic Ridge, causes the rocks to plot away from the ocean-floor basalt fields on popular trace-element diagrams intended to identify tectonic affinities of basalts.

The upper parts of the Macquarie Island oceanic lithosphere section can be thought of as a vertical slice through a magma column, differentiating at shallow levels. The layered and massive gabbros that underlie the basalts and dolerites are composed essentially of olivine, plagioclase and clinopyroxene. Olivine and plagioclase are cumulate phases in the layered rocks, clinopyroxene is postcumulus. Mineral compositions of the gabbros, particularly those of the layered rocks, are closely resembled by phenocryst compositions in the basalts and dolerites. Plagiogranites and trondheimites are unknown from the island, and norites very rare. Thus, Macquarie Island basalts, dolerites and gabbros form a distinctive igneous association that ought to make Macquarie Island-type ophiolite complexes from major ocean basins an easily recognized ophiolite type in continental orogenic terranes, even when dismembered.

INTRODUCTION

Various methods of chemical characterization of igneous rocks from different tectonic settings have been proposed, particularly since advances in instru-

**Present address:* Max-Planck-Institut für Chemie, Saarstrasse 23, D6500 Mainz, Federal Republic of Germany.

0009-2541/80/0000—0000/$02.25

mental analysis techniques have made available a large number of rock and mineral analyses for isotopes and major, minor and trace elements.

Particular attention has been paid to the ocean-floor basalts. Early results suggested that these basalts were of distinctive and intriguingly uniform major-element composition (Engel et al., 1965; Kay et al., 1970; Cann, 1971). This uniformity seemed to extend to some of their trace elements and to their Sr-isotope characteristics. And when Cann (1970) remarked that their Ti, Y, Zr and Nb abundances fell within a fairly restricted range that was not only distinctive but also apparently strongly resistant to change by secondary processes, he started one of the great growth industries of modern igneous geochemistry.

For if their Ti, Y and Zr abundances could identify ocean-floor basalts even when they were altered and metamorphosed, this offered a geochemical means of tracing to their source the ophiolite complexes with sheeted dyke complexes that had been suspected to be fragments of former oceanic lithosphere, and whose presence among continental rocks in orogenic terrains might mark a suture line where an ocean basin has been eliminated during plate collision.

Geochemical methods were developed that used abundances of P, Ti, Cr, Sr, Y, Zr, Nb and the rare-earth elements to determine the tectonic settings of basalts (Pearce and Cann, 1971, 1973; Bloxam and Lewis, 1972; Jakes and Gill, 1970; Pearce et al., 1975; Floyd and Winchester, 1975). It was soon shown that many of the lavas and dykes of two of the well-developed ophiolite complexes, the Troodos complex and the Macquarie Island complex, resembled ocean-floor basalts in their Ti, Y and Zr abundances (Pearce and Cann, 1971; Varne and Rubenach, 1972). The problem of determining the original tectonic setting of ophiolite complexes seemed solved, and the Troodos complex became widely accepted as a type example of oceanic lithosphere created at a spreading mid-oceanic ridge.

Yet it has since been shown that some of the volcanic rocks of ophiolite complexes, including the Troodos complex, may possess characteristics similar to those of island-arc tholeiites (Miyashiro, 1973, 1975; Pearce, 1975), boninites (Varne and Brown, 1978; Cameron et al., 1979, 1981), and LREE-depleted magnesian olivine-poor tholeiites (Duncan and Green, 1980). Similar volcanic rocks could form in a variety of settings, in back-arc or inter-arc basins in island-arc environments (Miyashiro, 1975; Pearce, 1975; Smewing et al., 1975; Dewey, 1976; Saunders and Tarney, 1979), in fore-arc settings (Cameron et al., 1981), or by shallow multistage melting of rising mantle, perhaps in an oceanic basin (Duncan and Green, 1980), or perhaps in the waning stages of magmatism associated with aborted continental rifting (Brown et al., 1981).

A growing recognition that many ophiolite complexes may not represent oceanic lithosphere derived from a spreading mid-oceanic ridge environment in a major ocean basin has been paralleled by re-appraisals of the extent of compositional variation of ocean-floor basalts. It had been known for some

time that alkaline basalts occurred on the Mid-Atlantic Ridge at 45°N (Muir et al., 1964). It has now been shown that segments of the ridge near 36°N, 45°N and 63°N have erupted volcanic rocks that are relatively enriched in some "incompatible" or "hygromagmatophile" trace elements (e.g., Hart et al., 1973; Schilling, 1973; Frey et al., 1974; Wood et al., 1979a) although still plotting within the ocean-floor basalt field on the Ti-Y-Zr discriminant triangle of Pearce and Cann (1973).

Arguments that Macquarie Island probably represents uplifted oceanic crust formed by spreading processes in a major ocean basin have been presented elsewhere (Varne et al., 1969; Varne and Rubenach, 1972, 1973; Miyashiro, 1975; Cameron et al., 1981). New geological, geochemical and geophysical data corroborate these arguments.

With the current controversy about the origin of many ophiolites, it seems timely to present some of the new geochemical information about the Macquarie Island ophiolite complex, and to use it to help reassess the characteristics of oceanic lithosphere.

ANALYTICAL METHODS

Major- and trace-element abundances were mostly determined using XRF methods (Norrish and Chappell, 1967; Norrish and Hutton, 1969). New bulk-rock analyses were carried out by B.J. Griffin and P. Robinson, using a Philips® PW1410 spectrometer. Earlier data from Varne and Rubenach (1972, 1973) are included. Electron microprobe analyses by B.J. Griffin and R. Varne were performed on the JEOL® JXA-50A scanning electron microscope, Central Science Laboratory, University of Tasmania, using an EDAX® EDS system (Griffin, 1979) and on the TPD®–Ortec® system, Australian National University (Reed and Ware, 1975). Representative analytical data are available on request from R. Varne.

REGIONAL SETTING OF THE MACQUARIE ISLAND OPHIOLITE COMPLEX

Macquarie Island lies on the Macquarie ridge (Fig. 1), ~ 1100 km SSW of the southern tip of New Zealand, the nearest major continental land mass. The island is elongated NNW along the ridge axis, and is ~ 37 km long and as much as 5 km wide although it is mostly narrower. Bathymetric data (Cullen, 1969; Hayes and Talwani, 1972) suggest that morphologically the island is part of the Macquarie ridge crest that breaks the surface.

The Macquarie Ridge is a narrow, arcuate ridge that runs south from New Zealand to join the Indian–Pacific ridge system. It has a rugged and complicated topography and in places has a double crest separated by a deep and narrow depression (Summerhayes, 1974). The ridge is locally topped by a flat platform ~ 160 m below sea-level where it may have been exposed in the Pliocene. A subsiduary ridge occurs east of the main ridge in the Macquarie Island region, separated from it by a narrow but deep trench, the Macquarie

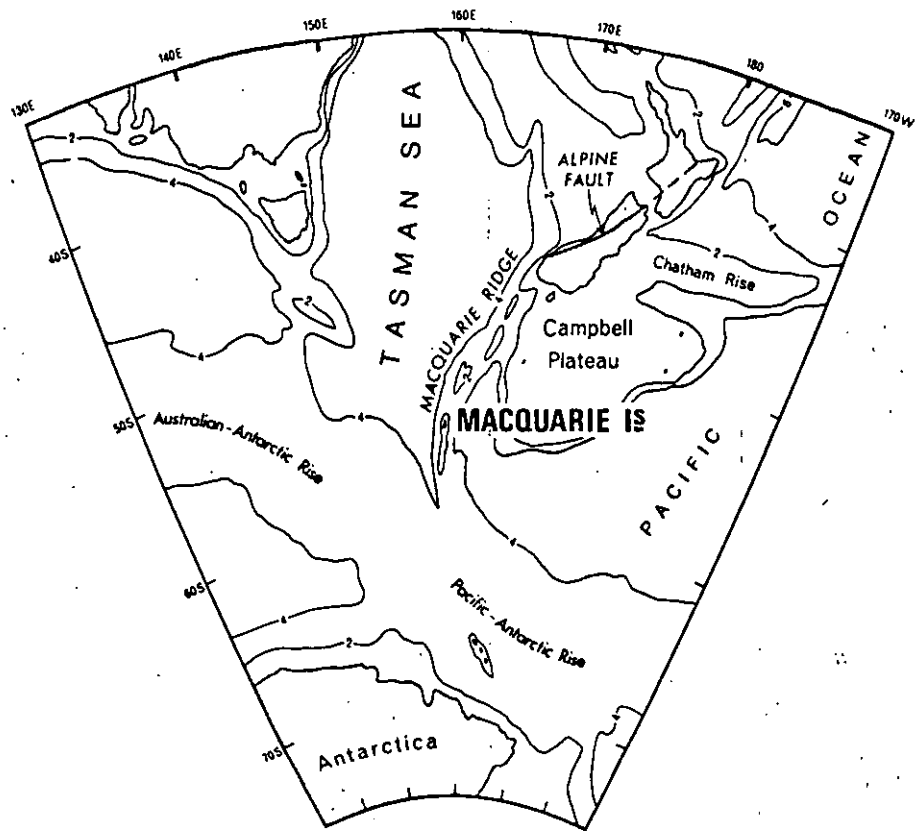

Fig. 1. Locality map. Isobaths at 2, 4 and 6 km.

trench. This trench contains undeformed sediments (Hayes and Talwani, 1972).

The Macquarie ridge is seismically active, and usually considered to mark the boundary between the Indian—Australian and the Pacific plates. Earthquakes are shallow, and first-motion analyses imply that the ridge is associated with normal, thrust and strike-slip faulting. Plate-tectonic analyses suggest that the predominant motion along the ridge is right-lateral strike-slip (Hayes and Talwani, 1972). Nevertheless, different parts of the ridge are probably also governed by extensional and compressional regimes as a consequence of the closeness of the ridge to the Pacific—Indian pole of relative motion. Marginal interactions between the plates associated with rapid recent motions of this pole (Griffiths and Varne, 1972; Le Pichon et al., 1973) have probably contributed to the complex structural development of the ridge, and incidentally to the exposure of part of it to form Macquarie Island.

Rocks similar to those of Macquarie Island have been dredged from the submerged ridge crest to north and south (Summerhayes, 1969; Watkins and Gunn, 1972), encountered at nearby DSDP sites *278*, *279* of Leg *29* (Oven-

shine et al., 1979; Schilling and Ridley, 1979), and occur in some much smaller islands also exposed along the ridge (Lugg et al., 1978).

Paleomagnetic pole positions derived from the island suggest that it forms part of the Indian—Australian plate (Williamson, 1979), and pillow lavas from the island have magnetic properties that correspond well with those of ocean-floor basalts (Butler et al., 1976; Levi et al., 1978).

A magnetic profile across the island shows a broad anomaly which is correlatable with similar anomalies in marine magnetic profiles around the island. This local anomaly probably forms part of Anomaly 7, which can be traced across the ridge and island to its termination at the Macquarie trench to the east (Williamson, 1974).

Magnetostratigraphic ages for Anomaly 7 lie within Late Oligocene time (Heirtzler et al., 1968; La Brecque et al., 1977), but poorly preserved coccoliths from calcareous oozes associated with pillow lavas from the northern part of the island suggest an Early, or perhaps Middle, Miocene age (Quilty et al., 1973). Radiometric and radiolarian studies that are underway may resolve this descrepancy.

GEOLOGY OF THE MACQUARIE ISLAND OPHIOLITE COMPLEX

The island is formed almost entirely of basalts, dolerites, gabbros and serpentinized peridotites. Here we summarize geological relationships described in more detail elsewhere (Mawson, 1943; Varne and Rubenach, 1972) and incorporate some results of recent investigations.

The northern part of the island is formed mainly of intrusive rocks whereas the southern part is formed mainly of extrusive rocks. The dolerite dyke swarms are a notable geological feature, and are composed almost entirely of series of narrow dykes lying parallel to sub-parallel to one another to form a sheeted dyke complex. Faulting is widespread on the island, and it is essentially composed of fault-bounded blocks, probably on all scales.

The volcanic rocks are commonly basaltic pillow lavas, accompanied by volcanic breccias and some massive lavas. Series of narrow basaltic dykes cut these volcanic rocks. Calcareous *Globerigina* oozes occur between pillows, whereas the volcanic sequences that contain massive lavas also include lenses of volcaniclastic sediments, and may have formed during periods of relatively high tectonic activity. The coarsely-grained sediments resemble talus-slope and rubble deposits. Graded bedding and truncated and concoluted laminae occur in the more finely-grained sediments.

The volcanic rocks are tilted. Dips range from near-horizontal up to 45° or more. Two strike directions are common, ~ 150° and ~ 230°. It has been argued that the tilting of the volcanic rocks occurred in two stages (Varne and Rubenach, 1972): the first stage involved tilting around horizontal axes that were near-horizontal and parallel to dyke-bedding plane intersections, and therefore caused variations only in dip; the second was a later rotation about vertical axes of the tilted rocks that caused the variations in strike. This inter-

pretation is supported by paleomagnetic studies (Williamson, 1979). The dykes seem to have been intruded originally in a near-vertical orientation striking east-southeast.

This ESE dyke orientation corresponds very well with the inferred orientation of the spreading axis of the Indian—Pacific ridge during Anomaly 7 time, as preserved by the present orientation of the linear marine magnetic anomalies in the region (Weissel and Hayes, 1972; Williamson, 1974).

Rotations of the crustal blocks of the island therefore apparently occurred first about horizontal axes parallel to the spreading axis, probably as an integral part of the spreading process (Ballard and van Andel, 1977). Later rotations about vertical axes could have been caused by recent strike-slip movements along the Macquarie ridge.

The Macquarie Island oceanic lithosphere section

The tilting of the fault-bounded blocks that make up the island, and their planation by marine erosion as they were brought up during the tectonism that formed the Macquarie ridge, has provided several partial sections through oceanic lithosphere. Deeper crustal levels are represented by the gabbro and peridotite masses of the northern part of the island. A relatively complete section is apparently preserved in coastal exposures from North Head, around the northern coast of Handspike Point, and from there to Eagle Point (Figs. 2 and 3).

The top of the section is represented by North Head, where the volcanic rocks are relatively fresh, and retain the magnetic properties of typical ocean-floor basalts (Butler et al., 1976). The rocks have suffered the smectite—carbonate alteration that is characteristic of ocean-floor weathering, and probably formed the uppermost 200 m of the volcanic pile. On the isthmus to the south of North Head the pillow lavas are metamorphosed at higher grades and some of the volcanic section is apparently missing. Another incomplete volcanic section in the south of the island is ~ 1.4 km thick, and exhibits a metamorphic succession through zeolite facies assemblages defined by the development of Na- and Ca-zeolites, particularly natrolite, thomsonite, analcite, wairakite and at the base, laumontite, into albite—chlorite—epidote—sphene assemblages of the lower greenschist facies (B.J. Griffin, in prep.). When the two sections are combined, it seems that the Macquarie Island lava pile may have been at least 1.6 km thick. Nevertheless, such attempts to reconstruct the volcanic stratigraphy of ocean crust must be treated sceptically. The very nature of the sea-floor spreading process, by which material is added laterally, makes it unlikely that true horizontal superimpositional stratigraphic successions are formed in the mid-oceanic ridge environment.

The dolerite dyke swarms exposed in both the northern and southern parts of the island display a widespread and distinctive actinolitic replacement of primary mafic minerals, with plagioclase commonly surviving little-altered (Varne and Rubenach, 1972; Banerjee et al., 1974; B.J. Griffin, in prep.), and

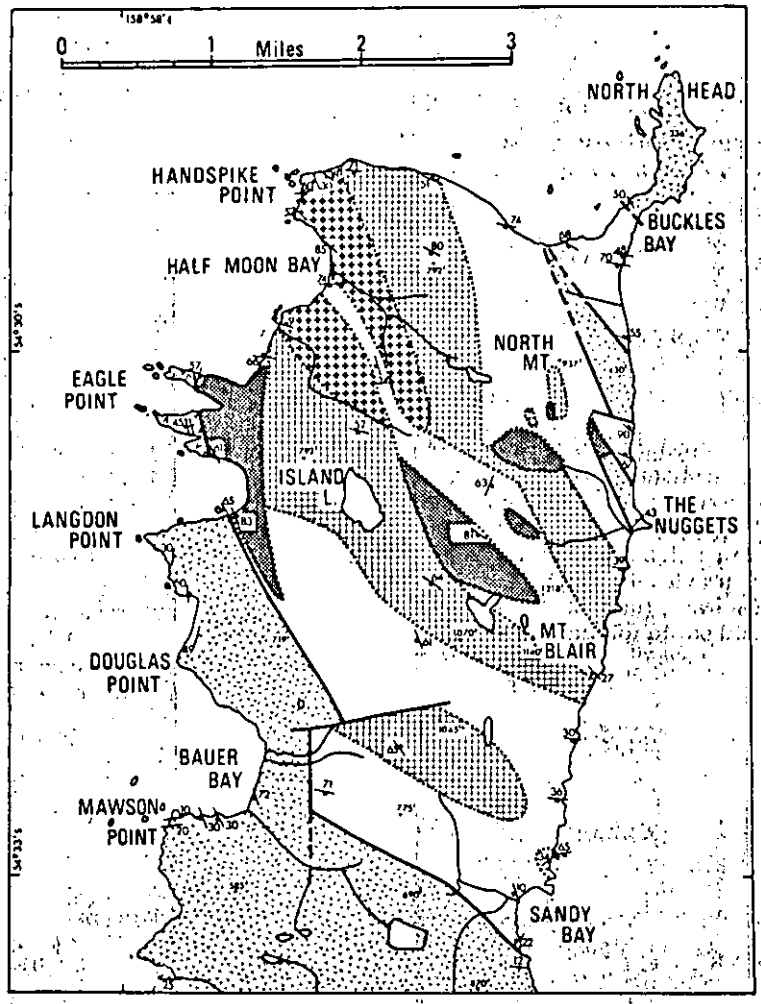

Fig. 2. Geological map of the northern part of Macquarie Island, with superficial deposits omitted, from Varne and Rubenach (1972).
Serpentinized peridotite bodies are marked by *heavy diagonal cross-hatching*; layered gabbro complex is marked by *crosses*; other gabbro masses are marked by *light cross-hatching*; extrusive volcanic rocks and associated sediments are marked by *vees*; dyke swarms are *blank*.
Strikes on lavas are shown with a *single tick*, and strikes on dykes are shown with a *double tick*. Faulted contacts are drawn as *heavy lines*, and gradational or uncertain contacts are drawn as *dotted lines*. Spot heights in feet (t ft. = 0.3048 m) above sea level. Vertical aerial photography has recently become available and the interior of the island is to remapped.

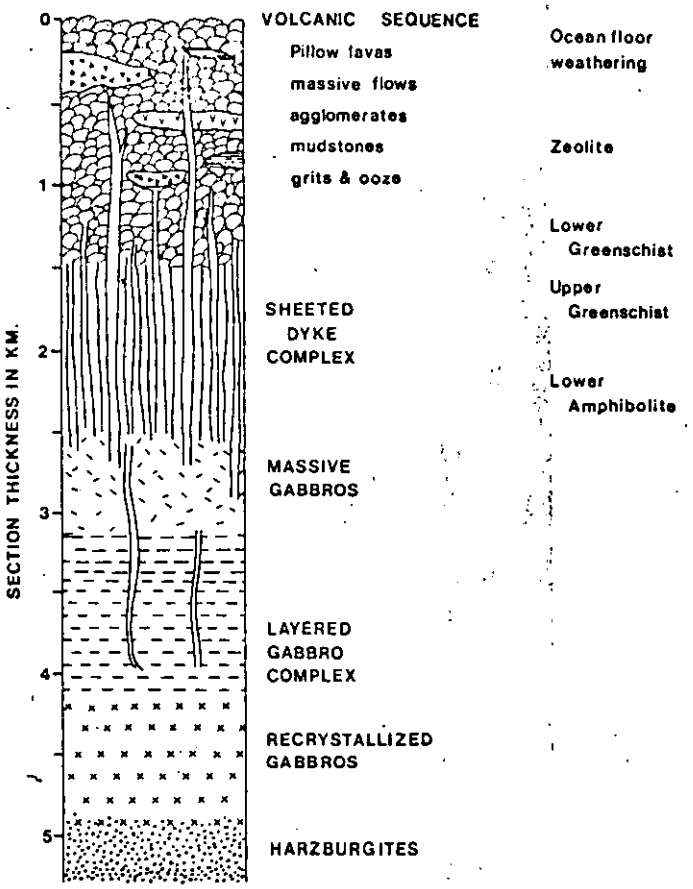

Fig. 3. A schematic section through Macquarie Island-type oceanic lithosphere. The section is based on the traverse from North Head to Eagle Point via Handspike Point (see Fig. 2), but is augmented by field data from elsewhere on Macquarie Island, as explained in the text.

locally the metamorphic grade lay within the amphibolite facies, the highest grade attained in the fine-grained igneous rocks. The thickness of the dyke swarms is at least 250 m (the elevation above sea-level of the island). If the dykes were vertical when emplaced, as has been argued, they could have been derived from a layer as much as 1 km in thickness.

The dolerite dyke swarms grade downwards into massive gabbros. Most of the dykes strike about 120° and dip at about 50° southwest, and the thicknesses of the gabbroic layers in the oceanic lithosphere section have been estimated by reconstructing a section from North Head to Eagle Point, and rotating it about a horizontal axis of 120° so that the dolerite dyke swarms become vertical or near-vertical. This brings many, but by no means all, of the layers of the layered gabbro complex into a near-horizontal attitude and puts the olivine-rich rocks at its base.

The rocks of the layered gabbro complex around Half Moon Bay (Fig. 2)

include wehrlite, plagioclase wehrlite, troctolite, olivine gabbro and gabbro, and are mineralogically fairly simple. They are composed mainly of olivine, plagioclase and clinopyroxene. Spinel is a scarce but widespread accessory mineral, and orthopyroxene occurs very rarely as thin rims around olivine or as tiny relict grains within clinopyroxene. Cumulate phenocryst phases are olivine, plagioclase and spinel. Clinopyroxene is always postcumulus, plagioclase is also postcumulus in some olivine-rich rocks.

Several massive gabbro masses outcrop on the east coast, and to the northeast of the layered gabbro complex (Fig. 2). They occur both above and below the layered rocks in the section, possess complicated intrusive contacts, contain inclusions of other gabbros, are in places deformed and are also cut by dykes. Their bulk chemical compositions are similar to those of some of the lavas and dykes (see Figs. 5 and 13 on pp. 295 and 302, respectively) and they range in texture from gabbroic to doleritic.

A zone of massive gabbros that have undergone high-temperature sub-solidus recrystallization occurs around Island Lake and north of Eagle Point (Fig. 2). They separate the wehrlites of the layered gabbro complex from the harzburgite at Eagle Point, and are composed essentially of clinopyroxene and plagioclase, with lesser amounts of olivine, and minor amounts of orthopyroxene, hornblende and spinel. The orthopyroxene occurs partly as a reaction product, rimming olivine in a vermicular intergrowth with plagioclase.

The harzburgite at Eagle Point is interleaved in a complex manner with thin gabbroic and doleritic sheets, and to the south is thrown against volcanic rocks along a major fault. Other, more-serpentinized, harzburgites also occur elsewhere on the island (Fig. 2).

Whether the location of the harzburgite at the base of the section, and the sandwiching of the layered gabbro complex between massive gabbros (Fig. 3), were features of the oceanic lithosphere when it was first formed or whether they developed shortly afterwards during tectonic adjustments, is not yet known.

Many other sections through oceanic lithosphere are available. But, as Coleman (1977) remarked:

> "Numerous models of mid-ocean spreading tied to observed petrologic relationships, have been published and they bear a startling similarity to the ophiolite sequences. Mainly because all these models draw heavily on spatial relationships observed for on-land ophiolites."

The schematic section through Macquarie Island-type oceanic lithosphere is useful in several ways: (1) it offers a guide to the geological relations in the lithosphere after removal from the spreading axis; (2) it will be shown that it provides some plausible constraints on the range of magmatic processes that may cause differentiation in spreading ridge environments similar to segments of the Mid-Atlantic Ridge near 45° N and the FAMOUS area near 36° N; and (3) it aids in the characterization of ophiolite complexes formed by spreading processes in major ocean basins.

The lavas and dykes of Macquarie Island are basaltic. Petrographic descriptions have been presented elsewhere (Mawson, 1943; Varne and Rubenach, 1972; Cameron et al., 1981). To summarize their characteristics, the rocks range from coarsely porphyritic to aphyric, and from almost wholly crystalline to almost wholly glassy. The most abundant phenocryst phase is plagioclase (An_{87-70}), followed by olivine (Fo_{89-85}), rare clinopyroxene ($Ca_{45}Mg_{55}$-Fe_5—$Ca_{38}Mg_{50}Fe_{12}$) and tiny euhedra of chrome spinel. Spinel compositions from Macquarie Island volcanics fall within the compositional field of spinels from Mid-Atlantic Ridge basalts (Cameron et al., 1981), and zoned plagioclase phenocrysts are progressively enriched in FeO from core to rim (Banerjee et al., 1974).

Slightly-altered groundmasses of both lavas and dykes exhibit continuous variation from assemblages of subcalcic augite, plagioclase, opaques and glass in subophitic textures, to less common and relatively alkaline assemblages of olivine, titanaugite, minor glass and rare kaersutitic amphibole in intersertal textures.

Normatively, the rocks vary from *ol*- and *hy*-bearing to mildly *ne*-bearing and rarely *Q*-bearing (Fig. 4). Within the analysed glasses the normative range

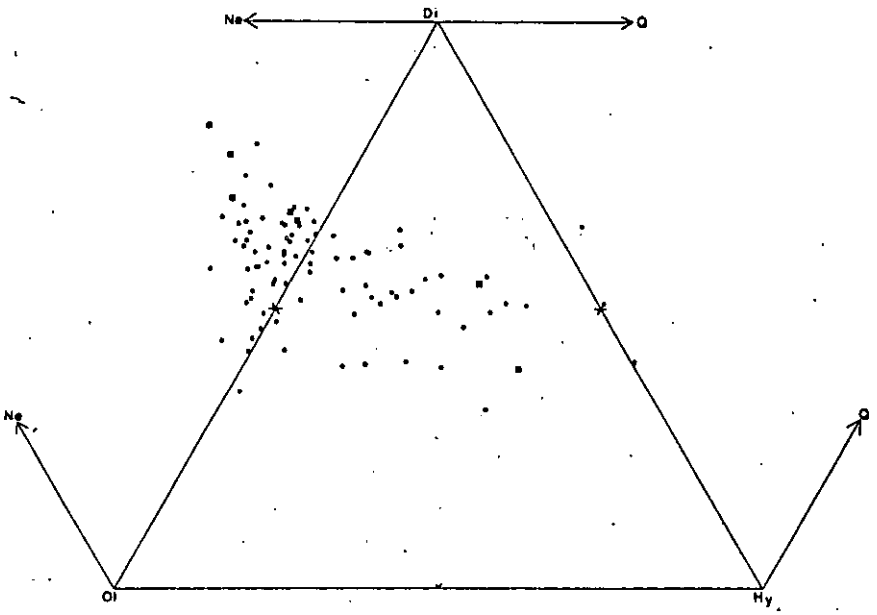

Fig. 4. Plot of relative proportions of normative *ol*, *hy*, *di*, *ne* and *Q* in Macquarie Island basalts (*open circles*), dolerites (*filled circles*), and volcanic glasses (*filled squares*). CIPW norm calculations were performed on major-element analyses recalculated volatile-free with Fe^{2+}: (total Fe) = 0.85. Two volcanic glasses, four basalts, and one dolerite have > 5 wt.% *ne*, and could be termed basanitoids.

is almost as great as within the crystalline rocks, although the data are fewer. The normative transition from *ol*- and *hy*-bearing to *ne*-bearing corresponds roughly with the appearance of groundmass olivine and titanaugite. The rocks plot within a fairly restricted field on an *AFM* triangular plot, similar to that at 45°N on the Mid-Atlantic Ridge, although with slightly higher Mg/(Mg + Fe) ratios (Fig. 5), that range from ~ 0.72 down to ~ 0.51 (Fig. 6).

Although there is almost complete overlap, comparison of the group of dykes with the group of lavas shows that the dykes tend to be less rich in *ne* and *di*, to include the few *Q*-normative rocks (Fig. 4), and to occupy a field nearer to the *F*-apex of the *AFM*-diagram (Fig. 5). The group of dykes is also displaced towards lower Mg/(Mg + Fe) ratios than the group of lavas (Fig. 6).

The Macquarie Island rocks have phenocryst assemblages similar to ocean-floor basalts (Varne and Rubenach, 1972; Cameron et al., 1981), and most resemble Bryan et al.'s (1976) Group-I rocks. Their normative range, and the scarcity of *Q*-normative varieties are also characteristic of ocean-floor basalts (cf. Aumento, 1968; Kay et al., 1970; Cann, 1971; Thompson et al., 1972; Bryan and Moore, 1977; Wood et al., 1979a, b).

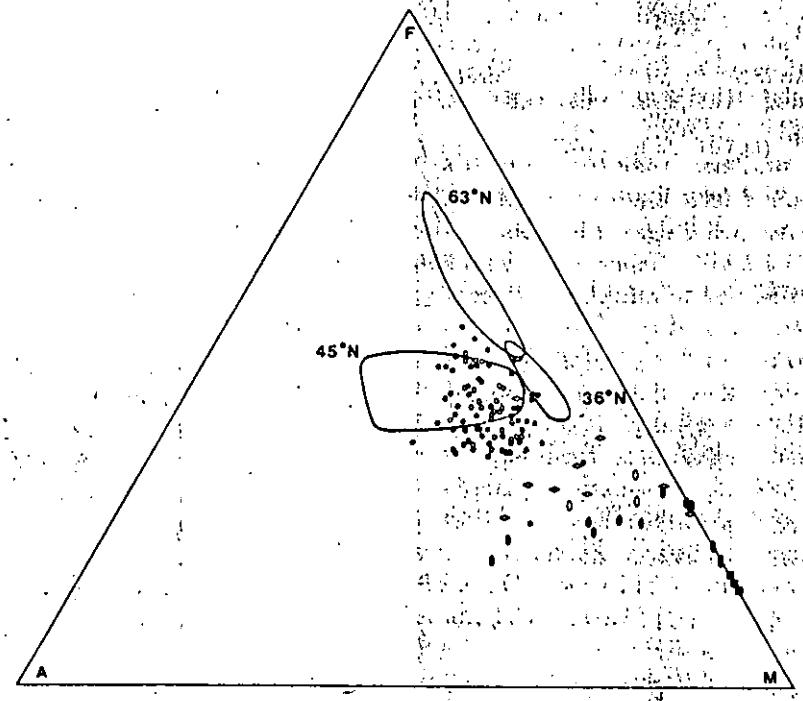

Fig. 5. *AFM*-diagram for Macquarie Island basalts (*open circles*), dolerites (*filled circles*), layered gabbros and wehrlites (*filled ellipses*), harzburgites (*filled squares*). Massive gabbros are shown by *open rhombs* except for those east of Handspike Point and above the layered rocks in the section (see Fig. 3), which are shown as *open ellipses*. Also outlined are fields of IPOD Leg-*49* basalts from the Mid-Atlantic Ridge (Wood et al., 1979a).

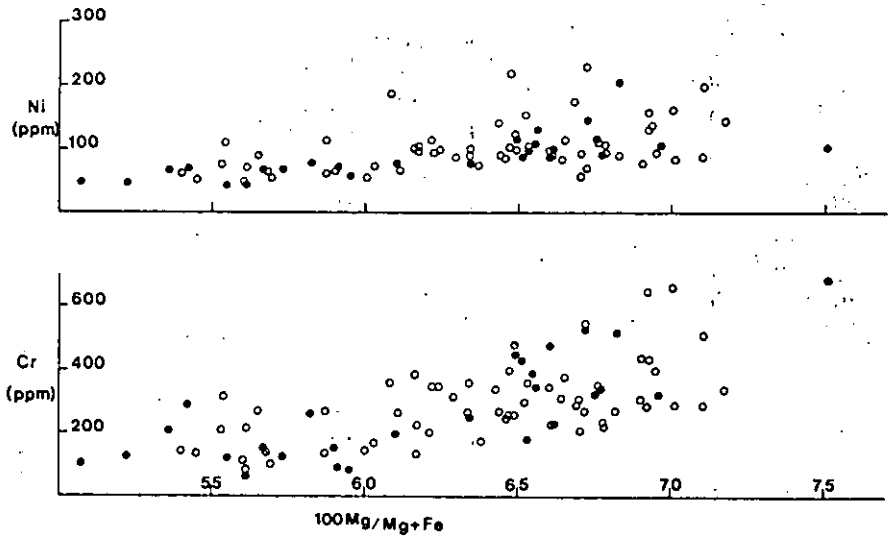

Fig. 6. Ni and Cr contents of Macquarie Island basalts (*open circles*) and dolerites (*closed circles*), plotted against 100 Mg/(Mg + Fe).

Trace-element characterization of the volcanic rocks

It has been shown that some trace elements in basaltic rocks are fairly resistant to the chemical changes that occur during the alteration and metamorphism of ocean-floor basalts (Cann, 1970; R. Hart, 1970; Thompson, 1973). Trace elements that have been used to characterize altered and metamorphosed basalts and assign them to particular tectonic environments include P, T, Cr, Sr, Y, Zr, Nb and the rare-earth elements (e.g., Pearce and Cann, 1971, 1973; Bloxam and Lewis, 1972; Floyd and Winchester, 1975).

On the Ti-Zr diagram of Pearce and Cann (1973) the Macquarie Island data fall mainly within the ocean-floor basalts (OFB) field, with some data points within the OFB—low-K tholeiite (LKT) field where overlap occurs with the low—K tholeiites of island arcs (Fig. 7). On their Ti—Zr—Y diagram (Fig. 8), the majority of the Macquarie Island data falls within the OFB field but some data points occur in the "within-plate" basalt WPB field defined by ocean island or continental basalts. On their Ti—Zr—Sr diagram (Fig. 9), the Macquarie Island data points define a band from the OFB field into the LKT field.

Thus, use of discriminant functions involving Ti, Zr, Y and Zr classifies most of the Macquarie Island rocks as ocean-floor basalts, but the remainder are unlike typical ocean-floor basalts (Varne and Rubenach, 1972). Similarly ambiguous results are achieved using the plots of Floyd and Winchester (1975), and the recent Zr—Zr/Y diagram (Fig. 10) of Pearce and Norry (1979). On the useful Ti—Cr diagram developed by Pearce (1975) to discriminate between ocean-floor basalts and island-arc tholeiites, the Macquarie Island rocks with Ti abundances generally greater than 5000 ppm and ranging

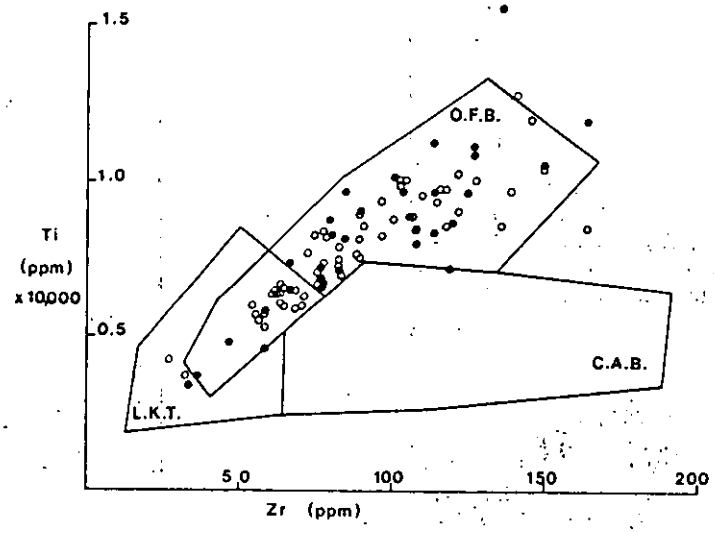

Fig. 7. Ti and Zr contents of Macquarie Island basalts (*open circles*) and dolerites (*closed circles*) plotted on a basalt classification and discrimination diagram of Pearce and Cann (1973). Ocean-floor basalts plot in the OFB field, and in the field that overlaps into the low-potassium tholeiite (LKT) field. Calc-alkali basalts (CAB) also plot in this overlapping field and in the CAB field.

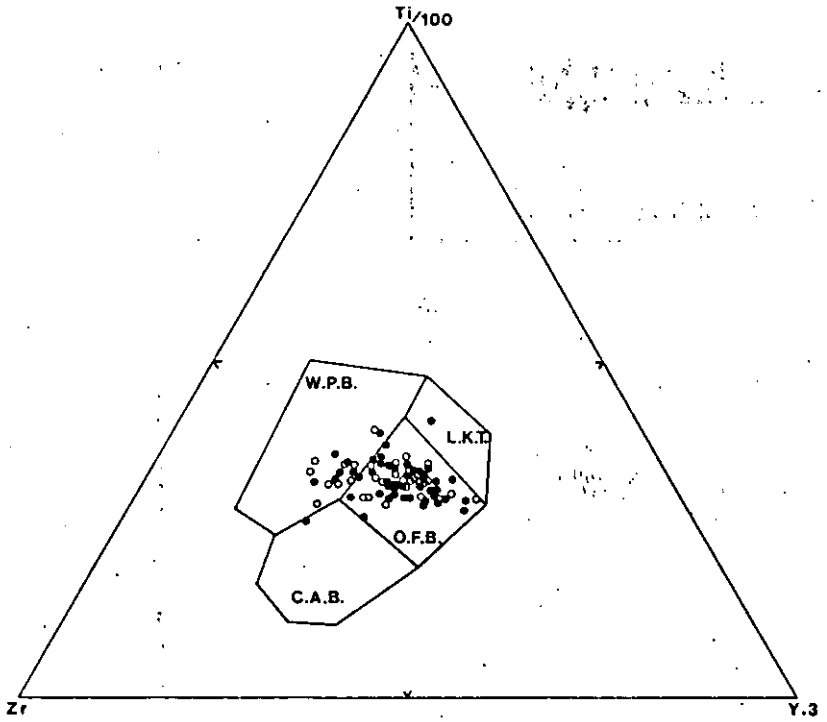

Fig. 8. Ti, Zr, and Y contents of Macquarie Island basalts (*open circles*) and dolerites (*filled circles*) in a discrimination triangle of Pearce and Cann (1973). Fields as in the caption to Fig. 7, with the addition of a "within-plate" basalt field (WPB).

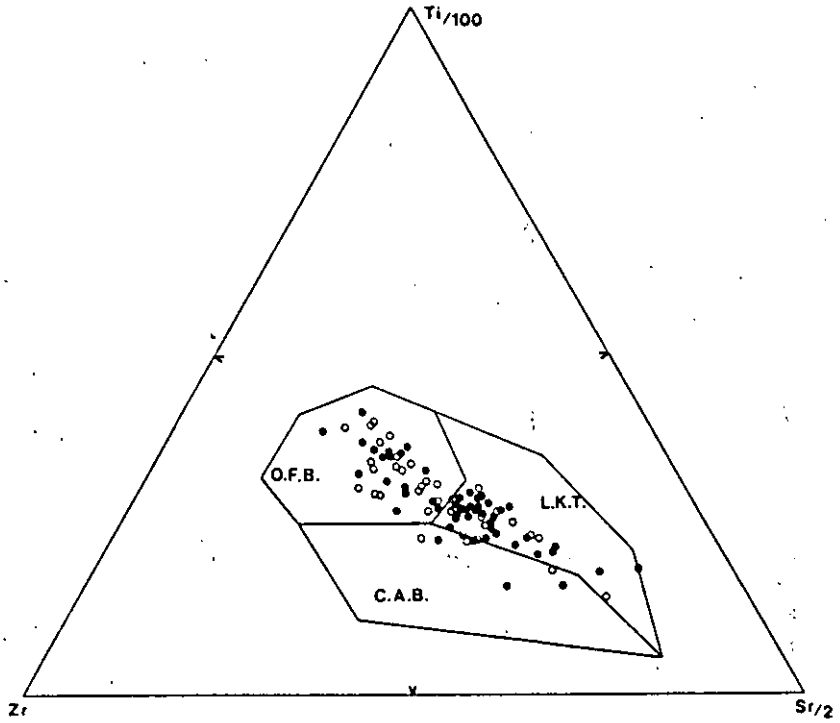

Fig. 9. Ti, Zr, and Sr contents of Macquarie Island basalts (*filled circles*) and dolerites (*open circles*) in a discrimination triangle of Pearce and Cann (1973). Fields as in the caption to Fig. 7.

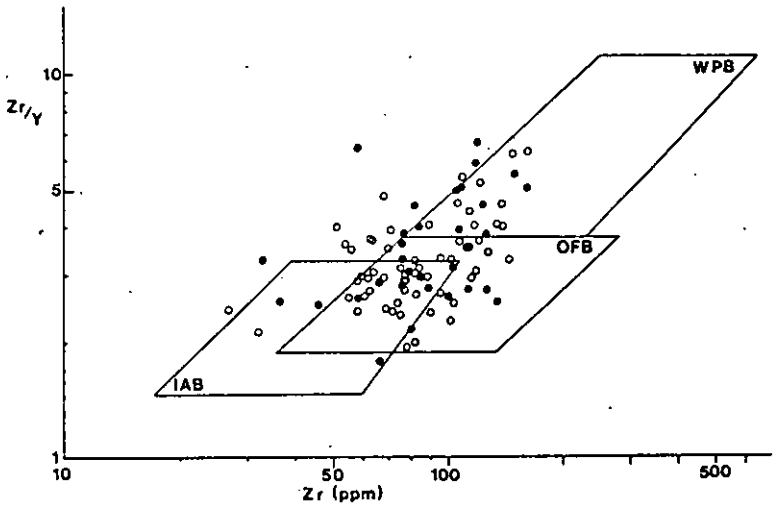

Fig. 10. Zr and Y contents of Macquarie Island basalts and dolerites plotted on the Zr—Zr/Y diagram of Pearce and Norry (1979). Fields as in the captions of Figs. 7 and 8.

up to 15,000 ppm (Fig. 7), and Cr abundances generally greater than 100 ppm and ranging up to 600 ppm (Fig. 6), would fall within the OFB field.

The Macquarie Island rocks that plot within the OFB fields tend to have relatively high Ti/Zr ratios, have Na/Na + K) ratios > 0.9, low K and K/Rb > 360, and relatively low Nb values. These resemble Engel et al.'s (1965) "depleted" oceanic tholeiites and Bryan et al.'s (1976) Group-I ocean-floor basalts.

The Macquarie Island rocks that plot outside the OFB fields tend to have relatively high Nb contents and low Zr/Nb, Y/Nb, Ti/Zr and K/Rb ratios, to be relatively enriched in K and Sr, and to be *ne*-normative.

These rocks are resembled by volcanics from the so-called "anomalous" ridge segments. Using large amounts of chemical analytical data, particularly for trace elements, Wood et al. (1979a) showed that few basalts from the Mid-Atlantic Ridge near 63° N (Reykjanes), 45° N and 36° N (the FAMOUS area) have the geochemical characteristics of Engel et al.'s (1965) "depleted" oceanic tholeiites.

On a Zr/Nb diagram (Fig. 11), rocks from near 36° N and 45° N on the Mid-Atlantic Ridge have Zr/Nb ratios in the range 3—7 and Nb contents generally higher than those of rocks from near 63° N where Zr/Nb ratios range from ~ 7 up to the high values of 18 or more that were formerly considered to be diagnostic of ocean-floor basalts (Pearce and Cann, 1973; Erlank and Kable, 1976). Most of the Macquarie Island rocks plot in the same fields as 36° N and 45° N rocks but range more widely when considered as a group (Fig. 11).

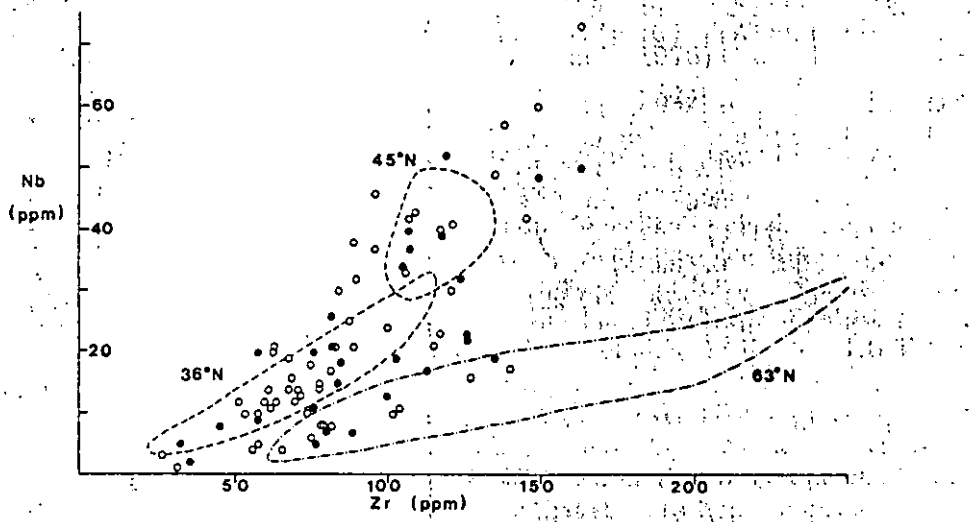

Fig. 11. Zr and Nb contents of Macquarie Island basalts and dolerites. Also outlined are fields for IPOD Leg-*49* basalts from the Mid-Atlantic Ridge (Wood et al., 1979a).

Evidence for low-pressure fractional crystallization

The great majority of the basalts and dolerites have phenocryst assemblages that strongly resemble the mineralogy of the layered gabbro complex.

Olivine from the layered rocks falls in the compositional range Fo_{87-82}, and was probably more magnesian in the serpentinized plagioclase dunites judging by their bulk-rock compositions (see Figs. 5 and 13). Plagioclase compositions lie in the compositional range An_{87-82}. The compositional ranges in the cumulate silicates therefore correspond reasonably well with the compositional ranges encountered in the same phases occurring as phenocrysts in the basalts and dolerites (Fig. 12). Preliminary data show that the spinels are like the spinel microphenocrysts in the volcanics but more analyses are needed. Postcumulus clinopyroxenes in the layered rocks are apparently heteradcumulus but are very similar to the rare phenocrysts of the volcanics, both in CaMgFe ratios (Fig. 12) and also in Al, Cr and Ti contents (not shown).

These mineralogical comparisons imply that the layered gabbro complex

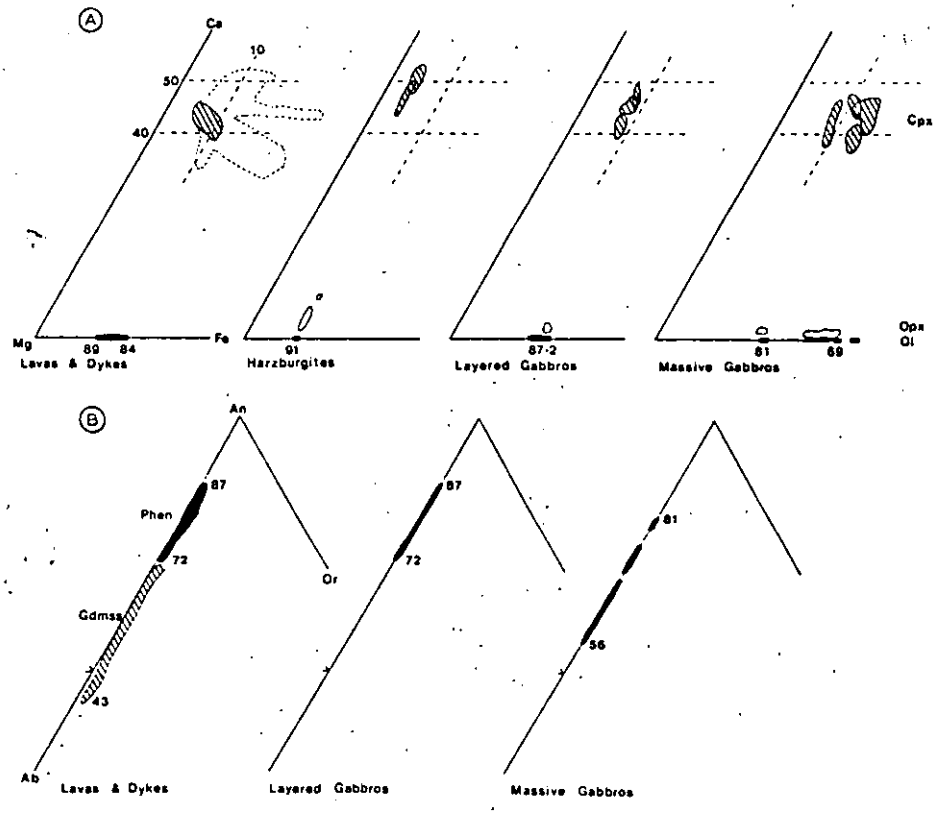

Fig. 12. Illustrations of the compositional ranges in CaMgFe contents of olivines and pyroxenes in: (A) basalts, dolerites, gabbros and peridotites; and (B) An and Ab contents of plagioclases from basalts, dolerites and gabbros.

is composed of cumulates complementary to the volcanic rocks. The conclusion can be tested by comparison with experimental studies of the distribution of Mg and Fe^{2+} between olivine and basic melts (Roeder and Emslie, 1970; Cawthorn et al., 1973; Ito, 1973; Duke, 1976; Bender et al., 1978). Basic liquids in equilibrium with the olivines of the layered rocks are calculated to have $Mg/(Mg + Fe^{2+})$ in the range 0.67 ± 0.02—0.58 ± 0.02, a range similar to that of the basalts and dolerites (Fig. 6). Conversely, the most magnesian basalts [$Mg/(Mg + Fe) \simeq 0.72$] could have been in equilibrium with olivines as magnesian as Fo_{91-89}. There is no obvious evidence that the harzburgite was a low-pressure cumulate from basaltic magma: the minerals of the harzburgite are more magnesian than the phenocrysts of the basaltic rocks (Fig. 12), and orthopyroxene does not occur as a phenocryst phase in the volcanics.

Fractionation of olivine and plagioclase, the cumulate phases in the layered gabbros and the common phenocrysts in the lavas and dykes, has been widely invoked to explain major-element compositional variability in ocean-floor basalts. Yet mixing calculations (Bryan et al., 1976; Thompson et al., 1980) suggest that the variability is only satisfactorily accounted for if clinopyroxene is also extracted, in spite of its rarity as a phenocryst phase. Varne and Rubenach (1972) pointed out that rapid eruption of a typical ocean-floor basalt magma from ~ 9 kbar pressure could lead to a situation where:

> "aluminous clinopyroxene stable at higher pressures would react with the magma, and plagioclase and olivine would be precipitated as the magma fractionally crystallized to move to a cotectic relationship at lower pressures."

It was argued that the rare clinopyroxene xenocrysts of ocean-floor basalts should prove to be highly aluminous if this suggestion were valid. However, the clinopyroxenes are not notably rich in Al and resemble the postcumulus clinopyroxenes in the layered rocks. This similarity, and the likelihood that the postcumulus clinopyroxene crystallized by heteradcumulate growth, implies that many of the basalts could have formerly been intercumulus liquids at shallow crustal levels (cf. Hodges and Papike, 1976; Brooks and Nielson, 1978).

Because the layered rocks are a mixture of cumulus and postcumulus phases similar in composition to the phenocrysts of the basalts and dolerites, their bulk compositions are unlike those of liquids. This compositional feature is displayed on a plot of CaO against $Mg/(Mg + Fe)$ (Fig. 13). The basalts and dolerites plot within a fairly restricted area, only slightly affected by plagioclase enrichment in some rocks. Most of the gabbros and peridotites, and all of the layered rocks, have bulk compositions with $Mg/(Mg + Fe)$ ratios higher than those of the fine-grained or glassy igneous rocks, with a scatter of CaO contents that reflects crystal fractionation effects involving olivine, plagioclase and clinopyroxene. The influence of marked variations in modal cumulate olivine and plagioclase is also clearly shown in the *AFM*-diagram (Fig. 5).

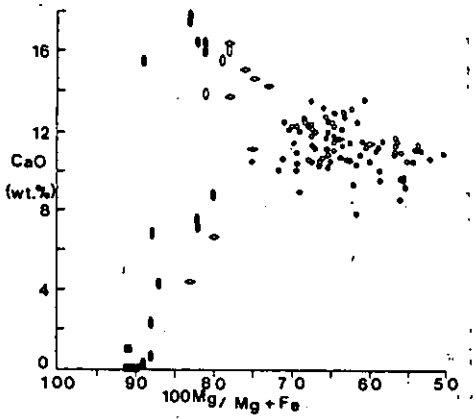

Fig. 13. CaO contents of Macquarie Island rocks, plotted against 100 Mg/(Mg E Fe). Basalts are shown by *open circles*, dolerites by *filled circles*, layered gabbros and wehrlites by *filled ellipses*. Gabbros from east of Handspike Point and above the layered gabbros in the section (see Fig. 3) are shown by *open ellipses*. Other massive gabbros are shown by *open rhombs* except for the massive gabbros from around Island Lake (see Figs. 2 and 3), shown by *filled rhombs*.

The massive gabbros have Mg/(Mg + Fe) ratios that range widely, but most are intermediate between those of the dykes and those of the layered rocks (Fig. 5). Those gabbros with Mg/(Mg + Fe) ratios similar to those of the basalts and dolerites have mineral compositions similar to those of phenocrysts and groundmass phases in the fine-grained rocks (Fig. 12).

The massive gabbros in the northwest of the island (Fig. 2), placed between the dyke swarms and the layered gabbro complex in the oceanic lithosphere section (Fig. 3), have Mg/(Mg + Fe) ratios intermediate between those of the dykes and those of the layered rocks (Fig. 5), as do the recrystallized massive gabbros south of the layered gabbro complex (Fig. 2) that in section appear beneath them, and above the harzburgite.

These compositional relationships indicate that the upper part of the Macquarie Island oceanic lithosphere section resembles a vertical slice through a differentiating column of magma. Much of the major-element compositional variability in the lavas and dykes is apparently the result of low-pressure fractional crystallization. Many of the magmas could have been intercumulus liquids in the layered gabbros, differentiating by adcumulate fractional crystallization. As a group, the dykes are more differentiated than the lavas. The strong resemblances between the Macquarie Island rocks and the volcanic rocks erupted near 36°N and 45°N on the Mid-Atlantic Ridge imply that similar fractionation processes and spatial relationships occur in these active "anomalous" ridge segments, and that a magma chamber may be at least episodically present, perhaps smaller than that proposed by Bryan and Moore (1977) but more substantial than that inferred by Nisbet and Fowler (1978).

DISCUSSION

Its oceanic environment, its tectonic setting, its magnetic properties, its pillow lavas and deep-sea sediments — these features all show that Macquarie Island is composed of oceanic crust.

The age of the rocks, the presence of dolerite dyke swarms, their structural history, and the linear magnetic anomaly patterns of the region are all consistent with the hypothesis that Macquarie Island oceanic lithosphere was formed by mid-Tertiary sea-floor spreading at the Indian—Antarctic—Pacific ridge far from any continent. Indeed, it is difficult to explain the origin of the rocks in any other way.

Macquarie Island therefore provides the opportunity to examine oceanic crust, using the same methodology and at the same scale as land-based studies of ophiolite complexes. The island is the connecting-link between the ophiolites of continental environments, and the in situ oceanic crust studied by dredge, drill and submersible.

Miyashiro (1975) commented that volcanic rocks could be used to assign ophiolite complexes to at least three classes. Class-I ophiolites are characterized by tholeiitic volcanics that display, at least in part, the compositional characteristics of island-arc magmatism. Such Class-I ophiolites may include the Troodos complex and may have formed in an island arc (Miyashiro, 1975), and inter-arc basin (Pearce, 1975; Smewing et al., 1975; Dewey, 1976; Sun and Nesbitt, 1978; Saunders and Tarney, 1979), in fore-arc settings (Cameron et al., 1981), or in the waning stages of aborted continental rifting (Brown et al., 1981). These are the complexes where orthopyroxene appears early, as a major cumulate phase in the ultramafics, and as a phenocryst phase in volcanic sequences that are proving to include high-Mg, low-TiO_2 andesites or basalts that are *hy*-rich and may have boninitic affinities (Kuroda and Shiraki, 1975; Varne and Brown, 1978; Cameron et al., 1979; Brown et al., 1981; Cameron et al., 1981).

Miyashiro's (1975) Class-II ophiolites are associated with tholeiitic volcanics similar to ocean-floor basalts, but showing more variation in SiO_2 contents and FeO^*/MgO ratios. Miyashiro (1975) suggested that Class-II ophiolites, like those of the Labrador Trough and the Yap Islands, may have formed in immature arcs or in mid-oceanic ridges. Broadly similar volcanics occur in the Mid-Atlantic Ridge from the Reykjanes Ridge at 63°N (Wood et al., 1979a) and from the Indian and Pacific Oceans (Bryan et al., 1976).

Miyashiro (1975) also distinguished Class-III ophiolites in which tholeiitic volcanics were accompanied by alkaline basalts, and included in this class the ophiolites of high-pressure metamorphic terranes, and those of Macquarie Island. Miyashiro (1975) suggested that some of these Class-III ophiolites could be derived from fracture zones, marginal sea floor or sea-mounts.

However, as has been shown, the volcanic rocks of Macquarie Island are strongly resembled by the volcanic rocks from the so-called "anomalous" Mid-Atlantic Eidge segments near 36° and 45°N, but span a compositional

range that is wider than that so far encountered at any single sea-floor site. In addition, the dykes and some of the gabbros tend to follow a more pronounced Fe-enrichment trend than do the lavas, and also include more *di*-poor and *Q*-rich compositions. The extent of the compositional range among the Macquarie Island volcanics is partly a consequence of sampling methods and exposure: the best-known Mid-Atlantic Ridge site, the FAMOUS area, has similarly been shown to include almost the complete compositional range encountered in the three major ocean basins (Bryan et al., 1976).

On Macquarie Island, the volcanics range from *ne*- to *Q*-normative, and include types that are relatively enriched in K, Sr, Rb, Nb and related elements but retain the characteristic phenocryst assemblages, the Ti, Ni, Cr, Y and Zr abundances, the major-element compositions, and the normative mineralogy of ocean-floor basalts. Their geochemical characteristics, which may be related to source-heterogeneities (Pearce and Norry, 1979), pose a problem for the widely-used trace-element discrimination diagrams, where the ocean-floor basalt fields were defined using compositional data from the so-called "normal" ridge segments. These diagrams are an efficient method of identifying "normal" ocean-floor basalts, but "abnormal" ocean-floor basalts like the more enriched Macquarie Island basalts and dolerites tend to plot away from the ocean-floor basalt field into the "within-plate" basalt field or into the low-K island arc tholeiite field or are left unclassified.

Similar "abnormal" ocean-floor basalts in ophiolite complexes may betray their origins by Nb contents in the range 20—60 ppm. High Nb contents are very rare in basalts and andesites from island arcs: even highly potassic and undersaturated mafic lavas from the Sunda arc have Nb contents of only ~ 15 ppm or less (Foden and Varne, 1980). In alkaline "within-plate" basalts, high contents of Nb are commonly accompanied by Ti and Zr contents that are much greater than those of ocean-floor basalts. It would be of great interest to find out if many of Miyashiro's (1975) Class-III ophiolites from high-pressure metamorphic terranes are Macquarie Island-type ophiolite complexes that could have been derived from "anomalous" ridge segments.

The mineralogy and chemical composition of the Macquarie Island plutonic rocks are almost exactly those that would be predicted from consideration of the mineralogy and major-element composition of the basalts and dolerites. There are no plagiogranites or trondheimites on Macquarie Island, norite is either very rare or absent, orthopyroxenites are unknown, and the harzburgites are the only rocks in which orthopyroxene is abundant. The olivine, plagioclase and clinopyroxene of the gabbros have compositions that are closely similar to those of the same phases in the basalts and dolerites. Orthopyroxene is unknown from the volcanic rocks, and is only a very rare constituent of the gabbros, where it seems to have formed by subsolidus or near-solidus reaction (R. Varne, in prep.).

The comagmatic character of the basalts, dolerites and gabbros of the Macquarie Island ophiolite complex implies that any Macquarie Island-type opjiolite complex derived from a similar tectonic setting ought to be recognizable from its field relations, petrology and geochemistry, unless it is extremely altered and dismembered.

ACKNOWLEDGEMENTS

The Antarctic Division of the Commonwealth of Australia Department of Science and the Environment generously arranged our transport to Macquarie Island and supported our field work there. Financial support for the work was provided by the University of Tasmania, and the Australian Research Grants Committee. Prof. D.H. Green and G.A. Jenner kindly commented on the manuscript.

REFERENCES

Aumento, F., 1968. The Mid-Atlantic Ridge near 45° N, II. Basalts from the area of Confederation Peak. Can. J. Earth Sci., 5: 1—21.

Ballard, R.D. and van Andel, Tj.J., 1977. Morphology and tectonics of the inner rift valley at lat. 36° 50'N on the Mid-Atlantic Ridge. Geol. Soc. Am. Bull., 88: 507—530.

Banerjee, S.K., Butler, R.F. and Stout, J.H., 1974. Magnetic properties and mineralogy of exposed oceanic crust on Macquarie Island. Z. Geophys., 40: 537—548.

Bender, J.F., Hodges, F.N. and Bence, A.E., 1978. Petrogenesis of basalts from the Project FAMOUS area: experimental study from 0 to 15 kbars. Earth Planet. Sci. Lett., 41: 277—302.

Bloxam, J.W. and Lewis, A.D., 1972. Ti, Zr and Cr in some British pillow lavas and their petrogenetic affinities. Nature (London), Phys. Sci., 237: 134—136.

Brooks, C.K. and Nielson, T.F.D., 1978. Early stages in the differentiation of the Skaergaard magma as revealed by a closely related suite of dike rocks. Lithos, 11: 1—14.

Brown, A.V., Rubenach, M.J. and Varne, R., 1981. Geological environment, petrology and tectonic significance of the Tasmanian Cambrian ophiolitic and ultramafic complexes. Proc. Int. Ophiolite Symp., Nicosia, 1979 (in press).

Bryan, W.B. and Moore, J.G., 1977. Compositional variations of young basalts in the Mid-Atlantic Ridge rift valley near 36° 49'N. Geol. Soc. Am. Bull., 88: 556—570.

Bryan, W.B., Thompson, G., Frey, F.A. and Dickey, J.S., 1976. Inferred geologic settings and differentiation in basalts from the deep-sea drilling project. J. Geophys. Res., 81: 4285—4304.

Butler, R.F., Banerjee, S.K. and Stout, J.H., 1976. Magnetic properties of oceanic pillow basalts: evidence from Macquarie Island. Geophys. J.R. Astron. Soc., 47: 179—196.

Cameron, W.E., Nisbet, E.G. and Dietrich, V.J., 1979. Boninites, komatiites and ophiolitic basalts. Nature (London), 280: 550—553.

Cameron, W.E., Nisbet, E.G. and Dietrich, V.J., 1981. Petrographic dissimilarities between ophiolitic and ocean-floor basalts. Proc. Int. Ophiolite Symp. Nicosia, 1979 (in press).

Cann, J.R., 1970. Rb, Sr, Y, Zr, and Nb in some ocean-floor basaltic rocks. Earth Planet. Sci. Lett., 10: 7—11.

Cann, J.R., 1971. Major element variations in ocean-floor basalts. Philos. Trans. R. Soc. London, Ser. A, 268: 495—505.

Cawthorn, R.G., Ford, C.E., Biggar, G.M., Bravo, M.S. and Clarke, D.B., 1973. Determination of liquid compositions in experimental samples: discrepancies between microprobe analysis and other methods. Earth Planet Sci. Lett., 21: 1—5.

Coleman, R.G., 1977. Ophiolites. Springer, Berlin, 229 pp.

Cullen, D.J., 1969. Macquarie Island, provisional bathymetry, scale 1:200,000. Island Series, N.Z. Oceanogr. Inst., Wellington.

Dewey, J.F., 1976. Ophiolite subduction. Tectonophysics, 31: 93—120.

Duke, J.M., 1976. Distribution of the period four elements among olivine, calcic clinopyroxene and mafic silicate liquid: experimental results. J. Petrol., 17: 499—521.

Duncan, R.A. and Green, D.H., 1980. Role of multistage melting in the formation of oceanic crust. Geology, 8: 22—26.
Engel, A.E.J., Engel, C.G. and Havens, R.G., 1965. Chemical characteristics of oceanic basalts and the upper mantle. Geol. Soc. Am. Bull., 76: 719—734.
Erlank, A.J. and Kable, E.J.D., 1976. The significance of incompatible elements in the Mid-Atlantic Ridge basalts from 45°N with particular reference to Zr/Nb. Contrib. Mineral. Petrol., 54: 281—291.
Floyd, P.A. and Winchester, J.A., 1975. Magma type and tectonic setting discrimination using immobile elements. Earth Planet. Sci. Lett., 27: 211—218.
Foden, J.D. and Varne, R., 1980. The petrology and tectonic setting of Quaternary—Recent volcanic centres of Lombok and Sumbawa, Sunda arc. In: R.W. Le Maitre and A. Cundari (Guest—Editors), Chemical Characterization of Tectonic Provinces. Chem. Geol., 30: 201—226 (this Special Issue).
Frey, F.A., Bryan, W.B. and Thompson, G., 1974. Atlantic Ocean floor: Geochemistry and petrology of basalts from Legs *2* and *3* of the Deep-Sea Drilling Project. J. Geophys. Res., 79: 5507—5527.
Griffin, B.J., 1979. Energy-dispersive analysis system calibration and operation with Tas-Sueds, an advanced interactive data-reduction package. Univ. Tasmania, Hobart, Tasmania, Dep. Geol. Publ. No. 343, pp. 1—46.
Griffiths, J.R. and Varne, R., 1972. Evolution of the Tasman Sea, Macquarie Ridge and Alpine Fault. Nature (London), Sci., 235: 83—86.
Hart, S.R., 1970. Chemical exchange between sea water and deep ocean basalts. Earth Planet. Sci. Lett., 9: 269—279.
Hart, S.R., Schilling, J.-G. and Powell, J.L., 1973. Basalts from Iceland and along the Reykjanes Ridge: Sr-isotope geochemistry. Nature (London), Phys. Sci., 246: 104—107.
Hayes, D.E. and Talwani, M., 1972. Geophysical investigation of the Macquarie ridge complex. In: D.E. Hayes (Editor), Antarctic Oceanology, II: The Australian—New Zealand Sector. Antarct. Res. Ser., 19: 211—234.
Heirtzler, J.R., Dickson, G.O., Herron, E.M., Pitman III, W.C., and Le Pichon, X., 1968. Marine magnetic anomalies, geomagnetic field reversals and motions of the ocean floor and continents. J. Geophys. Res., 73: 2119—2136.
Hodges, F.N. and Papike, J.J., 1976. DSDP Site *334*: Magmatic cumulates from oceanic layer *3*. J. Geophys. Res., 81: 4135—4151.
Ito, K., 1973. Analytical approach to estimating the source rocks of basaltic magmas: Major elements. J. Geophys. Res., 78: 412—431.
Jakeš, P. and Gill, J.B., 1970. Rare earth elements and the island arc tholeiite series. Earth Planet. Sci. Lett., 9: 17—28.
Kay, R., Hubbard, N.J. and Gast, P.W., 1970. Chemical characteristics and origin of oceanic ridge volcanic rocks. J. Geophys. Res., 75: 227—255.
Kuroda, N. and Shiraki, K., 1975. Boninite and related rocks of Chichi-jima, Bonin Islands, Japan. Rep. Fac. Sci. Shizuoka Univ., 10: 145—155.
La Brecque, J.L., Kent, D.V. and Cande, S.C., 1977. Revised magnetic polarity time-scale for Late Cretaceous and Cenozoic time. Geology, 5: 330—335.
Le Pichon, X., Francheteau, J. and Bonnin, J., 1973. Plate Tectonics. Elsevier, Amsterdam, 300 pp.
Levi, S., Banerjee, S.K., Beske-Diehl, S. and Moskowitz, B., 1978. Limitations of ophiolite complexes as models for the magnetic layer of the oceanic lithosphere. Geophys. Res. Lett., 5: 473—476.
Lugg, D.J., Johnstone, G.W. and Griffin, B.J., 1978. The outlying islands of Macquarie Island. Geograph. J., 144: 277—287.
Mawson, D., 1943. Macquarie Island, its geography and geology. In: Australasian Antarctic Expedition 1911—1914, Govt. Print. Off., Sydney, N.S.W., Sci. Rep. Sect. A:5.

Miyashiro, A., 1973. The Troodos ophiolitic complex was probably formed in an island arc. Earth Planet. Sci. Lett., 19: 218—224.
Miyashiro, A., 1975. Classification, characteristics, and origin of ophiolites. J. Geol., 83: 249—281.
Muir, I.D., Tilley, C.E. and Scoon, J., 1964. Basalts from the northern part of the rift zone of the Mid-Atlantic Ridge. J. Petrol., 5: 409—434.
Nisbet, E.G. and Fowler, C.M.R., 1978. The Mid-Atlantic Ridge at 37 and 45°N: some geophysical and petrological constraints. Geophys. J.R. Astron. Soc., 54: 631—660.
Norrish, K. and Chappell, B.W., 1967. X-ray fluorescent spectrography. In: J. Zussman (Editor), Physical Methods in Determinative Mineralogy. Academic Press, London, pp. 161—214.
Norrish, K. and Hutton, J.T., 1969. An accurate X-ray spectrographic method for the analysis of a wide range of geological samples. Geochim. Cosmochim. Acta, 33: 431—455.
Ovenshine, A.T., Winkler, G.R., Andrews, P.B. and Gostin, V.A., 1979. Chemical analyses and minor element composition of Leg 29 basalts. In: J.P. Kennett, R.E. Houtz et al., Initial Reports of the Deep Sea Drilling Project, Vol. 29. U.S. Government Printing Office, Washington, D.C., pp. 1097—1102.
Pearce, J.A., 1975. Basalt geochemistry used to investigate past tectonic environments on Cyprus. Tectonophysics, 25: 41—67.
Pearce, J.A. and Cann, J.R., 1971. Ophiolite origin investigated by discriminant analyses using Ti, Zr and Y. Earth Planet. Sci. Lett., 12: 339—349.
Pearce, J.A. and Cann, J.R., 1973. Tectonic setting of basic volcanic rocks determined using trace element analyses. Earth Planet. Sci. Lett., 19: 290—300.
Pearce, J.A. and Norry, M.J., 1979. Petrogenetic implications of Ti, Zr, Y and Nb variations in volcanic rocks. Contrib. Mineral. Petrol., 69: 33—47.
Pearce, T.H., Gorman, B.E. and Birkett, T.C., 1975. The TiO_2—K_2O—P_2O_5 diagram: and non-oceanic basalts. Earth Planet. Sci. Lett., 24: 419—426.
Quilty, P.G., Rubenach, M. and Wilcoxon, J.A., 1973. Miocene ooze from Macquarie Island. Search, 4: 163—164.
Reed, S.J.B. and Ware, N., 1975. Quantitative electron microprobe analysis of silicates using energy dispersive X-ray spectrometry. J. Petrol., 16: 499—519.
Roedder, P.L. and Emslie, R.F., 1970. Olivine—liquid equilibrium. Contrib. Mineral. Petrol., 29: 275—289.
Saunders, A.D. and Tarney, J., 1979. The geochemistry of basalts from a back-arc spreading centre in the East Scotia Sea. Geochim. Cosmochim. Acta, 43: 555—572.
Schilling, J.-G., 1973. Iceland mantle plume: geochemical study of Reykjanes Ridge. Nature (London), 242: 565—571.
Schilling, J.-G. and Ridley, W.I., 1979. Volcanic rocks from DSDP Leg *29*: Petrography and rare earth abundances. In: J.P. Kennett, R.E. Houtz et al., Initial Reports of the Deep Sea Drilling Project, Vol. 29. U.S. Government Printing Office, Washington, D.C., pp. 1103—1107.
Smewing, J.D., Simonian, K.O. and Gass, I.G., 1975. Metabasalts from the Troodos massif, Cyprus: genetic implication deduced from petrography and trace element geochemistry. Contrib. Mineral. Petrol., 51: 49—64.
Summerhayes, C.P., 1969. Marine geology of the New Zealand Sub-antarctic sea floor. N'Z. Dep. Sci. Ind. Res., Bull. 190, 94 pp.
Summerhayes, C.P., 1974. Macquarie—Balleny Ridge. In: A.M. Spencer (Editor), Mesozoic—Cenozoic Orogenic Belts: Data for Orogenic Studies. Scottish Academic Press for the Geological Society, London, pp. 379—381.
Sun, S.-S. and Nesbitt, R.W., 1978. Geochemical regularities and genetic significance of ophiolitic basalts. Geology, 6: 689—693.
Thompson, G., 1973. A geochemical study of the low-temperature interaction of seawater and oceanic igneous rocks. EOS (Trans. Am. Geophys. Union), 54: 1015—1018.

Thompson, G., Shido, F. and Miyashiro, A., 1972. Trace element distributions in fractionated oceanic basalts. Chem. Geol., 9: 89—97.

Thompson, G., Bryan, W.B. and Melson, W.G., 1980. Geological and geophysical interpretation of the Mid-Cayman Rise spreading center: geochemical variation and petrogenesis of basalt glasses. J. Geol., 88: 41—55.

Varne, R. and Brown, A.V., 1978. The geology and petrology of the Adamsfield ultramafic complex. Contrib. Mineral. Petrol., 67: 195—207.

Varne, R. and Rubenach, M.J., 1972. Geology of Macquarie Island and its relationship to oceanic crust. In: D.E. Hayes (Editor), Antarctic Oceanology, II. The Australian—New Zealand Sector. Antarct. Res. Ser., 19: 251—266.

Varne, R. and Rubenach, M.J., 1973. Geology of Macquarie Island in relation to tectonic environment. In: P.J. Coleman (Editor), The Western Pacific: Island Arcs, Marginal Seas, Geochemistry, University of Western Australia Press, Perth, W.A.

Varne, R., Gee, R.D. and Quilty, P.G.J., 1969. Macquarie Island and the cause of oceanic linear magnetic anomalies. Science, 166: 230—233.

Watkins, N.D. and Gunn, B.M., 1971. Petrology, geochemistry, and magnetic properties of some rocks dredged from the Macquarie ridge. N.Z. J. Geol. Geophys., 14: 153—168.

Weissel, J.K. and Hayes, D.E., 1972. Magnetic anomalies in the southeast Indian Ocean, In: D.E. Hayes (Editor), Antarctic Oceanology, II. The Australia—New Zealand Sector. Antarct. Res. Ser., 19: 165—196.

Williamson, P., 1974. Recent studies of Macquarie Island and the Macquarie Ridge Complex. Bull. Aust. Soc. Explor. Geophys., 5: 19—22.

Williamson, P., 1979. The palaeomagnetism of outcropping oceanic crust on Macquarie Island. J. Geol. Soc. Aust., 25: 387—394.

Wood, D.A., Tarney, J., Varet, J., Saunders, A.D., Bougault, H., Joron, J.L., Treuil, M. and Cann, J.R., 1979a. Geochemistry of basalts drilled in the North Atlantic by IPOD Leg *49*: implications for mantle heterogeneity. Earth Planet. Sci. Lett., 42: 77—97.

Wood, D.A., Joron, J.-L. and Treuil, M., 1979b. A re-appraisal of the use of trace elements to classify and discriminate between magma series erupted in different tectonic settings. Earth Planet. Sci. Lett., 45: 326—336.

#7

B. J. Griffin

on

EROSION AND RABBITS ON MACQUARIE ISLAND: SOME COMMENTS

Reprinted with original pagination from

VOLUME 114 OF

THE PAPERS AND PROCEEDINGS OF

The Royal Society of Tasmania

Edited by M. R. Banks and published by the Society

May 1980

Hobart, Tasmania

T. J. Hughes, Government Printer, Tasmania

Papers and Proceedings of the Royal Society of Tasmania, Volume 114, 1980.

(ms. received 24.4.1979)

EROSION AND RABBITS ON MACQUARIE ISLAND: SOME COMMENTS

by B.J. Griffin
Geology Department, University of Tasmania

(with one plate)

ABSTRACT

GRIFFIN, B.J., 1980 (31 v): Erosion and rabbits on Macquarie Island: some comments. *Pap. Proc. R. Soc. Tasm.*, 114: 81-83 (incl. one plate). ISSN 0080-4703. Department of Geology, University of Tasmania, Hobart, Tasmania, Australia.

Rapid emergence and subsequent glacial and periglacial action on Macquarie Island have placed it in a state of high erosional activity. The dominant processes are mass erosion through landslips, soil creep slumping and solifluction. Fluvial and aeolian erosion are only important in very restricted areas. Rabbit activity has had a minimal effect on the overall rates of erosion although appearing significant in some localised areas.

INTRODUCTION

Macquarie Island is widely recognised as an extremely interesting area in terms of most natural sciences. This brief report looks at erosion processes on the island and the effects of the rabbit population on these processes and their rates of operation. the 34 km by 3 km island lies almost midway between the Australian mainland and the Antarctic continent, and is a subaerial exposure of the Macquarie Ridge. Physically it is dominated by a 200-300 m high plateau bounded by very steep slopes and cliffs with only very minor low-lying coastal terraces. These raised marine terraces are of middle to late Holocene age, indicating an average uplift rate of the island between 1.5 and 4.5 m per 1000 years (Colhoun and Goede 1973).

Geologically Macquarie Island is at present considered to represent Miocene oceanic crust generated in a spreading ridge environment (Varne and Rubenach 1972). The northern tip and southern three-quarters of the island are composed of basaltic pillow lavas and associated dolerite dykes. The remaining northern quarter is composed of more massive units of coarser-grained gabbros and ultramafic rocks.

The Colhoun and Goede (1974) have shown that former ice action on the island was dominated by local plateau, valley and cirque glaciers which covered, at their maximum extent, some 40% of the island, rather than by complete over-riding of an easterly moving ice sheet (Mawson 1943). Present landforms are dominantly of former periglacial and glacial origin. The current climatic conditions are humid periglacial.

PREVIOUS STUDIES OF EROSION

Few observations have been made of erosion processes on Macquarie Island. However various workers in other disciplines have made some brief comments. Taylor (1935) suggested that rabbit grazing is having catastrophic effects, in terms of erosion, on the grassland areas of Macquarie Island. This view was strongly supported by Costin and Moore (1960). They suggested that on the steeper slopes, which include grassland slopes in excess of 70° up to an altitude of 300 m, elimination of the stabilizing dominants, *Poa foliosa* and *Stilbocarpa polaris*, by rabbit grazing will almost certainly increase the incidence of minor landslips, resulting in the stripping of blanket bog peats and the development of screes. They finally suggested that small landslips in otherwise intact slopes often initiate an irreversible trend towards soil loss.

CURRENT OBSERVATIONS AND DISCUSSION

Soil creep is the major erosion mechanism on Macquarie Island. This is a continuous process with material gradually moving downslope under gravity. On Macquarie Island the soil-rock interface is permanently saturated; a result of the continuous heavy drizzle and low mist that characterise the weather conditions on the island. Precipitation is rarely heavy and many of the water channels on the island today are relict meltwater channels which are generally underfit (Colhoun and Goede 1974). Consequently today fluvial erosion does not play a major role on Macquarie Island.

The most spectacular form of mass movement, namely landslips, are very common on Macquarie Island. This is not surprising because the mass movement mantle is in a permanent state of instability and only requires a suitable trigger to move more rapidly as a landslip. During the three months 1975/76 summer field season it was observed that a number of landslips occurred immediately after the heaviest rainfall period of the summer. This correlation of landslips occurring after heavy rain periods has also been observed subsequently (G. Copson, *pers. comm.*). Another recognised trigger is large earthquakes and as Macquarie Island is seismically very active, earthquakes as well as heavy rain periods form the major triggers for the landslip activity. The irreversible soil loss trend after landslips suggested by Costin and Moore (1960) has not been observed by the author. On most of the slopes on both coasts it is possible to see landslip areas in various stages of revegetation (plate 1a). Bare rock is only exposed, if at all, at the head of the slip and this is quickly covered by collapse of upslope material.

PLATE 1a. - Recent and revegetated landslips on steep coastal tussock slopes near Nuggets Point at the northern end of Macquarie Island.

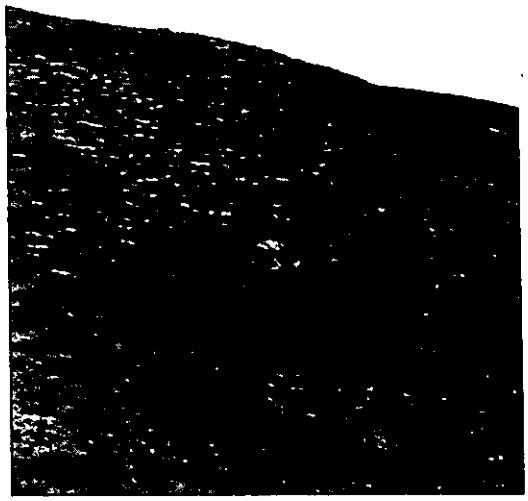

PLATE 1b.- Terracettes on a grassed hillslope.

Many of the grassland slopes contain small terraces or terracettes (plate 1b). These are commonly misnamed "sheep tracks" throughout rural mainland Australia and on Macquarie Island some workers have similarly misinterpreted these features as due to rabbit tracks or squats. Actually these features are usually a result of creep processes, solifluction and or occasionally small scale slumping.

Wind is another erosive agent on Macquarie Island; during the three month 1975/6 summer the average wind speed was 26 km per hour. However because of the moist surface environment wind deflation effects are drastically reduced relative to those in drier environments. Moist clay has strong interparticle adhesion so that only during the rare dry periods if ever, are the clays deflated. Coarser material is more susceptible and fossil aeolian dunes deposited along the natural wind 'funnel' between Sandy Bay on the east coast and Bauer Bay on the west coast are being eroded through wind deflation. Observations suggest that this was initiated by rabbits burrowing on the windward side of the dunes. Erosion of raised marine ridges on the coastal terraces is probably also a result of similar rabbit activity. These areas are very small relative to the whole island and insignificant in terms of the overall erosion processes.

It has also been suggested that rabbits have increased the incidence of landslips by weakening an area through burrowing. No evidence has been presented on this and a visual comparison of the island today with photographs taken at about the time of introduction of rabbits would suggest that the rate of occurrence has not significantly altered. Furthermore areas of burrowing petrel colonies, which have a higher burrow density than rabbits, are not obviously more eroded than adjacent areas.

In summary, the major processes active on Macquarie Island are various forms of mass movement. Although rabbits may have severe botanical effects on the ecology, they have had little effect on the erosion of Macquarie Island. It is invalid to compare Macquarie Island with mainland Australia because of the major climatic differences and such comparisons are misleading.

ACKNOWLEDGEMENTS

Many people have provided fruitful discussion and advice on this topic, in particular Mr. G. Copson, Dr. E. Colhoun and Dr. J. Jenkins. Mr. G. Copson is thanked for supplying the photographs. The National Parks and Wildlife Service of Tasmania, the Australian Antarctic Division and the University of Tasmania have provided logistic support and funding for two visits to the island and this is gratefully acknowledged.

REFERENCES

Colhoun, E.A., and Goede, A., 1973: Fossil Penguin Bones, ^{14}C Dates and the raised marine terraces of Macquarie Island: some comments. *Search*, 4(11): 499-501.

_____, 1974: A reconnaissance survey of the glaciation of Macquarie Island. *Pap. Proc. R. Soc. Tasm.*, 108: 1-19.

Costin, A.B., and Moore, D.M., 1960: The effects of rabbit grazing on the grasslands of Macquarie Island. *J. Ecol.*, 48: 729-732.

Cumpston, J.S., 1968: Macquarie Island. ANARE *Scientific Reports, Series A*, 93.

Mawson, D., 1943: Macquarie Island: its geography and geology. *Australasian Antarctic expedition 1911-1914 Scientific Reports, Series A*, 5.

Taylor, B.W., 1955: The flora, vegetation and soils of Macquarie Island. *Australian National Antarctic Research Expedition Reports, Series B.*, 11.

Varne, R., and Rubenach, M.S., 1972: Geology of Macquarie Island and its relationship to oceanic crust. *Amer. Geophys. Union, Antarctic Research Series*, 19: 251.